



*Official Journal of the  
Malaysian Medical Association*

# *The Medical Journal of Malaysia*

**July 2022**

**Volume: 77**

**Supplement: 1**



# MJM

*Official Journal of the  
Malaysian Medical Association*

Volume 71 Supplement 1 July 2022

## EDITORIAL BOARD

*Editor In Chief*

**Prof Datuk Dr Lekhraj Rampal**

*Editor*

**Dr Liew Boon Seng**

*Editors*

**Assoc Prof Dr Subapriya Suppiah**

**Prof Dato' Dr NKS Tharmaseelan**

**Prof Dr Baharudin Abdullah**

**Dr Philip Rajan Devesahayam**

**Prof Dr Victor Hoe Chee Wai**

**Dr Terence Ong Ing Wei**

*Editorial Manager*

**Ms Mahaletchumy Alagappan**

PP 2121/01/2013 (031329)

MCI (P) 124/1/91

ISSN 0300-5283

The Medical Journal of Malaysia is published six times a year.  
MJM is published bimonthly ie. January, March, May, July, September and November.

**All articles which are published, including editorials, letters and book reviews  
represent the opinion of the authors and are not necessarily those of the  
Malaysian Medical Association unless otherwise expressed.**

*Copyright reserved © 2022*  
Malaysian Medical Association

**Advertisement Rates:**

Enquiries to be directed to the Secretariat.

**Subscription Rates:**

Price per copy is RM100.00 or RM360.00 per annum, for all subscribers.

**Secretariat Address:**

Malaysian Medical Association  
4th Floor, MMA House, 124, Jalan Pahang, 53000 Kuala Lumpur.  
Tel: (03) 4042 0617, 4041 8972, 4041 1375 Fax: (03) 4041 8187  
E-mail: [info@mma.org.my](mailto:info@mma.org.my) / [mjm@mma.org.my](mailto:mjm@mma.org.my)  
Website: [www.mma.org.my](http://www.mma.org.my)

Printed by: Digital Perspective Sdn. Bhd.  
42-1, Level 1, Plaza Sinar, Taman Sri Sinar, 51200 Kuala Lumpur. Tel: 03-6272 3767  
Email: [dpsbkl@gmail.com](mailto:dpsbkl@gmail.com)

The *Medical Journal of Malaysia (MJM)* welcomes articles of interest on all aspects of medicine in the form of original papers, review articles, short communications, continuing medical education, case reports, commentaries and letter to Editor. Articles are accepted for publication on condition that they are contributed solely to *The Medical Journal of Malaysia*.

**NOTE: MJM is published bimonthly ie. January, March, May, July, September and November.**

#### REQUIREMENTS FOR ALL MANUSCRIPTS

Please ensure that your submission to MJM conforms to the International Committee of Medical Journal Editors Recommendations for the Conduct, Reporting, Editing, and Publication of Scholarly Work in Medical Journals.

Neither the Editorial Board nor the Publishers accept responsibility for the views and statements of authors expressed in their contributions.

The Editorial Board further reserves the right to reject papers read before a society. To avoid delays in publication, authors are advised to adhere closely to the instructions given below.

#### MANUSCRIPTS

Manuscripts should be submitted in English (British English). Manuscripts should be submitted online through *MJM Editorial Manager*, <http://www.editorialmanager.com/mjm>.

Instructions for registration and submission are found on the website. Authors will be able to monitor the progress of their manuscript at all times via the *MJM Editorial Manager*. For authors and reviewers encountering problems with the system, an online Users' Guide and FAQs can be accessed via the "Help" option on the taskbar of the login screen.

MJM charges a one-time, non-refundable Article Processing Charge (APC) upon submission. Waiver of the APC applies only to members of the editorial board, and authors whose articles are invited by the editor. In addition, recipients of the MJM Reviewer Recognition Award from the previous year may enjoy a waiver of the APC for the next calendar year (e.g. recipients of MJM Reviewer Recognition Award 2022 will enjoy waiver of APC for articles submitted between January and December 2023).

#### The MJM processing fee is based on the categories stated below:

- MJM
1. MMA Member - RM 400.00
  2. Non-Member - RM 600.00
  3. Overseas - USD 150.00

#### MJM Case Reports (effective 1st July 2022 up to further notice):

1. MMA Member - RM 200.00
2. Non-Member - RM 300.00
3. Overseas - USD 100.00

The MJM Article Processing Charge is a non-refundable administrative fee. Payment of the APC does not guarantee acceptance of the manuscript. Submitted articles will only be sent for reviews once the MJM APC has been successful completed.

All submissions must be accompanied by a completed **Copyright Assignment Form, Copyright Transfer Form and Conflict of Interest Form** duly signed by all authors. Forms can be download from MJM website at <https://www.e-mjm.org/>

Manuscript text should be submitted as **Microsoft Word** documents. Tables and flowcharts should be submitted as **Microsoft Word** documents. Images should be submitted as separate **JPEG files** (minimum resolution of 300 dpi).

#### PEER REVIEW PROCESS

All submissions must include at least two (2) names of individuals who are especially qualified to review the work. All manuscripts submitted will be reviewed by the Editor in-charge before they are sent for peer review. Manuscripts that are submitted to MJM undergo a double-blinded peer review and are managed online. Proposed reviewers must not be involved in the work presented, nor affiliated with the same institution(s) as any of the authors or have any potential conflicts of interests in reviewing the manuscript. The selection of reviewers is the prerogative of the Editors of MJM.

#### ELIGIBILITY AS AN AUTHOR

MJM follows the recommendation of the International Committee of Medical Journal Editors (ICMJE) for eligibility to be consider as an author for submitted papers. The ICMJE recommends that authorship be based on the following four (4) criteria:

1. Substantial contributions to the conception or design of the work; or the acquisition, analysis, or interpretation of data for the work; AND
2. Drafting the work or revising it critically for important intellectual content; AND
3. Final approval of the version to be published; AND
4. Agreement to be accountable for all aspects of the work in ensuring that questions related to the accuracy or integrity of any part of the work are appropriately investigated and resolved.

#### TYPES OF PAPERS

##### Original Articles:

Original Articles are reports on findings from original unpublished research. Preference

for publications will be given to high quality original research that make significant contribution to medicine. Original articles shall consist of a structured Abstract and the Main Text. The word count for the structured abstract should not exceed 500 words. The main text of the articles should not exceed 4000 words, tables/illustrations/figures/images up to five (5) and references up to 40. Manuscript describing original research should conform to the IMRAD format, more details are given below.

Original articles of cross-sectional and cohort design should follow the corresponding STROBE check-lists; clinical trials should follow the CONSORT check-list.

##### Review Articles:

Review Articles are solicited articles or systematic reviews. *MJM* solicits review articles from Malaysian experts to provide a clear, up-to-date account of a topic of interest to medical practice in Malaysia or on topics related to their area of expertise. Unsolicited reviews will also be considered, however, authors are encouraged to submit systematic reviews rather than narrative reviews. Review articles shall consist of a structured Abstract and the Main Text. The word count for the structured abstract should not exceed 500 words. Systematic Review are papers that presents exhaustive, critical assessments of the published literature on relevant topics in medicine. Systematic reviews should be prepared in strict compliance with MOOSE or PRISMA guidelines, or other relevant guidelines for systematic reviews.

##### Short Communications:

Shorts communication are short research articles of important preliminary observations, findings that extends previously published research, data that does not warrant publication as a full paper, small-scale clinical studies, and clinical audits. Short communications should not exceed 1,500 words and shall consist of a Summary and the Main Text. The summary should be limited to 100 words and provided immediately after the title page. The number of tables/illustrations/figures/images should be limited to three (3) and the number of references to ten (10).

##### Continuing Medical Education (CME) Articles:

A CME article is a critical analysis of a topic of current medical interest. The article should include the clinical question or issue and its importance for general medical practice, specialty practice, or public health. It shall consist of a Summary and the Main Text. The summary should be limited to 500 words and provided immediately after the title page. Upon acceptance of selected articles, the authors will be requested to provide five multiple-choice questions, each with five true/false responses, based on the article. For guideline, please refer to: Sivalingam N, Rampal L. Writing Articles on Continuing Medical Education for Medical Journals. *Med J Malaysia*. 2021 Mar;76(2):119-124.

##### Case Reports:

Papers on case reports (one to five cases) must follow these rules: Case reports should not exceed 2,000 words; with a maximum of two (2) tables; three (3) photographs; and up to ten (10) references. It shall consist of a Summary and the Main Text. The summary should be limited to 250 words and provided immediately after the title page. Having a unique lesson in the diagnosis, pathology or management of the case is more valuable than mere finding of a rare entity. Being able to report the outcome and length of survival of a rare problem is more valuable than merely describing what treatment was rendered at the time of diagnosis. There should be no more than seven (7) authors.

Please note that all Case Reports will be published in the new MJM Case Reports Journal ([www.mjmcasereports.org](http://www.mjmcasereports.org)).

##### Commentaries:

Commentaries will usually be invited articles that comment on articles published in the same issue of the *MJM*. However, unsolicited commentaries on issues relevant to medicine in Malaysia are welcomed. They should not exceed 2,000 words. They may be unstructured but should be concise. When presenting a point of view, it should be supported with the relevant references where necessary.

##### Letters to Editor:

Letters to Editors are responses to items published in *MJM* or to communicate a very important message that is time sensitive and cannot wait for the full process of peer review. Letters that include statements of statistics, facts, research, or theories should include only up to three (3) references. Letters that are personal attacks on an author will not be considered for publication. Such correspondence must not exceed 1,500 words.

##### Editorials:

These are articles written by the editor or editorial team concerning the *MJM* or about issues relevant to the journal.

#### STRUCTURE OF PAPERS

##### Title Page:

The title page should state the brief title of the paper, full name(s) of the author(s) (with the surname or last name bolded), degrees (limited to one degree or diploma), affiliation(s), and corresponding author's address. All the authors' affiliations shall be provided after the authors' names. Indicate the affiliations with a superscript number at the end of the author's degrees and at the start of the name of the affiliation. If the author is affiliated to more than one (1) institution, a comma should be used to separate the number for the said affiliation.

Do provide preferred abbreviated author names for indexing purpose, e.g. L Rampal (for Lekhraj Rampal), BS Liew (for Liew Boon Seng), B Abdullah (for Baharudin Abdullah), Hoe VC (for Victor Hoe Chee Wai).

Please indicate the corresponding author and provide the affiliation, full postal address and email.

Articles describing Original Research should consist of the following sections (IMRAD format): Abstract, Introduction, Materials and Methods, Results, Discussion, Acknowledgment and References. Each section should begin on a fresh page. Scientific names, foreign words and Greek symbols should be in italic.

## Abstract and Key Words:

A structured abstract is required for Original and Review Articles. It should be limited to 500 words and provided immediately after the title page. Below the abstract provide and identify three (3) to 10 key words or short phrases that will assist indexers in cross-indexing your article. Use terms from the medical subject headings (MeSH) list from Index Medicus for the key words where possible. Key words are not required for Short Communications, CME articles, Case Reports, Commentaries and Letter to Editors.

## Introduction:

Clearly state the purpose of the article. Summarise the rationale for the study or observation. Give only strictly pertinent references, and do not review the subject extensively.

## Materials and Methods:

Describe your selection of the observational or experimental subjects (patients or experimental animals, including controls) clearly, identify the methods, apparatus (manufacturer's name and address in parenthesis), and procedures in sufficient detail to allow other workers to reproduce the results. Give references to established methods, including statistical methods; provide references and brief descriptions of methods that have been published but are not well-known; describe new or substantially modified methods, give reasons for using them and evaluate their limitations.

Identify precisely all drugs and chemicals used, including generic name(s), dosage(s) and route(s) of administration. Do not use patients' names, initials or hospital numbers. Include numbers of observation and the statistical significance of the findings when appropriate.

When appropriate, particularly in the case of clinical trials, state clearly that the experimental design has received the approval of the relevant ethical committee.

## Results:

Present your results in logical sequence in the text, tables and illustrations. Do not repeat in the text all the data in the tables or illustrations, or both: emphasise or summarise only important observations in the text.

## Discussion:

Emphasise the new and important aspects of the study and conclusions that follow from them. Do not repeat in detail data given in the Results section. Include in the Discussion the implications of the findings and their limitations and relate the observations to other relevant studies.

## Conclusion:

Link the conclusions with the goals of the study but avoid unqualified statements and conclusions not completely supported by your data. Avoid claiming priority and alluding to work that has not been completed. State new hypotheses when warranted, but clearly label them as such. Recommendations, when appropriate, may be included.

## Acknowledgements:

Acknowledgements of general support, grants, technical assistance, etc., should be indicated. Authors are responsible for obtaining the consent of those being acknowledged.

## Referencing guide:

The Medical Journal of Malaysia, follows the Vancouver numbered referencing style. Citations to someone else's work in the text, should be indicated by the use of a number. In citing more than one article in the same sentence, you will need to include the citation number for each article. A hyphen should be used to link numbers which are inclusive, and a comma used where numbers are not consecutive. The following is an example where works 1,3,4,5 have been cited in the same place in the text.

Several effective drugs are available at fairly low cost for treating patients with hypertension and reducing the risk of its sequelae.<sup>1,3,5</sup>

The list of all of the references that are cited in the article should be presented in a list labelled as 'References'. This reference list appears at the end of the paper. Authors are responsible for the accuracy of cited references and these should be verified by the author(s) against the original documents before the manuscript is submitted. It is important that the author should never place in the list of references a document that he or she has not seen. The Journals names should be abbreviated according to the style used in the Index Medicus. All authors when six or less should be listed; when seven or more list only the first six and add et al.

If you are citing the author's name in your text, you must insert the citation number as well. Jewell BL (8) underlined that as focus in the SARS-CoV-2 pandemic shifts to the emergence of new variants of concern (VOC), characterising the differences between new variants and non-VOC lineages will become increasingly important for surveillance and maintaining the effectiveness of both public health and vaccination programme. If you are citing more than one author's name in your text and you want to cite author names in your text, use 'et al.' after the first author. Example: Rampal et al. (9) highlighted that the disregard of the manuscript guidelines and instruction to authors of the journal you submit, is one of the common reasons for 'Rejection' of the article.

## Example references Journals:

### Standard Journal Article

Rampal L and Liew BS. Coronavirus disease (COVID-19) pandemic. *Med J Malaysia* 2020; 75(2): 95-7.

Rampal L, Liew BS, Choolani M, Ganasegeran K, Pramanick A, Vallibhakara SA, et al. Battling COVID-19 pandemic waves in six South-East Asian countries: A real-time consensus review. *Med J Malaysia* 2020; 75(6): 613-25.

NCD Risk Factor Collaboration (NCD-RisC). Worldwide trends in hypertension prevalence and progress in treatment and control from 1990 to 2019: a pooled analysis of 1201 population-representative studies with 104 million participants. *Lancet* 2021; 11; 398(10304): 957-80.

## Books and Other Monographs:

### Personal Author(s)

Goodman NW, Edwards MB. 2014. *Medical Writing: A Prescription for Clarity*. 4 th Edition. Cambridge University Press.

### Chapter in Book

McFarland D, Holland JC. Distress, adjustments, and anxiety disorders. In: Watson M, Kissane D, Editors. *Management of clinical depression and anxiety*. Oxford University Press; 2017: 1-22.

### Corporate Author

World Health Organization, Geneva. 2019. WHO Study Group on Tobacco Product Regulation. Report on the scientific basis of tobacco product regulation: seventh report of a WHO study group. WHO Technical Report Series, No. 1015.

NCD Risk Factor Collaboration (NCD-RisC). Rising rural body-mass index is the main driver of the global obesity epidemic in adults. *Nature* 2019; 569: 260-64.

World Health Organization. Novel Coronavirus (2019-nCoV) Situation Report 85, April 14, 2020. [cited April 2020] Accessed from: <https://www.who.int/docs/defaultsource/coronaviruse/situationreports/20200414-sitrep-85-covid-19>.

## Online articles

**Webpage:** Webpage are referenced with their URL and access date, and as much other information as is available. Cited date is important as webpage can be updated and URLs change. The "cited" should contain the month and year accessed.

Ministry of Health Malaysia. Press Release: Status of preparedness and response by the ministry of health in and event of outbreak of Ebola in Malaysia 2014 [cited Dec 2014]. Available from: [http://www.moh.gov.my/english.php/database\\_stores/store\\_view\\_page/21/437](http://www.moh.gov.my/english.php/database_stores/store_view_page/21/437).

## Other Articles:

### Newspaper Article

Panirchellum V. 'No outdoor activities if weather too hot'. *the Sun*. 2016; March 18: 9(col. 1-3).

### Magazine Article

Rampal L. World No Tobacco Day 2021 -Tobacco Control in Malaysia. *Berita MMA*. 2021; May: 21-22.

## Tables:

All tables and figures should have a concise title and should not occupy more than one printed page. The title should concisely and clearly explain the content of the table or figure. They should be numbered consecutively with Roman numerals (e.g Table I) and figures with Arabic numerals (e.g. Figure 1), and placed after the sections of the manuscript which they reflect, particularly the results which they describe on separate pages. Cite tables in the text in consecutive order. Indicate table footnotes with lower-case letters in superscript font. Place the information for the footnote beneath the body of the table. If a table will be submitted as a separate document, the filename should contain the surname of the first author and match its label in the manuscript (e.g., SMITH Table 1). Vertical lines should not be used when constructing the tables. All tables and figures should also be sent in electronic format on submission of the manuscript as supplementary files through the journal management platform. Clinical Photographs should conceal the subject's identity. Tables and flow-charts should be submitted as Microsoft Word documents. Images should be submitted as separate JPEG files (minimum resolution of 300 dpi).

## Photographs of Patients:

Proof of permission and/or consent from the patient or legal guardian must be submitted with the manuscript. A statement on this must be included as a footnote to the relevant photograph.

## Colour reproduction:

Illustrations and diagrams are normally reproduced in black and white only. Colour reproductions can be included if so required and upon request by the authors. However, a nominal charge must be paid by the authors for this additional service; the charges to be determined as and when on a per article basis.

## Abbreviations:

Use only standard abbreviations. The full-term for which an abbreviation stands should precede its first use in the abstract, article text, tables, and figures, unless it is a standard unit of measurement. Abbreviations shall not be used in the Title. Abbreviations should be kept to a minimum.

## Formatting of text:

Numbers one to ten in the text are written out in words unless they are used as a unit of measurement, except in tables and figures. Use single hard-returns to separate paragraphs. Do not use tabs or indents to start a paragraph. Do not use the automated formatting of your software, such as hyphenation, endnotes, headers, or footers (especially for references). Submit the Manuscript in plain text only, removed all 'field codes' before submission. Do not include line numbers. Include only page number.

## BEST PAPER AWARD

All original papers which are accepted for publication by the MJM, will be considered for the 'Best Paper Award' for the year of publication. No award will be made for any particular year if none of the submitted papers are judged to be of suitable quality.

- Role of somatostatin receptor SSRT5-AS1 in predicting biomarkers of primary androgen deprivation therapy on prostate cancer in Indonesian population 1  
*Indrawarman Soerohardjo, Irianiwati Widodo, Andy Zulfiqar, Didik Setyo Heriyanto, Sumadi Lukman Anwar*
- Social determinants of health protocol adherence among adults during COVID-19 pandemic in Yogyakarta, Indonesia 5  
*Supriyati Supriyati, Fahmi Baiquni, Tri Siswati, Hemi Endah Widyawati, Riadini Rahmawati, Ratri Kusuma Wardani*
- Improvement of quality in clinical care for patients with benign prostatic hyperplasia: Cost effectiveness analysis 10  
*Johannes Cansius Prihadi, Firdaus Hafidz, Hanevi Djasri*
- Triple-action of the standardized antidiabetic polyherbal extract; Synacinn™ through upregulation of GLUT4 and inhibition of DPP(IV),  $\alpha$ -amylase, and  $\alpha$ -glucosidase activity 16  
*Hassan Fahmi Ismail, Zanariah Hashim, Dayang Norulfairuz Abang Zaidel, Siti Nurazwa Zainol, Fatahiya Mohamed Tap, Fadzilah Adibah Abdul Majid, Nor Hafizah Zakaria*
- Vascular remodeling and association with inflammation in the heart of obesity model 23  
*Dwi Cahyani Ratna Sari, Wiwit Ananda Wahyu Setyaningsih, Yaura Syifanie, Alya Kamila, Fauziyatul Munawaroh, Nur Arfian, Nungki Anggorowati*
- Gastric perforation in a 5-day-old infant: A case report 28  
*Luh Putu Neolita Pradnya Wineni, Ariandi Setiawan*
- Increased CD4/CD8 T-cell ratio : A risk factor for mortality in patients with coronavirus disease 2019 31  
*Adika Zhulhi Arjana, Komang Agus Trisna Amijaya, Sagita Adventia, Teguh Triyono, Umi Solekhah Intansari*
- Unusual radiological findings of pediatric jejunojejunal intussusception: A case report 35  
*Fransiska Kusumowidagdo, Dian Adi Syahputra, Vita Indriasari*
- Risk factors for failure of hydrostatic reduction in children with intussusception in Hasan Sadikin General Hospital 38  
*Dikki Drajat Kusmayadi, Laura Kurnia Agnestivita, Vita Indriasari*
- Mature Jejunal Teratoma in adolescents: A case report 42  
*N Wisnu Sutarja, Ariandi Setiawan, Fendy Matulatan*
- Coping with Coronavirus disease 2019: current state review and SWOT analysis to improve the urological services in Southeast Asia 45  
*Aria Danurdoro, Indrawarman Soerohardjo, Allen Soon Phang Sim, Raden Danarto, Dong Nguyen, Jose Benito A. Abraham, Supachai Sathidmangkang*
- Predictive accuracy of the APACHE IV scores on mortality and prolonged stay in the intensive care unit of Dr Sardjito Hospital 53  
*Yunita Widayastuti, Wildan Arsyad Zaki, Untung Widodo, Akhmad Yun Jufan, Bhirowo Yudo Pratomo*
- Cholelithiasis in children: A characteristic study 59  
*Emiliana Lia, Kharuli Amri*
- Circulating levels of Interferon-Gamma in patients with neovascular age-related macular degeneration in Yogyakarta 62  
*Supanji Supanji, Ayudha Bahana Ilham Perdamaian, Firman Setya Wardhana, Muhammad Bayu Sasongko, Mohammad Eko Prayogo, Angela Nurini Agni, Chio Oka*

## CONTENTS

Page

- 
- Network pharmacology for deciphering molecular mechanism of mahogany in dyslipidemia treatment of menopausal conditions 66  
*Afivah Dewi Anggraeni, Dhiya Ulhaq Salsabila, Bayu Anggoro, Adam Hermawan*
  - Assessment of association between PD-L1 expression and clinicopathological characteristics of Indonesian patients with high grade bladder urothelial carcinoma 78  
*Hanggoro Tri Rinonce, Theresia Hening Dwi Ambarwati, Muh Syaebani, Maria Fransiska Pudjohartono, Stella Adevida, Paranita Ferronika, Irianiwati Widodo*
  - Neutrophil-to-lymphocyte ratio, platelet-to-lymphocyte ratio, and absolute lymphocyte count as mortality predictor of patients with Coronavirus Disease 2019 84  
*Farida Anwari, Martina Kurnia Rohmah, Iif Hanifa Nurrosyidah, Acivrida Mega Charisma, Adinugraha Amarullah, Geo Firmanda A*



# Role of somatostatin receptor SSRT5-AS1 in predicting biomarkers of primary androgen deprivation therapy on prostate cancer in Indonesian population

Indrawarman Soerohardjo, MD<sup>1</sup>, Irianiwati Widodo, PhD<sup>2</sup>, Andy Zulfiquar, MD<sup>1</sup>, Didik Setyo Heriyanto, PhD<sup>2</sup>, Sumadi Lukman Anwar, PhD<sup>3</sup>

<sup>1</sup>Division of Urology, Faculty of Medicine, Public Health, and Nursing UGM, Yogyakarta, Indonesia, <sup>2</sup>Department of Anatomical Pathology, Faculty of Medicine, Public Health and Nursing, Universitas Gadjah Mada/Dr. Sardjito Hospital, Yogyakarta, Indonesia, <sup>3</sup>Division of Surgical Oncology, Department of Surgery, Faculty of Medicine, Public Health and Nursing, Universitas Gadjah Mada/Dr. Sardjito Hospital, Yogyakarta, Indonesia

## ABSTRACT

**Introduction:** Androgen deprivation therapy (ADT) has been the pivotal strategy for treating advanced prostate cancers. Despite the high efficacy of ADT in prohibiting tumor growth, >50% cases of prostate cancer will develop into an aggressive variant known as castration resistant prostate cancer (CRPC). This study aimed to evaluate the potential role SSRT5-AS1 expression as a biomarker for response to ADT in prostate cancer.

**Materials and Methods:** In total, 36 patients diagnosed with prostate cancer at Dr. Sardjito General Hospital, Yogyakarta, Indonesia were enrolled from 2015 and 2019. The expression of SSRT5-AS1 in primary tumors was quantified using quantitative real-time polymerase chain reaction.

**Results:** The mean age of patients enrolled in this study was  $69.07 \pm 8.7$  years, and the mean of prostate-specific antigen in patients was  $141.22 \pm 112.28$  ng/ml. Compared with the median, a higher expression of SSTR5-AS1 had more significant prognostic value than the variable shorter time to CRPC ( $p=0.043$ ).

**Conclusion:** This study demonstrated that high expression of SSRT5-AS1 is a promising biomarker to predict response to ADT in patients with prostate cancer.

## KEYWORDS:

ADT, prostate cancer, SSRT5-AS1, CRPC, biomarkers

## INTRODUCTION

Prostate cancer (PCa) is a tumor pathology with the highest incidence in men and is strongly influenced by the hormonal milieu, especially androgens.<sup>1</sup> The use of hormonal therapy for treating PCa dates back to 1941 when American surgeons initiated endocrine manipulation. Ever since then, androgen deprivation therapy (ADT) has become the gold standard for both locally advanced and metastatic PCas.<sup>1,2</sup> After receiving ADT, PCa progresses into a variant that no longer responds to ADT. This variant is termed castration resistant PCa (CRPC).<sup>3</sup> The time required for this variant to develop is known as the time to CRPC. This time reportedly differs among patients

with PCa, which has led to emerging issues to find biomarkers to facilitate treatment selection to PCa patients. ADT is associated with several significant side effects that can affect the quality of a patient's life. Consideration must be given for implementing ADT in patients who had benefited less from this therapy, to avoid morbidity associated with androgen deprivation.

CRPC is marked by disease progression despite continuous hormonal manipulation, such as with ADT, with a profile that may present a continuous increase in serum prostate-specific antigen (PSA), clinical and radiological progression of pre-existing disease, and appearance of new metastases. Because CRPC is typically unresponsive to ADT and patients show differing time to develop CRPC, the occurrence of this condition is considerably challenging in the clinical scenario. This is because diagnostic options with current biomarkers often lead to over-diagnosis and over treatment owing to limited specific biomarkers to guide clinical decision-making.<sup>4,6</sup> Indeed, new treatment and diagnostic modalities still need to be developed, and significant efforts are being implemented with advances being reached in basic, translational, and clinical research fields. However, diagnostic approaches are still limited, particularly in advanced disease states owing to the heterogeneity and complexity of the disease. Hence, specific biomarkers are required to help in clinical settings to identify early responses to treatment outcomes and to identify patients who are most likely to benefit from ADT.<sup>6</sup>

Notably, PCa has a marked endocrine nature with other non-sex hormones such as somatostatin, which is also related with normal prostate and PCa development. Several studies have reported the role of somatostatin receptor signaling pathway (SSRT) in different types of tumors with SSRT5 expression, which is more pre-dominant in all tissue samples, especially SSTR5-AS1.<sup>7,9</sup> However, the role of SSTR5-AS1 in PCa is still unclear. Therefore, we evaluated the prognostic significance of SSTR5-AS1 overexpression in patients with PCa and time to develop CRPC. The goal of the study was to increase the knowledge of therapy resistant PCa by incorporating novel biomarkers, which could help improve predictive and prognostic models.

Corresponding Author: Indrawarman Soerohardjo  
Email: indrawarman@ugm.ac.id

**Table I: Characteristics of patients**

Variables	Mean ( $\pm$ SD)/ count (%)
Age, years	69.07( $\pm$ 8.7)
PSA, ng/ml	141.22 ( $\pm$ 112.28)
Time to CRPC, month	25.7 ( $\pm$ 18.36)
ISUP Groups (%)	
1	5 (13.9%)
2	4 (11.1%)
3	1 (2.8%)
4	9 (25%)
5	17 (47.2%)
Surgical castration (%)	
Yes	16 (44.4%)
No	20 (55.6%)
T staging (%)	
T1a	4 (11.1%)
T1b	2 (5.6%)
T1C	9 (25%)
T2a	2 (5.6%)
T2b	10 (27.8%)
T2C	7 (19.4%)
T3C	2 (5.6%)
N staging (%)	
Nx	29 (80.6%)
N0	4 (11.1%)
N1	3 (8.4%)
M staging (%)	
M0	18 (50%)
M1B	18 (50%)
Comorbidities (%)	
Cerebrovascular	10 (27.8%)
Dyslipidemia	16 (44.4%)
ESRD	7 (19.4%)
T2DM	13 (36.1%)

ESRD=end-stage renal disease; T2DM:type 2 diabetes mellitus

**Table II: Predictive value time to CRPC**

Variable	Time to CRPC	p value
High expression of SSTR5-AS1	19.40 $\pm$ 5.9.55	0.043
Low expression of SSTR5-AS1	30.96 + 3.18	
Surgical castration	32.12 + 3.9	0.132
Medical castration	22.63 + 4.17	
High volume diseases	26.75 + 3.48	0.728
Low volume diseases	28.67 + 4.7	
PSA > 20 ng/ml	24.85 + 3.13	0.072
PSA < 20 ng/ml	37.88 + 6.25	

p values were calculated using Tarone-ware test

## MATERIALS AND METHODS

### Patients

In total, 36 patients who were diagnosed with PCa from RSUP Dr. Sardjito General Hospital(SGH), Yogyakarta, Indonesia between 2015 and 2019 were enrolled. Patients who received hormonal therapy as the primary treatment were enrolled. All clinical and demographic data were gathered from electronic medical records of SGH. Patients who received local therapy were excluded. This study received approval from the Medical and Health Research Ethics Committee, Universitas Gadjah Mada (KE/0158/02/2020).

The primary endpoint of this study was response to hormonal therapy, described as time to achieve CRPC. CRPC was defined as secondary radiographic or clinical progress of metastases during hormonal therapy or/and increase of PSA values during hormonal therapy after achieving nadir values with a testosterone level of <50 ng/ml. Clinical staging was

determined by unified tumor, node, and metastases criteria according to the EAU 2021 guidelines<sup>5</sup> and using the digital rectal examination, magnetic resonance imaging, computed tomography with contrast, or bone survey.

The pathological results on this study were categorized according to the 2005 International Society of Urological Pathology (ISUP) score that is currently being used as a risk stratification parameter in the 2021 EAU guidelines of prostate cancer.<sup>5</sup>

### Quantitative Real-Time Polymerase Chain Reaction (qRT-PCR)

Methods previously described by Indrawarman et al. were used.<sup>10</sup> In addition, this study was conducted in compliance Helsinki Declaration, and the study was registered with International Standard Randomized Controlled trial register (ISRCTN) under the reference no 24834343.<sup>11</sup>



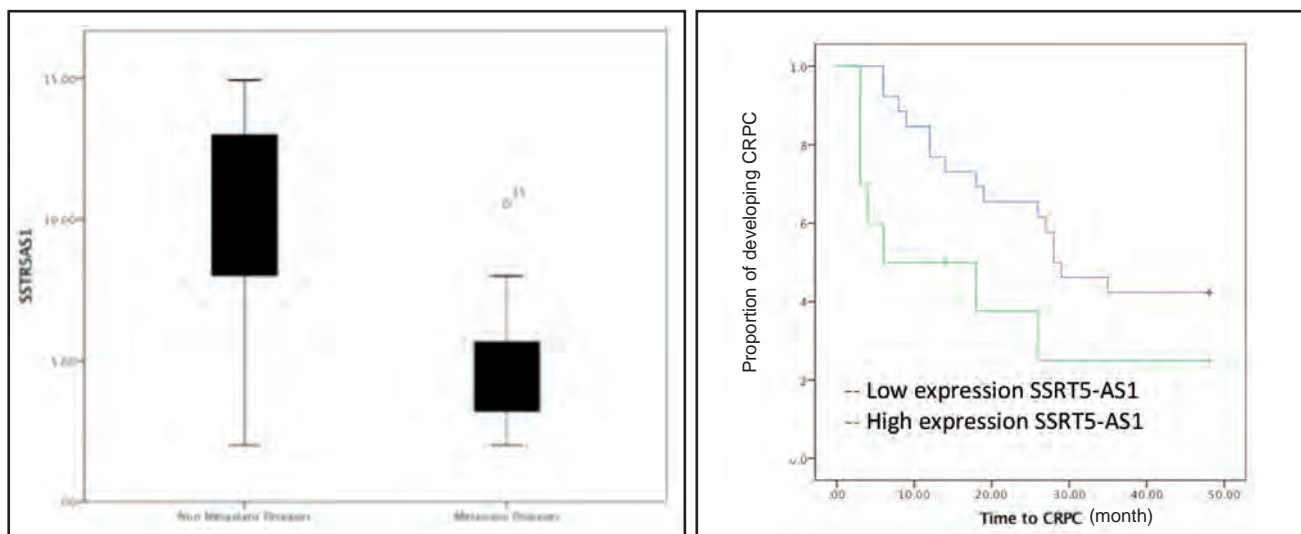


**Fig. 1:** The expression of SSRT5-AS1 in patients with prostate cancer with no metastases and bone metastases at diagnoses ( $p < 0.001$ ) (left) and Kaplan-Meier estimates of time to CRPC in patients with prostatic cancer who received ADT for expressions of SSRT5-AS1 (right).

RNAs were extracted from formalin-fixed and paraffin-embedded biopsied samples of PCa tissues and two additional samples of benign prostatic hyperplasia (normal references). Hybrid-R™ Isolation Kit (GeneAll, Seoul-South Korea) was used to extract total RNAs, and NEXpro™ qRT-PCR Kit (NextPro, Seoul-South Korea) was used to assess SSRT5-AS1 expression. The primer pair sequences used for the quantification were as follows: 5'-ACTACAGGTGCCATCAGACC-3' (forward) and 5'-GGTGTGCTGAAAAGGGTCC (reverse). Amplification conditions comprised an initial denaturation step at 95°C for 10 min, followed by 40 cycles at 95°C for 20 s, at 55°C for 40 s, and at 72°C for 60 s. The extension step was conducted at 72°C for 5 min. Amplification of samples using q-PCR was performed using BiONEERExicycle™ 96 (BioNEER, Daejeon, South Korea). RB1 and TP53 expression was determined by the cycle threshold values and was normalized using GADPH, as previously described.

## RESULTS

The mean age of patients was  $69.07 \pm 8.7$  years, and the mean PSA was  $141.22 \pm 112.28$  ng/ml. Most patient who was enrolled were classified to have high risk, with 47.2% patients being in ISUP 5 group and 25% being in ISUP 4 group. In this study, patients were castrated using LHRH agonist approximately 55.6% of enrolled patients, and 44.4% patient were surgical castrated.

To further examine the association of SSRT5-AS1 with tumor spread, we evaluated SSRT5-AS1 expression in both patients with non-metastatic disease and patients with metastatic diseases.

At diagnosis, the expression SSRT5-AS1 in the metastatic disease group was significantly lower than that in the non-metastatic disease group ( $p < 0.001$ ).

However, the metastatic status in this study showed similar time to CRPC after receiving castration (Tarone-ware  $p = 0.728$ ). The expression of SSRT5-AS1 was also similar between patients with PSA value at diagnosis  $> 20$  ng/ml and those with PSA value  $< 20$  ng/ml. However, time to CRPC in patients with PSA  $> 20$  ng/ml reached faster than in other groups. However, results showed no statistically significant correlation in PSA level and SSRT5-AS1 expression.

In addition, compared with median, higher expressions of SSRT5-AS1 had more significant prognostic value than shorter time to CRPC (Figure 1) (mean:  $19.40 \pm 5.95$ ,  $p = 0.043$ ) compared to patient with lower expression of SSRT5-AS1 (Figure 1). Meanwhile, the method of castration, diseases volume according CHARTED study, and PSA value  $> 20$  were not statistically significant predictors of time to develop CRPC in this pilot study (Table II).

## DISCUSSION

Somatostatin receptors (SSTRs) are commonly expressed on neuroendocrine tumors (NETs), and their expression has been correlated with disease prognosis in various types of cancer.<sup>11-13</sup> To function biologically and activate its signaling pathway, somatostatin needs to bind with five somatostatin receptor family gene products (SSTR1 to SSTR5).<sup>11-12</sup> The development of NET and SSTRs over expression by CRPC has been associated with negative or worse prognosis.<sup>14-16</sup> However, the context of NET in PCa is still debatable owing to the mechanism by which it develops and the clinical significance. However, some studies have reported the presence of neuroendocrine cells in PCa.<sup>17-18</sup>

The methods of castration did not show statistical significance. This finding was consistent with that reported by a previous study.<sup>5-6,19</sup> In addition, this study also revealed that metastatic volume by charted study and the initial PSA value did not show statistical significance. This result may be attributed to small sample power.

However, patients with high SSTR5-AS1 expression had shorter time to CRPC after receiving ADT as single therapy. Thus, this indicated that these patients benefit less from single ADT. Our study is the first to evaluate SSTR5-AS1 in a clinical setting for predicting the time CRPC in Asian population. Previously, Ramnarine et al. reported that patients with high expression who underwent prostatectomy plus adjuvant ADT had worse metastasis-free survival than those with low expression of SSTR5-AS1. However, for patient who did not receive ADT as adjuvant therapy had similar metastasis-free survival.<sup>20</sup>

Remarkably, the overexpression of SSTR5 has been indicated as a potential oncogenic factor, presenting as either aggressiveness or high proliferation rate in adenocarcinomas of the lung, squamous cell carcinomas of the lung, and small lung cancer.<sup>21</sup> Mass et al. reported a decrease in SSTR1-4 expression and overexpression of SSTR5, which possibly resulted from the evolution of tumor cells to elude cell cycle control by somatostatin, which can subsequently act as a growth advantage. However, the knowledge about the role of SSTR5 in PCa is still very limited and its therapeutic potential remains unknown.<sup>20-21</sup>

## CONCLUSION

To investigate the prognostic value of SSTR5, we measured the expression of SSTR5-AS1 in patients with PCa treated with ADT. Our results showed no apparent correlation between the expression of SSTR5-AS1 with disease metastasis and PSA score. However, our results illustrated a correlation between the expression of SSTR5-AS1 and time to CRPC, which indicated that the expression of SSTR5-AS1 could be considered as a biomarker to predict response to therapy in PCa.

Currently, there is no standard for the cut-off of overexpression of SSTR5-AS1 that can be used as a biomarker for disease progression. Future studies with larger populations are needed to validate and conform our findings. Additionally, further population studies should consider ethnicity in sample characteristics to determine if this biomarker is limited to the Javanese population.

## REFERENCES

- Rajput R and Sehgal A. Endocrine manipulations in cancer prostate: A review. *Indian JEndocrinolMetab* 2012; 16(Suppl 2): S199-204.
- Rebello RJ, Oing C, Knudsen KE, Loeb S, Johnson DC, Reiter RE, et al. Prostate cancer. *Nat Rev Dis Primers* 2021; 7(1): 9.
- Sountoulides P, Rountos T. Adverse effects of androgen deprivation therapy for prostate cancer: Prevention and management. *Int schRes Notices* 2013; 2013: 8.
- Savelli G, Muni A, Falchi R, Zaniboni A, Barbieri R, Valmadre G, et al. Somatostatin receptors over-expression in castration resistant prostate cancer detected by PET/CT: Preliminary report of in six patients. *Ann Transl Med* 2015; 3(10): 145.
- Madu CO and Lu Y. Novel diagnostic biomarkers for prostate cancer. *J Cancer* 2010; 1: 150-77.
- Atkinson AJ, Colburn WA, DeGruttola VG, DeMets DL, Downing GJ, Hoth DF, et al. Biomarkers and surrogate endpoints: Preferred definitions and conceptual framework. *Biomarkers Definitions Working Group. Clin Pharm Therap* 2001; 69: 89-95.
- Mottet N, van den Bergh RCN, Briers E, Van den Broeck T, Cumberbatch MG, De Santis M, et al. EAU-EANM-ESTRO-ESUR-SIOG guidelines on prostate cancer-2020 update. Part 1: Screening, diagnosis, and local treatment with curative intent. *EurUrol* 2021; 79(2): 243-62.
- Tian S, Lei Z, Gong Z, Sun Z, Xu D, Piao M. Clinical implication of prognostic and predictive biomarkers for castration-resistant prostate cancer: A systematic review. *Cancer Cell Int* 2020; 20: 409.
- Karavitakis M, Msaouel P, Michalopoulos V, and Koutsilieris M. Pattern of somatostatin receptors expression in normal and bladder cancer tissue samples. *Anticancer Res* 2014; 34(6): 2937.
- Morichetti D, Mazzucchelli R, Stramazotti D, Lopez-Beltran A, et al. Immunohistochemical expression of somatostatin receptor subtypes in prostate tissue from cystoprostatectomies with incidental prostate cancer. *BJU Int* 2010; 106(7): 1072.
- Hansson J, Bjartell A, Gadaleanu V, Dizzei N, and Abrahamsson PA. Expression of somatostatin receptor subtypes 2 and 4 in human benign prostatic hyperplasia and prostatic cancer. *Prostate* 2002; 53(1): 50.
- Soerohardjo I, Widodo I, Heriyanto DS, Zulfiqqar A, Anwar, Sumadi L. Down-regulation of RB1 and TP53 as potential predicting biomarkers for castration-resistant prostate cancer (CRPC): Indonesian retrospective cohort study. *Ann Med Surg* 2020; 60: 549.
- Soerohardjo I, Zulfiqqar A. Assessing demographic, clinical and pathological determinants of advanced prostate cancer in Indonesia for delayed diagnosis, treatment, and risk for secondary progression and survival [cited Dec 2021]. Available from: <http://www.isrctn.com/ISRCTN24834343>.
- Qian ZR, Li T, Ter-Minassian, M, ang J, Chan JA, Brais LK, et al. Association between somatostatin receptor expression and clinical outcomes in neuroendocrine tumors. *Pancreas* 2016; 45(10): 1386.
- Maas M, Mayer L, Hennenlotter J, Stühler V, Walz S, Scharpf M, et al. Prognostic impact of somatostatin receptor expression in advanced bladder cancer. *Urol Oncol* 2020; 38(12): 935.e17.
- Ruscica M, Magni P, Steffani L, Gatto F, Albertelli M, Rametta R, et al. Characterization and sub-cellular localization of SS1R, SS2R, and SS5R in human late-stage prostate cancer cells: Effect of mono- and bi-specific somatostatin analogs on cell growth. *Mol Cell Endocrinol* 2014; 382(2): 860.
- Usmani S, Orevi M, Stefanelli A, Alberto Z, Ofer NG, Claudio B, bNeuroendocrine Differentiation in castration resistant prostate cancer. *Nuclear Medicine radiopharmaceuticals and imaging techniques: A narrative review. Crit Rev Oncol/Hematol* 2019; 138: 29.
- Berruti A, Dogliotti L, Mosca A, Tarabuzzi R, Torta M, Mauro M, et al. Effects of the somatostatin analog lanreotide on the circulating levels of chromogranin-A, prostate-specific antigen, and insulin-like growth factor-1 in advanced prostate cancer patients. *Prostate* 2001; 47(3): 205.
- Spieth ME, Lin YG, Nguyen TT. Diagnosing and treating small-cell carcinomas of prostatic origin. *Clin Nucl Med* 2002; 27(1): 11.
- Savelli G, Muni A, Falchi R, Zaniboni B, Valmadre G, Minari C, et al. Somatostatin receptors over-expression in castration resistant prostate cancer detected by PET/CT: Preliminary report of in six patients. *Ann Transl Med* 2015; 3(10): 145.
- Klotz L, O'Callaghan C, Ding K, Toren P, Dearnaley D, Higano CS, et al. Nadir testosterone within first year of androgen-deprivation therapy (ADT) predicts for time to castration-resistant progression: A secondary analysis of the PR-7 trial of intermittent versus continuous ADT. *J Clin Oncol* 2015; 33(10): 1151.
- Ramnarine VR, Alshalalfa M, Mo F, Nabavi N, Erho N, Takhar M, et al. The long noncoding RNA landscape of neuroendocrine prostate cancer and its clinical implications. *GigaScience* 2018; 7(6): gij050.
- Maas M, Mayer L, Hennenlotter J, Stühler V, Walz S, Scharpf M, et al. Prognostic impact of somatostatin receptor expression in advanced bladder cancer. *Urol Oncol* 2020; 38(12): 935.e17.

# Social determinants of health protocol adherence among adults during COVID-19 pandemic in Yogyakarta, Indonesia

Supriyati Supriyati, Dr<sup>1,2</sup>, Fahmi Baiquni, MPH<sup>2</sup>, Tri Siswati, Dr<sup>3</sup>, HERNI Endah Widyawati, S.Tr.Gz<sup>3</sup>, Riadini Rahmawati, STP<sup>2</sup>, Ratri Kusuma Wardani, S.Gz<sup>4</sup>

<sup>1</sup>Department of Health Behavior, Environment, and Social Medicine, Faculty of Medicine, Public Health and Nursing, Universitas Gadjah Mada, Yogyakarta, Indonesia, <sup>2</sup>Center of Health Behavior and Promotion, Faculty of Medicine, Public Health and Nursing, Universitas Gadjah Mada, Yogyakarta, Indonesia, <sup>3</sup>Health Polytechnic of the Yogyakarta Ministry of Health, Yogyakarta, Indonesia, <sup>4</sup>Sleman Health and Demographic Surveillance System (Sleman HDSS) Faculty of Medicine, Public Health and Nursing, Universitas Gadjah Mada, Yogyakarta, Indonesia

## ABSTRACT

**Introduction:** Coronavirus disease (COVID-19) must be controlled by involving all stakeholders, including the community. Community protocol compliance with COVID-19 health guidelines is essential. This study assessed the social determinants of health on community protocol compliance with COVID-19 health guidelines among adults in Yogyakarta, Indonesia.

**Materials and Methods:** This study was a mixed-method study of 461 adults from February through May 2021 in Yogyakarta Province. We collected data through an online survey, focus group discussions, and in-depth interviews. Logistic regression was used to analyze the results.

**Results:** Most respondents (86%) always wore masks, followed social distancing (51.8%), and washed their hands regularly (99%). Subjects older than 45 years, women, and community leaders demonstrated greater compliance with COVID-19 health protocols compared to other people. On the other hand, the occupation has become a healthy lifestyle practice indicator.

**Conclusion:** Gender, age, educational level, economics, and social status were determinants of health protocol adherence among adults in Yogyakarta. Therefore, health providers need to consider social determinants for health promotion approaches and COVID-19 prevention and control strategies.

## KEYWORDS:

*guidelines adherence; health promotion; protocol compliance; social determinant of health*

## INTRODUCTION

Following the discovery of two cases in Indonesia on March 02, 2020, coronavirus disease 2019 (COVID-19) has been spreading rapidly. The World Health Organization (WHO) data on July 7, 2021, showed a total of 2,379,397 confirmed cases in Indonesia, with 62,908 deaths.<sup>1</sup> The official Indonesian government website (covid19.go.id) listed the highest number of cases in Java Island, concentrating on the Special Capital Region of Jakarta/*Daerah Khusus Ibukota* (DKI) Jakarta, followed by West Java, Central Java, and East Java.<sup>1</sup>

Since the beginning, the Indonesian government has implemented several strategies and policies to combat the pandemic. The strategy is to form a task force to promote social restrictions and handle testing, tracing, as well as treatment campaigns to prevent the spread of the disease.<sup>2</sup> Indonesia also started vaccinations in January 2021. As of July 7, 2021, 14 million people received complete vaccinations.<sup>3</sup> That number covered 7% of the national target.<sup>1,4</sup> This effort was still not optimal in preventing the spread of COVID-19.<sup>5</sup>

Preventive measures, such as the COVID-19 health protocols aimed at prevention of direct contact with infected or possibly infected persons, wearing masks, avoiding mass gatherings, regular washing hands, avoiding touching face, as well as disinfecting surfaces.<sup>6</sup> Denford et al.<sup>7</sup> claimed that community levels of adherence vary depending on their perceptions regarding their potential exposure to the virus, the benefits or requirements to adopt the measures, and their faith in the effectiveness of the measures. Studies have also found that sociodemographic factors, such as gender, educational level, occupational types, and age were associated with adults' adherence to COVID-19 health protocols.<sup>8,9</sup>

Studies regarding community adherence to COVID-19 prevention measures in Indonesia are scarce. A study in Central Java showed that community adherence in Indonesia varied based on protocols used. The results showed that 31% of respondents abided by stay-at-home protocols. The protocol adopted by most respondents was handwashing with soap (88.2%).<sup>10</sup> A study in Bali showed that community adherence to health protocols was associated with perceived social norms, perceived benefits, and gender.<sup>11</sup> These studies showed how social determinants become factors that contribute to health protocol adherence in Indonesia.

The WHO defines social determinants as "non-medical factors that influence health outcomes." Socioeconomic and political context may indirectly affect health outcomes through changes in individual health behaviours, material circumstances and psychosocial factors.<sup>12</sup> Therefore, contextual factors are important in explaining health outcomes and behaviours, including the adherence to health protocols in preventing the spread of COVID-19.

Corresponding Author: Supriyati Supriyati  
Email: supriyati@ugm.ac.id

By July 2021, the Special Region of Yogyakarta was among the top ten provinces with a high prevalence of COVID-19 sectors in Indonesia. Approximately 2.9% of COVID-19 cases in Indonesia had occurred in that province.<sup>1</sup> Yogyakarta Province is also one of the primary tourist destinations in Indonesia. The pandemic has severely impacted the socio-economic conditions there. Exploration of community adherence to health protocols in the province, especially regarding socially determinant factors, can help local governments improving the adherence and prevent the spread of COVID-19 in the community. The outcome may also provide insights into the essential social determinants affecting protocol adherence in vital tourism industries. Therefore, this study aimed to assessing the social determinants of adherence to health protocols among adults in the Special Region of Yogyakarta, Indonesia.

## MATERIALS AND METHODS

A mixed-method study with an explanatory sequential design<sup>13</sup> was conducted in Yogyakarta Special Province, Indonesia, in the first half of 2021. The population enrolled were adults aged 18 to 59 years old, from Sleman, Kulon Progo, Gunung Kidul, Bantul, and Yogyakarta City. This paper is the second publication of research entitled Policy Analysis of the Social Action of the Healthy Lifestyle, or *Gerakan Masyarakat Hidup Sehat* (GERMAS).

A cohort of 461 people volunteered for the study. We collected data via an online survey using Google Form, focus group discussions, and in-depth interviews. The online survey was conducted during February–May 2021, with 499 people completed the survey. Unfortunately, 50 people did not match the inclusive criteria. They may not have lived in from Yogyakarta Special Province, or they were less than 18 or over 60 years old. Thus, 50 respondents were excluded, and we included 449 respondents for further analysis. The minimum sample needed was 385 respondents.

We developed the questionnaire with content validation. We delivered the online questionnaire through Instagram and WhatsApp messaging applications. The questionnaire covered the five points of health protocols to prevent COVID-19, including physical distancing, hand washing, mask-wearing, mobility restriction, and crowd avoidance; and the sociodemographic variables include gender, age, education level, economic status, occupational, and social status. The questions were favourable and unfavourable.

We categorised the educational level into low (elementary and junior high school), middle (senior high school), and high (diploma and higher education). Low economic status defined as monthly income below three million rupiahs (approximately \$208 USD); middle economic status when their income ranging between three to six million rupiahs, and high economic status for those with monthly income above six million rupiahs (approximately \$416 USD) monthly income. While for occupational type, we categorize them into four groups, namely: students (including diploma/higher education students), formal workers (employers, teachers, lecturers, police, and military officers), non-formal workers (traders, entrepreneurs, labourers, farmers, and fishers), as well as not working (stay-at-home

parent, retired, and not working). This study conducted logistic regression for the quantitative data ( $p < 0.05$ ).

In addition, the focus group discussion and in-depth interview guidelines were developed according to the survey results. We conducted focus group discussions to elaborate and confirm the quantitative data. The qualitative informants were among stakeholders from various sectors, including provincial and districts officers, such as health officers, the provincial planning board of Yogyakarta, community leaders, as well as the Indonesian Society for Health Promotion and Education of Yogyakarta. The ethical committee of the Faculty of Medicine, Public Health, and Nursing, Universitas Gadjah Mada, approved this research protocol (KE/FK/0310/EC/2021). Informed consent were obtained from all the participants.

## RESULTS

Most respondents were women (79.7%) and over 45 years old (39.9%). Only 29.4% of respondents were community leaders, as noted in Table I. Table I shows that most respondents had high levels of education (63.7%), low economic status (58.8%).

Most respondents complied with health protocols. Mask use (86.6%) and hand washing (94.6%) were the health protocols with the highest level of compliance in Yogyakarta. One-third of the respondents removed their masks while talking and some did not wear their masks properly (Table II).

Table II shows maintaining physical distancing, staying at home, and avoiding crowds had the lowest scores for health protocol adherence among adults in Yogyakarta.

The qualitative data showed that many community stakeholders promoted the health protocols. In this pandemic, all the stakeholders (government and private sectors) were actively involved in health protocol promotional activities.

“...Most stakeholders were involved in the health protocol campaign...They were not limited to the health officer only...” (In-depth interview, health promotion officer)

There were many sectors participate in the health matters during COVID-19 pandemic. The health promotion division of the provincial health office had empowered the existing network for health protocols and the healthy lifestyle campaign. There were massive social media campaign through the WhatsApp group of the local leader, Instagram, and YouTube. In addition, the provincial and district level Yogyakarta government issued many regulations related to the health protocols for COVID-19 prevention and control.

This study illustrates a significant correlation between sociodemographic variables, e.g., sex, age, education level, occupation, and social status, with health protocols that covered physical distancing, mask wearing, restricted mobility, as well as avoiding crowds ( $p < 0.05$ ). In contrast, there was no significant correlation between socio-demographics and handwashing behaviour. In this study,



**Table I: Demographic Characteristics of the respondents**

Respondent characteristics (n = 449)	f	%
Gender		
Men	91	20.27
Women	358	79.73
Age		
18–35 years old	138	30.7
36–45 years old	132	29.4
>45 years old	179	39.9
Education level		
Low	21	4.7
Middle	142	31.6
High	286	63.7
Economic status		
Low	264	58.8
Middle	157	35.0
High	28	6.2
Occupation		
Unemployed	151	33.6
Formal worker	239	53.2
Informal worker	37	8.2
Student	22	4.9
Social status		
Citizen	317	70.6
Community leader	132	29.4

**Table II: Health protocol adherence**

Variable	Respondent	%
Wearing a mask		
Wears mask	389	86.64
Wears two-layer fabric mask or medical mask	435	94.65
Wears their mask while talking	300	66.82
The mask covers mouth and nose	367	81.74
Handwashing	448	99.78
Physical distancing	248	55.23
Stays at home	284	63.25
Avoids social gathering	287	63.92

almost all respondents (99.78%) had good hand washing practices.

Table III shows that sex, age, education level, occupation, as well as social status were the social determinants of health protocol compliance among adults in Yogyakarta. Education levels and age were the most substantial social determinants of health protocol compliance in Yogyakarta. Respondents who were over 45 years old had the highest compliance level toward health protocols.

Social status, represent by the community leader, contributed to the health protocol compliance. Respondents who were community leaders have high levels of compliance toward health protocol. Community leaders are public figures. Hence, the pleasant habit and practices of the community leaders will lead to good habits among people. We excluded the handwashing variable from Table III because of the correlation analysis result. There was no significant correlation between sociodemographic and handwashing behaviours.

## DISCUSSION

This study showed that the Yogyakarta community had high compliance with health protocol. Also, there were social determinant of the health protocol compliance, such as education level, age, social status, sex, as well as social status. The socio ecological model suggests assessing social determinants to investigate the health status and health behaviour.<sup>14</sup> Moreover, many factors, including social determinants of health, contribute to the health status and health behaviours.<sup>15</sup> In line with the previous study, this result proved that age and gender were the social determinants of the community adherence toward health protocol among adult in Yogyakarta.<sup>8,9</sup> Moreover, the level of community compliance toward health protocol was varied.<sup>7</sup> Even though most people had high levels of compliance, one-third of respondents did not obey the social restrictions. Many stakeholders supported the health protocols campaign in Yogyakarta, both from government and private sectors. Indeed, they were provided infrastructure to support the health protocol practices. The participation of various stakeholders in the public health intervention will lead to the program's sustainability.<sup>16</sup>

**Table III: Logistic regression of the association between sociodemographic factors, including mask use, physical distancing, restricted mobility, and avoiding crowds**

	Physical distancing			Avoiding crowds			Restricted Mobility			Use a mask properly		
	OR	p-Value	95% CI	OR	p-Value	95% CI	OR	p-Value	95% CI	OR	p-Value	95% CI
Sex (vs male)												
Female	1.67	0.03	1.05 - 2.66	1.61	0.05	1.00 - 2.56	1.64	0.04	1.03 - 2.61			
Age (vs 18-35 years old)												
36-45 years old	1.42	0.15	0.88 - 2.30	1.38	0.20	0.85 - 2.24	1.11	0.67	0.68 - 1.80			
>45 years old	3.03	0.00	1.91 - 4.81	2.23	0.00	1.39 - 3.56	2.10	0.01	1.31 - 3.36			
Education (vs low)												
Middle												
High												
Occupation (vs unemployed)												
Formal worker	0.41	0.00	0.27 - 0.63	0.49	0.00	0.32 - 0.77	0.66	0.06	0.43 - 1.02			
Non-formal worker	0.86	0.70	0.40 - 1.83	0.73	0.42	0.33 - 1.58	0.91	0.82	0.42 - 1.97			
Students	0.32	0.02	0.13 - 0.81	0.29	0.01	0.12 - 0.72	0.37	0.03	0.15 - 0.91			
Social status (vs Citizen)												
Community leader	1.71	0.01	1.12 - 2.60							3.39	0.04	1.06 - 10.86
										2.3	0.12	0.80 - 6.73



COVID-19 has influenced all aspects of life, just as many factors have determined community compliance with health protocols. Therefore, public health intervention is considered a social determinant of health.<sup>17,18</sup> Public health intervention and need assessment are essential.<sup>19</sup>

## CONCLUSION

This study concludes that education level, age, and social status were the social determinant of health protocol compliance. Government should adjust strategies to improve health protocol compliance according to target characteristics, such as education level, age, and social status.

## ACKNOWLEDGMENT

We express our gratitude to the Mental and Spiritual Development Bureau of the Yogyakarta Special Province local government that supported this study.

## CONFLICT OF INTEREST

We declare that there is no conflict of interest in this study.

## REFERENCES

1. Satuan Tugas Penanganan COVID-19. Peta Sebaran 2020. [cited July 2021]. Available from: <https://covid19.go.id/peta-sebaran>
2. Djalante R, Lassa J, Setiamarga D, Sudjatma A, Indrawan M, Haryanto B, et al. Review and analysis of current responses to COVID-19 in Indonesia: Period of January to March 2020. *Prog Disaster Sci* 2020 ; 6: 100091.
3. World Health Organization Indonesia. Coronavirus Disease Situation Report World Health Organization. *World Heal Organ [Internet]*. 2020;33(November):1–20. [cited July 2021]. Available from: [https://www.who.int/docs/default-source/searo/indonesia/covid19/external-situation-report-33-11-november-2020.pdf?sfvrsn=f338094a\\_2](https://www.who.int/docs/default-source/searo/indonesia/covid19/external-situation-report-33-11-november-2020.pdf?sfvrsn=f338094a_2)
4. Direktorat Jenderal Pencegahan dan Pengendalian Penyakit Kementerian Kesehatan Republik Indonesia. Surat Edaran Nomor HK.02.02/1/368/2021, tanggal 11 Februari 2021, tentang Pelaksanaan Vaksinasi COVID-19 pada Kelompok Sasaran Lansia, Komorbid dan Penyintas COVID-19, serta Sasaran Tunda [Internet]. Vol. 4247608, Kementerian Kesehatan RI. Jakarta: Direktorat Jenderal Pencegahan dan Pengendalian Penyakit Kementerian Kesehatan Republik Indonesia; 2021. p. 613–4. [cited July 2021]. Available from: [https://ppid.temanggungkab.go.id/assets/file\\_master/Surat\\_Edaran\\_Pelaksanaan\\_Vaksinasi\\_COVID-19\\_pada\\_Kelompok\\_Sasaran\\_Lansia\\_cap.pdf](https://ppid.temanggungkab.go.id/assets/file_master/Surat_Edaran_Pelaksanaan_Vaksinasi_COVID-19_pada_Kelompok_Sasaran_Lansia_cap.pdf)
5. Olivia S, Gibson J, Nasrudin R. Indonesia in the Time of Covid-19. *Bull Indones Econ Stud* 2020; 56(2): 143–74.
6. Lotfi M, Hamblin MR, Rezaei N. COVID-19: Transmission, prevention, and potential therapeutic opportunities. *Clin Chim Acta* 2020; 508: 254–66.
7. Denford S, Morton KS, Lambert H, Zhang J, Smith LE, Rubin GJ, et al. Understanding patterns of adherence to COVID-19 mitigation measures: a qualitative interview study. *J Public Health (Bangkok)* 2021; 43(3): 508–16.
8. Carlucci L, D'Ambrosio I, Balsamo M. Demographic and Attitudinal Factors of Adherence to Quarantine Guidelines During COVID-19: The Italian Model. *Front Psychol* 2020; 11: 1–13.
9. Hills S, Eraso Y. Factors associated with non-adherence to social distancing rules during the COVID-19 pandemic: a logistic regression analysis. *BMC Public Health* 2021; 21(1): 352.
10. Disemadi HS, Handika DO. Community compliance with the covid-19 protocol hygiene policy in Klaten Regency, Indonesia. *Leg J Ilm Huk* 2020; 28(2): 121–33.
11. Indrayathi PA, Januraga PP, Pradnyani PE, Gesesew HA, Ward PR. Perceived Social Norms as Determinants of Adherence to Public Health Measures Related to COVID-19 in Bali, Indonesia. *Front Public Heal* 2021; 9.
12. Solar O, Irwin A. A conceptual framework for action on the social determinants of health 2010; 79.
13. Creswell JW, Clark VLP. Designing and conducting mixed methods research. Third Edit. Los Angeles: SAGE Publications Ltd.; 2018. 520 p.
14. Lee D, Paul C, Pilkington W, Mulrooney T, Diggs SN, Kumar D. Examining the effects of social determinants of health on COVID-19 related stress, family's stress and discord, and personal diagnosis of COVID-19. *J Affect Disord Reports* 2021; 5: 100183.
15. Kawachi I, Berkman LF. Social Capital, Social Cohesion, and Health. In: *Social Epidemiology* [Internet]. Oxford, UK: Oxford University Press; 2014. p. 290–319.
16. Akwanalo C, Njuguna B, Mercer T, Pastakia SD, Mwangi A, Dick J, et al. Strategies for Effective Stakeholder Engagement in Strengthening Referral Networks for Management of Hypertension Across Health Systems in Kenya. *Glob Heart* 2019; 14(2): 173.
17. Nussbaumer-Streit B, Mayr V, Dobrescu AI, Chapman A, Persad E, Klerings I, et al. Quarantine alone or in combination with other public health measures to control COVID-19: a rapid review. *Cochrane Database Syst Rev* 2020. 8; (4): 1–44.
18. Supriyati S, Silvano F, Mandariska RP, Saragih DP, Gunawan C, Wuragil AI, et al. Barrier to health protocol adherence during exercise among youth in the COVID-19 pandemic era. *J Community Empower Heal* 2021; 4(1): 8-15.
19. Supriyati S, Angraeny DK, Carissa TM, Sheila AP, Qisthi SA, Rianti M, et al. Preparing new normal: the health literacy assessment on the Covid-19. *Ber Kedokt Masy* 2021; 37(1): 27.

# Improvement of quality in clinical care for patients with benign prostatic hyperplasia: Cost effectiveness analysis

Johannes Cansius Prihadi, PhD<sup>1,2</sup>, Firdaus Hafidz, PhD<sup>3</sup>, Hanevi Djasri, PhD<sup>3</sup>

<sup>1</sup>Department of Surgery, Sub Urology, School of Medicine and Health Sciences Atma Jaya Catholic University of Indonesia, Indonesia, <sup>2</sup>Department of Urology, St Carolus Hospital, Indonesia, <sup>3</sup>Department of Health Policy and Management, Faculty of Medicine, Public Health, Nursing, University of Gajah Mada, Indonesia, Yogyakarta, Indonesia

## ABSTRACT

**Introduction:** Currently, St. Carolus Hospital (SCH), Jakarta, Indonesia is using a combination therapy for patients with benign prostatic hyperplasia (BPH) based on the clinical practice guidelines (CPG). In this study, we used two methods of administering combination therapy, namely, the standard method and the modified method. To date, no research has been conducted to reduce the cost burden of BPH medication without reducing the quality of service. Thus, this study aimed to compare the clinical outcomes and quality of life (QoL) of the modified therapeutic method with those of the standard therapeutic method and perform cost-effective analysis of the two therapeutic methods available at SCH.

**Materials and Methods:** The study design used was a retrospective cohort. Data were obtained from medical records at SCH and interviews. Decision tree analysis was used for this study based on clinical outcomes and costs. Clinical outcomes and costs were compared between the standard and modified therapy models. Interviews were conducted to obtain cost data from a societal perspective. Then, the data were analyzed using SPSS statistics program and MS Excel.

**Results:** A total of 100 BPH patients met the inclusion criteria. The mean age in the standard therapy and modified therapeutic method groups was 66.92 (SD±6.67) and 67.10 (SD 8.49) years, respectively. At the start of therapy, the mean international prostate symptom score (IPSS) in the standard method group was lower than that in the modified group (15 vs 17), but the mean Qmax in both groups was the same (9 ml/s). In addition, the mean QoL score in both groups was 4 (not satisfied). At the end of therapy, there was an improvement in the IPSS, Qmax and QoL was observed in both groups. In the Mann Whitney statistical test, there was no significant difference in IPSS and QoL was found between the standard therapeutic method group and the modified therapeutic method group ( $P = 0.07$  and  $P = 0.498$ ). In the unpaired T test, there was a significant difference in Qmax was found between the standard method group and the modified method group ( $p = 0.039$ , 95%CI, -3.20529 to -0.8769). The effectiveness of standard therapeutic methods and modified therapy methods is 82% and 90%, respectively. The average cost of standard therapeutic methods is greater than that of modified therapeutic methods per visit. Furthermore, the average cost-effectiveness ratio of the

modified therapeutic method is lower than that of the standard therapeutic method.

**Conclusion:** The Modified therapeutic method has better results regarding the maximum urinary flow rate compared with the standard therapeutic method. The modified therapeutic method is also more cost-effective than the standard therapeutic method. This study can be used as the basis for service standards in hospitals and national health technology assessments as a policy direction for the national health insurance benefit package.

## KEYWORDS:

*Benign prostate hyperplasia, combine therapy, cost, cost-effective analysis*

## INTRODUCTION

The prevalence rate of lower urinary tract symptoms (LUTS) worldwide varies widely, and it is significantly increasing with age. The number of patients with LUTS worldwide is approximately 2.3 billion people or 45.8% of the world population in 2018, which shows an 18.4% since 2008.<sup>1</sup> The incidence of benign prostatic hyperplasia (BPH) in Indonesia remains unknown, but based on the data obtained from Cipto Mangunkusumo Hospital (RSCM) from 1994 until 2013; a total 3,804 cases of BPH with a mean age of the patients 66.61 years have been reported. In addition, Hasan Sadikin Hospital reported 718 cases of BPH, from 2012 to 2016, with a mean age of patients 67.9 years old.<sup>2</sup>

The treatment of choice is a major factor contributing to the cost of treatment from medical therapy (a combination of alpha blockers and 5-alpha reductase inhibitor (5-ARI)) to invasive action, such as transurethral resection of prostate.

The combination of alpha blocker and 5-ARI has been proven to be more effective than monotherapy based on studies from several countries.<sup>3,4</sup>

The high prevalence rate of BPH can cause a huge economic burden and medical costs to the authorities. The cost of BPH treatment in the UK is estimated around £ 180 million annually, of which 60% are due to complications from BPH. Long-term treatment will also increase costs, thereby causing a heavy burden to the government and society.<sup>5</sup>

Corresponding Author: Firdaus Hafidz  
Email: hafidz.firdaus@ugm.ac.id

In addition, cost-effectiveness analysis (CEA) has been conducted to evaluate the BPH medical therapy in several American and European countries, which shows that combination of pharmacological therapy is more cost-effective than monotherapy.<sup>3,4,6-9</sup>

At present, St. Carolus Hospital (SCH), Jakarta, Indonesia is using combination therapy for patients with BPH, based on the clinical practice guidelines (CPG). Thus, in this study, we used two methods of administering combination therapy. Based on the CPG, in the standard method, the combination drug is given for 6 months every day and routine follow-up is conducted every month. On the contrary, in the modified method, the drug is given every day for 3 months, and then the administration of drug is continued intermittently for 3 months, and follow-up is conducted once a month in the first 3 months and then once at the end of 6 months.

In this study, we compare the objective clinical outcome and quality of life (QoL) of the modified therapeutic method with those of the standard therapeutic method and perform cost-effective analysis of the two therapeutic methods available at SCH.

## MATERIALS AND METHODS

The study design used was a retrospective cohort. Data were obtained from the medical and financial record of SCH. Interviews were also conducted with BPH patients in regard to their international prostate symptoms score (IPSS) and QoL. Decision tree analysis was performed in this study with financing and clinical outcomes as parameters. The inclusion criteria were as follows men above 50 years who were diagnosed with BPH from urologist, and currently taking Tamsulosin (0.4 mg) and Dutasteride (0.5 mg). We excluded patients with prostate cancer or other diseases that can cause LUTS except BPH. All patients who refused and didn't complete the routine follow up were also excluded. Then we divided the patients into standard therapy method group (Group 1), and modified therapy method (Group 2). Clinical outcomes and costs were then analyzed between the two groups.

## RESULTS AND DISCUSSION

### 1. Respondent Characteristics

BPH is a benign enlargement of the prostate in elderly men. Patients aged 60-69 and 70-79 were the largest age group included in this study at SCH. All respondents in Group 1 showed moderate symptoms, whereas in Group 2, 49 patients showed moderate symptoms, and one people had severe symptoms (IPSS > 20). Group 1 had fewer patients with IPSS (16-19) compared with Group 2 (44% vs 68%, Table I). The quality of life (QoL) of patients in both groups at the beginning of therapy showed dissatisfaction and unhappiness toward their condition. In all 86% of the patients in Group 1 were "mostly dissatisfied" with their condition, whereas only 60% of the patients in Group 2 were "mostly dissatisfied" with their condition. However, a total of 20 patients (40%) in Group 2 reported "unhappiness", whereas only six patients (12%) in Group 1 reported "unhappiness". The majority of patients in both groups had

an initial maximum urinary flow rate (Qmax) of < 10 mL/s (86% in Group 1, 66% in Group 2) (Table I).

### 2. Clinical Outcomes and Effectiveness

Group 1 was given standard combination therapy for BPH (Tamsulosin 0.4 mg q.d. and Dutasteride 0.5 mg q.d.) continuous for 6 months, and routine follow-up was conducted every month. On the contrary Group 2 was given modified combination therapy using the same drugs, but the administration of the drug was continued for the first 3 months and then every 2 days for the last 3 months. Follow-up was also conducted monthly for the first 3 months, and at the end of 6 months. The data during each follow-up was collected and analyzed the basis of clinical improvement and costs.

### Post Therapy IPSS, QoL and Qmax

Improvement on IPSS was observed in both groups. A total of 37 people in Group 1 (74%) had an IPSS of 4-7, and only 13 (26%) patients had an IPSS  $\geq$  8. Meanwhile, 41 patients (82%) in Group 2 had an IPSS of 4-7, and 9 patients (18%) had an IPSS  $\geq$  8. Forty-seven patients in Group 2 showed improvement in IPSS compared with Group 1 (50 patients, 94% vs 100%) with different mean improvements (7.22 vs 8.20). Based on the statistical analysis, using Shapiro-Wilk test to evaluate the normality of post therapy IPSS, we found that the data were nonparametric in both groups. We then analyzed the data using Mann Whitney test to compare both groups ( $p = 0.077$ ).  $p > 0.05$  indicates no significant difference between IPSS of groups 1 and 2. (Table II)

At the end of therapy, Group 1 and Group 2 showed a "mostly satisfied" QoL (52% vs 50%). Mixed feeling and dissatisfied QoL were also observed in both groups, but most of the patients showed improvement. Forty-seven patients (94%) in Group 1 showed improvement in QoL, whereas 46 patients (92%) in Group 2 showed improved same mean improvement. Normality test using the Shapiro-Wilk test on post-therapy QoL showed that the data were nonparametric ( $p < 0.001$ ). Therefore, statistical analysis was conducted using the Mann Whitney test with a significance value of 0.498.  $p$  value  $> 0.05$ , indicates no significant difference in QoL between two groups. (Table II)

The Maximum urinary flow rate (Qmax) at the end of therapy in both groups mostly showed Qmax  $> 10$  mL/s. The number of patients that had Qmax  $> 10$  mL/s was greater in group 2 than in group 1 (90% vs 82%). The number of patients that had improved Qmax during 6 months of therapy was 41 (82%) in Group 1, and 45 (90%) in group 2 with different mean improvement (4.19 vs 5.20; Table III). Normality test on post-therapy Qmax showed normal distribution of data. We used unpaired T-test with  $P = 0.039$ .  $P < 0.05$ , indicates significant difference in Qmax after therapy between the two therapy groups. (Table II).

### Effectiveness of Therapy

Effectiveness of therapy can be seen from the improvement of IPSS, QoL score, and Qmax. Effectiveness of each parameter in both groups can be seen in Table III.

**Table I: Age group of distribution, initial IPSS, QoL, Qmax of BPH patients in the standard therapeutic method and modified therapeutic method at St. Carolus Hospital**

Characteristics	Standard Method		Modified Method	
	Total	%	Total	%
Age				
50-59	4	8	12	24
60-69	30	60	17	34
70-79	14	28	20	40
≥ 80	2	4	1	2
Initial IPSS				
8-11	0	0	1	2
12-15	28	56	14	28
16-19	22	44	34	68
≥ 20	0	0	1	2
Initial QoL				
Mixed about equally satisfied and dissatisfied	1	2	0	0
Mostly dissatisfied	43	86	30	60
Unhappy	6	12	20	40
Initial Qmax				
< 10 mL/s	43	86	33	66
≥ 10 mL/s	7	14	17	34

**Table II: IPSS, QoL, Qmax at the end of the therapy in the standard therapeutic method and modified therapeutic method at St. Carolus Hospital**

Post Therapy	Standard Method		Modified Method	
	Total	%	Total	%
IPSS				
0-3	0	0	0	0
4-7	37	74	41	82
≥ 8	13	26	9	18
Changes in IPSS				
Improved	50	100	47	94
Not Improved	0	0	3	6
QoL				
Pleased	9	18	7	14
Mostly satisfied	26	52	27	50
Mixed about equally satisfied and dissatisfied	10	20	9	22
Mostly dissatisfied	5	10	7	14
Changes in QoL				
Improved	47	94	46	92
Not Improved	3	6	4	8
Qmax				
< 10 mL/s	9	18	5	10
≥ 10 mL/s	41	82	45	90

**Table III: Effectiveness of standard therapy and modified therapy method**

Effectiveness	Standard Method	Modified Method
IPSS	7.22	8.20
QoL	1.88	2.06
Qmax	4.19	5.20

**Table IV: Direct cost, indirect cost, and the average cost between the standard and modified therapy groups**

Cost	Standard Method	Modified Method
Direct Cost	Rp 278,866,476	Rp 219,814,417
Indirect Cost	Rp 18,000,000	Rp 12,000,000
Total	Rp 296,866,476	Rp 231,814,417
Average Cost in 6 Months	Rp 5,937,330	Rp 4,636,288
Average Cost / Visit	Rp 989,555	Rp 927,258

Table V: ACER and ICER based on IPSS, QoL and Qmax

Method	ACER			ICER		
	IPSS	QoL	Qmax	IPSS	QoL	Qmax
Standard	822,345	3,158,154	1,415,672			
Modified	565,401	2,250,625	891,251	-1,327,593	-7,228,007	-1,290,715

Group 2 has shown to be more effective with regard to of IPSS, QoL and Qmax improvement compared with group 1.

### 3. BPH Clinical Service Cost

The Cost of BPH clinical services at SCH includes direct cost and indirect cost. Direct cost includes medical and non-medical cost, whereas indirect cost includes consumption cost, transportation and cost incurred by caretakers of patients. Cost difference was found between the two groups. The cost in Group 2 was cheaper than that in Group 1, both direct cost and indirect cost. In Group 1, the total cost of illness reached was Rp 296,866,746 in 6 months and the average cost per visit was Rp. 989,555. By contrast, in Group 2, the total cost of illness reached was Rp, 231,814,417 in 6 months and the average cost per visit was Rp. 927,258 (Table IV).

Based on the higher level of effectiveness in QoL, and the lower cost of medical services in Groups 2 compared with Group 1, we performed CEA which was expressed in the form of average cost-effectiveness ratio (ACER) and incremental cost-effectiveness ratio (ICER). The ACER of Group 2 was smaller than that of Group 1. Therefore, group 2 can be considered as more cost-effective compared with Group 1. Based on the indicators of clinical quality, including IPSS, QoL and Qmax, the ICER Group 2 was -1,327,593, -7,228,007, and -1,290,715 respectively. This result indicates the improvements in the effectiveness and cost savings of modified therapeutic methods (Table V).

## DISCUSSION

BPH is a benign enlargement of the prostate in elderly men. Patients aged 60-69 years and 70-79 years were the largest age group included in this study at SCH. LUTS caused by BPH are progressive complaints, which occur at the age of 70 years or more.<sup>4</sup> Some researchers reported that BPH began at the age of 50. Patients with BPH will then be assessed on the basis of the degree of complaint and QoL using the IPSS, and the maximum urinary flow rate using uroflowmetry. At present, medical therapy is given for patients with moderate or severe complaints. The Indonesian Association of Urologists recommends daily combination therapy for 6 months among patients with moderate to severe symptoms.<sup>2</sup> However, long-term treatment will cause a large increase in costs which can cause a heavy burden to the government and society.<sup>5</sup> Therefore, finding a cost-effective therapy without losing the quality of the clinical outcome is necessary.

The initial severity of complaints by the patients determines the treatment option, cure rate, and complications that will occur in the future. In Europe, 63% patients with BPH come with moderate to severe complaints.<sup>4</sup> In several other studies,

improvement in complaints was observed after combination therapy.<sup>8,10</sup> This finding is consistent with the result of this study, where patients in combination therapy showed improvement in complaints. However, modified therapeutic methods provide greater improvement when compared with standard therapeutic methods.

In this study with regard to the QoL, patients in both groups at the beginning of therapy showed dissatisfaction and unhappiness toward their condition. This situation caused the patients to come for treatment. This result is also in accordance with several other studies, that is people with BPH come for treatment if it interferes with daily life and activities.<sup>8</sup> QoL has improved after receiving either standard therapy or modified therapy. The improvement in QoL showed almost the same percentage in both groups. Early combination therapy reduces prostate growth progression and reduces the incidence of acute urinary retention; thus, giving early combination therapy will improve the QoL patients with BPH.

The maximum urinary flow rate (Qmax) examined by uroflowmetry in both groups showed an inadequate flow of urine (obstruction). Obstruction was found in 86% of patients in the standard method group and 66% of patients in the modified method group. Qmax in both groups improved after combination therapy. The modified therapeutic method group showed a higher Qmax improvement than the standard therapeutic method group within 6 months of clinical observation.

The high prevalence rate of BPH causes a huge economic burden and medical costs. The cost of BPH treatment in the United Kingdom is approximately £ 180 million annually, of which 60% are due to complications from BPH. Medical costs were also found to be 1.1 billion USD in the US per year.<sup>10</sup> Evaluation of BPH medical therapy in several American and European countries shows that combination medical therapy is more cost effective than monotherapy.<sup>3,4,6-9</sup>

The medical costs of the modified therapeutic method are less than that of the standard method. The cost per visit of the modified therapeutic method is also less than that of the standard therapeutic method. CEA is the conversion of cost and effectiveness in the form of a ratio. CEA is expressed as the ACER and ICER. The effectiveness of this study based on the clinical quality indicators shows different values. The maximum urinary flow rate is an objective indicator of clinical quality compared with other indicators, and it showed a significant difference in statistical tests in favor to the modified therapeutic method. Given its better effectiveness and lower clinical service costs, the ACER in the modified method group is smaller. ACER does not show real



economic value compared with ICER.<sup>12</sup> The ICER is more important than ACER, because it shows the degree of cost effectiveness of an intervention. In addition, the ICER of the modified therapeutic method is more cost-effective, where one clinical quality effectiveness value can reduce costs by Rp. 890,225.

Research on clinical quality and cost provides an understanding of the importance of coordination and collaboration with clinicians. Management encourages peer groups or medical staff to perform therapy in accordance with CPG; conduct clinical evaluations or audits of high-volume, high-risk, and high-cost cases; and monitor and evaluate the applicable CPG in hospitals. Therefore, collaborative care will be created in hospitals. Our study shows the importance of the role of head management in the hospital for clinical values in Continuous Quality Improvement. Hospital leaders can encourage cross-functional team performance among health professionals by setting budgets on clinical services. Data on the successful cost-effective health services can be used as an adequate promotional value.

Moreover, a comprehensive understanding of the application of pharmacoeconomic studies is necessary. Cost-effectiveness analysis is widely used to compare two or more health interventions that have different degree of effectiveness.<sup>13-15</sup> The existence of the HTA (Health Technology Assessment) team and the committee for quality improvement in hospitals are necessary because it can ensure that the dimensions of quality run well in the hospital. Understanding the quality of services related to clinical quality is a common need for clinicians and management in accordance with the dimensions of health service quality. The Institute of medicine defines six dimensions of health service quality: patient safety, effectiveness, efficiency, patient-centered, punctuality and equity. The modified BPH therapy method that is conducted in this study also pays attention to other quality dimensions such as patient safety, where patients are monitored in the same way as standard therapeutic methods. Another dimension of quality that can be observed is patient centeredness, where this study can also answer patients desire not to take medication every day for life. Therefore, the modified therapeutic method conducted in this study for patients will be low-cost service to be implemented in the future. This modified therapeutic method will be great help to the National Health Insurance (JKN) of Indonesia with regard to of balancing cost-effectiveness while maintaining service quality.

Ensuring the quality of hospital health services based on the dimensions of health service quality, requires directors of hospital with meta-leadership quality. Quality of service must be the indispensable part of the hospitals. This way, a hospital with services that are affordable, feasible and of good quality will be achieved.

## CONCLUSION

Clinical quality indicators, including IPSS, maximum urinary flow rate, and QoL have improved in both combinations therapeutic methods. The modified therapeutic method was more effective in improving clinical IPSS and maximum urinary flow rate than the standard therapeutic method.

A significant relationship was found between the maximum urinary flow rate in the standard therapeutic and the modified therapeutic groups.

The total and average cost of therapy for clinical services of patients with BPH in the modified therapeutic methods was less than that of the standard therapeutic methods. Furthermore, the cost-effectiveness ratio of the modified therapeutic method group was less than that of the standard therapeutic method group.

## REFERENCES

1. Zhang AY and Xu X. Prevalence, burden, and treatment of lower urinary tract symptoms in men aged 50 and older: A systematic review of the literature. SAGE; 2018:4.
2. IAU. Panduan Penatalaksanaan Klinis Pembesaran Prostat Jinak. Ikatan Ahli Urologi Indonesia; 2017: 1-38.
3. Walker A, Doyle S, Posnett J, Hunjan M. Cost-effectiveness of single-dose tamsulosin and dutasteride combination therapy compared with tamsulosin monotherapy in patients with benign prostatic hyperplasia in the UK. *BJU Int* 2013; 112:638-46.
4. Geitona M, Karabela P, Katsoulis IA, Kousoulakou H, Lyberopoulou E, Bitros E, et al. Dutasteride plus tamsulosin fixed dose combination first line therapy versus tamsulosin monotherapy in the treatment of benign prostatic hyperplasia: a budget impact analysis in the Greek healthcare setting. *BMC Urol* 2014; 14:78.
5. McAninch JM, Lue TF. Smith & Tanaho's General Urology 18th edition. Lange. 2013
6. Udeh EI, Ofoha CG, Adewole DA, and Nnabugwu II. A cost-effective analysis of fixed-dose combination of dutasteride and tamsulosin compared with dutasteride monotherapy for benign prostatic hyperplasia in Nigeria: a middleincome perspective; using an interactive markov model. *BMC Cancer* 2016; 16:405.
7. DerSarkissian M, Xiao Y, Sheng MD, Lefebvre P, Swensen AR, and Bell CF. Comparing clinical and economic outcomes associated with early initiation of combination therapy of an alpha blocker and dutasteride or finasteride in men with benign prostatic hyperplasia in the United States. *J Manag Care Spec Pharm* 2016.
8. Erman A, Masucci L, Krahn MD, and Elterman DS. Pharmacotherapy vs surgery as initial therapy for patients with moderate to severe benign prostate hyperplasia: a cost effectiveness analysis. *BJU Int* 2018; 879-88.
9. Bahia RL, Araujo DV, Pepe C, Javaroni V, Trindade M, Camargo CM. Cost-effectiveness analysis of medical treatment of benign prostatic hyperplasia in the Brazilian public health system. *Int Braz JUrol* 2012; 38(5).
10. Kim HW, Moon DG, Kim HM, Hwang JH, Kim SC, Nam SG, et al. Effect of shifting from combination therapy to monotherapy of alpha blocker or 5 ARI on prostate volume and symptoms in patients with benign prostatic hyperplasia. *Korea JUrol* 2011; 681-6
11. Speakman M, Kirby R, Doyle S, Ioannou C. Burden of male lower urinary tract symptoms (LUTS) suggestive of benign prostatic hyperplasia (BPH) – focus on the UK. *BJU Int* 2015; 115:508–19.
12. Haslinda NI, Juni MH, Rosliza AM, Faisal I. Designing and conducting cost effectiveness analysis studies in healthcare. *IJPHCS* 2017; 4: 62-76.



13. Eisenberg JM, Schulman KA, Glick H, and Koffer H. Pharmacoeconomics: Economic evaluation of pharmaceuticals. In: Strom BL, Editor. Pharmacoeconomics, John Wiley & Sons Ltd.; 1994: 469-493.
14. Sanchez LA. Applied pharmacoeconomics: Evaluation and use of pharmacoeconomic data from literature. Am J Health Syst Pharm1999; 56:1630-40.
15. Sanchez LA, Lee JT. Applied pharmacoeconomics: Modeling data from internal and external resources. Am J Health Syst Pharm2000; 57:146-158.

# Triple-action of the standardized antidiabetic polyherbal extract; Synacinn™ through upregulation of *GLUT<sub>4</sub>* and inhibition of *DPP(IV)*, $\alpha$ -amylase, and $\alpha$ -glucosidase activity

Hassan Fahmi Ismail, PhD<sup>1,2</sup>, Zanariah Hashim, PhD<sup>2</sup>, Dayang Norulfairuz Abang Zaidel, PhD<sup>3</sup>, Siti Nurazwa Zainol<sup>3</sup>, Fatahiya Mohamed Tap, PhD<sup>4</sup>, Fadzilah Adibah Abdul Majid, PhD<sup>1</sup>, Nor Hafizah Zakaria, PhD<sup>1</sup>

<sup>1</sup>Institute of Marine Biotechnology, Universiti Malaysia Terengganu, 21030 Kuala Nerus, Terengganu, Malaysia, <sup>2</sup>Department of Bioprocess and Polymer Engineering, School of Chemical & Energy Engineering, Faculty of Engineering, Universiti Teknologi Malaysia, 81030 Johor Bharu, Johor, Malaysia, <sup>3</sup>Proliv Life Science, Taman Ukay Bistari, 68000 Ampang, Selangor, Malaysia, <sup>4</sup>Faculty of Chemical Engineering, Universiti Teknologi Mara, Bukit Besi, 23200 Dungun, Terengganu, Malaysia

## ABSTRACT

**Introduction:** Synacinn™ is a standardized polyherbal supplement for diabetes mellitus which is formulated from *Andrographis paniculata*, *Curcuma xanthorrhiza*, *Cinnamomum zeylanicum*, *Eugenia polyantha*, and *Orthosiphon stamineus*.

**Materials and Methods:** This study aimed to elucidate the antidiabetic potential of Synacinn™ on three specific actions, including 1) the insulin sensitivity and glucose transport on dexamethasone-induced insulin-resistance 3T3-L1 adipocytes, 2) the inhibitory capacity on postprandial enzyme activity ( $\alpha$ -amylase and  $\alpha$ -glucosidase), and 3) the inhibitory activity of hepatic *DPP(IV)* enzyme.

**Results:** Results showed that insulin resistance of 3T3-L1 adipocytes may be developed by prolonging the exposure of 1 $\mu$ g/ml of dexamethasone for >48 hours. The insulin-resistance condition was minimized by the treatment of 10  $\mu$ g/ml of Synacinn™ which significantly improved the insulin-stimulated glucose utilization by 10.6%. Meanwhile, insulin-stimulated glucose utilization in normal adipocytes was also attenuated by 9.2%. At the cellular level, Synacinn™ attenuated glucose utilization mainly by upregulating *GLUT<sub>4</sub>* protein expression by 1.71 fold. Additionally, Synacinn™ is a potent inhibitor for the activity of  $\alpha$ -amylase and  $\alpha$ -glucosidase with *IC<sub>50</sub>* of 0.467 mg/mL and 0.245 mg/mL, respectively. Synacinn™ also controlled the glycemic index through inhibition of hepatic *DPP(IV)* enzyme with *IC<sub>50</sub>* of 1.11 mg/mL.

**Conclusion:** Results suggested that Synacinn™ reduced diabetes mellitus through sensitizing the cellular glucose utilization, reducing the postprandial carbohydrate degradation, and inhibiting the hepatic *DPP(IV)* enzyme function.

## INTRODUCTION

In recent decades, new drugs and drug classes have become available for type-2 diabetes mellitus (T<sub>2</sub>DM) patients that act at different sites of actions including sulfonylureas, meglitinides, biguanides, thiazolidinediones, *DPP(IV)*

inhibitors, and  $\alpha$ -amylase and  $\alpha$ -glucosidase inhibitor.<sup>1,2</sup> Physicians would prescribe these drugs based on the level of glucose and hemoglobin 1C (Hb1C), which may include a single or combination of oral therapy drugs.<sup>1</sup> Despite advanced research on drug development, DM therapies require lifelong drug consumption to control the glycemic condition at a healthy level. Unfortunately, these drugs have limitations and unwanted side effects. For example, metformin increases glucose uptake in body tissues and inhibits gluconeogenesis in the liver, but it causes gastrointestinal problems,<sup>2</sup> hepatotoxicity<sup>3</sup> and is not suitable for patients with kidney problems.<sup>4</sup> Meanwhile, sulphonylureas, an insulin release stimulator, is only ideal for T<sub>2</sub>DM patients.<sup>5</sup> Potentially natural therapies derived from the plants (single compounds, a group of compounds or whole extract) have become a popular choice to reduce and prevent the DM traditionally.<sup>6,7</sup>

Synacinn™, a traditional polyherbal supplement is recommended for the treatment of DM, and has symptoms including tiredness and high blood glucose level. Synacinn™ is formulated from five herbs, including *Andrographis paniculata*, *Curcuma xanthorrhiza*, *Cinnamomum zeylanicum*, *Eugenia polyantha*, and *Orthosiphon stamineus*. Qualitative and quantitative HPLC fingerprinting of this formulation has been critically developed as reported by Zainol et al.<sup>8</sup> Synacinn™ contains gallic acid, catechin, rosmarinic acid, curcumin, cinnamaldehyde, and andrographolide which are known as therapeutic agents against various diseases. Herb-drug interaction analysis also recommended that Synacinn™ could be consumed separately from a drug known to be metabolized by all tested CYP450 enzymes.<sup>9</sup> It is believed that the synergistic outcomes of this combination involved multiple mechanisms, ultimately in covering all the possible effects of DM in the body. Synacinn™ at 250 (b.i.d.) mg kg<sup>-1</sup> normalizes the blood glucose level, total glyceride, and cholesterol in STZ-induced rats.<sup>10</sup> It also protects the liver, kidney, and pancreas from the damage caused by STZ administration.<sup>10</sup> However, the fundamental mechanism behind the antihyperglycemic event is still unknown. This study investigated the reversal of insulin-resistance conditions using an *in-vitro* model developed by the acute exposure of dexamethasone (DEX) on 3T3-L1 adipocytes.

Corresponding Author: Fadzilah Adibah Abdul Majid  
Email: f.adibah@umt.edu.my

Subsequently, the utilization of glucose and intracellular protein expression was assessed. Furthermore, Synacinn™ was also examined for its ability to inhibit the postprandial enzymes  $\alpha$ -amylase and  $\alpha$ -glucosidase as well as hepatic DPP(IV) activity.

## MATERIALS AND METHODS

### Materials

Standardized water extract of Synacinn™ was supplied by Naturemedics Laboratories Sdn. Bhd. Terengganu, Malaysia. DEX, 3-isobutyl-1-methylxanthine (IBMX), insulin, and rosiglitazone (ROS) were purchased from Sigma Aldrich (St. Louis, MO, USA). 3-(4,5-dimethylthiazol-2-yl)-2,5-diphenyltetrazolium bromide (MTT) was purchased from Invitrogen (Carlsbad, CA, USA). Mouse 3T3-L1 preadipocyte was purchased from American Type Culture Collection, Manassas, USA. Dulbecco's Modified Eagle's medium (DMEM), fetal bovine serum (FBS), and penicillin strep (PS) were purchased from Gibco, Life Technologies (Rockville, MD, USA).

### Cells maintenance and differentiation

3T3-L1 preadipocytes were cultured and maintained between 80% and 90% confluency in DMEM supplemented with 10% of FBS and 1% of PS. To initiate differentiation, two-days post confluent cells were incubated with differentiation medium (DMEM supplemented with 10% FBS, 0.5 mM IBMX, 2 mM DEX, and 1.7 mM insulin). After 48–72 h, spent media was replaced by DMEM supplemented with 10% FBS and 1.7 mM insulin. Differentiated adipocytes were maintained in DMEM until day ten.

### Cytotoxicity assay

All procedures were referred to Ismail et al.<sup>11</sup> with slight modifications. Preadipocytes were treated with Synacinn™ ranging from 5 to 10000  $\mu$ g/mL diluted in DMEM for 24 h. MTT solution was added to each well and incubated for 4 hours at 37°C. The developed formazan was dissolved in 200  $\mu$ L of DMSO and analyzed using microplate reader (Biotec, ELx 808, Vermont, USA) at 570 nm via the KC Junior program. Treatment was conducted in six replications. Untreated cells were used as controls.

### Induction and validation of insulin resistance in adipocytes

Fully differentiated adipocytes were serum-starved and treated with 1  $\mu$ M of DEX diluted in DMEM for 24, 48, and 72 h. Upon completion of insulin-resistance induction, cells were treated with 50  $\mu$ M ROS for 48 h. The development of insulin resistance was considered successful if the glucose utilization was significantly lower ( $p < 0.05$ ) than that of the control.

### Synacinn™ treatment on insulin-sensitive and insulin-resistance adipocytes

Prior to Synacinn™ treatment, cells were starved for 3 h in the basal DMEM. Normal and insulin-resistance adipocytes were treated with Synacinn™ at concentrations of 1, 10, and 100  $\mu$ g/mL with and without the 1  $\mu$ g/mL of insulin. After 48 h of incubation, spent media were collected, and glucose utilization was assayed using the Cobas C111. Subsequently, cells were lysed, and the supernatant was collected and stored at -80°C for protein analysis. ROS was used as a positive

control. Treatment was conducted in triplicates.

### Western blotting

Samples (30  $\mu$ g) were separated by electrophoresis, transferred and blocked by the 5% of skimmed milk. Primary antibody anti-GLUT4 (1:2000) (PA519621, Thermo Scientific), IRS-1 (1:2000) (PA11057, Thermo Scientific), PI3K (1:2000) (4257P, Cell Signaling Technology), AKT (1:2000) (4691P, Cell Signaling Technology), were added for overnight incubation at 4°C with the continuous shaking. Then, the membrane was incubated with a secondary antibody-AP conjugate (1:7500) (0031210, Thermo Scientific) for 1 h at room temperature. The developed band was scanned and quantified using ImageJ.

### DPP (IV) inhibitor assay

DPP(IV) inhibition assay was conducted according to the DPP(IV) inhibitor screening assay kit (Cayman; 700210). Reaction was initiated by mixing 30  $\mu$ L of assay buffer, 10  $\mu$ L of DPP(IV) enzyme, 10  $\mu$ L of samples, and 50  $\mu$ L of substrate solution. The mixture was incubated for 30 min at 37°C. Fluorescence reading was obtained by using an excitation wavelength of 355 nm and an emission wavelength of 458 nm with a multimode reader (Varioskan Flash, Thermo Scientific).

### $\alpha$ -Amylase inhibitor assay

The activity of  $\alpha$ -amylase was assayed according to the manufacturer protocol (Abcam; ab102523) with modification. A total of 5  $\mu$ L of 0.5U/ $\mu$ L *Aspergillus oryzae*  $\alpha$ -amylase was preincubated with 45  $\mu$ L of samples for 30 min at 37°C. Total amount of 100  $\mu$ L reaction mix was added to each reaction and mixed carefully. The mixtures were allowed to react for 20 min, followed by the measurement of absorbance at 405 nm. Acarbose was used as a positive control. Percent of inhibition was calculated by using Equation(1).

$$\%inhibition = \frac{OD_{control} - OD_{sample}}{OD_{control}} \times 100 \quad (1)$$

### $\alpha$ -Glucosidase inhibitor assay

The inhibitory activity of  $\alpha$ -glucosidase was conducted according to the procedures provided by the QuantiChrom™  $\alpha$ -Glucosidase Assay Kit (DAGD-100) with modifications. About 10  $\mu$ L of 1.0U/mL of  $\alpha$ -glucosidase from baker's yeast was preincubated with 10  $\mu$ L of samples for 15 min at 37°C. A total of 200  $\mu$ L of working reagent was added and allowed to react for 30 min. The reaction was measured at 405nm. Acarbose was used as a positive control. Percent of inhibition was calculated using the Equation(1) mentioned above.

### Statistical analysis

All data were expressed in mean  $\pm$  standard error (SEM). Statistical analysis was performed using SPSS program with one-way ANOVA and Tukey test. Significant differences were considered as  $p < 0.05$ .

## RESULTS

### Effect of Synacinn™ on insulin-resistance in-vitro model Development of insulin-resistance adipocytes by dexamethasone

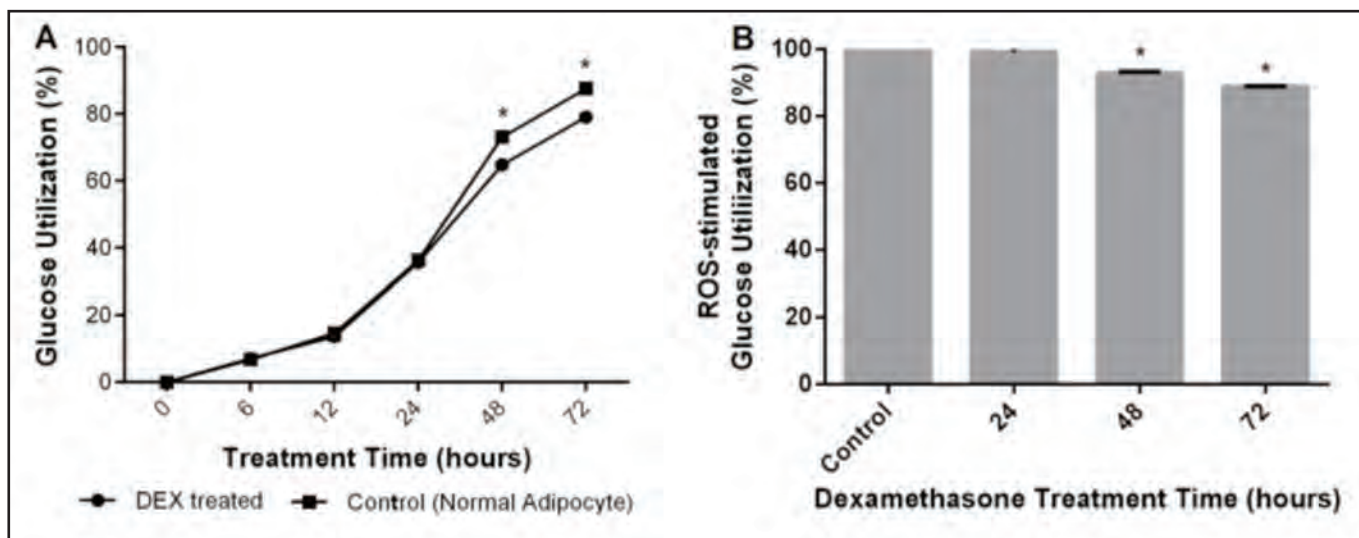


**Fig. 1:** A) Insulin-stimulated glucose utilization during the induction of insulin resistance by DEX. [\*] Significant differences ( $p < 0.05$ ) of 8.3% and 8.5% were quantified at 48 h and 72 h, respectively, as compared to control. Treatment was carried out in triplicates. B) Validation of insulin-resistance model by rosiglitazone (ROS). Significant differences of 7.1% and 11.2% were measured at 48 h and 72 h of treatment, respectively.

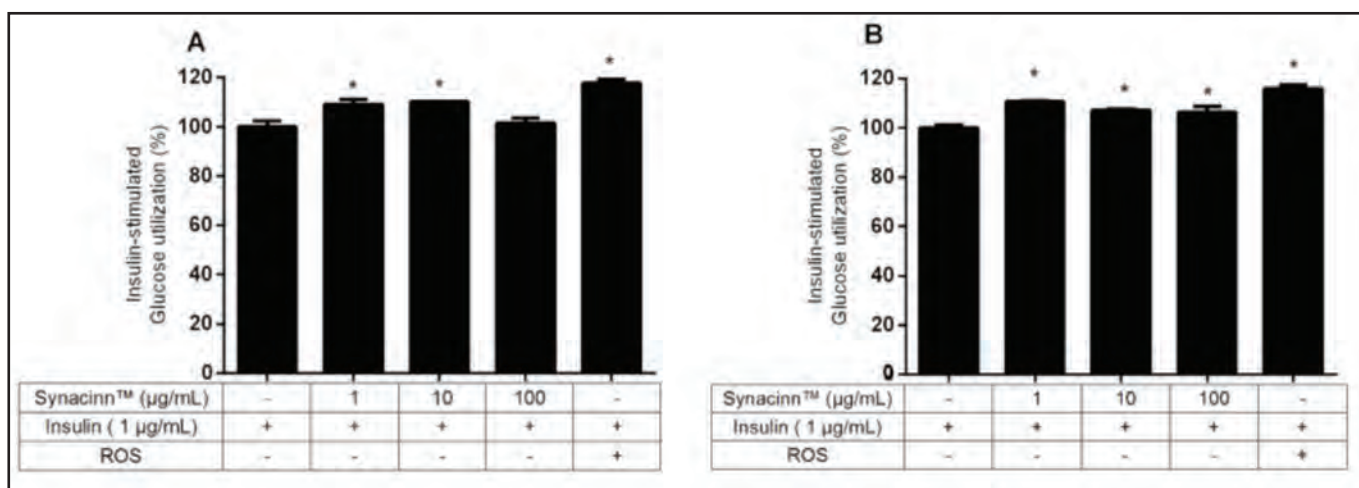


**Fig. 2:** Effect of Synacinn™ on insulin-stimulated glucose utilization. A) Effect of Synacinn™ on glucose utilization in normal adipocytes. B) Effect of Synacinn™ on the glucose utilization in insulin resistant adipocytes. Rosiglitazone (ROS) was used as a positive control. [\*] Significance was considered as  $p < 0.05$ .

Induction of insulin resistance by DEX was carried out in the presence of insulin, which manifests the condition in the human body. As illustrated in Fig 1 (A), treatment of 1µM DEX for 72 h showed a time-dependent inhibition on glucose utilization. The presence of DEX partially disturbed the glucose utilization starting at 48 h of treatment, and continuously inhibited until the end of the experiment. Significant differences ( $p < 0.05$ ) of 8.3% and 8.5% were quantified at 48 h and 72 h of DEX treatment, respectively, as compared to the control (normal adipocytes).

In addition, following the induction of DEX, the insulin-resistance condition was validated in the presence of 50µM ROS as presented in Fig 1 (B). The ROS-stimulated glucose

utilization was consistent with the results in Fig 1. Significant differences were observed starting at 48 h (7.1%) and 72 h (11.2%).

Synacinn™ sensitized the insulin-stimulated glucose utilization in normal adipocytes and insulin-resistance adipocytes

Glucose utilization stimulated by insulin is predominant in insulin-sensitive tissues like muscles and adipose. In this study, normal adipocytes and insulin-resistance adipocytes were treated with Synacinn™ for 48 h, and the glucose concentration in spent media was measured to estimate the utilization of glucose by cells. As in Fig. 2 (A), insulin-stimulated glucose utilization in normal adipocytes was



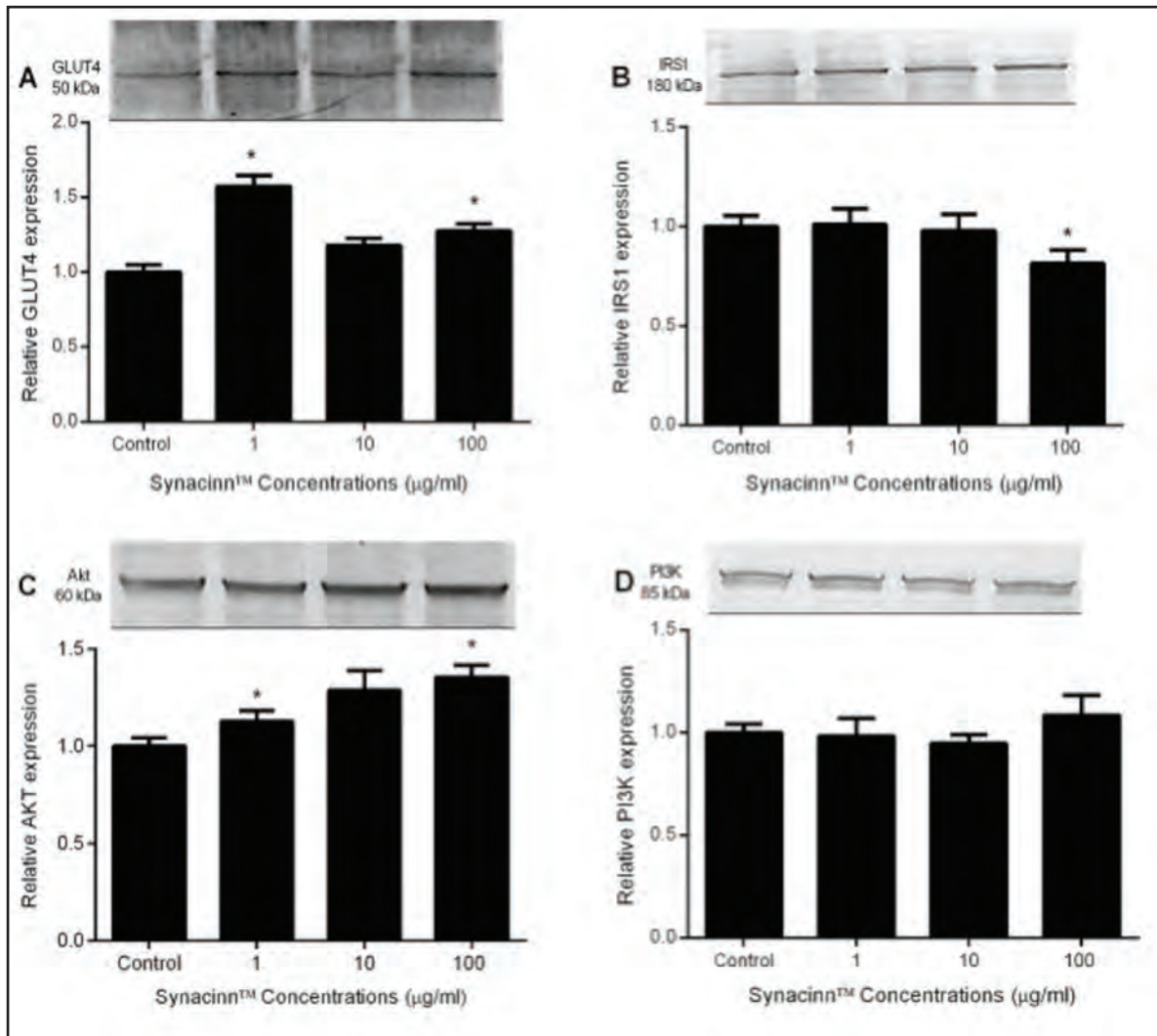


**Fig. 3:** Effect of Synacinn™ on the expression of insulin signaling pathway proteins in normal adipocytes. A) Relative expression of *GLUT4*, B) relative expression of *IRS-1*, C) relative expression of *AKT*, and D) Relative expression of *PI3K*. [\*]Significance was considered as  $p < 0.05$ .

significantly increased during the treatment of Synacinn™. At a concentration of 1 and 10 µg/mL, Synacinn™ significantly ( $p < 0.05$ ) attenuated glucose utilization by 9.2% and 10.2%, respectively. However, total of 100 µg/mL failed to increase the glucose utilization. As expected, ROS as positive control enhanced the glucose utilization by 17.6%.

The effect of Synacinn™ on glucose utilization was further investigated using DEX-induced insulin-resistance adipocytes. Fig.2 (B) demonstrates that Synacinn™ in the presence of insulin restored the impaired glucose utilization process. In comparison with the control (insulin only), significant improvement ( $p < 0.05$ ) on glucose utilization was observed with 10.6%, 7.2%, and 6.3% increment for 1, 10, and 100 µg/mL of Synacinn™ treatment, respectively.

Synacinn™ increased glucose utilization through upregulation of *GLUT4*

Previously, it was discovered that Synacinn™ enhanced glucose utilization in normal and insulin resistant

adipocytes. Further analysis of the expression of proteins related to the insulin signaling pathway has shown that Synacinn™ treatment on normal adipocytes enhances the expression of *GLUT4* and *AKT*. The total *GLUT4* expression was markedly increased during the treatment of all concentrations with 1.55-, 1.17-, and 1.28-fold for 1, 10, and 100 µg/mL, respectively (Fig.3A). Meanwhile, the expressions of *AKT* were increased by 1.13-, 1.29-, and 1.22-fold during treatment of similar doses of Synacinn™ (Fig.3C). No changes in the expression of *IRS-1* and *PI3K* were detected upon Synacinn™ treatment (Fig.3B and Fig.3D).

The treatment of Synacinn™ on insulin resistant adipocytes showed that Synacinn™ treatment in the presence of insulin specifically improved the expression of total *GLUT4* (Fig.4). Treatment of 1, 10, and 100 µg/mL Synacinn™ significantly increased the total *GLUT4* expression by 1.39-, 1.71-, and 1.59-fold, respectively (Fig.4A). However, the changes of expression of *IRS-1*, *AKT*, and *PI3K* were not significant during Synacinn™ treatment.

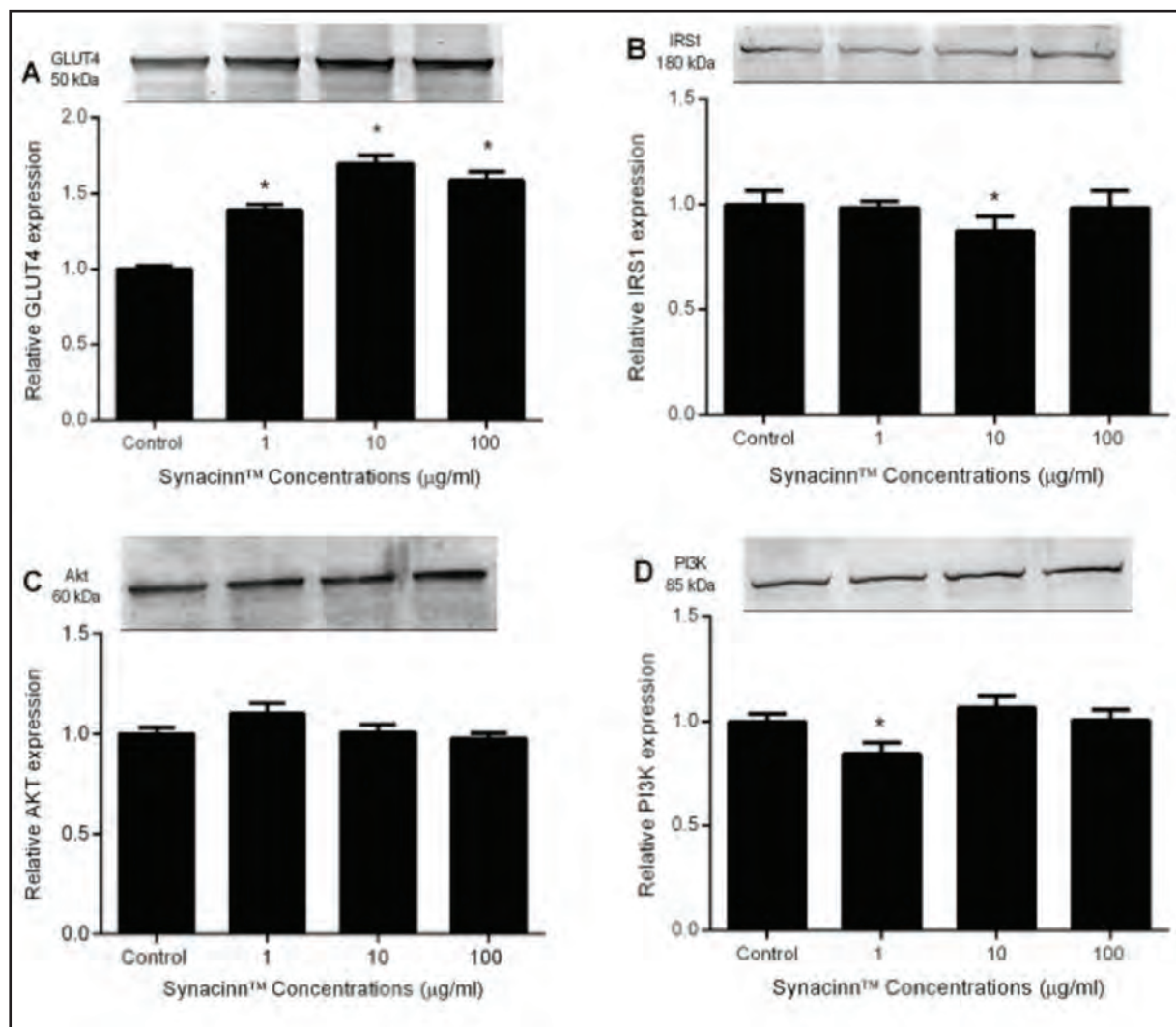


**Fig. 4:** Effect of Synacinn™ on the expression of insulin signaling pathway proteins for insulin-resistance adipocytes. A) Relative expression of *GLUT4*, B) relative expression of *IRS-1*, C) relative expression of *AKT*, and D) relative expression of *PI3K*. [\*] Significance was considered as  $p < 0.05$

#### Effect of Synacinn™ on the inhibition of *DPP(IV)*, $\alpha$ -amylase, and $\alpha$ -glucosidase activities

Another route of antidiabetic therapies is by inhibiting *DPP(IV)* enzyme activity from converting glycogen in the liver to glucose, which in turn will increase the glycemic index in the blood. In this study, adose-dependent inhibition trend was observed during the treatment of Synacinn™ on *DPP(IV)* activity (Fig 5). At the highest tested concentration, 4 mg/mL, Synacinn™ inhibited 94.3% of its activity with  $IC_{50}$  of 1.11 mg/mL.

The antidiabetic effect of Synacinn™ was further analyzed on the inhibition activity of the postprandial enzymes  $\alpha$ -amylase and  $\alpha$ -glucosidase as presented in Fig. 6. A dose-dependent inhibition was achieved by Synacinn™ toward the activity of both enzymes. At the highest concentration of 4 mg/mL, Synacinn™ inhibited 98.5% of  $\alpha$ -amylase activity and 96.6% for  $\alpha$ -glucosidase with  $IC_{50}$  of 0.467 mg/mL and 0.245 mg/mL, respectively.

#### DISCUSSION

Synacinn™, a polyherbal supplement for DM, is formulated from five different types of Malaysian herbs, including *A. paniculata*, *C. zeylanicum*, *C. xanthorrhiza*, *E. polyantha*, and *O. stamineus*. It is believed that this combination triggers a synergistic mechanism ultimately to overcome all the possible effects of DM. In a recent study, *in-vitro* pharmacodynamics tests were conducted to identify the antidiabetic potential of the standardized extract of Synacinn™. We discovered that this novel polyherbal formulation is a multifunctional mediator for DM with the following abilities: 1) increases the glucose utilization in normal and insulin-resistance adipocytes through upregulation of *GLUT4*, 2) inhibits the activities of the postprandial enzymes, and 3) inhibits *DPP(IV)* enzyme activities.

To investigate the mechanism of action of Synacinn™, the *in-vitro* insulin-resistance model that mimics T2DM was



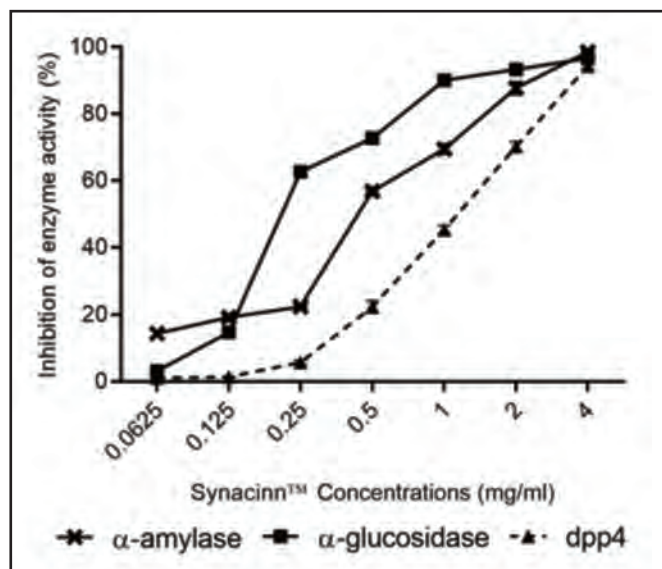


**Fig. 5:** Effect of Synacinn™ on the activity of hepatic *DPP(IV)*,  $\alpha$ -amylase, and  $\alpha$ -glucosidase. Dose-dependent inhibition was observed for the *DPP(IV)* enzyme activity with a maximum inhibition at 4 mg/mL (94.3%) ( $IC_{50}$  = 1.11 mg/mL) For  $\alpha$ -amylase and  $\alpha$ -glucosidase, the maximum inhibition were 98.5% ( $IC_{50}$  = 0.467 mg/mL) and 96.6% ( $IC_{50}$  = 0.245 mg/mL), respectively.

developed by treating the *3T3-L1* adipocytes with 1  $\mu$ M DEX with the presence of insulin for 72 h. During the development of insulin resistance, we discovered that the disturbance of insulin-stimulated glucose utilization was initiated at 48 h and worsened at 72 h of DEX treatment. This condition was further validated by 50  $\mu$ M ROS, which produced similar results. In contrast with Sangeetha et al.<sup>12</sup> in the absence of insulin, 50% reduction in glucose uptake during the insulin-resistance state was achieved as early as 24 hours. The differences suggested that insulin might have a protective mechanism toward the early stage of DEX-induced insulin resistance. However, the protective effect was later diminished at a longer treatment period. In addition, no phenotypic changes such as cell death, changes in size and shape (data not shown) were observed during this period, suggesting that the inhibitory effect of glucose utilization was due to the resistance imposed on the cells. ROS has been reported to improve insulin sensitivity in in-vitro insulin-resistance models, such as *3T3-L1* adipocytes, human embryonic kidney 293 (*HEK 293*), and *C2C12* skeletal muscle cells.<sup>12-14</sup> As a *PPAR* $\gamma$  ligand, ROS binds specifically and activates the *PPAR* $\gamma$  nuclear receptor. The activated *PPAR* $\gamma$  binds to the retinoid X receptor and forms a complex. This complex will assist the transcription of another gene especially in insulin signaling and adipogenesis pathway.<sup>15</sup> In isolated fetal rat primary brown adipocytes, ROS treatment has correspondingly increased the expression of *IRS-1* and *IRS-2* Tyr phosphorylation, which subsequently activates the *PI3K* and *AKT* proteins. The mRNA level of *GLUT4* was not changed, but ROS increases the translocation of *GLUT4* to the plasma membrane resulting in a significant increase of basal and insulin-stimulated glucose uptake.<sup>16</sup> ROS was also shown to improve glucose transport in vastus lateralis muscles and adipocytes of Goto-Kakizaki diabetic rats and independently

increase the expression of *PKC- $\zeta$ / $\lambda$*  without the improvement in the activation of *PI3K* and *PKB*.<sup>17</sup>

Synacinn™, a standardized polyherbal supplement, is designed to reduce DM and its complications. In a recent study, it was confirmed that Synacinn™ increases glucose utilization in normal adipocytes and reverses DEX-induced insulin resistance in *3T3-L1* adipocytes. Interestingly, lower concentrations of Synacinn™ were more potent in sensitizing insulin-stimulated glucose utilization. Even though the improvement was not as good as ROS within the tested period, it was postulated that for a longer time, Synacinn™ exhibited a promising effect as a glucose-lowering agent. Among the phytochemicals in Synacinn™ that have such an effect on adipocytes are gallic acid and andrographolide.<sup>18-20</sup> Meanwhile, 5  $\mu$ M rosmarinic acid increases glucose uptake by 86% in L6 rat myotubes.<sup>21</sup>

In insulin-responsive tissue like muscles and adipose, glucose transportation is regulated by a cascade of intracellular phosphorylation event insulin signaling pathway. Cellular analysis on the insight of DEX-induced insulin resistance identified dephosphorylating several downstream proteins in the insulin signaling pathways including *IRS-1*, *PI3K*, and *AKT*, which subsequently inhibit the translocation of *GLUT4* from the cytosolic compartment to the cellular membrane.<sup>22,23</sup> In this study, we discovered that the effect of Synacinn™ was dominant in restoring glucose transportation rather than repairing the insulin signal transduction. The restoration of glucose utilization in adipocytes was in fact, mainly stimulated by upregulation of *GLUT4* level, and not by other downstream proteins in the insulin signaling pathway, such as *IRS-1*, *PI3K*, and *AKT*. The expression of *GLUT4* was hyped up to 1.5-fold suggesting that more glucose will be transported into the cells. Even though Synacinn™ does not improve *IRS-1*, *PI3K*, and *AKT* expression in insulin-resistance adipocytes, it is postulated that these proteins' activity is sufficient to enhance *GLUT4* activity. Similar results were demonstrated by 10  $\mu$ M gallic acid showed the enhancement of *GLUT4* translocation without any stimulation on the *AKT* and *AMPK* phosphorylation.

In this study, we also discovered that Synacinn™ controls the glycemic index through inhibition of *DPP(IV)* enzyme. Dose-dependent inhibition of the activity of this enzyme was observed (Fig. 6), where the optimum concentration was at 4 mg/mL. Curcumin, gallic acid, and rosmarinic acid have shown potential as natural sources of *DPP(IV)* inhibitor.<sup>24</sup> The inhibition of *DPP(IV)* enzyme activity influences the blood glucose level by prolonging the half-life of active glucagon-like peptide-1 (*GLP1*) to stimulate the insulin secretion, increase beta-cell mass, inhibit glucagon secretion, reduce the rate of gastric emptying, and induce satiety.<sup>25</sup>

The control of postprandial hyperglycemia may be achieved by slowing the absorption of glucose through the inhibition of the carbohydrate hydrolyzing enzymes ( $\alpha$ -amylase and  $\alpha$ -glucosidase). Inhibitors of these enzymes delay carbohydrate digestion and prolong the overall carbohydrate digestion time, causing a reduction in the rate of glucose absorption and consequently blunting the postprandial blood glucose rise. While most individual herbs in the formulation have

been reported to inhibit carbohydrate hydrolyzing enzymes, Synacinn™ as in polyherbal combination exerts greater potential as an inhibitor for  $\alpha$ -amylase and  $\alpha$ -glucosidase with  $IC_{50}$  of 0.467 mg/ml and 0.245 mg/ml. In comparison, the binary water-ethanolic extract of *Andrographis paniculata* exhibited higher  $IC_{50}$  for  $\alpha$ -amylase (35.7 mg/mL) and  $\alpha$ -glucosidase (4.63 mg/mL).<sup>26</sup>

## CONCLUSION

To summarize, the multifunctional standardized polyherbal formulation, Synacinn™, modulates hyperglycemic control through three specific mechanisms of action including: 1) enhancing cellular glucose transportation through upregulation of *GLUT4*, 2) inhibiting postprandial enzymes activities, which delay the degradation and absorption of polysaccharide, and 3) altering the gluconeogenesis process in the liver by inhibiting hepatic *DPP(IV)* enzyme activities.

## ACKNOWLEDGMENT

This research was supported by Research University Grant, Universiti Teknologi Malaysia (RUG: 10H27); NRGs, Ministry of Agriculture, Malaysia (4H016); and Fundamental Research Grant Scheme, Ministry of Higher Education, Malaysia (59424).

## REFERENCES

- Nathan DM, Buse JB, Davidson MB, Heine RJ, Holman RR, Sherwin R, et al. Management of Hyperglycemia in Type 2 Diabetes: A Consensus Algorithm for the Initiation and Adjustment of Therapy. *Diabetes Care* 2006;29(8):1963.
- Siavash M, Tabbakhian M, Sabzghabae AM, Razavi N. Severity of Gastrointestinal Side Effects of Metformin Tablet Compared to Metformin Capsule in Type 2 Diabetes Mellitus Patients. *J Res Pharm Pract* 2017;6(2):73-6.
- Miralles-Linares F, Puerta-Fernandez S, Bernal-Lopez MR, Tinahones FJ, Andrade RJ, Gomez-Huelgas R. Metformin-Induced Hepatotoxicity. *Diabetes Care* 2012;35(3):e21.
- Hsu WH, Hsiao PJ, Lin PC, Chen SC, Lee MY, Shin SJ. Effect of metformin on kidney function in patients with type 2 diabetes mellitus and moderate chronic kidney disease. *Oncotarget* 2017;9(4):5416-23.
- Kalra S, Aamir AH, Raza A, Das AK, Azad Khan AK, Shrestha D, et al. Place of sulfonylureas in the management of type 2 diabetes mellitus in South Asia: A consensus statement. *Indian J Endocrinol Metab* 2015;19(5):577-96.
- Katiyar D, Singh V, Gilani SJ, Goel R, Grover P, Vats A. Hypoglycemic herbs and their polyherbal formulations: a comprehensive review. *MedicChem Res* 2015;24(1):1-21.
- Prabhakar PK, Doble M. Effect of Natural Products on Commercial Oral Antidiabetic Drugs in Enhancing 2-Deoxyglucose Uptake by 3T3-L1 Adipocytes. *Ther Adv Endocrinol Metab* 2011;2(3):103-14.
- Zainol SN, Fadhilina A, Rentala SV, Pillai R, Yalaka M, Bansal I, et al. Analytical method cross validation by HPLC for identification of five markers and quantification of one marker in Synacinn™ formulations and its in vivo bone marrow micronucleus test data. *Data in Brief* 2021;36:107001.
- Nur Syukriah Ab R, Fadzilah Adibah Abd M, Mohd Effendy Abd W, Ain Nabihah Z, Siti Nurazwa Z, Hassan Fahmi I, et al. Evaluation of Herb-Drug Interaction of Synacinn™; and Individual Biomarker through Cytochrome 450 Inhibition Assay. *Drug Metab Lett* 2018;12(1):62-7.
- Ab Rahman NS, Abdul Majid FA, Abd Wahid ME, Ismail HF, Tap FM, Zainudin AN, et al. Molecular docking analysis and anti-hyperglycemic activity of Synacinn™ in streptozotocin-induced rats. *RSC Adv* 2020;10(57):34581-94.
- Ismail HF, Hashim Z, Soon WT, Rahman NSA, Zainudin AN, Majid FAA. Comparative study of herbal plants on the phenolic and flavonoid content, antioxidant activities and toxicity on cells and zebrafish embryo. *J Tradit Complement Med* 2017;7(4):452-65.
- Sangeetha KN, Shilpa K, Jyothi Kumari P, Lakshmi BS. Reversal of dexamethasone induced insulin resistance in 3T3L1 adipocytes by 3beta-taraxerol of *Mangifera indica*. *Phytomedicine* 2013;20(3-4):213-20.
- Jiang G, Dallas-Yang Q, Biswas S, Li Z, Zhang BB. Rosiglitazone, an agonist of peroxisome-proliferator-activated receptor gamma (PPARgamma), decreases inhibitory serine phosphorylation of IRS1 in vitro and in vivo. *Biochem J* 2004;377(Pt 2):339-46.
- Meshkani R, Sadeghi A, Taheripak G, Zarghooni M, Gerayesh-Nejad S, Bakhtiyari S. Rosiglitazone, a PPARgamma agonist, ameliorates palmitate-induced insulin resistance and apoptosis in skeletal muscle cells. *Cell Biochem Funct* 2014;32(8):683-91.
- Kroker AJ, Bruning JB. PPAR Res 2015;2015:816856.
- Hernandez R, Teruel T, Lorenzo M. Rosiglitazone produces insulin sensitisation by increasing expression of the insulin receptor and its tyrosine kinase activity in brown adipocytes. *Diabetologia* 2003;46(12):1618-28.
- Kanoh Y, Bandyopadhyay G, Sajjan MP, Standaert ML, Farese RV. Rosiglitazone, insulin treatment, and fasting correct defective activation of protein kinase C-zeta/lambdab by insulin in vastus lateralis muscles and adipocytes of diabetic rats. *Endocrinol* 2001;142(4):1595-605.
- Prasad CN, Anjana T, Banerji A, Gopalakrishnapillai A. Gallic acid induces GLUT4 translocation and glucose uptake activity in 3T3-L1 cells. *FEBS Lett* 2010;584(3):531-6.
- Jin L, Shi G, Ning G, Li X, Zhang Z. Andrographolide attenuates tumor necrosis factor-alpha-induced insulin resistance in 3T3-L1 adipocytes. *Molec Cell Endocrinol* 2011;332(1):134-9.
- Chen CC, Lii CK, Lin YH, Shie PH, Yang YC, Huang CS, et al. *Andrographis paniculata* Improves Insulin Resistance in High-Fat Diet-Induced Obese Mice and TNF $\alpha$ -Treated 3T3-L1 Adipocytes. *Am J Chin Med* 2020;48(5):1073-90.
- Vlavcheski F, Naimi M, Murphy B, Hudlicky T, Tsiani E. Rosmarinic Acid, a Rosemary Extract Polyphenol, Increases Skeletal Muscle Cell Glucose Uptake and Activates AMPK. *Mol* 2017;22(10).
- Buren J, Liu H, Jensen J, Eriksson J. Dexamethasone impairs insulin signalling and glucose transport by depletion of insulin receptor substrate-1, phosphatidylinositol 3-kinase and protein kinase B in primary cultured rat adipocytes. *Euro J Endocrinol* 2002;146(3):419-29.
- Brown PD, Badal S, Morrison S, Ragoobirsingh D. Acute impairment of insulin signalling by dexamethasone in primary cultured rat skeletal myocytes. *Mol Cell Biochem* 2007;297(1-2):171-7.
- Chalichem NSS, Gonugunta C, Krishnamurthy PT, Duraiswamy B. DPP4 Inhibitors Can Be a Drug of Choice for Type 3 Diabetes: A Mini Review. *Am J Alzheimer Dis other Demen* 2017;32(7):444-51.
- Shivanna Y, Raveesha KA. Dipeptidyl peptidase IV inhibitory activity of *Mangifera indica*. *J Nat Prod (India)*. 2010;3:76-9.
- Mohamed EAH, Siddiqui MJA, Ang LF, Sadikun A, Chan SH, Tan SC, et al. Potent  $\alpha$ -glucosidase and  $\alpha$ -amylase inhibitory activities of standardized 50% ethanolic extracts and sinensetin from *Orthosiphon stamineus* Benth as anti-diabetic mechanism. *BMC Complement Alternat Med* 2012;12(1):176.

# Vascular remodeling and association with inflammation in the heart of obesity model

Dwi Cahyani Ratna Sari, PhD<sup>1</sup>, Wiwit Ananda Wahyu Setyaningsih, MSc<sup>1</sup>, Yaura Syifanie, MD<sup>2</sup>, Alya Kamila, MD<sup>2</sup>, Fauziyatul Munawaroh, MD<sup>1,3</sup>, Nur Arfian, PhD<sup>1</sup>, Nungki Anggorowati, PhD<sup>4</sup>

<sup>1</sup>Department of Anatomy, Faculty of Medicine, Public Health and Nursing, Universitas Gadjah Mada, Yogyakarta, Indonesia, <sup>2</sup>Undergraduate Student Faculty of Medicine, Public Health and Nursing, Universitas Gadjah Mada, Yogyakarta, Indonesia, <sup>3</sup>Master Program of Biomedical Sciences, Faculty of Medicine, Public Health and Nursing, Universitas Gadjah Mada, Yogyakarta, Indonesia, <sup>4</sup>Department of Anatomical Pathology, Faculty of Medicine, Public Health and Nursing, Universitas Gadjah Mada, Yogyakarta, Indonesia

## ABSTRACT

**Introduction:** Obesity alters several metabolic activities, subsequently leading to the development of cardiovascular diseases. The insulin resistance-induced obesity stimulates vasodilatation and vasoconstriction imbalance, which ends up in cardiac vascular remodeling. Therefore, we aimed to investigate the effect of obesity in cardiac diseases with a focus on inflammatory mediators associated with endothelial dysfunction.

**Materials and Methods:** Rats (3 months old, weighing 200 g) were divided into control (n=6) and the obese groups, which included rats fed on a high-fat diet (HFD, n=6 in each subgroup) for 1 month (OB1), 2 months (OB2), and 4 months (OB4). Then, the rats were sacrificed, and their hearts were harvested for histological quantification as well as the quantification of the mRNA expression of inflammatory mediators, eNOS, and ppET-1 by reverse transcriptase-polymerase chain reaction (RT-PCR). Sirius Red staining was performed to assess vascular remodeling, while immunohistochemistry of CD68 was performed to assess the localization of macrophage.

**Results:** HFD-induced obesity was significantly manifested in the obese groups relative to that in the control group. It was followed by an increase in the mRNA expression of inflammatory mediators in the obese groups when compared to that in the control group. Long-term obesity promoted vascular remodeling, which was noted in the OB4 group, along with downregulation of the eNOS mRNA expression and the upregulation of the ppET-1 mRNA expression.

**Conclusion:** Obesity associated with inflammation and vascular remodeling in the heart.

## KEYWORDS:

Obesity, inflammatory mediators, vascular remodeling, eNOS, ppET-1

## INTRODUCTION

Obesity is a condition marked by the presence of excess fat tissues in several areas of the body that results in a high body

mass index (BMI). It has been known that people with BMI >30 are categorized as obese and that they may be at a greater risk to several health problems.<sup>1,2</sup> The prevalence of obesity has increased over several past decades in both developed and developing countries. In 2013, more than 50% of the population in Oceania, North Africa, and the Middle East countries were recorded as obese.<sup>3</sup> According to The Indonesian National Basic Health Research, the prevalence of people with BMI score >27 in Indonesia has increased since 2007, namely by 10.5%, 14.5%, and 21.8% in the years 2007, 2013, and 2018 respectively.<sup>4,5</sup>

Obesity is associated with heart failure, atrial fibrillation, sudden cardiac death, and myocardial steatosis.<sup>6,7,8,9</sup> High BMI correlates with a high level of fat mass and free fatty acid (FFA), which has a severe effect on the cardiovascular system.<sup>10</sup> An accumulation of adipose tissue increases the release of adipokines<sup>11</sup> and pro-inflammatory cytokines, such as IL-6 and TNF- $\alpha$ ,<sup>12</sup> which results in the infiltration of immune cells.<sup>13</sup> Hypertrophy and hyperplasia of the adipose tissues lead to lipotoxicity and alter lipid metabolism. An increase in the lipid metabolism promotes macrophage infiltration and activation mediated by nuclear factor kappa-light-chain-enhancer of the activated B cells (NF- $\kappa$ B) pathway. An increase in the level of FFA, cardiomyocyte fatty acid uptake exceeds the mitochondrial oxidative capacity, ultimately forming inclusions of lipid within the cardiomyocytes, also known as cardiac steatosis. This condition leads to lipotoxicity of the hearts.<sup>14</sup>

Inflammation contributes to the development of early endothelial dysfunction that leads to the development of atherosclerotic plaque. The acute phase protein and inflammatory mediators in circulation aggravates myocardial fibrosis and endothelial dysfunction. Imbalance vasodilator and vasoconstrictor agent are regulated by phosphatidylinositol 3-kinase-dependent (PI3K) and mitogen-activated protein kinase, respectively, in vascular endothelial tissues. Measuring the diameter and blood flow in coronary arteries is regarded as the gold standard to assess endothelial function.<sup>15,16</sup> This study was performed to explore the effect of obesity in the cardiovascular system with a focus on inflammatory mediators associated with endothelial dysfunction.

Corresponding Author: Dwi Cahyani Ratna Sari  
Email: dwi.cahyani@ugm.ac.id



## MATERIALS AND METHODS

### *Animal study*

This study was conducted according to the ethical approval of the Ethical Committee of Medical Research and Health of Faculty of Medicine, Public Health, and Nursing, Universitas Gadjah Mada (ethical expediency number KE/FK/0385/EC/2019). The rats were maintained at 25°C–30°C with 50%–60% humidity, under a dark-light cycle of 12:12 h.

Sprague–Dawley rats (age: 3 months, weight: 180–200 g) were divided into 4 groups, namely control group that received standardized food (Control, n = 6) and obese groups that were fed with a high-fat diet (HFD). The obese groups consisted of rats with obesity for 1-month (n = 6, OB1), obesity for 2 months (n = 6, OB2), and obesity for 4 months (n = 6, OB4) groups. Lee Index ( $(\sqrt[3]{\text{weight(grams)}})/\text{naso-anal length (mm)}$ ) was used to determine the level of obesity. At the due date, the rats were sacrificed, and their hearts were harvested. The area under the coronary sulcus was immersed in an RNA preservation solution (Favorgen, FARSS100) for RNA extraction, and the apex was immersed in 4% paraformaldehyde.

### *RNA Extraction and cDNA synthesis*

The heart of rat was extracted according to the procedural technique described by the manufacturer of the Genezol RNA Solution (GENEzol™, Cat. No. GZR100). Then, 3000 ng of total RNA was used to synthesis the cDNA. The synthesis of cDNA was performed using the cDNA Synthesis Kit (SMOBio, RP1400) with the PCR condition of 25°C for 10 min, 42°C for 50 min, and 85°C for 5 min.

### *Reverse transcriptase PCR (RT-PCR)*

Assessment of the mRNA expression of inflammatory mediators was done using CD68 (forward 5'-TGTTGCTTCCCAAGCAG-3' and reverse 5'-AAGAGAAGCATGGCCCAAG-3'), NFκB (forward 5'-CACTCTCTTTTGGAGGT-3' and reverse 5'-TGGATATAAGGCTTTACG-3'), and MCP-1 (forward 5'-GCTGTAGTATTTGTCACCAAGCTC-3' and reverse 5'-ACAGAAGTGCTTGAGGTGGT-3'). The mRNA expression of eNOS was assessed using forward 5'-CCGGCGCTACGAAGAATG-3' and reverse 5'-AGTGCCACGGATGGAAATT-3') and the ppET-1 performed using forward 5'-GTCGTCCCCTATGGACTAGG-3' and reverse 5'-ACTGGCATCTGTTCCCTTGG-3'). PCR conditions were denaturation at 94°C for 10 s, annealing at 60°C for 30 s, and extension at 72°C for 1 min, followed by the final extension phase end step at 72°C for 10 min. The RT-PCR was performed by mixing cDNA, Taq master mix (Promega, GoTaq Green, M7122), and primers. The PCR products were analyzed on 2% agarose gel along with a 100-bp DNA ladder (Bioron, Germany, Cat. No. 306009). The internal control used HRPT-1 (forward 5'-AGACGTTCTAGTCTGTGGC-3' and reverse 5'-ATCAAAGGGACGCAGCAAC-3') and β-actin (forward 5'-GCAGATGTGGATCAGCAAGC-3' and reverse 5'-GGTGAAAACGCAGCTCAGTAA-3'), was used to normalize the expression.

### *Immunohistochemistry staining of CD68*

The samples were cut into 4-μm-thick paraffin sections and placed in coated-object glass, followed by deparaffinizing

with xylene and rehydration with grading alcohol. Next, the antigen was retrieved using heat-induced antigen retrieval methods, followed by blocking peroxidase with 3% H2O2 in the PBS solution. Then, the slides were incubated with the blocking serum for 20 min and incubated with mouse 1st polyclonal antibody anti-CD68 (Abcam®, ab955; 1:300) overnight. On the following days, the slides were incubated with antibodies (Biocare Medical®, STUHRP700L10), and diaminobenzidine tetrahydrochloride (DAB) (Biocare Medical®, STUHRP700L10). The results were captured under a light microscope (Olympus CX22®) through the Optilab software with 400x magnification.

### *Statistical analysis*

Data were analyzed using the SPSS 22 software, and the normality test was performed by using Shapiro–Wilk. Normally distributed data were analyzed using One-way ANOVA and independent t-test. The significant value was determined if the *p*-value was less than 0.05.

## RESULTS

### *HFD feeding stimulated obesity in conjunction with the severity of cardiac inflammation*

According to the Lee Index, at the end of study, we showed that HFD feeding for 1, 2, and 4 months significantly caused obesity in Sprague-Dawley rats (*p* = 0.000). Starting at week 8, the body weight increased gradually, which was noted in OB2 (*p* = 0.009) and OB4 (*p* = 0.006) when compared to that in the control group. At week 12 and week 16, a remarkable escalation of the body weight in OB4 was noted to that in the control group (*p* = 0.000).

With an increase in the body weight, the inflammatory cytokines were upregulated. Long-term obesity provoked cardiac inflammation, which was obvious in the OB4 groups. The mRNA expression of NFκB, MCP1, and CD68 in the OB4 group was markedly elevated when compared to that in the control group (*p* < 0.05). However, the mRNA expression of NFκB and MCP1 in the OB1 group was not statistically different when compared to that in the control group (Fig. 1).

### *Obesity enhanced cardiac vascular remodeling via an imbalance of vasodilator and vasoconstrictor agent*

Finally, to evaluate the functional alteration induced by obesity, our results suggested a significant difference between the control and OB groups (*p* < 0.01). This alteration was accompanied by the downregulation of eNOS mRNA expression and the upregulation of ppET-1 mRNA expression in obese groups, particularly in the OB4 group (*p* < 0.05) (Fig. 2).

## DISCUSSION

Our results demonstrated that an HFD stimulates vascular remodeling mediated by the upregulation of inflammatory cytokines. It has been understood that obesity-induced low-grade inflammation as a result of the enlargement of adipocytes that leads to hypoxia and reactive oxygen species (ROS) development.<sup>17,18</sup> The circulating inflammatory mediators contribute to the development of cardiac inflammation in a time-dependent manner (Fig. 1). Abdominal white adipocyte tissue inflammation has also

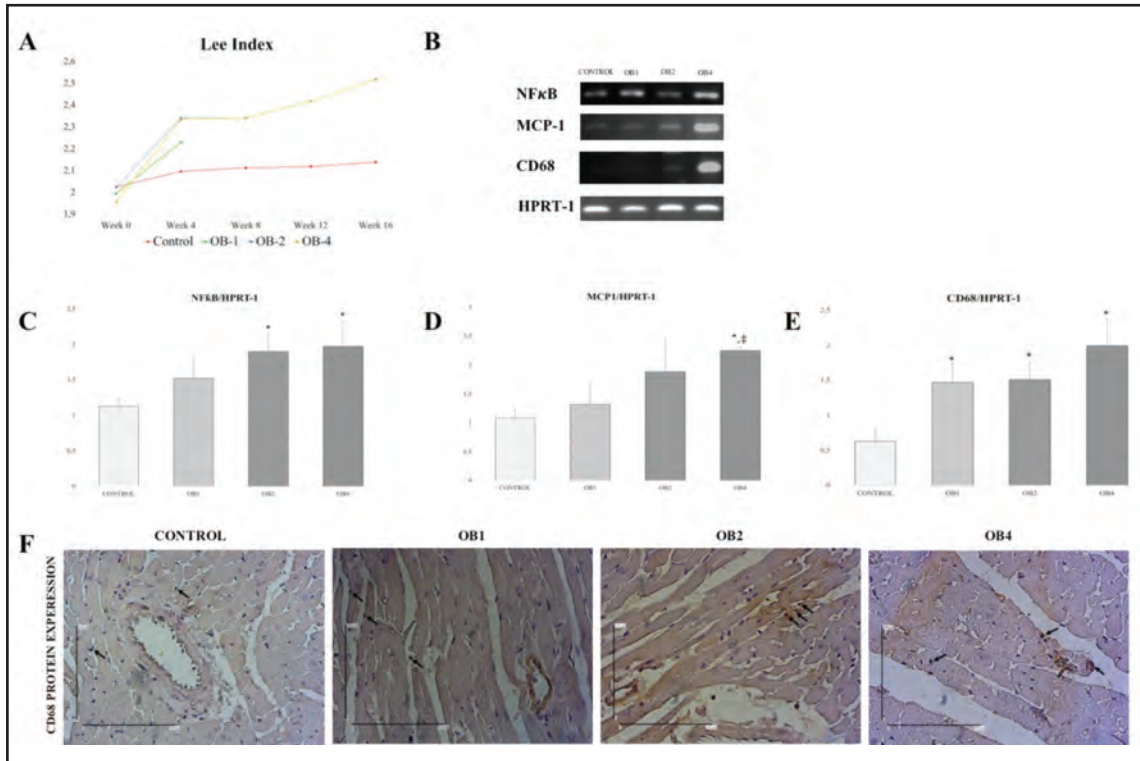


**Fig. 1:** Obesity associated with an increase in the level of inflammatory mediators. A. Bar chart of Lee Index. B. Representative figures of inflammatory mediators. C–E. Quantification of NFκB, MCP-1, and CD68 mRNA expression. F. CD68 protein expression.

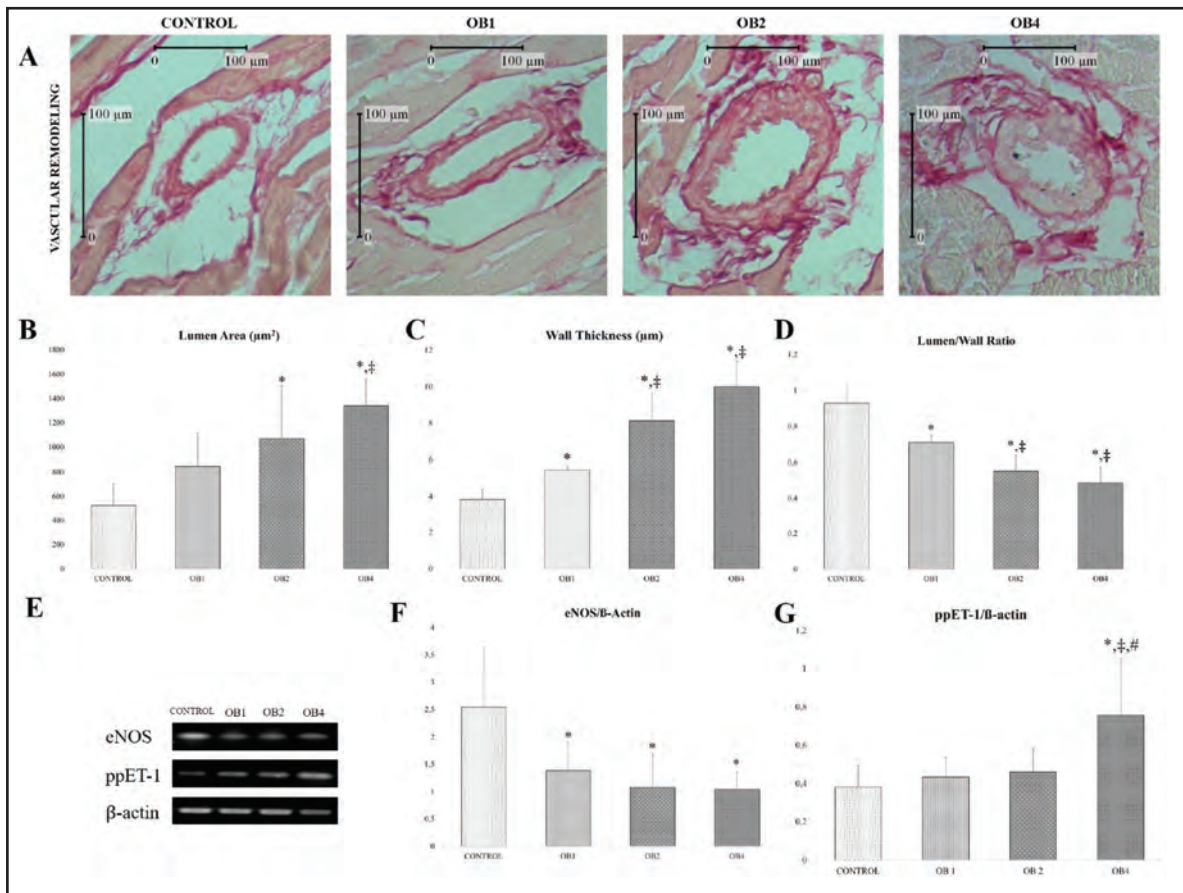


**Fig. 2:** Obesity-induced vascular remodeling. A. Representative figures of vascular remodeling by Sirius Red staining. B. Quantification of the lumen area. C. Quantification of the wall thickness. D. Quantification of the lumen/wall ratio. E. Representative figures of the eNOS and ppET mRNA expression. F. Quantification of the eNOS mRNA expression. G. Quantification of the eNOS mRNA expression.

been correlated with the development of cardiovascular diseases, such as atherosclerosis and diabetes mellitus type 2. The nuclear factor  $\kappa$ B (NF $\kappa$ B) luciferase reporter assay activity in an HFD showed markedly higher activity when compared to that in the abdominal region of low-fat-diet-fed male mice.<sup>19</sup> In obese db/db mice, the blockade of NF $\kappa$ B alleviated the oxidative stress and improved the cardiac function.<sup>18</sup> The FFA secreted by adipocyte tissues are recognized by Toll-like receptor 2/4 (TLR2/4), which is highly expressed in the cardiac tissues of HFD-induced mice model. Downstream of TLR, the activation of MyD88, an adaptor protein, plays a crucial role in inducing pro-inflammatory cytokine through the phosphorylation of I $\kappa$ B, which eventually leads to nuclear translocation of NF $\kappa$ B and the production of pro-inflammatory genes expression, including MCP-1.<sup>20-22</sup> Hypoxia and oxidative stress promote cardiac inflammation through HIF-1 $\alpha$ . HFD feeding enhances the upregulation of mRNA and protein HIF-1 $\alpha$  in adipocyte tissues in a time-dependent manner.<sup>23</sup> The crosstalk between NF $\kappa$ B and HIF-1 $\alpha$  has been well-documented. The proximal promoter of HIF-1 $\alpha$  contained a NF $\kappa$ B binding-site at -197/-188 bp under hypoxia. This condition promotes an increase in the NF $\kappa$ B activity and enhanced inflammatory response.<sup>24,25</sup>

Saturated fatty acid *per se* induces the NLRP3 inflammasome activation, which leads to IL-1 $\beta$  release in macrophage cell culture in a dose-dependent manner.<sup>26</sup> Macrophage and adipocyte cells expressed an abundance of CCR2 under metabolic disorders. This increment is in accordance with the elevation of CCL2 or MCP1 in the adipose tissues of obese rodents.<sup>27-29</sup> The circulating MCP-1 extricated by adipose tissues were doubled in obese diabetic (db/db) mice model when compared to that in lean mice as a control. An elevation of circulating MCP-1 level was positively correlated with an elevation of BMI, waist circumference, IL-6, and HOMA and negatively correlated with the HDL-cholesterol level.<sup>30</sup> Our result suggests that an elevation of MCP-1 was demonstrated in HFD feeding for 4 months (Fig. 1). Higher MCP-1 level has been strongly correlated to the development of atherosclerosis.<sup>30,31</sup> It promotes the recruitments of monocytes into the subendothelial layers. After entering the subendothelial layers, monocytes differentiate into macrophages that produce foam cells of the fatty streak. The deletion of CCR2 has been correlated with the attenuation of macrophage accumulation in the atherosclerotic lesion in apoE null mice with HFD feeding.<sup>32,33</sup>

CD68 is a glycosylated type-1 transmembrane glycoprotein that is mostly expressed by macrophages, other mononuclear phagocytes, and endothelial cells mainly located in the endosomal compartment. Upon responding to the inflammatory stimuli, CD68 was upregulated, and it is demonstrated an ability to bind modified LDL, phosphatidylserine, and apoptotic cells.<sup>34</sup> Long-term inflammation accelerates an increase in M1 macrophage polarization, which in turn markedly increases the CD68 expression. Injection of inflammatory proteins, TNF $\alpha$ , demonstrated a significantly higher intimal plaque formation in accordance with an increase in the CD68 protein expression.<sup>35</sup> In addition, an excess of oxidative stress, DNA damage, high glucose, and ceramides present in a chronic state of obesity, can develop cellular senescence,

which produces senescence-associated secretory phenotype (SASP). This SASP can stimulate further inflammation by secreting more IL-6, TNF- $\alpha$ , MCP1, and other cytokines. With other cellular senescence effects such as extracellular matrix dysfunction and pathological angiogenesis, the accumulation of cells undergoing cellular senescence may lead to aging or age-related disorders, including heart failure and atherosclerotic diseases.<sup>36</sup>

Obesity is commonly accompanied by insulin resistance, the elevation of leptin, and an alteration of the renin-angiotensin system that may cause sodium retention resulting in increased fluid volume which increases markedly by dilatation of the artery. Although the vein is known as the capacitance vessel, increased fluid volume causes dilation of the arterial lumen under the condition of increased body fluid volume. The disturbing vasodilation effect of chronic inflammation may occur in a longer obesity period, which ideally occurs in 6 months, although the longest obesity period in this study was only 4 months.<sup>37-39</sup> However, our results demonstrated thickening of the vascular wall in the obese groups (Fig. 2). In response to the higher lumen area, the wall thickens to compensate for luminal enlargement in order to normalize the stress on the wall.<sup>40</sup> Other than compensating for the wall stress, an increased level of insulin may increase the arterial wall thickness through the direct trophic effect of smooth muscle cells, the generation of ROS, protein kinase C, and activation of NF $\kappa$ B, which stimulates the growth and proliferation of vascular smooth muscle cells.<sup>41</sup> Metabolic changes due to obesity enhances the downregulation of the PI3K/Akt pathway, resulting in a decrease eNOS mRNA expression in 2 months obese-prone Sprague-Dawley rats fed on a HFD.<sup>42</sup>

Deposition of foam cells may increase the vascular wall thickness, which then stimulates the proliferation of vascular smooth muscle cells. The proliferation of vascular smooth muscle is often associated with an imbalance of vasoconstrictor and vasodilator agents represented by the upregulation of ppET-1 mRNA expression and the downregulation of eNOS mRNA expression in long-term obesity. Long-term obesity shown by the OB4 group involved enhanced upregulation of the ppET-1 mRNA expression caused by increased oxidative stress and chronic inflammation.<sup>43,44</sup>

## CONCLUSION

Obesity associated with inflammation and vascular remodeling in the heart.

## ACKNOWLEDGMENTS

We thank Mr. Mulyana for his animal maintenance support. This study was funded by Nutrifood Research Center Grant 2021 with No.SP/LG NFI-20. Some of the data had been used for completing the undergraduate program (Bachelor of Medicine) for Alya Kamila and Yaura Syifanie from the School of Medicine, Faculty of Medicine, Public Health, and Nursing, Universitas Gadjah Mada.



## REFERENCES

1. World Health Organization. Obesity and overweight fact sheet No. 311. World Health Organization; 2018.
2. GBD. Obesity collaborators. Health effects of overweight and obesity in 195 countries over 25 years. *N Engl J Med* 2017; 377(1): 13–27.
3. Ng M, Fleming T, Robinson M, Thomson B, Gratez N, Margono C, et al. Global, regional, and national prevalence of overweight and obesity in children and adults during 1980–2013: a systematic analysis for the Global Burden of Disease Study 2013. *Lancet* 2014; 384(9945): 766–81.
4. Kenchaiah S, Evans JC, Levy D, Wilson PWF, Benjamin EJ, Larson MG, et al. Obesity and the risk of heart failure. *N Engl J Med* 2002; 347(5): 305–13.
5. Huxley RR, Lopez FL, Folsom AR, Agarwal SK, Loefer LR, Soliman EZ, et al. Absolute and attributable risks of atrial fibrillation in relation to optimal and borderline risk factors: the atherosclerosis risk in communities (ARIC) study. *Circulation* 2012; 123(14): 612–24.
6. Adabag S, Huxley RR, Lopez FL, Chen LY, Sotoodehnia N, Siscovick D, et al. Obesity related risk of sudden cardiac death in the atherosclerosis risk in communities study. *Heart* 2015; 101(3): 215–21.
7. Mcgavock JM, Victor RG, Unger RH, Szczepaniak LS. Review adiposity of the heart, revisited. *Coll Am Physicians* 2017; 144(7): 517–25.
8. Ortega FB, Lavie CJ, Blair SN. Obesity and cardiovascular disease. *Circ Res* 2016; 118(11): 1752–70.
9. Halberg N, Wernstedt I, Scherer PE. The adipocyte as an endocrine cell. *Endocrinol Metab Clin North Am* 2009; 37(3): 1–15.
10. Tilg H, Moschen AR. Inflammatory mechanisms in the regulation of insulin resistance. *Mol Med* 2008; 14(3–4): 222–31.
11. Wisse BE. The inflammatory syndrome: the role of adipose tissue cytokines in metabolic disorders linked to obesity. *J Am Soc Nephrol* 2004; 15(11): 2792–800.
12. Zhang Y, Ren J. Role of cardiac steatosis and lipotoxicity in obesity cardiomyopathy. *Hypertension* 2011; 57(2): 148–50.
13. Muniyappa R, Sowers JR. Role of insulin resistance in endothelial dysfunctions. *Rev Endocr Metab Disord* 2013; 14(1): 5–12.
14. Csige I, Ujvárosy D, Szabó Z, Lorincz I, Paragh G, Harangi M, et al. The impact of obesity on the cardiovascular system. *J Diabetes Res* 2018; 2018: 3407306.
15. Cercato C, Fonseca FA. Cardiovascular risk and obesity. *Diabetol Metab Syndr* 2019; 11(74): 74.
16. Mariappan N, Elks CM, Sriramula S, Guggilam A, Liu Z, Borkhsenius O, et al. NF- $\kappa$ B-induced oxidative stress contributes to mitochondrial and cardiac dysfunction in type II diabetes. *Cardiovasc Res* 2010; 85(3): 473–83.
17. Carlsen H, Haugen F, Zadelaar S, Drevon CA, Blomhoff R. Diet-induced obesity increases NF $\kappa$ B signaling in reporter mice. *Genes Nutr* 2009; 4: 215–22.
18. Ko HJ, Zhang Z, Jung DY, Jun JY, Ma Z, Jones KE, et al. Nutrient stress activates inflammation and reduces glucose metabolism by suppressing AMP-activated protein kinase in the heart. *Diabetes* 2009; 58(11): 2536–46.
19. Liu T, Zhang L, Joo D, Sun SC. NF- $\kappa$ B signaling in inflammation. *Signal Transduct Target Ther* 2017; 2: 1–9.
20. Yu M, Zhou H, Zhao J, Xiao N, Roychowdhury S, Schmitt D, et al. MyD88-dependent interplay between myeloid and endothelial cells in the initiation and progression of obesity-associated inflammatory diseases. *J Exp Med* 2014; 211(5): 887–907.
21. He Q, Gao Z, Yin J, Zhang J, Yun Z, Ye J. Regulation of HIF-1  $\alpha$  activity in adipose tissue by obesity-associated factors: adipogenesis, insulin, and hypoxia. *Am J Physiol Endocrinol Metab* 2011; 300(5): E877–85.
22. Grolach A, Bonello S. The cross-talk between NF $\kappa$ B and HIF-1: further evidence for a significant. *Biochem J* 2008; 19: 17–9.
23. Garvey JF, Taylor CT, McNicholas WT. Cardiovascular disease in obstructive sleep apnoea syndrome: the role of intermittent hypoxia and inflammation. *Eur Respir J* 2009; 33(5): 1195–205.
24. Karasawa T, Kawashima A, Usui-Kawanishi F et al. Saturated fatty acids undergo intracellular crystallization and activate the NLRP3 inflammasome in macrophages. *Arter Thromb Vasc Biol* 2018; 744–56.
25. Panee J. Monocyte Chemoattractant Protein 1 (MCP-1) in obesity and diabetes. *Cytokine* 2012; 60(1): 1–12.
26. Weisberg SP, Mccann D, Desai M, Rosenbaum M, Leibel RL, Ferrante AW. Obesity is associated with macrophage accumulation in adipose tissue. *J Clin Invest* 2003; 112(12): 1796–808.
27. Weisberg SP, Hunter D, Huber R, Lemieux J, Slaymaker S, Vaddi K, et al. CCR2 modulates inflammatory and metabolic effects of high-fat feeding. *J Clin Invest* 2006; 116(1): 115–24.
28. Kanda H, Tateya S, Tamori Y et al. MCP-1 contributes to macrophage infiltration into adipose tissue, insulin resistance, and hepatic steatosis in obesity. *J Clin Invest* 2006; 116(6): 1494–505.
29. Kim CS, Park HS, Kawada T, Kim JH, Lim D, Hubbard NE, et al. Circulating levels of MCP-1 and IL-8 are elevated in human obese subjects and associated with obesity-related parameters. *Int J Obes (Lond)* 2006; 30(9): 1347–55.
30. Gonzalez-Quesada C, Frangogiannis NG. Monocyte Chemoattractant Protein (MCP-1)/CCL2 as a biomarker in acute coronary syndromes. *Curr Atheroscler Rep* 2010; 11(2): 131–138.
31. Harrington JR. The role of MCP-1 in atherosclerosis. *Stem Cells* 2000; 18(1): 65–66.
32. Chistiakov DA, Killingsworth MC, Myasoedova VA, Orekhov AN, Bobryshev YV. CD68/macrosialin: not just a histochemical marker. *Lab Invest* 2017; 97(1): 4–13.
33. Lee SG, Oh J, Bong SK, Kim JS, Park S, Kim S, et al. Macrophage polarization and acceleration of atherosclerotic plaques in a swine model. *PLOS ONE* 2018; 13(3): e0193005.
34. Tchkonina T, Zhu Y, van Deursen JV, Campisi J, and Kirkland JL. Cellular senescence and the senescent secretory phenotype: therapeutic opportunities. *J Clin Invest* 2013; 123(3): 966–72.
35. Wildman RP, Mehta V, Thompson T, Brockwell S, Sutton-Tyrrell K. Obesity is associated with larger arterial diameters in Caucasian and African-American young adults. *Diabetes Care* 2004; 27(12): 2997–9.
36. Korshunov VA, Berk BC. Flow-induced vascular remodeling in the mouse: a model for carotid intima-media thickening. *Vasc Biol* 2003; 23(12): 2185–91.
37. Madsen AN, Hansen G, Paulsen SJ, Lykkegaard K, Tang-Christensen M, Hansen HS, et al. Long-term characterization of the diet-induced obese and diet-resistant rat model: a polygenetic rat model mimicking the human obesity syndrome. *J Endocrinol* 2010; 206(3): 287–96.
38. Kozakova M, Palombo C, Morizzo C, Hojlund K, Hatunic M, Balkau B, et al. Obesity and carotid artery remodeling. *Nat Publ Gr* 2015; 5: 1–8.
39. Stapleton PA, James ME, Goodwill AG, and Frisbee JC. Obesity and vascular dysfunction. *Pathophysiology* 2008; 15(2): 79–89.
40. Garcia-Prieto CF, Hernandez-Nuno F, Rio DD, Ruiz-Hurtado G, Aranguiz I, Ruiz-Gayo M, et al. High-fat diet induces endothelial dysfunction through a down-regulation of the endothelial AMPK – PI3K – Akt – eNOS pathway. *Mol Nutr Food Res* 2014; 59(3): 1–13.
41. Donato AJ, Gano LB, Eskurza I, Silver AE, Gates PE, Jablonski K, et al. Vascular endothelial dysfunction with aging: endothelin-1 and endothelial nitric oxide synthase. *Am J Physiol Heart Circ Physiol* 2009; 297(1): H425–32.
42. Weil BR, Westby CM, Guilder Van GP, Greiner JJ, Stauffer BL, and DeSouza CA. Enhanced endothelin-1 system activity with overweight and obesity. *Am J Physiol Heart Circ Physiol* 2011; 301(3): H689–95.

# Gastric perforation in a 5-day-old infant: A case report

Luh Putu Neolita Pradnya Wineni, MD<sup>1</sup>, Ariandi Setiawan, MD<sup>2</sup>

<sup>1</sup>Pediatric Surgery Resident, Airlangga University Faculty of Medicine, Dr. Soetomo Regional Public Hospital, Surabaya, East Java, Indonesia, <sup>2</sup>Pediatric Surgeon, Department of Surgery, Pediatric Surgery Division, Airlangga University Faculty of Medicine, Dr. Soetomo Regional Public Hospital, Surabaya, East Java, Indonesia

## SUMMARY

**Gastric perforation in a new-born signifies a surgical emergency requiring immediate attention. Therefore, early diagnosis is expected to lead to a better prognosis. Any infant presenting with sudden and severe abdominal distention should be suspected of gastric perforation. Diagnosis is confirmed by pneumoperitoneum in the plain abdominal X-ray, including anteroposterior and lateral views. In this study, we report a case of a 5-day-old neonate, who was diagnosed with gastric perforation and accordingly proceeded with primary surgical repair.**

## INTRODUCTION

Gastric perforation in neonates is a serious and life-threatening condition associated with high morbidity and mortality rates. Spontaneous gastric perforation has been reported in approximately 1 in 2900 live births and accounts for 10-15% of all gastrointestinal perforation cases in neonates and children.<sup>1,2</sup>

Siebold in 1926 was the first to describe spontaneous gastrointestinal perforation. Stern, in his research, reported surgical repair, while Leger, in 1950, described the first successful repair of gastric perforation in neonates.<sup>3,4,7</sup> The causes of neonatal gastric perforation can be categorized into two groups: spontaneous/idiopathic or traumatic/iatrogenic. Spontaneous or idiopathic gastric perforation refers to that caused by unidentified underlying diseases and accounts for most cases. Meanwhile, iatrogenic gastric perforation case is usually caused by gastric tube insertion or intubation attempts.<sup>2,9</sup>

## CASE REPORT

A 5-day-old female infant presented with sudden abdominal distention since a day prior to her admission. Further history was taken from her parents, and we identified that her entire abdomen was distended and improved after the insertion of orogastric tube at the previous hospital. The frequency of her bowel movement found to be normal, ranging from 3 to 4 times a day with soft consistency. She had fever since abdominal distention and her abdominal skin appeared reddish on examination. The patient was referred from Walisongo General Hospital in Gresik and was treated with intravenous D10 (300 cc/24-h), ceftiofur (150mg /12-h), and santagesik (30 mg/8-h).

Antenatal history revealed that the patient was born a second pregnancy that was routinely checked by a midwife.

Antenatal ultrasonography (USG) was performed once during pregnancy by an obstetrician-gynecologist to present normal finding. Due to placenta previa, she was delivered by cesarean section at 38 – 39th week of gestation, with a birth weight of 3000 g and an APGAR score of 7 – 8.

The patient appeared lethargic and icteric (zone 2 on Kramer's scale) during her physical examination. The abdomen was found distended with reddish abdominal skin (Fig. 1A). Her bowel sounds decreased on auscultation, while the dullness of liver diminished on percussion. From rectal touché examination, we found that the tonus of sphincter ani collapse and mucosal surface was normal. Faeces, without blood, was found on the post-examination gloves. Urine output was 18 cc/2-h during the observation period at the emergency department (equal to 3 cc/kg/h).

The complete blood count test, result: hemoglobin 12.5 g/dL, WBC 3,980/uL, and platelets 139,000/uL. Her serum electrolytes levels were as follows: sodium 131 mEq/L, potassium 6.7 mEq/L, and chlorides 96 mEq/L. Her bleeding time was within normal limits. We performed plain thoracoabdominal X-ray or babygram as well as left lateral decubitus (LLD) imaging to reveal pneumoperitoneum, and the tip of the orogastric tube that appeared outside of the gastric contours, extending to the pelvic cavity. The LLD view revealed free intraperitoneal air (Fig. 1B).

Based on the results of her clinical examination and the subsequent workups, we suspected perforation of a hollow organ, and thus an emergency surgery was accordingly performed via explorative laparotomy for the primary repair of gastric perforation.

Prior to incision, 90 mg of intravenous cefazolin was administered as the surgery was considered susceptible to contamination. The surgical field was then disinfected, and the patient was draped with sterile surgical drapes. Upon transversal supraumbilical incision, air and faecal matters burst out when we reached the peritoneal cavity. Gastric perforation with a diameter of approximately 5 cm was identified at the posterior aspect of the gastric fundus near the greater curvature. Several minor tissues surrounding the stomach was detected in the slough. We also observed grade II-III intestinal adhesion. The peritoneal cavity lavage was accordingly performed. The minor tissues of the stomach were excised, and primary suturing of the perforated region was performed using 4.0 silk thread via simple interrupted and overhecting sutures. Further evaluation of the intestines including jejunum, ileum, and colon revealed no

Corresponding Author: Luh Putu Neolita Pradnya Wineni  
Email: wineini@gmail.com



**Fig. 1:** A. The patient's abdomen appeared distended and reddish with dilated veins. B. Babygram revealed pneumoperitoneum and the tip of the orogastric tube appeared outside of gastric contours and the LLD view showed free intraperitoneal air.

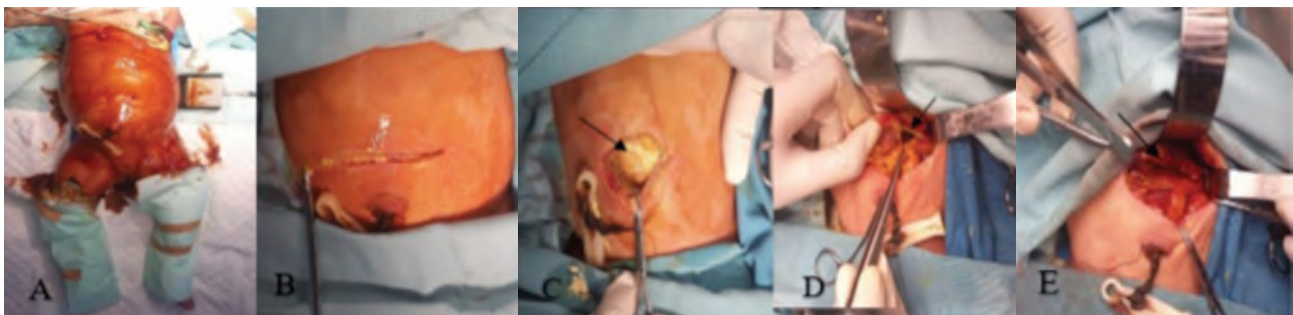


**Fig. 2:** A. Disinfecting the surgical field and draping the patient. B. Transversal supraumbilical incision. C. Air and fecal matters burst out when the peritoneal cavity was reached (arrow). D. Gastric perforation with a diameter of approximately 5 cm detected at the posterior aspect of gastric fundus near the greater curvature (arrow). E. Primary suturing using a 4.0 silk thread simple interrupted overhecting sutures (arrow).

abnormalities. Another peritoneal lavage was then performed, and the surgical incisions were closed. We did not perform any histopathological investigation.

The patient was admitted to the Neonatal Intensive Care Unit (NICU) for her post-operative care. Her respiration status deteriorated 8 h post-op, requiring mechanical ventilation as follows: PEEP 2, FiO<sub>2</sub> 35%, and the oxygen saturation was maintained >90%. She also went into a hypotensive state, but her hemodynamic status improved after resuscitation using intravenous saline, blood transfusion, and dopamine. Her abdomen was soft on palpation, showing no distention and discoloration. Total parenteral nutrition was administered via central vein catheter.

On the second day post-op, the patient was hemodynamically stable, and the ventilator parameters were reduced to the following: PEEP 3, FiO<sub>2</sub> 25%, and oxygen saturation > 90%. She was weaned-off the ventilator on the fifth day post-op when her condition had clearly improved. She was able to breath spontaneously supported by a nasal cannula. On the tenth day post-op, she resumed breastfeeding with no evidence of vomiting or bowel obstruction. She was finally discharged after 25 days of hospitalization, and we found that she even gained weight.

## DISCUSSION

Neonatal gastric perforation is classified as either spontaneous (idiopathic) or traumatic. However, in most cases, the aetiology is most likely multifactorial.<sup>3,5</sup> Sudden and unexplained abdominal over-distention that leads to organ perforation is regarded as a spontaneous one. Most cases presented in the first 7 days of life with various clinical manifestation.<sup>1,6</sup>

Chieh-Mo Lin et al. outlined that gastric acidity in a newborn is exceptionally high during the first week of life. While this does not indicate potential causality, it can possibly contribute to gastric perforation.<sup>8</sup> Another study by Chen et al. analyzed that preterm neonate with gastric perforations is at 4.21-times higher risk of mortality than full-term neonates.<sup>4</sup>

Infants with gastric perforation may present with respiratory distress, hemodynamic instability, and even symptoms suggestive of shock such as hypothermia, cyanosis, poor peripheral perfusion, and diminished urine output. The abdomen may also appear distended in a short amount of time, which may be a sign of peritoneal irritation.<sup>4</sup> In our case report, the patient was a 5-day-old infant who presented with sudden abdominal distention since 1 day before admission. We also recorded a history of fever that started at



the same time has the onset of distention. On clinical examination, marked abdominal distention, reddish abdominal skin, with dilated veins were observed. Bowel sounds were decreased on auscultation, and no liver dullness was found on percussion. Urine output upon observation at emergency department was 18 cc/2-h (equal to 3 cc/kg/h).

Laboratory studies are performed to aid diagnosis in gastric perforation cases, such as blood cultures, leukocytes count, haemoglobin, haematocrit, platelet count, electrolytes profile, and blood gas analysis.<sup>1,5</sup> In this patient, we observed workup results as follows: haemoglobin 12.5 g/dL, WBC3,980/uL, and platelet 139,000/uL. Serum electrolytes level were as follows: sodium 131 mEq/L, potassium 6.7 mEq/L, and chlorides 96 mEq/L.

Plain abdominal X-ray was also performed to aid diagnosis, which showed massive pneumoperitoneum indicated by the presence of air under diaphragm that extended laterally as well as subcutaneous emphysema, pneumoscrotum, ascites, or even the tip of oro- or nasogastric tube that extends beyond the gastric contours.<sup>2,3,6</sup> The plain thoracoabdominal X-ray or babygram as well as LLD view X-ray of this patient showed pneumoperitoneum and the tip of orogastric tube that appeared outside of the gastric contours, extending to pelvic cavity.

The initial management included hemodynamic stabilization by administering bolus intravenous fluid or blood transfusion, the administration of broad-spectrum antibiotic in case of infection, and primary peritoneal drainage to achieve better clinical outcome.<sup>1,2,7,8</sup> We performed early resuscitation on our patient but no primary peritoneal drainage, since emergency surgery could be arranged immediately, and the patient was placed in an optimal condition prior the surgery.

The main therapy for gastric perforation is surgical exploration, which is started via a transversal supraumbilical incision and evacuation of the peritoneal fluid, followed by exploration of the perforation site. When gastric perforation is not detected, careful exploration of the gastroesophageal junction, duodenum, small intestines, and large intestines must be performed. If gastric perforation is detected, which is usually near the greater curvature, then it must be closed in one or two layers and can be strengthened using an omental patch. After repairing the perforation, the peritoneal cavity lavage is usually performed using a warm saline solution.<sup>5,7,8</sup> In this patient, we performed explorative laparotomy and primary repair on the site of gastric perforation. No histopathological investigation was performed in this study and hence we could not identify the cause of the perforation.

Supportive care and resuscitation measures were continued post-op, broad-spectrum antibiotic administration, gastric acid suppression therapy, total parenteral nutrition, as well as gastric decompression. Enteral nutrition was started after the patient's condition had stabilized. Several of surgeons perform contrast studies prior to initiation of enteral nutrition.<sup>7,8,16</sup> The present patient was admitted to the (NICU)

for post-operative care. Her respiration status deteriorated 8 h post-op and required mechanical ventilation. She also went into a hypotensive state, hence we performed resuscitation using intravenous saline, blood transfusion, and dopamine. Total parenteral nutrition was administered via the central vein catheter. The next day, the patient's condition had improved, and she was weaned-off the ventilator on her fifth day post-op. On the tenth day post-op, she resumed breastfeeding and was finally discharged after 25 days of hospitalization.

The clinical factor associated with poor prognostic outcome included sepsis, metabolic acidosis, and hyponatremia. Early diagnosis and identification of perforation and appropriate supportive treatment was deemed essential for the best possible clinical outcome.<sup>1,4,9</sup>

## CONCLUSION

Gastric perforation in newborns is a serious and life-threatening condition. Newborns, especially those of premature or low birth weight, who present with progressive abdominal distention with or without pneumoperitoneum should be suspected of gastric perforation.

Initial management of gastric perforation includes early diagnosis, resuscitation, stabilization, and surgical exploration. Early resuscitation can serve as a primary management for neonates to immediately stabilize their general condition prior to the main surgery, in order to achieve the best possible clinical outcome.

## REFERENCES

1. Adam CA and Robert KM. Gastric perforation in newborn surgery, 4th ed. CRC Press; 2018:65-570.
2. Holcomb GW, Murphy JP, St Peter SD. Lesions of the Stomach in Holcomb and Ashcraft's Pediatric Surgery. 7th edition. Elsevier Health Sciences. 2019; 478-88.
3. Duran R, Inan M, Vatansever U, Aladağ N, Acunaş B. Etiology of neonatal gastric perforations: review of 10 years' experience. *Pediatr Int* 2007; 49(5):626-30.
4. Chen TY, Liu HK, Yang MC, Yang YN, Ko PJ, Su YT, et al.. Neonatal gastric perforation: a report of two cases and a systematic review. *Medicine* 2018;97(17).
5. Oztürk H, Onen A, Otçu S, Dokucu AI, Gedik S. Gastric perforation in neonates: analysis of five cases. *Acta Gastro-Enterol Belg* 2003;66(4):271-3.
6. Cardiel-Marmolejo LE, Peña A, Urrutia-Moya L, Crespo-Smith D, Morales-Vivas CA, Camacho-Juárez KV, and Roque-Ibáñez C. Neonatal gastric perforation: a case report. *Rev Medica del Hosp Gen de Mex* 2018; 81:36-40.
7. Prashant SP, Abhaya G, Paras LK. Gastric perforation in two neonates: Spontaneous? Secondary to feeding tube: A case report. *SM J Pediatr Surg* 2016;2(1):1009.
8. Kshirsagar AY, Vasisth GO, Ahire MD, Kanojiya RK, Sulhyan SR. Acute spontaneous gastric perforation in neonates: a report of three cases. *Afr J Paediatr Surg* 2011;8(1):79.
9. Kim E. Gastric perforation in a newborn. *J Pediatr Surg Case Rep* 2019; 43:87-9.
10. Desouki K, Osman MK. Gastric perforation in neonates: analysis of five cases. *Ann Pediatr Surg* 2006;2(1):45-7.

# Increased CD4/CD8 T-cell ratio : A risk factor for mortality in patients with coronavirus disease 2019

Adika Zhulhi Arjana, MD, Komang Agus Trisna Amijaya, MD, Sagita Adventia, MD, Teguh Triyono, PhD, Umi Solekhah Intansari, PhD

Department of Clinical Pathology and Laboratory Medicine, Faculty of Medicine Public Health and Nursing, Universitas Gadjah Mada, Yogyakarta, Indonesia

## ABSTRACT

**Introduction:** Although CD4 and CD8 T-cells are the main subset of T-lymphocytes, their roles in COVID-19 infection and severity remain unclear. This study aimed to determine the role of increased CD4/CD8 T-cells ratio as a risk factor for cases of 28-days in-hospital mortality in COVID-19 patients.

**Materials and Methods:** This study employed a prospective cohort design. Inclusion criteria were confirmed COVID-19 cases with a positive polymerase chain reaction report. CD4 and CD8 T-cells absolute counts were measured by flow cytometry. The CD4/CD8 ratio was calculated by dividing the absolute count of CD4 by that of CD8 T-cells.

**Results:** A total of 85 subjects were followed for 28 days. The mean age of the subjects was 52.64 years, and majority of them were females (51.8%). Twenty-eight (32.9%) subjects died within 28 days of follow-up. Receiver operating characteristics analysis obtained an area under curve of 0.68 with the cut-off value 1.26 with  $p = 0.005$ . Kaplan–Meier’s analysis obtained Hazard Ratio 2.91 (95%CI 1.377–6.161;  $p = 0.0052$ ).

**Conclusion:** Subjects with an increase in CD4/CD8 T-cells ratio  $>1.26$  had a 2.91-times risk of 28 days in-hospital mortality.

## KEYWORDS:

CD4/CD8 T cells ratio, T cell lymphocyte, COVID-19, mortality risk, laboratory testing, SARS COV-2

## INTRODUCTION

The pathophysiological process of SARS COV-2 infection is not as yet clearly understood, including the underlying death mechanism in COVID-19 patients, which is suspected to be due to the occurrence of a cytokine storm that has a direct impact on cardiac cell damage.<sup>1</sup> Several cytokines whose level increases under the condition include INF- $\gamma$ , IL-1 $\beta$ , IL-6, IL-8, IL-12, and TNF- $\alpha$ , which were known to cause acute respiratory distress syndrome (ARDS).<sup>2</sup> Another hypothesis suggests the occurrence of bacterial sepsis as a secondary infection.<sup>3</sup> Several studies have shown traces of SARS-CoV-2 virus in cases of death occurring in several hematological laboratory parameters such as neutrophil to lymphocyte

ratio, relative lymphocytopenia, and platelet to lymphocyte ratio through a cytokine storm mechanism.<sup>2,4,5</sup>

Lymphocytopenia was a common finding in COVID-19 patients that may be a critical factor associated with disease severity and mortality.<sup>6</sup> The mechanism of lymphopenia could be explained by several possible theories, including (i) direct viral infection of lymphocytes, (ii) viruses infecting the lymphatic organs, (iii) apoptosis of lymphocytes due to a cytokine storm, and (iv) inhibition of lymphocyte metabolism that suppresses their proliferation.<sup>5</sup> The development mechanism of this laboratory finding remains unclear. The examination of the CD4/CD8 T-cell ratio will provide an overview of the response of the T-lymphocyte subset. This ratio is often employed in monitoring patients infected with the human immunodeficiency virus (HIV). A CD4/CD8 T-cell ratio  $<1$  indicates a weakened immune system as the number of CD4 T-cells decreases and their proportion is replaced by those of CD8 T-cells. The decrease in this ratio illustrates the weak level of patient immunity resulting in an increased risk of infection.<sup>7</sup> On the other hand, an increase in the ratio of CD4/CD8 T-cells indicates an increase in the rapid immune response against viruses.

This study aimed to determine the role of CD4/CD8 T-cell ratio increment as a risk factor for the occurrence of death in COVID-19 patients.

## MATERIALS AND METHODS

This study employed a prospective cohort design. The inclusion criteria were confirmed adult COVID-19 patients (based on the results of the COVID-19 polymerase chain reaction [PCR] examination) and having received treatment at Dr. Sardjito Hospital (SH), both as an inpatient or an outpatient. Patients who were pregnant and who had history of impaired immune system were excluded. Subjects were recruited from December 2020 to March 2021, on the first day of confirmed COVID-19 based on their PCR report. Patients agreed to participate in the study by signing an informed consent form either by themselves or their entitled family member. This research received ethical approval from the ethics committee of the Faculty of Medicine, Public Health and Nursing Universitas Gadjah Mada with the approval number KE/FK/0398/EC/2021.

Corresponding Author: Umi Solekhah Intansari  
Email: umintansari@ugm.ac.id



**Table I: Subject characteristics**

Parameter	n (%)
Age (year), Median (range)	57 (18–83)
Male	41 (48.2)
Female	44 (51.8)
Severity	
Mild	9 (10.6)
Moderate	28 (32.9)
Severe	47 (55.3)
Critical	1 (1.2)
Length of stay (days), median (range)	12 (2–67)

**Table II: Initial laboratory parameters at hospital admission**

Parameter	Mean (± SD) / Median (range)
Hb (g/dL)	11.33 (± 2.51)
Leukocyte count (x10 <sup>3</sup> cell/μL)	8.54 (2.11–31.37)
Lymphocyte count (x10 <sup>3</sup> cell/μL)	1.26 (± 0.65)
Lymphocyte percentage (%)	13 (1.6–37.6)
CD4 cell count (cell/μL)	254 (13–1066)
CD4 cell percentage (%)	30.66 (3.61–68.96)
CD8 cell count (cell/μL)	222 (21–1049)
CD8 cell percentage (%)	23.96 (2.65–52.76)
CD4/CD8 ratio	1.27 (0.26–5.72)

**Table III: Clinical outcome and laboratory examination results**

Parameter	Survivor N = 57	Dead N = 28	p
Age, median (min–max)	51 (18–72)	63 (35–83)	<0.0001
Male, n (%)	22 (53.7)	19 (46.3)	0.0117
Female, n (%)	35 (79.5)	9 (20.5)	
Severity			<0.001
Mild, n (%)	7 (77.8)	2 (22.2)	
Moderate, n (%)	28 (100)	0 (0)	
Severe, n (%)	22 (53.2)	25 (46.8)	
Critical, n (%)	0 (0)	1 (100)	
Length of treatment (days), median (min–max)	13 (10–67)	10 (2–27)	0.0241
Laboratory parameter			
Hb (g/dL), mean ± SD	11.42 (± 2.63)	11.24 (± 2.45)	0.8234
Leukocyte count (x10 <sup>3</sup> cell/μL), median (min–max)	8.03 (2.11–31.37)	10.15 (3.69–30.03)	0.0787
Lymphocyte count (x10 <sup>3</sup> cell/μL), mean ± SD	1.41 (± 0.69)	0.99 (± 0.47)	0.0075
Lymphocyte percentage (%), median (min–max)	15.2 (4.5–37.6)	7.3 (1.6–32.9)	0.0010
CD4 cell count (cell/μL), median (min–max)	340 (39–1066)	219 (13–869)	0.0033
CD4 percentage (%), median (min–max)	30.32 (9.26–68.96)	31.45 (3.61–43.98)	0.8959
CD8 cell count (cell/μL), median (min–max)	255 (62–902)	109 (21–1049)	0.0016
CD8 percentage (%), median (min–max)	26.87 (7.81–51.39)	18.65 (2.65–52.76)	0.0021
CD4/CD8 ratio, median (min–max)	1.18 (0.35–5.72)	1.51 (0.26–3.95)	0.0136

Blood samples were obtained from the selected subjects (3 mL of the blood in an EDTA tube) within 24 hours of confirmed COVID-19 tests. Complete blood count analysis was performed with Sysmex XN-1000. Blood samples were then examined by flow cytometry using FACS Canto II with the lyse wash principle. The samples were incubated with CD3 FITC, CD4 PE, and CD8 FITC reagents for 15 min in a dark room and read within 2 hours of incubation. The parameters measured included complete blood count and CD4 and CD8 cells count.

The recruited subjects underwent treatment according to the standard of care at SH. The outcome measured in this study

was death within 28 days of hospitalization (28 days in-hospital mortality). Follow-up was conducted for subjects for 28 days after being confirmed positive for COVID-19 and the outcome of death was recorded. The outcomes were categorized as survivors or dead. The survivors were subjects who were declared recovered and discharged from SH or being treated within 28 days. Meanwhile, the subjects who died within 28 days of treatment were categorized as dead.

Categorical data was presented in the form of frequency and proportion. Data with normal distribution are presented in the form of mean ± standard deviation (SD). Data with abnormal distribution are presented in the form of the

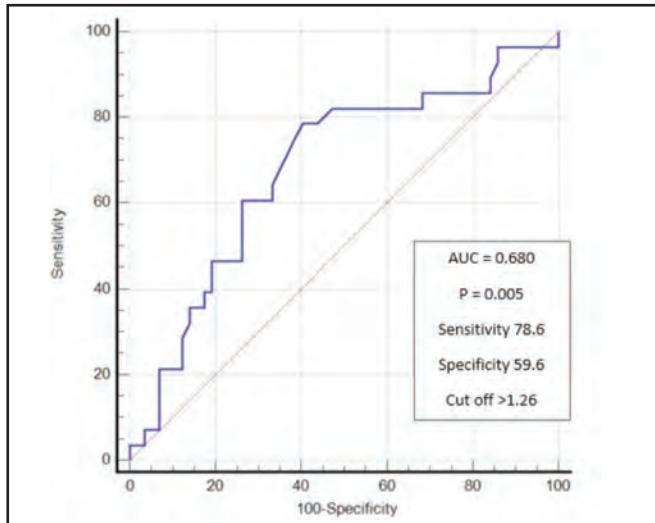


**Fig. 1:** ROC analysis of CD4/CD8 ratio toward mortality outcome in 28 days of treatment.

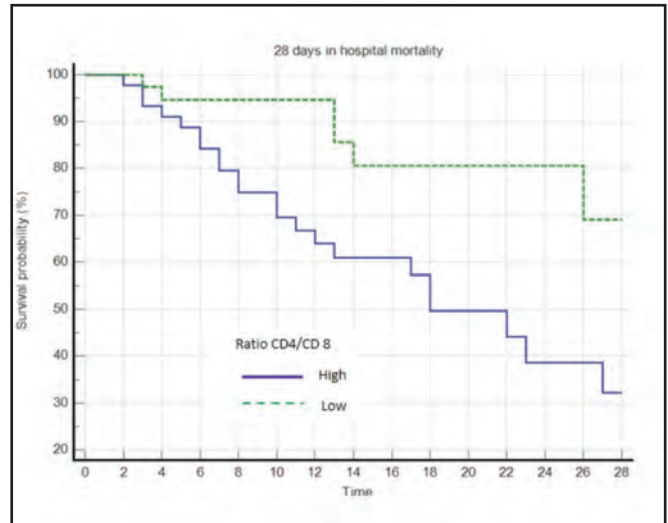


**Fig. 2:** Kaplan-Meier curve analysis of survival with CD4/CD8 ratio toward mortality outcome in 28 days of treatment.

median (min-max). Statistical analysis was performed by the Receiver Operating Characteristics (ROC) curve to obtain the cutoff value, and Kaplan-Meier analysis was performed to assess the prognosis of death. All statistical analyzes were performed using the Medcalc software, and  $p < 0.05$  was considered to indicate statistical significance.

## RESULTS

A total of 85 subjects were included in this study. The mean age of the subjects was 52.64 years and majority of the subjects were women (51.8%). A total of 47 subjects (55.3%) were admitted to the hospital with severe conditions. The length of stay at the hospital varied between 2 and 67 days (Table I).

Fifty subjects (65.8%) had a lymphocyte count of  $<18\%$  with an overall median of 13%. The median percentage of CD4 T-cells was 30.66%, while that of CD8 T-cells was 23.96%. The overall CD4/CD8 T-cell ratio ranged widely from 0.26 to 5.72 (Table II).

Twenty-eight subjects (32.9%) died within 28 days of hospitalization. The fastest length of treatment was 2 days in the dead group and 10 days in the survivor group. There was a significant difference between the groups for the ratio of CD4/CD8 T-cells, with the median in the dead group being significantly higher ( $p < 0.05$ ) (Table III). ROC analysis for the ratio of CD4/CD8 T-cells obtained an area under curve of 0.68, with a cutoff value of 1.26 and  $p = 0.005$  (Figure 1). A total of 45 subjects (52.94%) showed a CD4/CD8 T-cell ratio  $>1.26$ .

Statistical analysis: proportion difference test using Chi-squared test, difference test with normal distribution using independent t-test, difference test with abnormal distribution using Mann-Whitney test.

The analysis was continued with Kaplan-Meier, obtaining a hazard ratio of 2.91 (95% CI 1.377–6.161;  $p = 0.0052$ ),

indicating that the subjects with an increased CD4/CD8 T-cell ratio of  $>1.26$  had a 2.91-times risk of death in 28 days of treatment (Fig. 2).

## DISCUSSION

The pathophysiology of COVID-19 in causing cytokine storms remains unclear. The involvement of T-cells in case progression also remains unclear. Preliminary evidence suggests that lymphocytopenia supports the aggravation of the disease.<sup>8</sup> The results of this study showed a similar finding, suggesting that the percentage of lymphocytes decreased in the dead group. These findings confirm the role of T-cells in the pathophysiology of COVID-19.

Previous studies have suggested a correlation between the proportion of a subset of T-cells and disease severity. Lower levels of CD4 and CD8 T-cells were associated with the severe and critically severe groups.<sup>9</sup> The results of this study showed similar findings in the dead group with significant differences.

T-cells, mainly consisting of CD4 and CD8 T-cells, play a major role in the adaptive immune system. T-cells act as a mediator of antibody responses produced by B cells.<sup>10</sup> Pathogenic exposure to CD4 T-cells either directly or mediated by dendritic cells trigger the differentiation of T-cells into their subsets, which then produce interleukin 12. This response ultimately triggers antibody production.<sup>11</sup> In terms of the response to infection with the SARS-CoV-2 virus, this exposure triggers the emergence of antibodies to the virus.<sup>12,13</sup> Likewise, CD8 T-cells that act as cytotoxic can eliminate cells infected with the SARS-CoV-2 virus through the abnormal recognition of MHC class 1.<sup>14,15</sup> The findings in this study indicate a fatigue response of CD4 and CD8 T-cells in patients with aggravation, leading to death.

Deaths that occur in COVID-19 patients are suspected to occur through 2 mechanisms, namely cytokine storm and secondary infection leading to bacterial sepsis.<sup>3,16,17</sup> The results

of this study demonstrated a quantitative decrease in the immune response in the dead group. An exhausted immune system is described by a decrease in the number of CD4 and CD8 T-cells. Although this study did not describe the kinetics of the two subsets of T-lymphocytes, the significant differences between the two groups could justify this point. Past studies conducted on infants of mothers confirmed positive COVID-19 showed normal levels of CD4 and CD8 T-cells in patients with negative results.<sup>18</sup> This finding indicates the kinetics of decreasing levels of CD4 and CD8 T-cells along with the fatigue level of the immune response.

The ratio of CD4/CD8 T-cells is a parameter that can indicate the function of adaptive immunity. This ratio is often used in monitoring patients with HIV to determine the condition of immunity and susceptibility to opportunistic infections.<sup>7,19</sup> In the case of COVID-19, this parameter could be used as a reference to assess the risk of secondary infection. Another study has indicated no significant difference in the CD4/CD8 T-cell ratio between different levels of severity.<sup>9</sup> This study reported that an increase in the ratio of CD4/CD8 T-cells >1.26 had a significantly higher risk of death. This mechanism is suspected in line with the increased risk of secondary infection.

## CONCLUSION

This study concludes that CD4/CD8 T-cell ratio >1.26 increases the risk of death of COVID-19 patients by 2.91-times. The limitations of the present study include that it did not measure the kinetics of the CD4/CD8 T-cell ratio and the examination of secondary infections in the subjects. Kinetic data is expected to assist in the analyses of the changes occurring in patients with varying clinical status as well as to confirm the current findings.

## ACKNOWLEDGMENT

The authors express gratitude to all subjects and PT. BD Indonesia for the aid of this study. This study was funded by Faculty of Medicine Public Health and Nursing, Universitas Gadjah Mada through Dana Masyarakat 2021 research grant.

## REFERENCES

1. Santoso A, Pranata R, Wibowo A, Al-Farabi MJ, Huang I, Antariksa B. Cardiac injury is associated with mortality and critically ill pneumonia in COVID-19: A meta-analysis. *Am J Emerg Med* 2021; 44: 352–7.
2. Li X, Xu S, Yu M, Wang K, Tao Y, Zhou Y, et al. Risk factors for severity and mortality in adult COVID-19 inpatients in Wuhan. *J Allergy Clin Immunol* 2020; 146:110–8.

3. Lin HY. The severe COVID-19: A sepsis induced by viral infection? And its immunomodulatory therapy. *Chin J Traumatol* 2020; 23: 190–5.
4. Xu P, Zhou Q, Xu J. Mechanism of thrombocytopenia in COVID-19 patients. *Ann Hematol* 2020; 146: 110–8.
5. Tan L, Wang Q, Zhang D, Ding J, Huang Q, Tang YQ, et al. Lymphopenia predicts disease severity of COVID-19: a descriptive and predictive study. *Signal Transduct Target Ther* 2020; 5: 33.
6. Xu Z, Shi L, Wang Y, Zhang J, Huang L, Zhang C, et al. Pathological findings of COVID-19 associated with acute respiratory distress syndrome. *Lancet Respir Med* 2020; 8: 420–2.
7. Sainz T, Serrano-Villar S, Díaz L, Tome MIG, Gurbindo MD, De José MI, et al. The CD4/CD8 ratio as a marker T-cell activation, senescence and activation/exhaustion in treated HIV-infected children and young adults. *AIDS* 2013; 27: 1513–6.
8. Oliveira DS, Medeiros NI, Gomes JAS. Immune response in COVID-19: What do we currently know? *Microb Pathog* 2020; 148: 104484.
9. Liu R, Wang Y, Li J, Han H, Xia Z, Liu F, et al. Decreased T cell populations contribute to the increased severity of COVID-19. *Clin Chim Acta* 2020; 508: 110–4.
10. Gorczynski R, Stanley J. *Clinical immunology*, 1st ed. Vademecum; 2013.
11. Abbas AK, Lichtman AH, and Pillai S. *Cellular and Molecular Immunology*. Saunders; 2008.
12. Long QX, Liu BZ, Deng HJ, Wu GC, Deng K, Chen YK, et al. Antibody responses to SARS-CoV-2 in patients with COVID-19. *Nat Med* 2020.
13. Randolph HE and Barreiro LB. Herd immunity: Understanding COVID-19. *Immunity* 2020; 52: 737–41.
14. Jiang Y, Wei X, Guan J, Qin S, Wang Z, Lu H, et al. COVID-19 pneumonia: CD8+ T and NK cells are decreased in number but compensatory increased in cytotoxic potential. *Clin Immunol* 2020; 218: 108516.
15. Ganji A, Farahani I, Khansarinejad B, Ghazavi A, Mosayebi G. Increased expression of CD8 marker on T-cells in COVID-19 patients. *Blood Cells Mol Dis* 2020; 83: 102437.
16. Khamis F, Memish Z, Bahrani M Al, Dowaiqi S Al, Pandak N, Bolushi Z Al, et al. Prevalence and predictors of in-hospital mortality of patients hospitalized with COVID-19 infection. *J Infect Public Health* 2021; 14: 759–65.
17. Chen X, Huang J, Huang Y, Chen J, Huang Y, Jiang X, et al. Characteristics of immune cells and cytokines in patients with coronavirus disease 2019 in Guangzhou, China. *Hum Immunol* 2020; 81: 702–8.
18. Liu P, Zheng J, Yang P, Wang X, Wei C, Zhang S, et al. The immunologic status of newborns born to SARS-CoV-2-infected mothers in Wuhan, China. *J Allergy Clin Immunol* 2020; 146: 101–9.
19. Serrano-Villar S, Gutiérrez C, Vallejo A, Hernández-Novoa B, Díaz L, Abad Fernández M, et al. The CD4/CD8 ratio in HIV-infected subjects is independently associated with T-cell activation despite long-term viral suppression. *J Infect* 2013; 66: 57–66.

# Unusual radiological findings of pediatric jejunojejunal intussusception: A case report

Fransiska Kusumowidagdo, MD<sup>1</sup>, Dian Adi Syahputra, MD<sup>2</sup>, Vita Indriasari, MD<sup>3</sup>

<sup>1</sup>Pediatric Surgery Division, Department of Surgery, Airlangga University, Soetomo General Hospital, Surabaya, Indonesia, <sup>2</sup>Pediatric Surgery Division, Department of Surgery, Syiah Kuala University, Zainoel Abidin Regional General Hospital, Banda Aceh, Indonesia, <sup>3</sup>Pediatric Surgery Division, Department of Surgery, Padjadjaran University, Hasan Sadikin General Hospital, Bandung, Indonesia

## SUMMARY

**Intussusception is a common cause of intestinal obstruction in children, especially in those of age <5 years. The typical signs and symptoms of this condition is colicky abdominal pain, bloody mucous stool, and palpated abdominal mass, with a classic target sign finding on abdominal ultrasound. In older children, the symptoms may vary, which necessitates investigation of the cause of intussusception, as it is often caused by a pathologic lead point. We report here the case of a 14-year-old girl with total bowel obstruction, hematochezia, a very dilated reverse C-shaped bowel loop, and intestinal pneumatosis on abdominal X-ray. During laparotomy, we detected jejunojejunal intussusception caused by jejunal polyp. After bowel resection and anastomosis, the patient recovered well and had no other events during follow-up.**

## INTRODUCTION

Intussusception is a condition in which one segment of the intestine telescope inside of another to cause obstruction, and it most commonly recorded in children aged 6 months to 3 years. Although it is mostly idiopathic, 4% of all cases may be caused by a pathological lead point (PLP) that is usually found in children of age >5 years or in adolescents.<sup>1</sup> Intestinal pneumatosis (IP) is described as an abnormal intramural gas of the digestive tract. The presentation of PI may suggest the occurrence of life-threatening conditions, such as gastrointestinal perforation, ischemic bowel, and bowel necrosis.<sup>2</sup> We report here the case of a 14-year-old girl with bowel obstruction and a very dilated reverse C-shaped bowel loop and IP on abdominal X-ray caused by jejunojejunal intussusception.

## CASE REPORT

A 14-year-old girl visited the Emergency Department (ED) of Soetomo General Hospital, Surabaya, Indonesia with intermittent colicky pain for the last 6 days, especially at the epigastric and left abdominal areas. The pain lasted for 5–10 min at each episode. Nausea and vomiting also occurred, eventually progressing to bilious vomiting. The patient did not have any bowel movements for the past 6 days and admitted to enable her to pass gas. At the ED, she had hematochezia with no mucous. Previously, she was admitted to a secondary hospital and then sent to our hospital. She was weak and somnolent at the time of admission,

tachycardic (172 beats per min) with raised body temperature to 38.3°C. The nasogastric tube production was bilious, 300 mL within 12 hours. There was no abdominal distention, bowel contour, or bowel movement. The bowel sound was decreased with muscular guarding. Digital rectal examination revealed collapsed ampulla, no mass, with fresh colored blood on the gloves. Laboratory findings were normal, but her C-Reactive Protein (CRP) level was raised to 27.2 mg/L (normal value: <6 mg/L). Central venous catheter insertion, fluid resuscitation, and broad-spectrum antibiotic administration were accordingly performed. A plain abdominal X-ray showed a reverse C-shaped dilated bowel with massive IP (Fig. 1). Further abdominal CT scan study revealed bowel obstruction due to jejunojejunal intussusception.

We performed exploratory laparotomy and found bloody peritoneal fluid and jejunojejunal intussusception with necrotic intussusception of the bowel, which could only be partially released. The intussusceptum was also necrotic with multiple perforations. We resected 48 cm of the jejunal segment from 10-cm distal to the Treitz ligament and performed end to end jejunojejunal anastomosis. After resecting, the bowel was opened, and we detected a jejunal polyp. We palpated the rest of the bowel and found no other polyp.

Histopathological examination revealed ulcerated jejunum with a wide ischemic and bleeding site, most of which were filled with lymphocytes, histiocytes, erythrocytes extravasation, and infarcted polyp. Multiple trapped air bubbles were found in the submucosa (Fig. 2). The polyp could not be evaluated further because it was probably already necrotic for quite some time, albeit there was no malignant cell.

After surgery, the patient has put nil per month for 2 days due to postoperative paralytic ileus, and oral feeding was started on the 3rd postoperative day. She received 3rd generation of cephalosporin and analgesics. The patient recovered uneventfully after 5 days of recovery time. She recovered well and, at 2 weeks of follow-up, the wound healed nicely. She had no gastrointestinal symptoms at 6 months and 2 years follow-up.

## DISCUSSION

Intussusceptions are a common cause of acute abdomen in

Corresponding Author: Fransiska Kusumowidagdo  
Email: fransiska.pedsurg@gmail.com



**Table I: Conditions associated with pneumatosis intestinalis**

<b>Pulmonary</b> Asthma COPD Emphysema Bronchitis Cystic Fibrosis	<b>Drug Induced</b> Corticosteroids Chemotherapy agents Lactulose Sorbitol Chloral hydrate	<b>Organ transplantation</b> Bone marrow e.g. for leukemia Kidney, Lung, Liver Graft versus host
<b>Gastrointestinal</b> IBD Diverticulitis Colitis Necrotizing enterocolitis Enteritis Toxic Megacolon Appendicitis Intestinal Obstruction Bowel stenosis Adynamic Ileus Malignancy Peptic Ulcer Celiac sprue	<b>Infectious</b> HIV and AIDS Virus (CMV, rota-, adeno-, varicella- zoster virus) Candida albicans Mycobacterium tuberculosis	<b>Autoimmune and systemic</b> Lupus variants Polymyositis Dermatomyositis Polyarteritis nodosa Scleroderma Sacroidosis
<b>Vascular</b> Mesenteric vascular disease Intestinal infarction and ischemia	<b>Iatrogenic</b> Blunt abdominal trauma Endoscopy Postsurgical intestinal anastomosis Jejunioileal bypass Barium enema Enteric tube placement PEEP ventilation	<b>Idiopathic (primary)</b>



**Fig. 1:** (left) abdominal X-ray showed reverse C shaped dilated (yellow arrow) bowel and multiple IP ;(right) abdominal CT scan revealed jejunojejunal intussusception (red arrow) with dilated proximal duodenojejunum.

children. In our case, the patient presented with acute abdominal pain, a sign of bowel obstruction, and rectal bleeding, which should have raised a high index of suspicion for a life-threatening condition due to bowel strangulation. After rapid resuscitation, subsequent acute abdomen imaging studies were performed without delaying the definitive surgical treatment.

The abdominal X-ray revealed large reverse C-shaped bowel consistent with the dilated third portion of the duodenum,

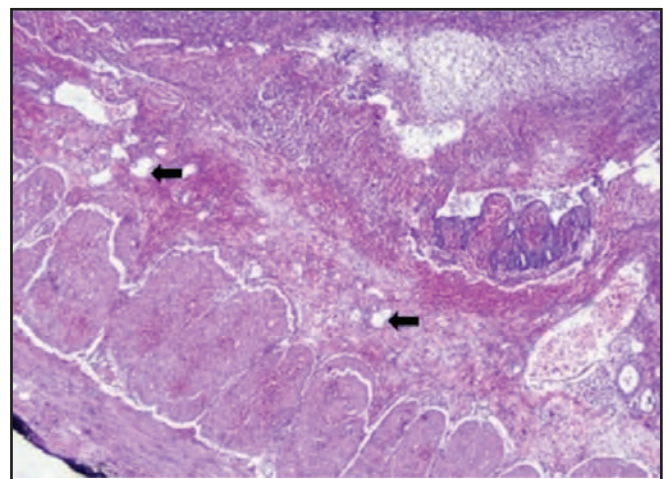


**Fig. 2:** Air bubbles (black arrow) trapped in the submucosal area (HE staining).

duodenojejunal junction, and proximal jejunum. The fixed retroperitoneal located distal duodenum, traction from the Treitz ligament, and narrow proximal jejunal mesentery made this reverse C-appearance possible. At the end of the reverse C-shaped bowel, we detected soft tissue mass opacity indicating intussuscepted bowel. There were also multiple linear and cystic-shaped lucency on the wall of proximal dilated part of the duodenum and jejunum, and the also in the walls of the jejunal intussusception, which was consistent with IP.

Computerized Tomography (CT) imaging is a common examination modality performed to detect IP as well as other signs of digestive pathology. The absence of bowel enhancement is a specific finding associated with ischemia that occurs during the late stage. IP with the associated absence of bowel enhancement, bowel wall thickening, mesenteric fat stranding, and ascites are prominent findings that indicate surgical situation.<sup>2</sup> In this case, the abdominal CT scan confirmed the X-ray findings, showed dilatation of the stomach, duodenum, and proximal jejunum. The intussuscepted bowel mass was also clearly depicted at the distal portion of the reverse C-shaped bowel. The heterogenous hypodensity at the proximal and medial portion of the C-shaped bowel may constitute the overlapping intraluminal gas, bowel wall edema, and multiple IP.

A massive intramural gas detected in this patient was considered as a rare finding in intussusception. It may appear in the intramural layer in a cystic, bubbly, curvilinear, or linear shape. In general, IP is classified into 2 types, primary and secondary IP.<sup>3</sup> Primary IP, found in approximately 15% of all IP cases, is a benign condition that is usually asymptomatic and caused by respiratory diseases, systemic diseases, after organ transplants, pathological process, endoscopic procedures, immunological imbalance, mucosal disruption, and other intraabdominal pathology. The management of primary IP depends on the cause and, not every case requires surgical management.<sup>1,4</sup> On the other hand, secondary IP is described as an air collection, forming a linear pattern that reflects on a pathological condition. Pear, in 1998, divided the cause of IP into 4 big groups: bowel necrosis, mucosal disruption, increased mucosal permeability, and pulmonary disease; while St. Peter divided IP based on pathology that reflected the origin of the gas: intraluminal gastrointestinal gas, bacterial gas, and pulmonary gas.<sup>5</sup> Various conditions associated with IP are described in Table I.

In our case, the IP was secondary, probably due to bowel mucosal disruption, caused by both leaked intraluminal gastrointestinal gas and gas-forming bacteria due to bacterial translocation after a long period of bowel obstruction that leads to distention and ischemia.

Intussusception in an older child is usually caused by PLP. It is different from the idiopathic intussusceptions that usually occur at ileocolon, the predilection of intussusceptions with PLP are at the caecocolic (2.5%) and jejunojejunal (2.5%).<sup>1</sup> In this patient, we detected a jejunojejunal intussusception caused by a jejunal polyp. Although rare, the jejunal polyp is often recorded as an intussusception caused in various ages, arising only from an obstruction to atresia.<sup>6-8</sup>

Some past studies have reported solitary jejunal polyp in association with Peutz-Jegher syndrome, but, in this case, we detected no signs of this syndrome such as dark skin freckling at the mouth, eye, nostril, or anus, and other polyps along the gastrointestinal tract.<sup>6,7</sup> Other causes included juvenile polyp, adenocarcinomatous polyp, and inflammatory fibrous polyp.<sup>9,10</sup> In this patient, due to an old ischemic cell, the pathologist only described an infarcted polyp, but could not differentiate the type of the polyp.

Treatment for IP is mostly performed conservatively unless signs of peritonitis or strangulation are detected. Cause of IP that can be managed medically: autoimmune disease, vascular disease, or drug-induced IP. In case of doubt, surgery decision making should depend on several points; concomitant critical CT findings (mesenteric ischemia, bowel obstruction, bowel perforation, portal venous gas), critical laboratory findings (Leukocyte/inflammatory marker increase, lactic acid increase, acidosis), conspicuous physical examination (muscle guarding, peritonitis, and bowel sounds), and past medical history and its medications. The decision to perform surgery should be tailored to the clinical conditions of patients and supported by meticulous examination.<sup>5</sup>

The ideal follow-up should be based on the probable diagnosis of the polyp, but the limitation, in our case, is that the histopathology of the polyp was inconclusive due to old infarction and bleeding. As it might have been an isolated juvenile polyp, we considered it as a benign polyp that did not necessarily need further evaluation.

## CONCLUSION

IP can be a sign of life-threatening conditions in children. Although it is most commonly seen in neonates with necrotizing enterocolitis, other pathology such as intussusception, gastrointestinal perforation, bowel ischemia, and necrosis must be considered seriously in older children.

## REFERENCES

1. Columbani PM, Scholz S. Intussusception. In: Coran AG, Adzick NS, Krummel TM, Laberge JM, Caldamone A, Shamberger R, Editors. *Pediatric Surgery*. 7th Edition. 2012: 1093-110.
2. Than VS, Nguyen MD, Gallon A, Pham MT, Nguyen DH, Boyer L, et al. Pneumatosis intestinalis with pneumoperitoneum: Not always a surgical emergency. *Radiol Case Rep* 2020; 15: 2459-63.
3. Koss LG. Abdominal gas cysts (pneumatosis cystoides intestinorum hominis); an analysis with a report of a case and a critical review of the literature. *AMA Arch Pathol* 1952; 53: 523-49.
4. Itazaki Y, Tsujimoto H, Ito N, Horiguchi H, Nomura S, Kanematsu K, et al. Pneumatosis intestinalis with obstructing intussusception: A case report and literature review. *World J Gastrointest Surg* 2016; 8: 173-8.
5. Khalil P, Huber-Wagner S, Ladurner R, Kleespies A, Siebeck M, Mutschler W, et al. Natural history, clinical pattern, and surgical considerations of pneumatosis intestinalis. *Eur J Med Res* 2009; 14: 231-9.
6. Ozer A, Sarkut P, Ozturk E, Yilmazlar T. Jejuno-duodenal intussusception caused by a solitary polyp in a woman with Peutz-Jeghers syndrome: a case report. *J Med Case Rep* 2014; 8: 13.
7. Kalavant A, Menon P, Mitra S, Thapa B, Narasimha Rao K. Solitary Peutz-Jeghers polyp of jejunum: A rare cause of childhood intussusception. *J Indian Assoc Pediatr Surg* 2017; 22: 245-7.
8. Parelkar SV, Sanghvi BV, Vageriya NL, Paradkar B, Samala DS, Oak SN. Neonatal jejunal polyp with jejunojejunal intussusception causing atresia: A novel cause. *J Pediatr Surg Case Rep* 2014; 2: 73-5.
9. Kwon KB, Shin MY, Kwon KW, Park JO. A case of jejunal juvenile polyp presented as intussusception. *Clin Exp Pediatr* 2005; 48: 453-6.
10. Kao Y-K, Chen J-H. Adult Jejuno-jejunal intussusception due to inflammatory fibroid polyp. *Medicine* 2020; 99(36): e22080.

# Risk factors for failure of hydrostatic reduction in children with intussusception in Hasan Sadikin General Hospital

Dikki Drajat Kusmayadi, SpBA(K), Laura Kurnia Agnestivita, MD, Vita Indriasari, Sp.BA(K)UG

Pediatric Surgery Division, Department of Surgery, Faculty of Medicine Padjadjaran University/Dr. Hasan Sadikin General Hospital, Bandung, Indonesia

## ABSTRACT

**Introduction:** Intussusception is a medical emergency caused by proximal insertion of the intestinal segment to its lumen, which results in ischemia, necrosis, and sepsis-associated mortality in pediatric patients. Intussusception is managed mainly by surgical reduction; hydrostatic reduction is a noninvasive alternative with lower risk of complications. The study was aimed to analyze the risk factors for the failure of hydrostatic reduction in children with intussusception at the Hasan Sadikin General Hospital. **Materials and Methods:** The medical records of children diagnosed with intussusception and treated with hydrostatic reduction during January 2010 and September 2019 were included. Variables of the study included age, sex, onset of symptoms, and outcome. Logistic regression analyses were performed to determine the significance and strength of correlation on the included characteristics with outcomes of hydrostatic reduction in the population. The  $p < 0.05$  was deemed significant.

**Results:** There were a total of 56 children with intussusception who were treated with hydrostatic therapy during the study period. The failure rate of hydrostatic therapy was 83.9%. Age, sex, onset of symptoms, and location of intussusception were not significantly associated with the failure of hydrostatic reduction ( $p > 0.05$ ). Dehydration was the only symptom significantly associated with the failure of hydrostatic reduction (OR 16.80;  $p = 0.001$ ).

**Conclusion:** Dehydration is significantly associated with the failure of hydrostatic reduction in children with intussusception.

## KEYWORDS:

*intussusception, dehydration, risk factor, pediatric*

## INTRODUCTION

Intussusception is a potentially life-threatening medical emergency caused by the insertion of the proximal portion of the intestine into the distal lumen of the intestine, which causes obstruction, followed by ischemia and subsequent intestinal necrosis in pediatric patients. Morbidity and mortality may occur due to sepsis related to intestinal necrosis; this condition is associated with higher morbidity and mortality in cases of delayed diagnosis and/or

treatment.<sup>1-6</sup> Fatalities associated with delayed diagnosis and/or treatment in children with intussusception has been reported to reach up to 20% in Indonesia.<sup>7</sup>

Intussusception requires immediate surgical reduction to treat; less-invasive alternative that may be utilized in treating intussusception in children is through hydrostatic reduction.<sup>8,9</sup> Management using hydrostatic reduction was associated with lower complication rates when compared to conventional surgical reduction.<sup>9,10</sup> The cure rates for hydrostatic reduction in previous studies were noted to be similar to that of conventional surgical reduction.<sup>10</sup> This study was aimed to analyze the variables correlated with the failure rate of hydrostatic reduction of pediatric patients with intussusception treatment in Hasan Sadikin General Hospital (HSGH).

## MATERIAL AND METHODS

An analytical study with retrospective data was performed in the HSGH. Data was collected from medical records and consisted of pediatric intussusception cases treated with hydrostatic reduction during January 2010 and September 2019. The inclusion criteria for the study were as follows: patients aged <18 years, diagnosed with intussusception, and treated with hydrostatic reduction at the HSGH. The patients were excluded from the study if they had incomplete medical record or had refused treatment. Consecutive sampling was performed in this study.

Dependent and independent variables in this study were collected from the medical records for children with intussusception who were treated at the HSGH between January 2010 and September 2019. The dependent variable of this study was the outcome of hydrostatic reduction. Independent variables of this study included age, sex, onset of symptoms (until management with hydrostatic reduction), location of intussusception, symptoms, and outcomes. The patients were grouped into 3 age groups: 0–12 months; 13 months–3 years; and >3 years. Onset to management was defined as time (in hours) from the first reported symptoms to receiving treatment for intussusception. Locations of intussusception were defined into ileoileal, ileocolic, ileocolocolic, ileocecal, and colocolic. The symptoms were defined as the chief complaint found during the initial presentation in the emergency department. The assessment of the outcome was defined postoperatively; unsatisfactory

Corresponding Author: Laura Kurnia Agnestivita  
Email: dr.laura.ka@gmail.com

**Table I: Baseline characteristics**

Variables	N = 56, count (%)
Body weight (kg), mean (± SD)	8.20 ± 2.60
Age	
0–12 months	50(89.3%)
13 months–3 years	3(5.4%)
>3 years	3(5.4%)
Sex	
Male	35(62.5%)
Female	21(37.5%)
Onset of symptoms	
<24 hours	31(55.4%)
> 24 hours	25(44.6%)
Location	
Ileoileal	2(3.6%)
Ileocolic	40(71.4%)
Ileocolocolic	5(8.9%)
Colocolic	6(10.7%)
Ileocecal	3(5.4%)
Bloody stool	
Yes	53(94.6%)
No	3(5.4%)
Vomiting	
Yes	51(91.1%)
No	5(8.9%)
Bloated stomach	
Yes	44(78.6%)
No	12(21.4%)
Dehydration	
Yes	45(80.4%)
No	11(19.6%)
Obstipation	
Yes	1(1.8%)
No	55(98.2%)
Diarrhea	
Yes	34(60.7%)
No	22(39.3%)
Hydrostatic reduction outcome	
Successful	9(16.1%)
Failed	47(83.9%)

hydrostatic reduction (assessed by Doppler ultrasonography) was continued with the conventional intestinal reduction. Descriptive statistics were employed to describe the frequency and percentage of categorical variables. Mean with standard deviation and median with range (min–max) were used to describe numerical variables. Chi-square test (with the alternative of Fisher's exact test) was applied to compare the differences between both the outcomes of hydrostatic reduction. The strength of correlation of a variable with the outcome of hydrostatic reduction was analyzed by logistic regression, with the values described in odds ratio (OR). The  $p < 0.05$  were deemed to be significant.

**RESULTS**

During the study period, there were a total of 180 children who were treated for intussusception. Of these, 56 children had received hydrostatic reduction for the treatment of intussusception. Mean body weight of the patients was 8.2 kg. The majority of the patients were aged 0–12 months. Most patients were males. Most the patients received treatment in <24 h since the first onset of symptoms; 25 patients had received delayed treatment (>24 h after the first onset of

symptoms). Ileocolic intussusception was the most prevalent location of intussusception. Bloody stool was the most commonly detected symptoms in patients with intussusception, followed by vomiting, dehydration, bloated stomach, diarrhea, and obstipation. Hydrostatic reduction success rate was low; only 9 out of 56 cases (16.1%) were successfully treated with hydrostatic reduction and 47 out 56 cases failed (83.9%). The remaining cases require conventional surgery after failure of hydrostatic reduction.

The success rate of hydrostatic reduction in treating intussusception was low in 0–12-month-old patients and in patients >3 years. No significant difference in terms of the outcomes between male and female patients ( $p = 0.231$ ) were noted. The onset of symptoms ( $p = 0.475$ ) was not significantly correlated with the hydrostatic reduction outcomes. Dehydration is the only symptom that was significantly correlated with worse outcome of hydrostatic reduction in this study (OR 16.80,  $p = 0.001$ ). Other symptoms included in this study were not significantly correlated with the outcome of hydrostatic reduction in treating intussusception.



**Table II: Patients' characteristics correlated with successful outcome**

Variables	N	%	OR	p
Age			N/A	
0–12 months	8	16		
13–3 years	0	0		
>3 years	1	33.3		
Sex			2.4	0.231
Male	4	11.4		
Females	5	23.8		
Onset of symptoms			1.70	0.475
<24 hours	4	12.9		
>24 hours	3	20.0		
Location			N/A	
Ileoileal	2	100		
Ileocolic	3	7.5		
Ileocolocolic	1	20		
Colocolic	2	33.3		
Ileocecal	1	33.3		
Blood stool			2.81	0.420
Yes	8	15.1		
No	1	33.3		
Vomiting			4.19	0.152
Yes	7	13.7		
No	2	40		
Bloated stomach			2.11	0.349
Yes	6	13.6		
No	3	25.0		
Dehydration			16.80	0.001***
Yes	0	0		
No	9	54.5		
Obstipation			N/A	
Yes	0	0		
No	9	16.4		
Diarrhea			3.88	0.079
Yes	3	8.8		
No	6	27.3		

OR=odds ratio

## DISCUSSION

In this study, hydrostatic reduction showed higher success rate in children aged <3 years. Previous study had hypothesized the correlation between the diameter of small intestines and the outcomes of hydrostatic reduction. In this case, younger children had smaller lumen diameter of small intestines. The smaller diameter may have caused difficulties in reducing the portion of the intestine that were strangulated on the distal part.<sup>11</sup>

Successful reduction in higher rates in female patients relative to that in male patients were noted in this study, although the difference was not significant. Physiological differences between both the sexes may have contributed to the difference in the outcomes of hydrostatic reduction for the management of intussusception. In females, food digestion rate was slower, and the colon was longer relative to those in males. Weaker peristaltic forces associated with the physiological difference mentioned above may have contributed to the higher success rate of hydrostatic reduction in female patients than in male patients.<sup>12</sup>

The onset of symptoms was not significantly correlated with the success of hydrostatic reduction; this study had found that delayed presentation and treatment of intussusception (as defined as >24 hours had elapsed from the first onset of the symptoms to receiving treatment) was more common when

compared to early treatment of intussusception (<24 hours). Khorana et al. noted the onset of symptoms to treatment was not correlated with the outcomes of hydrostatic therapy (with presentation ranging from 1 hour to the maximum of 120 hours). Hydrostatic reduction was indicated as an alternative to conventional surgery in treating intussusception; it may be performed even in individuals with delayed presentation of intussusception and still garner similar outcomes.<sup>10,13</sup>

In this study, intussusception of the ileocolic region was the most prevalent location of intussusception. The ileocolic region had numerous free-hanging structures of the abdominal region. Anatomical variations of the cecum and ileus may have contributed to the development of ileocolic intussusception, such as decreased cecum rigidity due to the absence of a secondary cecum and taenia coli; papillary structure of the ileocecal valve; and longitudinal muscle fibers of the colon around the valve. Decreased rigidity by anatomical variation may have caused intussusception due to the prolapse of the ileocolic segment.<sup>14,15</sup>

Several symptoms are associated with higher risk of failure in hydrostatic reduction. In this study, patients with dehydration showed significantly higher risk of failure in treatment using hydrostatic reduction; other symptoms, such as bloody stool and other gastrointestinal symptoms were not associated with the failure of hydrostatic reduction; however, patients with bloody stools were present in relatively higher

rate when compared to those with other symptoms listed. Dehydration may be related to the hardening of the feces; reduction of intestinal content requires higher pressure to treat through hydrostatic reduction; as such, it was associated with higher risk of failure of hydrostatic reduction in patients with dehydration.<sup>11,16</sup> In a previous study by Ekenze et al., patients with bloody stool were at higher risk for gastrointestinal complication and intestinal resection, while patients with bloody stool often presented with a higher prevalence of intestinal angulation, strangulation, and/or compression. Bloody stool was associated with a reduction of the venous blood flow of the intestine.<sup>17</sup> The study showed different findings related to the risk factors associated with the failure of hydrostatic reduction by He et al.; in the referenced study, bloody stool was significantly associated with the failure of hydrostatic reduction (OR 9.27;  $p < 0.05$ ).<sup>18</sup> Conversely, in this study, bloody stool, despite the higher prevalence-failed treatment group, was not significantly associated with the failure of hydrostatic reduction. Katz et al. had noted that dehydration (mild, moderate, and severe) was significantly associated with the failure of hydrostatic reduction;<sup>19</sup> this study had found the similar results that patients with dehydration is significantly associated with failure of hydrostatic reduction in children with intussusception.

There were several limitations for this study. The disease is relatively rare and performed only at a single institution (with the consideration that the said institution is a tertiary referral hospital); as such, the sample may not be wholly representative of the characteristics of the patients in West Java, Indonesia. In this study, there were several patients who had experienced delays in treatment for >24 hours; there were some cases in which the patients had only sought treatment after experiencing the symptoms up to a week's period. In cases of extreme delays, there was a probable confounding factor in the evolution of symptoms (which may explain the current study to have several differences with previous studies performed outside Indonesia). Despite these limitations, this is one of the first studies to discuss the risk factors associated with the failure of hydrostatic reduction in treating children with intussusception, particularly in West Java, Indonesia.

## CONCLUSION

Dehydration in pediatric intussusception cases is significantly associated with the failure of hydrostatic reduction in children with intussusception. Age, sex, and other gastrointestinal symptoms were not significantly associated with the failure of hydrostatic reduction.

## ACKNOWLEDGMENTS

The authors would like to express their gratitude to the Hasan Sadikin General Hospital Pediatric Surgery division for aiding with the data collection for the patients included in this study.

## REFERENCES

1. Chu A, Liacouras CA. Ileus, adhesions, intussusception, and closed-loop obstructions. In: Behrmen K, Editor. *Nelson textbook of pediatrics*, 20th Edition. Elsevier; 2015: 1812–4.
2. Ramachandran P. Intussusception in pediatric surgery diagnosis and management. Puri P and Hollwarth M, Editors. Springer: Dordrecht Heidelberg; 2009: 80-100.
3. Kartono D. Invaginasi. In: *Kumpulan kuliah ilmu bedah*. Reksoprodjo S and Pusponegoro AD, Editors. Binarupa Aksara; 2010: 60-82.
4. Pendergast LA, Wilson M. Intussusception: A sonographer's perspective. *J Diagn Med Sonogr* 2003; 19(4): 231–8.
5. Fallan ME. Intussusception in pediatric surgery, 4th Edition. Ashcraft KW, Holder TM, Editors. W B Saunders Company; 2005.
6. World Health Organization. Acute intussusception in infants and children. Incidence, clinical presentation and management: A global perspective. World Health Organization; 2002: 1–98.
7. Sukmawati S, Santoso H, Suandi IKG. Manifestasi gastrointestinal akibat alergi makanan. *Sari Pediatr* 2016; 7(3): 132.
8. Hooker RL, Hernanz-Schulman M, Yu C, Kan JH. Radiographic evaluation of intussusception: Utility of left-side-down decubitus view. *Radiology* 2008; 248(3): 987–94.
9. Columbani PM, In SSI, AGC, NSA. Tm K, and J-ML. Shamberger RC. In: *Caldamone AA, Editor. Pediatric surgery*, 7th Edition. Saunders; 2012: 508–16.
10. Khorana J, Singhavejsakul J, Ukarapol N, Laohapensang M, Wakhanrittee J, Patumanond J. Enema reduction of intussusception: The success rate of hydrostatic and pneumatic reduction. *Ther Clin Risk Manag* 2015; 11: 1837–42.
11. Xiaolong X, Yang W, Qi W, Yiyang Z, Bo X. Risk factors for failure of hydrostatic reduction of intussusception in pediatric patients: A retrospective study. *Medicine (Baltimore)* 2019; 98(1): e13826.
12. Karlstadt RG, Hogan DL, Foux-Orenstein A. Normal physiology of the gastrointestinal tract and gender differences. *Princ Gen Specif Med* 2004; 43(2): 377–96.
13. Khorana J, Singhavejsakul J, Ukarapol N, Laohapensang M, Siritwongmongkol J, Patumanond J. Prognostic indicators for failed nonsurgical reduction of intussusception. *Ther Clin Risk Manag* 2016; 12: 1231–7.
14. Young AK. Intestinal intussusception. *Br Med J* 1884; 2(1241): 706–8.
15. Scheyé T, Dechelotte P, Vanneuville G. Etiopathogenic theory of ileoceocolic intussusception. *Anat Clin* 1985; 7(2): 103–6.
16. Fallon SC, Lopez ME, Zhang W, Brandt ML, Wesson DE, Lee TC, et al. Risk factors for surgery in pediatric intussusception in the era of pneumatic reduction. *J Pediatr Surg* 2013; 48(5): 1032–6.
17. Ekenze SO, Mgbor SO. Childhood intussusception: The implications of delayed presentation. *Afr J Paediatr Surg* 2011; 8(1): 15–8.
18. He N, Zhang S, Ye X, Zhu X, Zhao Z, Sui X. Risk factors associated with failed sonographically guided saline hydrostatic intussusception reduction in children. *J Ultrasound Med* 2014; 33(9): 1669–75.
19. Katz M, Phelan E, Carlin JB, and Beasley SW. Gas enema for the reduction of intussusception: Relationship between clinical signs and symptoms and outcome. *AJR Am J Roentgenol* 1993; 160(2): 363–6.

# Mature Jejunal Teratoma in adolescents: A case report

N Wisnu Sutarja, MD, Ariandi Setiawan, MD, Fendy Matulatan, MD

Pediatric Surgery Division, Department of General Surgery, Medical Faculty of Airlangga University, Dr. Soetomo Hospital, Surabaya, Indonesia

## SUMMARY

Jejunal teratoma (JT) is a rare type of extragonadal teratoma. To date, the subject of mature jejunal teratomas has not yet been discussed in the literature. This type of teratoma contains cystic, solid, and calcified components. JT may be suspected on a computed tomography (CT) scan, which can describe the various features of the germinal layer components, followed by normal laboratory results of alpha fetoprotein (AFP) and  $\beta$ -human chorionic gonadotropin ( $\beta$ -hCG). This case report describes that of a teenager with a mature JT whose chief complaints were recurrent general weakness due to anemia and an abdominal mass. The patient was initially treated with non-operative management; however, his symptoms remained unresolved, and he accepted surgical intervention. No additional chemotherapy or radiotherapy was required after complete tumor excision. The patient no longer complained of general weakness following surgery.

## INTRODUCTION

Jejunal teratomas (JT) are very rare neoplasms, and no publication discussing this type of tumor is yet available. JT contain cystic, solid, and calcified components. This type of tumor may be suspected on a computed tomography (CT) scan, which can describe the various features of the germinal layer components, followed by normal laboratory results of alpha fetoprotein (AFP) and  $\beta$ -human chorionic gonadotropin ( $\beta$ -hCG). In this report, we discuss the case of a teenager with a mature jejunal teratoma.

## CASE REPORT

A 15-year-old male arrived at Dr. Soetomo Hospital (SH), Surabaya, Indonesia with a chief complaint recurrent general weakness due to anemia. This problem was solved temporarily by repeated hospitalization within the last 1 year for recurrent transfusion. The patient's appetite and sleeping quality was good, his daily activities were within normal limits. Our patient had no motor or sensory complaints. Every time he felt weak, his hands and face turned pale and then he was admitted to the peripheral hospital. The patient denied other complaints such as headache, fever, bloody stool, blood in urine, history of trauma, or spontaneous bleeding from other places whenever he felt weak. The patient didn't have medical record about the laboratory value from peripheral hospital. When his anemia had been resolved, he felt fit and was discharged from the hospital. His last transfusion was 2 months before this admission. When arrive in SH, the patient was found to be anemic, which required transfusion until his condition improved and

acceptable for operation of his lump. He had a painless lump in his lower left abdomen which was recognized by his mother since he was a 3-days-old neonate and increased in size as the patient grew older. The patient reported no other lumps grew elsewhere on his body. The patient had a good appetite, never complained of abdominal distension, no blood in his feces, had normal bowel habits, and never had other digestive problems. His urine was clear and yellow, and no complaints regarding his urination were made. The patient's weight was stable in the last 1 year, and he had no history of other diseases or high blood pressure. No peripheral blood smear examination nor fecal occult blood test (FOBT) was previously performed.

The patient had no family history of recurrent anemia, tumor, cancer, or similar complaints. The patient's mother was 24 years old when the patient was conceived. Routine checks by the midwife and an ultrasound examination of the womb by an obstetrician revealed that the fetus was normal. On physical examination, the patient's weight was 54 kg, and his vital signs, heart, and lungs were normal. His conjunctiva was anemic. In abdominal examination, we obtained the impression of a mass lump in the left lower quadrant with the skin surface was normal as the surrounding mass, normal bowel sounds, tympanic percussion, palpation of a single solid mass, flat surface, with firm impression boundaries, fixed at the base, painless, mass size 11 × 8 × 6 cm, does not cross the midline. No palpable enlarged lymph nodes were found in the head, neck, axilla, or inguinal regions. Liver and spleen impressions were within normal limits. Both testes were palpable within normal limits. The rectal digital examination, we found that the ampulla recti did not collapse, and no palpable impression of an intraluminal or extraluminal mass was noted, hand gloves was visible feces without blood. Motor and sensory functions were within normal limits. Laboratory testing showed normal tumor markers of  $\alpha$ FP < 1.3 and  $\beta$ hCG < 2.0, blood count show Hb = 8.0 g/dL. Other laboratory values were within the normal range.

The results of physical examination revealed an intra-abdominal mass with anemia; thus, further radiological examination was recommended. Abdominal ultrasound on 1 month before operation revealed a donut-shaped intraluminal mass in the left lower quadrant of the abdomen; this mass appeared to lead to intussusception, but no symptoms of intussusception that matched the patient's clinical condition. A Computed Tomography (CT) Scan with contrast of the abdomen was then performed for further investigation.

Corresponding Author: N Wisnu Sutarja  
Email: wisnuflycrick@gmail.com



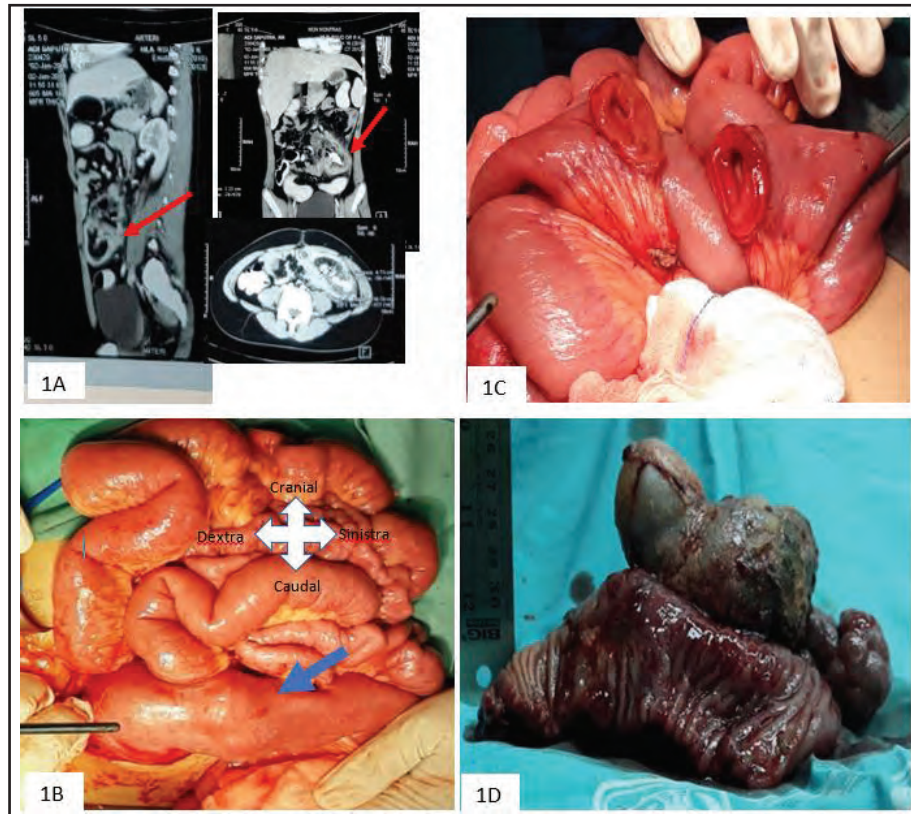


**Fig. 1:** (A) Abdominal CT scan with contrast showing a mass (red arrow). (B) Intraoperative mass attached to interintestine (blue arrow). (C) Intraoperative jejunum after tumor resection. (D) Cut section of tumor specimen.

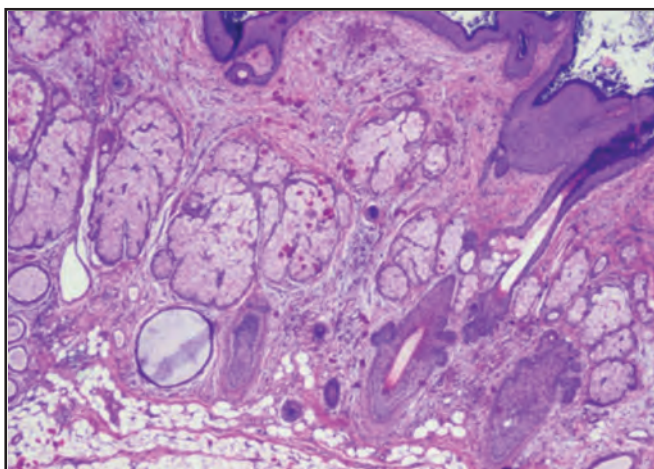


**Fig. 2:** Histopathology of the teratoma (magnification, 10x).

CT scan with contrast of the abdomen on 1 week after ultrasonography showed a lesion with solid components, fat, and calcification. The lesion measured  $10.7 \times 7.72 \times 4.71$  cm and was located in the left parailiac region. Contrast administration showed enhancement of the edges, septa, and solid parts of the lesion. Figure (1A) shows the lesion in the lower left quadrant of the patient's abdomen.

From the laparotomy, we found clear peritoneal fluid. The tumor was located in the intraluminal jejunum and the jejunum attached to the left white line, sigmoid, and

terminal ileum, which was pulled to the left. Release of intestinal adhesion followed by tumor evaluation was then performed (Fig 1B). The intraluminal tumor in the jejunum was observed approximately 40 – 52 cm (about 12 cm long) distal to the ligament of Treitz. The tumor was freed from the surrounding tissue and then total tumor was resected along with the surrounding jejunum for about 20 cm (Fig 1C, 1D). After opening the resected jejunum, there was single heterogenous (solid and cystic) oval mass tightly attached with mesenteries side of jejunum, with size  $11\text{cm} \times 10\text{cm} \times 5\text{cm}$ , no ulceration, no hemorrhage as shown in Figure (1D). On further exploration, we obtained liver had sharp edges, a flat surface, and a normal red color. No mesenteric lymph node enlargement was noted. After the intact resection of the jejunum with tumor, end-to-end jejunum anastomosis were performed.

Macroscopic examination of the anatomical pathology of the tumor revealed that the preparation contained portions of jejunum tissue weighing 275 g, 3.5 cm in proximal jejunum diameter, and 3 cm in distal jejunum diameter. The outer surface was partly smooth and partly covered with fat. On the slices, the mass was observed as sebaceous tissue, bone, teeth, and hair, measuring  $10\text{cm} \times 9.5\text{cm} \times 4.5\text{cm}$ . Some cysts measuring 1.2 cm in diameter with a yellowish-gray color and dense, chewy consistency were noted.

Microscopic findings showed sections of intestinal tissue with tumor growth consisting of skin epidermis, sebaceous glands, hair follicles, skin adnexa, glandular epithelium, hard bone tissue, fatty tissue, squamae, and calcifications, as shown in



Figure 2. The tumor had grown to the serous layer. No glial tissue and neuroepithelial components were seen. The ends of the resection were tumor free. No tumor was seen in the surrounding seven lymph nodes.

## DISCUSSION

The most common prevalence for gastrointestinal teratoma is gastric teratoma, but gastric teratoma alone accounts for less than 1% from total of teratomas.<sup>1,2</sup> The most frequent teratoma is sacrococcygeal teratoma (45% of all teratoma or 1 out of every 40,000 humans). To the best of our knowledge, there is no publication describing mature JT has yet been published. Small intestinal teratomas are believed to occur as a result of incomplete totipotential cell division in the subserosa of the jejunum in early life. However, the exact mechanism of this type of tumor remains unknown because of its rarity.<sup>3</sup>

This disease is usually diagnosed based on the patient's history, physical examination of the intra-abdominal mass, laboratory results revealed normal AFP and  $\beta$ -hCG values, and abdominal contrast CT scan. In our study, the results of the CT scan showed a lesion with solid components, fat, and calcifications. The lesion was a little bit bigger in width by operation 1 month after the CT scan was taken.

Teratoma is a common form of germ cell tumor (GCT). This tumor can develop congenitally or during childhood.<sup>4,5,6</sup> Because the tumor in our case was observed as early as when the patient was 3 days old, it may have developed congenitally. Mature teratomas show insignificant tumor growth. Our patient showed no clinical complaints or signs of distant spread, which often appears in immature or malignant tumors. Surgical removal of the tumor was performed only after the patient's repeated complaints of anemia as a teenager. His family was also afraid of operating option explained why he had just operated the lump when he was 15 years old. The patient's repeated anemia may be due to microscopic bloody stool, unfortunately we didn't perform FOBT to confirm this supposition. The type of anemia could not be identified because peripheral blood smear test was not conducted. While this type of tumor is not likely to metastasize to the bone marrow, this belief could not be confirmed because no peripheral blood smear test was performed. Surgery revealed a tumor located approximately 40 cm distal to the ligament of Treitz, which is still part of the jejunum. The jejunal with intraluminal tumor attach to the surrounding tissue confirmed that the tumor had been growing over a long period, but no signs of mesenteric or locoregional spread were noted, as supported by the patient's good liver and good mesenteric conditions. Thus, the tumor could be removed completely.

Macroscopic and microscopic pathological examination of the tumor showed sebaceous tissue, bone, teeth, hair, fatty tissue, squamous, and skin. These findings explained that tumor contains parts of endoderm, ectoderm, and mesoderm where each part can differentiate into many different tissues.<sup>5,6</sup> Different types of tissue from these three germ

layers lead to a teratoma. From the end of the tumorresection, histopathologic examination revealed no glial cells or neuroepithelial components. This finding indicates the absence of malignancy (i.e., a mature teratoma).

Chemotherapy is recommended for patients with grades 2 and 3 congenital immature teratomas after surgical resection.<sup>3,7</sup> Our type of JT was mature, no additional chemotherapy or radiotherapy was required after complete tumor excision. The variation of serum AFP level could be an indicator of tumor recurrence and of the need of further chemotherapy for patient with teratoma, especially in immature teratoma.<sup>3</sup> In our case, three months follow up after operation of this patients show normal AFP and  $\beta$ -hCG values, and 1.5 years after operation also no sign recurrent general weakness, no sign of recurrent abdominal mass.

## CONCLUSION

Teratomas are a type of GCT that can occur in various tissues, including the jejunum. Mature JT are a very rare type of tumor. No case report of a mature jejunal teratoma has previously been published. Our patient underwent surgery at the age of 15 years, which, in theory, could increase the risk of tumor malignancy. However, the patient showed good clinical and laboratory results before and during surgery, and no tumor spread was noted. Anatomical pathology also indicated a good prognosis. Histopathological results suggested a mature teratoma. Workup for the tumor markers  $\alpha$ FP and  $\beta$ -hCG 3 months after the operation show normal values. Our patient had recurrent anemia prior to surgery, which could have been caused by occult blood from the mass. Unfortunately, we did not perform FOBT or peripheral blood smear to confirm the true cause of anemia. Approximately 1.5 years after surgery, no complaint of abdominal mass or general weakness due to anemia was made. The prognosis of this patient was good.

## REFERENCES

1. Sowińska PE. Neuroendocrine tumors: Clinical, histological and immunohistochemical perspectives and case report - mature teratoma in a 16-year-old girl. *Pathophysiology* 2021;28:373-86.
2. Pankaj H, Kartik CM, Anjan D, Bidyut D. Childhood gastric teratoma: A case report. *India. Indian J Pediatr Surg* 2018; 2(2): 139-41.
3. Szu TC, Hong SL, Jin CS, Chia TS. Congenital immature teratoma originating from the jejunum. *J Pediatr Surg* 2007;42:1600-3.
4. Jeong HC, Cha SJ, Kim GJ. Rapidly grown congenital fetal immature gastric teratoma causing severe neonatal respiratory distress. *J Obstet Gynaecol Res* 2012; 38: 449-51.
5. Jean ML, Pramod SP, Kenneth S. Teratomas and other germ cell tumours. In: Goerge WH, Patric M, Shawn DSP, Editors. *Holcomb and Ascaft Pediatric Surgery, 7th Edition*. Elsevier; 2020:1066-2020.
6. Rescorla FJ. Teratomas and other germ cell tumours. In: Arnold GC, Editor. *Textbook of pediatric surgery, 7th Edition*. Elsevier; 2012: 507-18.
7. Lam KY, Lo CY. Teratoma in the region of adrenal gland: A unique entity masquerading as lipomatous adrenal tumor. *Surgery* 1999;126:90-4.

# Coping with Coronavirus disease 2019: current state review and SWOT analysis to improve the urological services in Southeast Asia

Aria Danurdoro, MD<sup>1</sup>, Indrawarman Soerohardjo, MD<sup>1</sup>, Allen Soon Phang Sim, MBChB<sup>2</sup>, Raden Danarto, MD<sup>3</sup>, Dong Nguyen, MD<sup>4</sup>, Jose Benito A. Abraham, MD<sup>5</sup>, Supachai Sathidmangkang, MD<sup>6</sup>

<sup>1</sup>Division of Urology, Department of Surgery, Faculty of Medicine, Public Health and Nursing, Universitas Gadjah Mada/Dr. Sardjito Hospital, Yogyakarta, Indonesia, <sup>2</sup>Department of Urology, Singapore General Hospital, Singapore, <sup>3</sup>Department of Urology, Annur Surgery Specialty Hospital, Yogyakarta, Indonesia, <sup>4</sup>Department of Urology, Binh Dan Hospital, Ho Chi Minh, Vietnam, <sup>5</sup>Department of Urology, National Kidney and Transplant Institute, Quezon City, Philippines, <sup>6</sup>Division of Urology, Department of Surgery, Faculty of Medicine, Vajira Hospital, Navamindradhiraj University, Bangkok, Thailand

## ABSTRACT

**Introduction:** We investigated the impact of Coronavirus Disease 2019 (COVID-19) pandemic on urological services by analyzing current attitudes and practices of urologists in the Southeast Asian (SEA) countries and create ways for improvement.

**Materials and methods:** Quantitative data were used as critical indicators of workload of urological services from each country in SEA. Qualitative data analysis was done to describe the current state of attitudes of urologists against COVID-19 in the region. A strengths, weaknesses, opportunities, and threats (SWOT) analysis was performed to formulate strategic action plans.

**Results:** A total of seven urologists from six SEA countries completed the survey. Approximately 21–40% reduction in elective surgeries and outpatient visits, as stated by 42.9% and 57.1% of respondents, respectively was noted. Collectively, most respondents (71.4%) experienced <20% reduction in emergency visits. Various strategies were utilized as reaction to the pandemic. These include utilization of virtual communication platforms, pre-surgical COVID-19 screening, and limited number of accepted outpatient appointments and surgeries. Face to face patient consultations were still considered needed by many urologists although most countries had prohibited direct patient contact. The national response of countries such as Malaysia, Singapore, Thailand, and Vietnam were successful in controlling the pandemic. However, Indonesia and Philippines struggled because of the limited testing and tracing capabilities. Through the SWOT analysis, strategies were identified which can help overcome COVID-19 and any other future pandemics: (1) restarting the urological services in a safe and sustainable manner; (2) optimizing financial and infrastructural capacities; and (3) regional collaboration to strengthen the health systems.

**Conclusion:** COVID-19 negatively impacted many health aspects, especially the delivery of urological services in SEA. Therefore, to ensure sustainability of urological services during the pandemic crisis, health care system

should focus on safe, resilient, and adaptive approach with regional collaboration.

## KEYWORDS:

*Southeast Asia; Urological Services; Urologist; Global Urology; Developing Countries; High-Income Countries; Low and Middle-Income Countries*

## INTRODUCTION

All countries worldwide are in the state of turmoil shortly after the emergence of a novel coronavirus disease 2019 (COVID-19) and its rapid global spread. Southeast Asia (SEA) was hit the earliest outside its origin in China. The first spread was reported in Thailand on January 13, 2020.<sup>1</sup> Furthermore, the 11 SEA countries including Brunei, Myanmar, Cambodia, Timor-Leste, Indonesia, Laos, Malaysia, Philippines, Singapore, Thailand, and Vietnam were greatly affected by the pandemic. As of July 15, 2021, the cumulative number of confirmed cases in 11 SEA countries reached over 19,000,000 patients. In order to combat the outbreaks, regional authorities have implemented numerous non-pharmaceutical interventions (NPIs) and preventative strategies like mandated quarantine and case isolation, restriction of all mass gatherings or public events, suspension of schools and other educational facilities, and large-scale social restriction including local and national lockdowns.<sup>2</sup>

Pandemic readiness and preparedness vary among SEA countries and there are several countries that are particularly vulnerable to this destructive outbreak. During this challenging time, urologists, as part of subspecialized healthcare resources may take an important leadership role: endeavoring to maintain patient care virtually, prioritizing patient safety, and protecting the larger community from potential coronavirus exposure. Generally surveying the impacts of COVID-19 on urological services, the rapid increase in the number of cases is overwhelming, as confirmed by many studies. However, less is known about the personal and daily experience of the practicing urologists in developing countries. Furthermore, a better understanding of potential factors may be helpful for urologists during this

Corresponding Author: Indrawarman Soerohardjo  
Email: indrawarman@ugm.ac.id

pandemic, such as collegial supports and coping strategies. The primary objective was to examine how the current COVID-19 pandemic affected the urological services in SEA countries, represented by the authors who are urologists in Indonesia, Malaysia, Philippines, Singapore, Thailand, and Vietnam. The secondary objective was to create strategies that will help improve the delivery of urological services.

## MATERIAL AND METHODS

A survey based on the hybrid-methods design was used. Quantitative and qualitative data from each participating urologists across SEA countries were collected to describe the primary objective.

### *Descriptive Quantitative Data and Qualitative Data Analysis*

The survey consisted of a 20-point questionnaire which was answered by each respective certified urologist. Convenience sampling was employed to include several urologists in the SEA. The questionnaire was based on standard urological clinical pathway per region's hospitals and their perception to several adaptive models of relevant urological services during COVID-19 pandemic. These urologists were asked to fill-out a quantitative survey and describe the daily urological practices in their respective hospitals through qualitative questions. Each country was classified based on gross national income per capita from the World Bank Country's status, to illustrate the possible impact of socio-economic welfare on national policy towards pandemic. The qualitative response was coded by the first and second authors. They assigned a code to each qualitative response after reading through all responses. Answers could be given to multiple coding categories. No statistical analyses were performed based on qualitative responses.

### *Strengths, Weaknesses, Opportunities, and Threats Analysis*

Strengths, weaknesses, opportunities, and threats (SWOT) analysis refers to assessing and evaluating the four elements of the acronym that influence a specific topic.<sup>3</sup> It is effective situation analysis techniques which comprehensively, systematically, and accurately assess the scenario of the case. This method helps formulate corresponding strategies, plans, and countermeasures in clinical decision-making and complicated systems analysis. Internal factors such as financial resources, healthcare resources and accessibility were identified as either strengths or weaknesses. In contrast, external factors such as policy trends, demographics, political and economic regulations were identified as opportunities or threats. Therefore, SWOT analysis was performed to develop prospective solutions meant to improve the collaborative development of urological services in SEA during the COVID-19 crisis.

## RESULTS

The questionnaires were sent to ten urologists, three of them refused to join the study and were classified as non-responder. Demographic data of the consultant urologists are displayed in Table I. All respondents were males, majority practicing in an academic institution and focusing primarily on stones and oncology subspecialties.

Regarding the epidemiological burdens, four out of seven respondents disclosed that they were working in COVID-19 managing hospitals, and two out of all participants were working in a hospital with a total of >30 COVID-19 cases. One respondent reported with cases of severe acute respiratory syndrome coronavirus 2 (SARS-COV-2) among colleagues in their department (Fig. 1).

Regarding preventive potential disruption in urological services, four urologists stated that their urological association in their country did not develop or apply specific COVID-19 guidelines. It was disclosed by five out of seven surgeons that their institution provides healthcare personnel training on COVID-19. Three out of seven respondents experienced COVID-19 testing with nasopharyngeal or oropharyngeal swab tests. Surgical masks were reported as the personal protective equipment (PPE) that was commonly provided in their hospitals (Fig. 1).

Numerical data to describe the current situation each country is summarized in Table II. With the relatively rapid action and effective measures designated to control the spread of the pandemic by each government, several countries such as Singapore, Thailand, Malaysia, and Vietnam had achieved impressive results compared with Indonesia and Philippines. It appears that the low and middle-income countries (LMICs) status did not necessarily affect the current pandemic status of the region.

The current situation and personal perspective of urologists from each country are described below.

### *Indonesia*

Indonesia was deeply affected by COVID-19, same as other developing countries. Despite being ranked as the largest economy in the region, Indonesia is struggling to cope with COVID-19 crisis.<sup>4</sup>

By mid July 2021, the proportions of death-related to COVID-19 reached to 69,210 cases, making it one of the highest number of cases in the world. The government gradually established the decentralized lockdowns but never reached the same rigidity level compared to other countries.<sup>5</sup> The implementation of polymerase chain reaction (PCR) testing across countries was low during that time.<sup>6</sup>

Danarto (An-Nur Surgery Specialty Hospital, Yogyakarta) noted that the spread of coronavirus in Indonesia had significantly impacted the urological services in general, shown by a drastic reduction during the earlier phase of the pandemic. However, this only lasted for eight weeks after the government decided to adjust the PSBB rules in many regions by early June 2020, resulting in a bounce-back rate of outpatient visits, elective surgeries, and ED visits. Due to the ongoing crisis, the Indonesian Urological Association took immediate action by releasing specific guidelines for urological services during COVID-19 pandemic to help local urologists make a clinical decision. With the current situation, Indonesia still has a long way to overcome the pandemic; thus, sustaining the urological services is going to be challenging with extra precautions, and utilization of PPE is mandatory.

### *Malaysia*

In Malaysia, the first COVID-19 case was diagnosed on January 25, 2020. They had the largest cumulative number of COVID-19 cases among SEA countries by March 21, 2020. The active cases had reached from <30 cases at the earlier March 2020 to 2,766 cases by the end of March 2020. Nevertheless, the outbreak was considered under control by early June 2020. Currently, Malaysia has entered its recovery from COVID-19 pandemic.<sup>7</sup> It took not less than eight months after the government announced the first case, and the country was recognized to successfully managed the pandemic by the World Health Organization (WHO).<sup>8</sup> One of the contributing factors was because to the Ministry of Health of Malaysia constructed prompt and responsive action for COVID-19, promulgated the Movement Control Order early March 2020, and strictly enforced mass testing and rapid contact tracing.<sup>9</sup>

Teng Aik Ong (University of Malaya, Kuala Lumpur) reported that urological services in his center had been back to almost normal. However, during the earlier phase COVID-19, there was a massive cut down in outpatient visits and the number of elective surgeries. In terms of current challenges, issues that need to be addressed include concerns over clearing the backlog of cases. Zoom platform is a new thing learned to have meetings and ward rounds. For the latest development, there was a resurgent of COVID-19 cases in Malaysia in the early part of 2021. However, the health care system had learned to cope with such surge. The clinical service was adjusted to the appropriate level to mitigate the spread of the disease, while maintaining adequate service to urgent and semi-urgent cases, such as uro-oncology. Such balancing act will be the strategy in the new normal.

### *Philippines*

As the second most populous country in the region, Philippines was affected by the pandemic quite early and currently is still struggling to defend against COVID-19.<sup>10</sup> At first, the Philippine government declared a state of a national public health emergency that engendered the formation of an Inter-Agency Task Force, enforcing multiple forms of home quarantines and lockdowns in regions with high number of COVID-19 cases.<sup>11</sup> These measures have continued in changing levels of severity until recently and the government is focusing now on escalating the number of mass testing to reproduce the success of better-performing countries such as Singapore and South Korea.<sup>12</sup>

Abraham and Zialcita of the National Kidney and Transplant Institute in Manila reported the Philippines' perspectives. Abraham stated that the pandemic had really caused a significant reduction in the delivery of urological services nationwide. This was mainly because of the prioritization of the pandemic related cases by the health care system. A concerted effort was made by the urological department to prioritize cases according to their severity, consistent with the guidelines set forth by the EAU. This prioritization has led to a reduction of cases being catered per day. The decline in case load was aggravated by fear of patients to seek medical help during the pandemic, thereby causing a drop in outpatient consultations. In order to overcome the risks of contracting the disease, several

practitioners applied control measures such as the widespread utilization of virtual consultations and specialized PPE. Many hospitals were challenged but specialized centers in the Philippines such as the National Kidney and Transplant Institute and St. Luke's Medical Center had resumed all elective surgeries and were able to cope with the pandemic. In fact, percutaneous nephrolithotomy, laparoscopy and robotic-assisted surgeries were offered to patients who needed them. The expedient preoperative evaluation of patients for COVID-19 infection was made possible with the GeneXpert® testing which allowed the prompt release of results within hours. Zialcita confirmed the importance of utilization of virtual consultations, such as Viber® and WhatsApp® platforms, in order to avoid face-to-face consultations. Dr Abraham also expressed the importance of preoperative evaluation with oropharyngeal and nasopharyngeal swab reverse transcription-polymerase chain reaction (RT-PCR) among patients and inclusive of their family members. In terms of organizational reactions to the pandemic, the Philippine Urological Association responded by arranging webinars to disseminate guidelines on the practice of urology during the pandemic, with the goals of optimizing the delivery of care while protecting the practicing physician from contracting the coronavirus disease.

### *Singapore*

No government was adequately prepared for this new pandemic, including Singapore as the most developed country in the region. However, since the first confirmed cases were reported in the country on January 23, 2020, Singapore has eventually achieved impressive results to surmount the spread of COVID-19 by enacting public health measures based on advice of experts to learn from the 2003 SARS pandemic.<sup>13</sup> This included a combination of social and workplace distancing, aggressive contact tracing, strict quarantine measures of infected and the closed contacts individuals, travel advisories, and entry restriction, which was then supported by high public compliance.<sup>14</sup> As of July 15, 2021, there were 62,804 cases with 36 deaths in Singapore.

Allen Sim (Department of Urology, Singapore General Hospital) expressed his gratitude that most of the positive cases are contained in dormitories with few positive community cases. Thus, the healthcare system is not overwhelmed. He explained that the urological services had not been much affected other than the decrease in volume during the peak of the pandemic. One of the critical issues now is that almost all meetings are conducted online, with many webinars readily available for all range of urological topics. Despite of the measures created, he expressed the craving for the international conferences and human physical interactions, which he believed many urologists are experiencing webinar fatigue and shared the same sentiment.

### *Thailand*

Being the first country to encounter the coronavirus in the region, Thailand is considered by many experts to have successfully handled the pandemic.<sup>15</sup> In total, 372,215 cases were detected, and 3,032 deaths by the mid of July 2021.



**Table I: Demographic data**

Variables	N = 7, count
Gender	
Male	7
Female	0
Years of practice	
1–5	1
6–10	1
>10	5
Country origin	
Indonesia	1
Malaysia	1
Philippines	2
Singapore	1
Thailand	1
Vietnam	1
Types of hospital/institution	
Academic hospital	4
Non-academic public hospital	1
Private practice	1
Mixture of public and private practices	1
Subspecialty field of urology	
General urology	5
Stones	6
BPH	4
Uro-oncology	6
Renal transplantation	3

**Table II: Summary of actual status of COVID-19 pandemic's burden across Southeast Asian region**

Country	Classification*	Population (in millions)†	Date first reported confirmed cases	No. confirmed cases**	No. of test performed**	CFR (%)	IFR (%)
Indonesia	Upper-middle income	267.0	March 2, 2020	2,670,046	22,373,873	2.6	2.6
Malaysia	Upper-middle income	32.7	January 25, 2020	867,567	15,866,357	0.7	0.7
Philippines	Lower-middle income	109.2	January 30, 2020	1,485,457	15,662,056	1.7	1.8
Singapore	High-income	6.2	January 23, 2020	62,804	14,751,144	<0.1	0.1
Thailand	Upper-middle income	69.0	January 13, 2020	372,215	8,129,670	0.8	0.8
Vietnam	Lower-middle income	98.7	January 23, 2020	38,239	8,434,266	0.4	0.4

Abbreviations: COVID-19, coronavirus disease 2019; CFR, case fatality rate; IFR, infection fatality rate

\*Classified according to the World Bank country income status.<sup>30</sup> According to official statistics of World Bank for 2021 fiscal year, calculated using the World Bank Atlas method, low-income economies are defined as those with a gross national income (GNI) per capita of \$1,035 or less in 2019; lower middle-income economies are those with a GNI per capita between \$1,036 and \$4,045; upper middle-income economies are those with a GNI per capita between \$4,046 and \$12,535; high-income economies are those with a GNI per capita of \$12,536 or more

†Data from U.S. and World Population Clock by United States Census Bureau,<sup>31</sup> as of July 15, 2020

\*\*Based on data reported to the registries as of July 15, 2020

Three months after the government established a state of emergency in late March 2020, most daily activities returned to normal in Bangkok and other royal territories. The early response was probably in disarray, but with improved coordination and communication, the government managed to respond better to the pandemic.<sup>16</sup>

It is suggested that robust central control and a well-developed health care system, complemented by near-universal health coverage, had been the key to such accomplishment. This allowed the successful implementation of active case finding, contact tracing, and other confinement protocols through the extensive and well-distributed network of healthcare providers. The country has been listed among the Global Health Security Index's top tier as the most prepared country for national health security.<sup>17</sup> Thailand has also become the highest adopter in compliance with mask-wearing in public places, which appears to have helped the slow spread of the virus.<sup>18</sup>

Supachai Sathidmangkang (Faculty of the Medicine Siriraj Hospital, Mahidol University, Bangkok) admitted that COVID-19 era has transformed healthcare activity into the new normal since the first confirmed cases on January 13, 2020. The number of COVID-19 cases had risen rapidly, overfilled hospital beds, medical personnel, and wearing of PPE keep patients and healthcare personnel safe. Regarding the impact on the urological services in his daily practices, he has been asked to limit his work in outpatient and surgical procedures. This resulted in a three-month backlog of cases of the non-urgent surgeries delayed because of the postponement. The preoperative COVID-19 screening protocol is compulsory for patients who needed to undergo surgery. He noted that the most crucial matter to consider is patient care based on prioritization and consequently the tiered surgery system is the key.

**Table III: SWOT analysis**

Influencing Factors	Influencing Factors	Weaknesses
	<ol style="list-style-type: none"> <li>1. Risk-stratify the elective surgery according to latest evidence<sup>32**</sup></li> <li>2. Specific guidelines for COVID-19 launched by several urological societies and groups<sup>32*</sup></li> <li>3. Growing recognition of urology as an essential part of a robust health system<sup>33*</sup></li> <li>4. Widely available resources<sup>34*</sup></li> </ol>	<ol style="list-style-type: none"> <li>1. Possibility to operate on large volume diseases caused by delay due to pandemic, lead to longer operating room time and more positive surgical margins*</li> <li>2. Geographical maldistributions of urological workforces in low and middle-income countries (LMIC)<sup>35*</sup></li> <li>3. Poor health insurance coverage in some countries<sup>36*</sup></li> <li>4. Large patient volumes<sup>34***</sup></li> </ol>
Strategies		
Opportunities	↑ S → ↑ O	W → ↑ O
<ol style="list-style-type: none"> <li>1. Surgery may be the safer option among various treatment modalities which requires multiple visits, e.g. chemotherapy and radiotherapy<sup>22****</sup></li> <li>2. Incorporation of technology in bridging the distance, e.g. telemedicine &amp; video conferencing<sup>23*</sup></li> <li>3. Task-sharing/hospital co-management and task-shifting<sup>29*</sup></li> </ol>	<ol style="list-style-type: none"> <li>1. Perform surgery based on risk stratification and wear the proper PPE<sup>32**</sup></li> <li>2. Enhance technical skills and appropriate knowledge among resident and non-urologist through additional training, webinars, podcast, etc.<sup>29**</sup></li> <li>3. Offers rewards or grants for HCW such as job promotion or recognition-of-services*</li> </ol>	<ol style="list-style-type: none"> <li>1. Allocate additional/extended work after hours or during weekend to cope the backlog<sup>37**</sup></li> <li>2. Expand the telemedicine usages, optimization of the OR schedules and augment with ambulatory surgery center, if necessary<sup>23*</sup></li> <li>3. Revitalize the advanced HCW e.g. the physician assistants, nurse practitioners, and advanced registered nurse<sup>29*</sup></li> </ol>
Threats	↑ S → T	
<ol style="list-style-type: none"> <li>1. Despite its benefits, the surgery risk stratification approach could potentially lead to worse disease progression<sup>22,32****</sup></li> <li>2. The long waiting list could create anxiety and deprived overall quality of life among patients<sup>38***</sup></li> <li>3. Shortage of PPE due to surging global demand &amp; depleted stockpiles<sup>28*</sup></li> <li>4. Healthcare personnel duty-hour restriction<sup>39**</sup></li> <li>5. Political inconsistencies among countries are unequivocally rising from religious, cultural, economic and government systems diversity*</li> <li>6. Catastrophic expenditure on surgery<sup>26*</sup></li> <li>7. Economic changes<sup>25*</sup></li> <li>8. Ethical obligations<sup>40**</sup></li> </ol>	<ol style="list-style-type: none"> <li>1. Perform critical analysis of the literature on surgical delay as a guide timing of treatment to minimize risk to patients and hospital resources<sup>32**</sup></li> <li>2. Perform a multi-disciplinary approach to consider all the aspects of each case, including the type and stage of disease, the age, the physical status, the psychological issues, and the availability of alternative treatments<sup>38**</sup></li> <li>3. Keep patients well-informed through website's posts, emails or texts<sup>23*</sup></li> <li>4. Relationship building among staffs<sup>23**</sup></li> </ol>	<ol style="list-style-type: none"> <li>1. Optimization in resource allocation according to benchmark for PPE required in urological procedures<sup>23*</sup></li> <li>2. Use effective shift duration and staff placement according to the routine tasks<sup>39*</sup></li> <li>3. Optimize workforce schedules<sup>39*</sup></li> <li>4. Ramping up telehealth to deliver services to keep staff on the job<sup>23*</sup></li> <li>5. Consider patient's perspective as a victim and vector of disease, while still putting forward the basic ethical principles (autonomy, non-maleficence, beneficence and justice) when encountered difficult judgment<sup>40**</sup></li> </ol>

S: Strengths, W: Weaknesses, O: Opportunities, T: Threats, ↑: Optimizing, : Eliminate

\*Administrative factors; \*\*Healthcare worker related factors;

\*\*\*Patient related factors; \*\*\*\*Disease related factors

### Vietnam

Vietnam is among the most successful countries to halt the COVID-19 and earned much international praise for its effective pandemic response.<sup>19</sup> Since its first confirmed cases on January 23, 2021 to July 31, 2021, Vietnam had detected 38,239 cases with only 138 deaths, compared to 5,829,724 detected cases with more than 100,000 deaths in France during the same timeline. One contributing factor was the ability of the government to fully implement strict enforcement of large-scale lockdown protocols and obligatory

quarantine with very high public compliance, utilizing its state apparatus of a centralized system of the government.<sup>20</sup>

In terms of the specific impact on urological services, Dong Nguyen (Binh Dân Hospital, Ho Chi Minh City) reported no significant changes during the pandemic. This was probably due to COVID-19 situation being relatively under control in the country. The Vietnam Urological Association did not develop specific guidelines, and Mr. Dong did not apply specific guidelines for his daily practices.

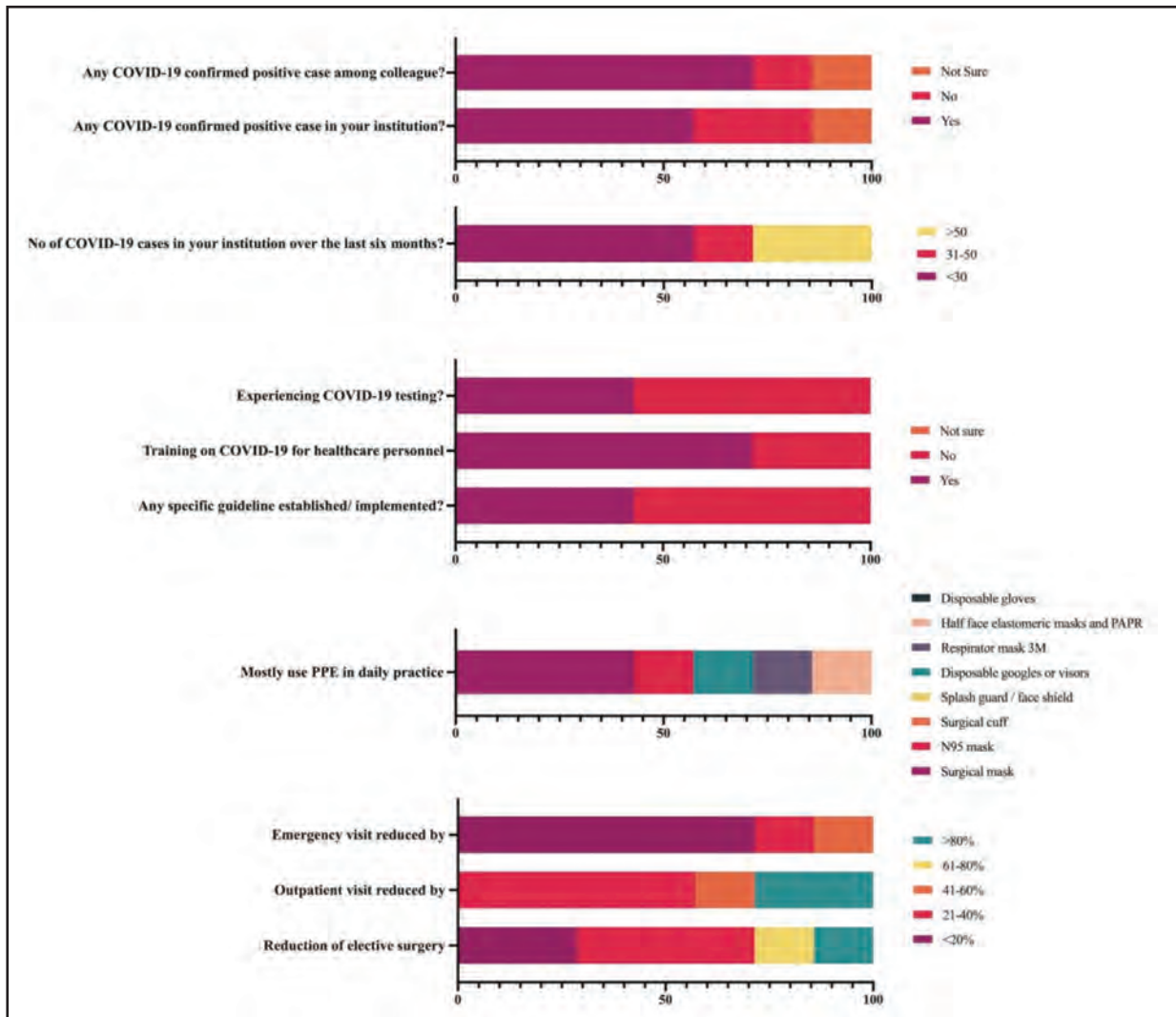


Fig. 1: Overview of the individual consultant urologist's statements on the questionnaire. For the full question texts, please refer to the questionnaire in the supplemental data.

## DISCUSSION

Through the SWOT analysis (See Table III), several strategies can be developed: (1) reboot the urological services safely and sustainably; (2) optimize financial and infrastructural capacities; and (3) regional collaboration to strengthen the health systems. Although these cannot cover all possible problems, these strategies aimed at urologists at SEA countries, and we tried to cover a wide range of situations encountered during the pandemic.

### *Reboot the urological services in a safe and sustainable manner*

Resumption, followed by a consistent delivery of specialized services such as urology during a pandemic crisis is essential. A delay can potentially lead to serious adverse events, which can result to an extensive procedure, and may complicate by worsening the disease condition and progression. However, the safety of both healthcare providers and patients is paramount. Proper strategy is effective to maintain the balance between the resumption of urological routine services while strengthening the efforts to curb the spread of COVID-19 through the following principles: (1) Determine if

the pandemic curve, the outbreak is within the region.<sup>21</sup> This is intended to engage relevant stakeholders and authorities to take necessary actions. Urological services, especially elective surgeries, should ideally be started when the curves flatten out, no vast surges or sustained spikes, and the community spreads is considerably under control. It is essential to note from the previous Spanish flu pandemic experienced, a second wave which was more lethal than the previous one. (2) Perform a reliable COVID-19 screening.<sup>22</sup> The gold standard is the molecular testing of upper or lower respiratory tract samples through RT-PCR. The rapid serology tests are less reliable due to antibodies' uncertain serodiagnostic power against SARS-COV-2. Nevertheless, this can be done as an alternative, by combining with chest computerized tomography as being adopted in some hospitals in Beijing. (3) Carry out a graded approach based on risk stratification for urological services based on the guidelines published by several groups and societies, and the provided objective perspectives on prioritizing patients during the pandemic. (4) Develop a well-planned non-surgical program for urological patients. Management of urological

patients often require non-surgical programs such as routine consultations and rehabilitation. This urges incorporation of technology in bridging the gap, such as telemedicine.<sup>23</sup> (5) Ensure sustainable efforts.<sup>24</sup> Without a dynamic system and continuity, the whole process will not be completed. The key strategy here is to maintain a steady but gradual services capacity and flexibility to adapt to the ever-changing situation. Start with small capacity of services, then adjust the number based on the epidemic curve in the SEA region. Maximize the procedure that can be done without hospitalization. Keep updated on the current development of the pandemic and adjust the health practices appropriately.

#### *Optimizing financial and infrastructural capacities*

There are several potential problems with the infrastructural and financial aspects of the government such as reduced access to urological facilities due to lockdown orders, reduced funds for most surgical cares due to ratcheting or reallocation of the state budget,<sup>25</sup> and most surgical cares have financially enormous spending.<sup>26</sup> These can be a hinderance to our efforts towards managing the pandemic.

The role of related stakeholders is essential, but a urologist may still contribute in several ways. First, by embracing adoption of technology to help patients with access challenges. Although still new and relatively low uptake, telemedicine is still the primary choice. Secondly, build a solid supply chain by promoting and empowering locally made PPEs.<sup>27</sup> The pandemic demands us to be creative, and utilization of the locally made PPE can be the perfect alternative while maintaining the high standards of production and quality control procedures. Thirdly, drastically reduce the expenditure in surgical cases & PPE using supply chain resilient concepts.<sup>28</sup> This is important to cope with the risk of enormous spending from surgical diseases and can be done through sustainability practices. Fourthly, divide the PPE stockpiles into emergency and routine care purposes.<sup>27</sup> The goal is to be prepared when pandemic-related emergency cases occur while maintaining routine urological care sustainability.

#### *Regional collaboration to strengthen the health systems*

The discrepancy of urologist distribution highlights an area for further improvement. The geographic proximity and close economic and structural ties of SEA countries call for multi-regional collaborations. This can be by information sharing from the experts to provide joint statements through additional training, webinars, podcast, etc. and may optimize patient care during the COVID-19 crisis.<sup>29</sup>

On a larger scale, the second phase of this and in any future pandemic, which many countries have not experienced, may need a regional capacity sharing system.<sup>29</sup> This allows us to share essential resources such as regional vaccines and PPEs. This will enable less developed countries to employ healthcare workforces from nearby countries through mutual recognition arrangements.

From this point forward, health security, in general, is a pivotal part of regional and national security and is best managed by a united SEA. Urologists should be prepared to contribute to further development by taking an important leadership role during this unprecedented time.

The limitations of the study include the small sample size, lack of diversity, and the recruitment methods with limited number of respondents. Larger studies are needed to expand the data from another developing country, to increase generalizability, and to compare unique experiences among urologists during the COVID-19 crisis.

## **CONCLUSIONS**

Several challenges and opportunities in SEA countries regarding continuing urological services during the COVID-19 pandemic were identified in this study. Each country has a unique approach and progress towards COVID-19 management. These findings helped us recognize potential areas for improvement and strategies to emphasize the safety for both patients and urologists. Thus, strengthening future collaboration by joint efforts should be implemented by recognizing the need for multi-stakeholder initiatives and involving all SEA members in an approach to ensure sustainability of urological services during a pandemic. Finally, the focus of urological services recovery should be based on resilient, adaptive, and sustainable approach.

## **ACKNOWLEDGMENT**

We acknowledge the contributions of the co-authors and participants of this survey for their collaboration throughout recruitment and data collection processes. We also thank Teng Aik Ong, MBBS (Department of Surgery, Faculty of Medicine, University of Malaya, Kuala Lumpur, Malaysia), and Hermenegildo Jose B. Zialcita, MD (Department of Urology, National Kidney and Transplant Institute, Quezon City, Philippines), for their contribution in updating the current situation in Malaysia and the Philippines.

## **REFERENCES**

1. Wu Y-C, Chen C-S, Chan Y-J. The outbreak of COVID-19: An overview. *J Chin Med Assoc* 2020; 83(3): 217–20.
2. Worldometers.info. COVID-19 Coronavirus pandemic [cited Oct 2020]. Available from: <https://www.worldometers.info/coronavirus/>
3. Gürel E, Tat M. SWOT analysis: a theoretical review. *J Int Soc Res* 2017; 10(51): 994–1006.
4. International Monetary Fund. World Economic Outlook, October 2020: A long and difficult Ascent [cited Oct 2020]. Accessed from: <https://www.imf.org/en/Publications/WEO/Issues/2020/09/30/world-economic-outlook-october-2020>
5. Gaduh A, Hanna R, Kreindler G, Olken B. Lockdown and mobility in Indonesia [cited Oct 2020]. Available from: <https://histecon.fas.harvard.edu/climate-loss/indonesia/index.html>
6. Hasan A, Susanto H, Kasim ME, Nuraini N, Triany D, aLestari BW. Superspreading in early transmissions of COVID-19 in Indonesia. *medRxiv*. 2020; 10: 1–4.
7. Ho JM, Sia JKM. Embracing an uncertain future: COVID-19 and MICE in Malaysia. *Local Dev Soc* 2020; 1(2): 190–204.
8. Lo Y-R. A country united in the face of the pandemic [cited Oct 2020]. Available from: <https://www.who.int/malaysia/news/commentaries/detail/a-country-united-in-the-face-of-the-pandemic>
9. Minhat HS, Kadir Shahar H. The trajectory of COVID-19 scenario in Malaysia: facing the unprecedented. *Curr Med Res Opin* 2020; 36(8): 1309–11.
10. Lau LL, Hung N, Wilson K. COVID-19 response strategies: Considering inequalities between and within countries. *Int J Equity Health* 2020; 19(1): 10–2.



11. Vallejo BM, Ong RAC. Policy responses and government science advice for the COVID 19 pandemic in the Philippines: January to April 2020. *Prog Disaster Sci* 2020; 7(2020): 1–7.
12. UP COVID-19 Pandemic Response Team. Modified community quarantine beyond April 30: Analysis and recommendations [cited Oct 2020]. Available from: <https://up.edu.ph/modified-community-quarantine-beyond-april-30-analysis-and-recommendations/>
13. Hsu LY, Chia PY, Vasoo S. A midpoint perspective on the COVID-19 pandemic. *Singapore Med J* 2020; 61(7): 381–3.
14. Woo JJ. Policy capacity and Singapore's response to the COVID-19 pandemic. *Policy Soc* 2020; 39(3): 345–62.
15. Lim W-S, Liang C-K, Assantachai P, Auyeung TW, Kang L, Lee W-J, et al. COVID-19 and older people in Asia: Asian Working Group for Sarcopenia calls to actions. *Geriatr Gerontol Int* 2020; 20(6): 547–58.
16. Shadmi E, Chen Y, Dourado I, Faran-Perach I, Furler J, Hangoma P, et al. Health equity and COVID-19: Global perspectives. *Int J Equity Health* 2020; 19(1): 1–16.
17. Cameron EE, Nuzzo JB, Bell JA, Nalabandian M, O'Brien J, League A, et al. Global Health Security Index [cited Oct 2020]. Available from: <https://www.ghsindex.org/country/thailand/>
18. Smith M. International COVID-19 Tracker Update [cited Sep 2020]. Available from: <https://yougov.co.uk/topics/health/articles-reports/2020/07/27/face-mask-use-surges-after-becoming-compulsory-sho>
19. World Health Organization. WHO Coronavirus Disease (COVID-19) Dashboard. 2020.
20. Van Nguyen H, Van Hoang M, Dao ATM, Nguyen HL, Van Nguyen T, Nguyen PT, et al. An adaptive model of health system organization and responses helped Vietnam to successfully halt the Covid-19 pandemic: What lessons can be learned from a resource-constrained country. *Int J Health Plann Manage* 2020; 35(5): 988–92.
21. Prevention CfDca. Interpretation of epidemic curves during ongoing outbreak investigations [cited Sep 2020]. Available from: <https://www.cdc.gov/foodsafety/outbreaks/investigating-outbreaks/epi-curves.html>
22. Dovey Z, Mohamed N, Gharib Y, Ratnani P, Hammouda N, Nair SS, et al. Impact of COVID-19 on prostate cancer management: Guidelines for urologists. *Eur Urol Open Sci* 2020; 20: 1–11.
23. Hilton L. Pandemic exacts economic toll: As practices reboot, urologists consider leaner staffs and operations. *Urol Times* 2020; 48(6): 1–26.
24. Liang LL, Tseng CH, Ho HJ, Wu CY. Covid-19 mortality is negatively associated with test number and government effectiveness. *Sci Rep* 2020; 10(1): 1–7.
25. Abiad A, Arao M, Dagli S, Ferrarini B, Noy I, Osewe P, et al. The economic impact of the COVID-19 outbreak on developing Asia [cited Nov 2020]. Available from: <https://www.adb.org/sites/default/files/publication/571536/adb-brief-128-economic-impact-covid19-developing-asia.pdf>
26. Gutnik L, Dieleman J, Dare AJ, Ramos MS, Riviello R, Meara JG, et al. Funding allocation to surgery in low and middle-income countries: a retrospective analysis of contributions from the USA. *BMJ Open* 2015; 5(11): 1–8.
27. Mazingi D, Navarro S, Bobel MC, Dube A, Mbanje C, and Lavy C. Exploring the impact of COVID-19 on progress towards achieving global surgery goals. *World J Surg* 2020; 44(8): 2451–7.
28. Park C-Y, Kim K, Roth S, Beck S, Kang JW, Tayag MC, et al. Global shortage of personal protective equipment amid COVID-19: supply chains, bottlenecks, and policy implications [cited Nov 2020]. Available from: <https://www.adb.org/publications/shortage-ppe-covid-19-supply-chains-bottlenecks-policy>
29. Falk R, Taylor R, Kornelsen J, Virk R. Surgical task-sharing to non-specialist physicians in low-resource settings globally: A systematic review of the literature. *World J Surg* 2020; 44(5): 1368–86.
30. World Bank Group. World Bank country lending groups country classification [cited Sep 2020]. Accessed from: <https://datahelpdesk.worldbank.org/knowledgebase/articles/906519>
31. United States Census Bureau. U.S. and world population [cited Oct 2020]. Accessed from: <https://www.census.gov/popclock/>
32. Heldwein FL, Loeb S, Wroclawski ML, Sridhar AN, Carneiro A, Lima FS, et al. A systematic review on guidelines and recommendations for urology standard of care during the COVID-19 pandemic. *Eur Urol Focus* 2020; 6(5): 1070–85.
33. Campaign NJ, MacDonagh RP, Mteta KA, and McGrath JS. Global surgery - How much of the burden is urological? *BJU Int* 2015; 116(3): 314–6.
34. Kumar R. A new era of Asian urology: a SWOT analysis. *Nat Rev Urol* 2016; 13(11): 685–9.
35. Metzler I, Bayne D, Chang H, Jalloh M, and Sharlip I. Challenges facing the urologist in low- and middle-income countries. *World J Urol* 2020; 38(11): 2987–94.
36. Van Minh H, Pocock NS, Chaiyakunapruk N, Chhorvann C, Duc HA, Hanvoravongchai P, et al. Progress toward universal health coverage in ASEAN. *Glob Health Action* 2014; 7(1): 1–12.
37. Desouky E. Urology after COVID-19: The post-apocalypse. *Urol Nephrol Open Access J* 2020; 8(4):109–12.
38. Soltany A, Hamouda M, Ghzawi A, Sharaq A, Negida A, Soliman S, et al. A scoping review of the impact of COVID-19 pandemic on surgical practice. *Ann Med Surg* 2020; 57: 24–36.
39. Dexter F, Parra MC, Brown JR, Loftus RW. Perioperative COVID-19 defense: An evidence-based approach for optimization of infection control and operating room management. *Anesth Analg* 2020; 131(1): 37–42.
40. Chubak BM, Gerrek ML, Kyprianou N. Urologic oncology: News and topics: Ethics of urologic care in the time of COVID-19. *Urol Oncol* 2020; 38(6): 557–9.

# Predictive accuracy of the APACHE IV scores on mortality and prolonged stay in the intensive care unit of Dr Sardjito Hospital

Yunita Widyastuti, PhD, Wildan Arsyad Zaki, MD, Untung Widodo, PhD, Akhmad Yun Jufan, MD, Bhirowo Yudo Pratomo, MD

Department of Anesthesiology and Intensive Therapy Faculty of Medicine, Public Health, and Nursing, Universitas Gadjah Mada, Indonesia

## ABSTRACT

**Introduction:** Acute Physiology and Chronic Health Evaluation (APACHE) is the most widely used scoring system in the intensive care unit (ICU). The APACHE IV showed a good level of discrimination and calibration on predicting mortality and prolonged stay (PLOS) in some countries. This study is aimed to determine the predictive accuracy of the APACHE IV score on mortality and PLOS at the ICU of Dr Sardjito General Hospital (SGH).

**Materials and Methods:** This study involved all adult patients at the ICU of SGH during 2018 that met the inclusion criteria. The discrimination of APACHE IV scores on mortality and PLOS was analyzed with Receiver Operating Characteristic Curve, and the optimal cut-off point was assessed with the Youden Index. The calibration of the APACHE IV score was assessed with the Hosmer-Lemeshow goodness-of-fit test, and a  $p$ -value of  $>0.05$  is considered a good calibration.

**Results:** From the data of 742 patients, only 476 were included. The overall mortality and PLOS rate was 25.4 % and 15.1 %, respectively. The mean of APACHE IV score was  $66.27 \pm 27.7$ . The area under the receiving curve with a 95% confidence interval for mortality is  $0.99(0.97-1.00)$  and for PLOS was  $0.68(0.62-0.74)$ . The optimal cut-off point of the APACHE IV score for mortality was 78.9, with a sensitivity of 0.96 and a specificity of 0.96. The optimal cut-off point of the APACHE IV score for PLOS is 62.5 (in the 6th percentiles), with a sensitivity of 0.72 and a specificity of 0.61. The calibration is good for mortality prediction ( $p=0.98$ ) but is poor for PLOS prediction ( $p=0.01$ ).

**Conclusion:** APACHE IV score has excellent accuracy for mortality prediction but is poor for PLOS prediction in patients in the ICU of SGH.

## KEYWORDS:

APACHE IV score, ICU, Mortality, PLOS, Prediction

## INTRODUCTION

The scoring system to predict the outcome of critically ill patients is needed for consideration of decision making, resources allocation, benchmarking, and stratification for clinical trials.<sup>1</sup> The accuracy of the risk prediction models are

measured by their good calibration, discrimination, and generalizability (good reproducibility of the score and transportability across geographic, time, and methodology). Some scores have excellent performance in the population they were originally developed. Still, some lose the accuracy when applied to different populations because of the differences in the population characteristic from where the score was initially created.<sup>2</sup> Population characteristics, the severity of disease, and health policy differ within and between countries from time to time; therefore, the risk prediction models require regular validation and refinement (for example, by recalibration).<sup>3</sup>

The intensive care unit (ICU) scoring system for intensive care has been developed since 1980 in response to demands for the evaluation and monitoring of health services. The system allows for a comparative audit and evaluation of intensive service research. Several assessment systems have been developed for critically ill patients to predict the likelihood of patients surviving in the hospital. Mortality and prolonged stay (PLOS) prediction in critically ill can benefit health services for quality improvement.<sup>1</sup>

The Acute Physiology and Chronic Health Evaluation (APACHE) and Simplified Acute Physiology Score (SAPS) are the most widely used scoring systems in the ICU.<sup>4</sup> The APACHE IV was introduced in 2006. The development of the APACHE IV system is based on 104 ICUs and 131,618 patients from the United States of America (USA).<sup>5</sup>

The APACHE IV score has a good level of discrimination and calibration with a broadly validated sample size and receiver operating characteristics (ROC) of 0.88.<sup>5</sup> The APACHE IV score can be used as an ICU benchmark by using the standardized number of mortality ratio to evaluate groups of patients.<sup>6</sup>

This study is aimed to assess the predictive accuracy of the APACHE IV score on mortality and PLOS of patients in a single tertiary hospital.

## MATERIAL AND METHODS

This retrospective study was based on the data of patients who were admitted to the ICU in SGH from January 1 to December 31, 2018. The study was conducted after the

Corresponding Author: Yunita Widyastuti  
Email: yunita.widya@ugm.ac.id

**Table I: Demographic Data of Research Participants**

Variable	TOTAL n(%)	Dead (n=119) n(%)	PLOS(70) n(%)
Gender			
Female	256(53.4)	45(37.8)	30(42.9)
Male	220(46.6)	74(62.2)	40(57.1)
Age (years)			
< 20	12(2.5)	3(2.5)	2(2.9)
21-40	144(30.3)	25(20.0)	17(24.3)
41-60	210(44.1)	32(26.9)	32(45.8)
60-80	100(21.0)	52(43.7)	16(22.9)
>80	10(2.1)	7(5.9)	3(4.3)
Diagnosis at Admission			
Medical	108(22.7)	63 (52.9)	38(54.3)
Post Neurosurgery	172(36.1)	16 (13.4)	18(25.7)
Post Orthopedic surgery	31(6.5)	1 (0.8)	0(0)
Post Urologic surgery	17(3.6)	1 (0.8)	0(0)
Post Digestive surgery	43(9.0)	23 (19.3)	5(7.1)
Post Oncologic surgery	10(2.1)	1 (0.8)	1(1.4)
Post-Obstetric-gynecologic surgery	47(9.9)	7 (5.9)	5(7.1)
Post-Thorax/Vascular surgery	48(10.1)	7 (5.9)	3(4.3)

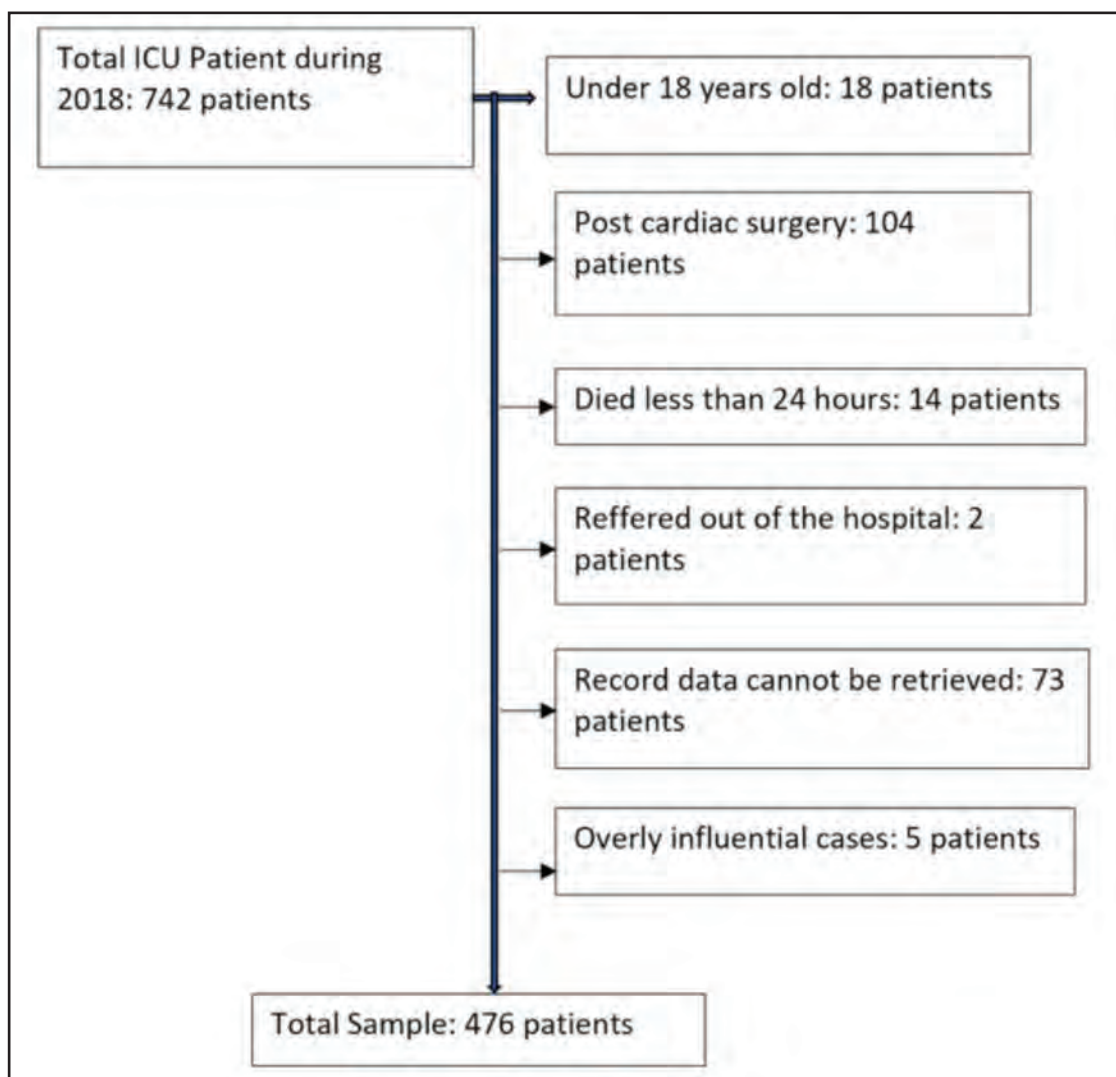


**Fig. 1: The study sampling**

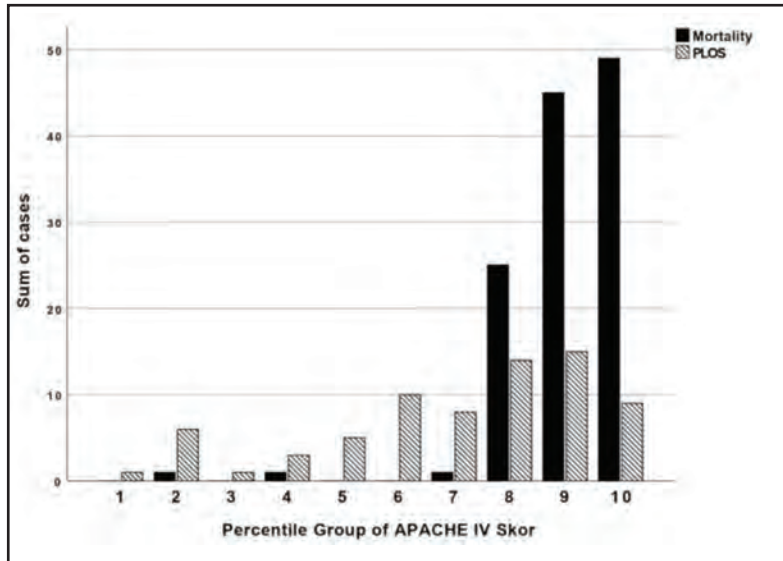


Fig. 2: The outcome based on the deciles of the acute physiology and chronic health evaluation (APACHE) IV.

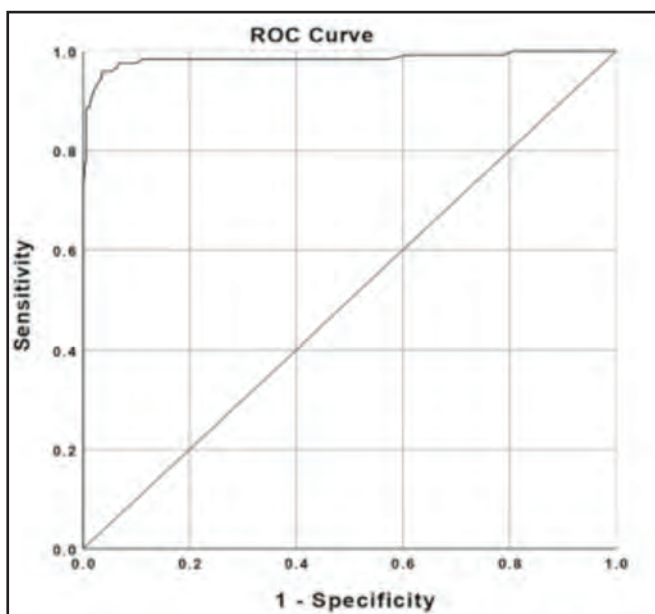


Fig. 3a: The discrimination of the acute physiology and chronic health evaluation (APACHE)IV score for mortality, the area under the curve (AUC) of Receiver Operating Characteristics (ROC) with 95% confidence interval (CI) for mortality: 0.99(0.97–1.00).

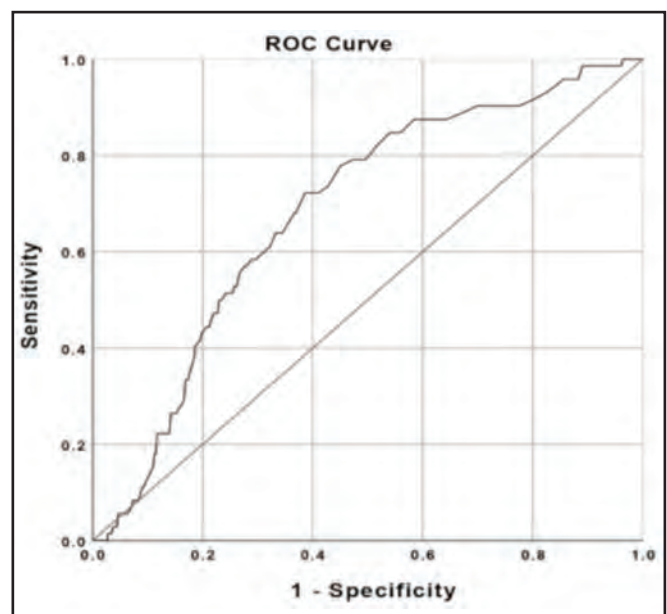


Fig. 3b: The discrimination of the acute physiology and chronic health evaluation (APACHE) IV score for PLOS, the area under the curve (AUC) of Receiver Operating Characteristics (ROC) with 95% confidence interval (CI) for a prolonged length of stay: 0.68 (0.62–0.74).

approval from the Ethical Committee No KE/FK/0684/EC/2019. The inclusion criteria in this study were all adult ( $\geq 18$  years old) patients admitted to the ICU of SGH. The exclusion criteria include the following: post-cardiac surgery, treatment  $< 24$  h, referred out of the hospital, and patients whose medical record data could not be collected during the sampling period. The dependent variable is mortality, defined as ICU mortality and PLOS as ICU stay  $> 7$  days. The independent variable in this study is the APACHE IV score.

The APACHE IV score was calculated according to the website ([http://www.mecriticalcare.net/icu\\_scores/apacheIV.php](http://www.mecriticalcare.net/icu_scores/apacheIV.php)), based on the patient's data in the first 24 h. The ROC producing an area under the curve (AUC) with 95% confidence intervals (CIs) was used to assess discrimination power. The optimal cut-off points of sensitivity and specificity were calculated using Youden Index. The calibration of the APACHE IV score was assessed with the Hosmer-Lemeshow goodness-of-fit test, and a p-value of  $> 0.05$  is considered a good calibration.



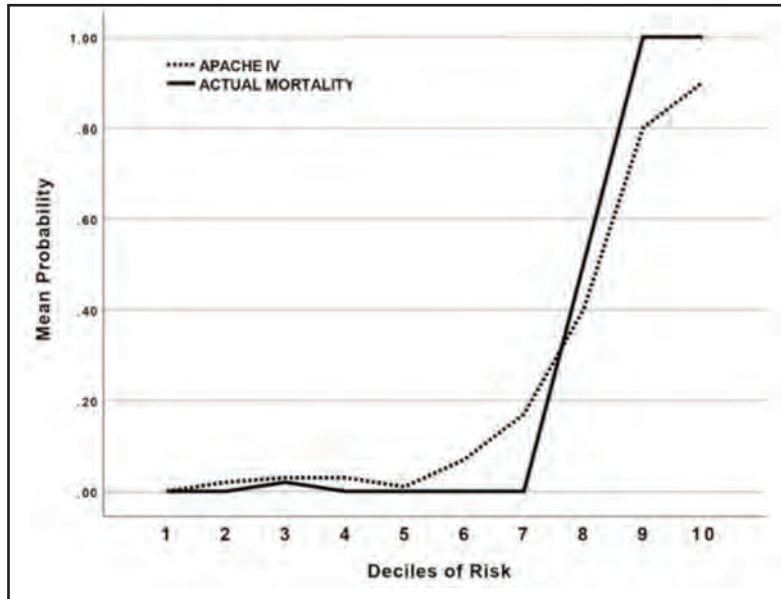


Fig. 4: The Observed versus Predicted Mortality by the acute physiology and chronic health evaluation (APACHE) IV score.

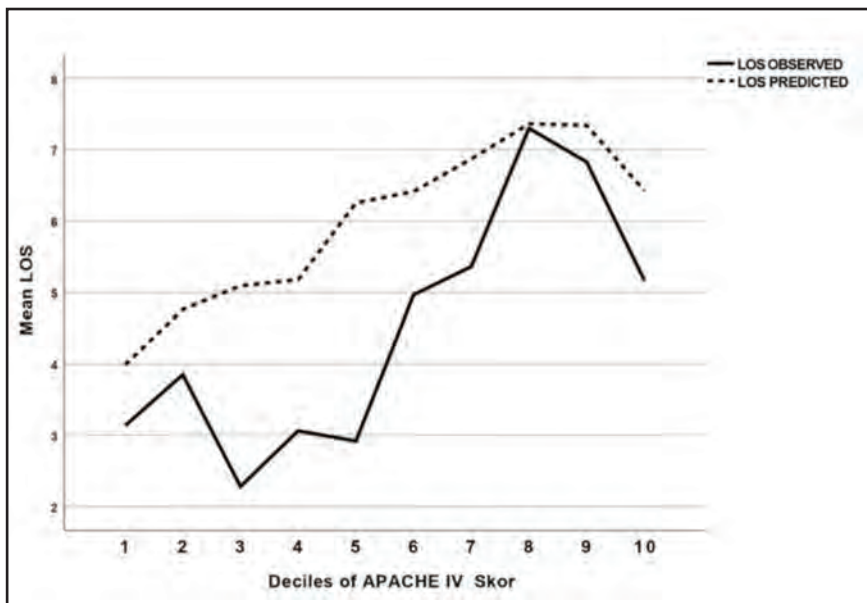


Fig. 5: The Observed versus Predicted prolonged length of stay by the acute physiology and chronic health evaluation (APACHE) IV score.

The ROC and Hosmer-Lemeshow tests were calculated using the Statistical Package for the Social Sciences (version 27.0 SPSS Inc., Chicago, IL, USA). Descriptive statistics were calculated with continuous data presented as mean  $\pm$ SD and categorical data presented as percentages. Overly influential variables were removed from the data.

**RESULTS**

The study was conducted on the medical records of 742 patients, but only 476 patients were included in the study sample (Fig. 1).

The baseline characteristics of the study group are presented in Table I. Of 476 patients, there were 220 males (46.6%), with an average age of  $48 \pm 16$  years. The mortality rate was 25.4%, the PLOS rate was 15.1%, and the APACHE IV score was underestimated at 23.4% and 6%, respectively. Male patients have a higher incidence of mortality (62.3%) and PLOS (58.3%). Patients aged 61–80 years had the highest mortality rate (44.1%), whereas 41–60 mostly experienced PLOS (45.8%).

Patients admitted to the ICU were divided into two large groups, namely, 108(22.7%) medical cases and 368 (77.3%) surgical cases, and most patients who died had a medical

admission diagnosis (52.9%) followed by digestive surgery 23(19.3%). Most patients with PLOS were diagnosed with a medical condition (52.8%), followed by a neurosurgery procedure 18 (25.7%) (Table 1).

Fig. 2 shows the outcome distribution of APACHE IV scores into deciles, which led that patients who died mainly in the APACHE score range 81–100 and patients who got PLOS especially were 61–80. The percentage of patients living was 100% in patients with APACHE IV scores of <40, whereas 100% of patients were dead in scores of >100, which reveal the fact that the greater the APACHE IV score, the higher the mortality rate, but not the same for PLOS.

The accuracy of the APACHE scores to discriminate the patients who died was excellent with AUC with a 95% CI for mortality: 0.99(0.97–1.00) (Fig. 3a). The AUC (95%CI) for PLOS was 0.68 (0.62–0.74), which is considered poor (Fig.3b). The optimal cut-off point of the APACHE IV score for mortality was 78.9 (in the 8th percentiles), with a sensitivity of 0.96 and specificity of 0.96. The optimal cut-off point for PLOS prediction was 62.5 (in the 6th percentiles), with a sensitivity of 0.72 and specificity of 0.61.

The calibration of the APACHE IV score for mortality was good with a p-value of 0.98, but poor for PLOS with a p-value=0.01. The APACHE score slightly overestimated the mortality in the low risk and underestimated the high risk (Fig.4). For PLOS prediction, the APACHE IV score tends to overestimate the length of stay (Fig. 5).

## DISCUSSION

This study revealed that the APACHE IV score consistently gives good discrimination in predicting mortality. The accuracy of predicting mortality was higher than the accuracy of predicting PLOS. This finding is consistent with another study.<sup>5-14</sup> The discrimination of the APACHE IV score for mortality prediction in our research is as good as in the original population, despite the different characteristics of a population. In our study, the age of ICU patients was younger, and the mean of the APACHE score was higher (66.27 vs 46.43).<sup>5</sup> The number of patients who died with the APACHE IV score of >100 was 59% in our study, whereas the original APACHE IV score was only 47%, and the remaining 39.7% had the APACHE IV score of 80–100.

The APACHE IV score is a physiology-based classification system that measures disease severity in a group of patients with a critical illness. The accuracy of the APACHE IV score plays a role in improving patient services. Its ability to provide mortality prognosis has been tested in USA and parts of Europe and Asia.<sup>5,7-9</sup>

The calibration of the APACHE IV score in predicting mortality is good. A study by Choi et al. also revealed the superiority of the APACHE IV calibration ( $p=0.905$ ) compared to the APACHE II score ( $p=0.805$ ).<sup>9</sup> Costa et al. (2011) prospectively examined APACHE IV, SAPS III, and MPMIII scores in critical patients with acute renal failure and showed good discrimination (AUROC 0.74) and calibration ( $p$ -value:0.574).<sup>14</sup> The calibration of the APACHE IV on mortality, especially in high-risk patients, is underestimated.

However, the overall calibration on mortality is still good. However, some studies showed that the mortality prediction of the APACHE IV was not accurate. The differences in patient characteristics, clinical practice, assurance, quality, and services of health care systems may make different outcomes. The study by Chan et al.<sup>15</sup> reported that the accuracy of the APACHE IV score for mortality prediction was poor. They conducted a retrospective study of a group of postoperative patients with surgical abdominal sepsis and showed that the APACHE IV score poorly predicted mortality. The other study also reported that the APACHE IV score did not accurately predict mortality in patients with trauma.<sup>16</sup>

Recently, the accuracy of the APACHE IV score was compared to the APACHE II and Sequential Organ Failure Assessment (SOFA) score for mortality in patients with Coronavirus disease in the ICU and showed that all scores had bad discrimination on overall population (the APACHE IV AUROC 0.67 vs 0.63 of APACHE II vs 0.53 of SOFA score). On the other hand, the APACHE IV had the best discriminative power of the three scoring systems in the subgroup of patients with low molecular weight heparin (APACHE IV AUROC 0.82 vs 0.7 of APACHE II vs 0.49 of SOFA score).<sup>17</sup>

The APACHE IV score lacked both discrimination and calibration in predicting PLOS and tends to overestimate prediction. Patients with PLOS in our population mainly were patients with a medical diagnosis, sepsis, and more than one organ failure. Thus, they tended to have a shorter length of stay because they died earlier than patients with a lower score. Another factor determining the inaccuracy of the APACHE IV score in predicting PLOS is the differences in time units to calculate the length of treatment from the time patients enter until discharge. The original study of APACHE scores used hours, whereas our study used days.<sup>6</sup> The APACHE IV scores have poor performance in patients with severe sepsis<sup>6</sup> and have poor accuracy in the length of stay prediction, especially in severe sepsis and trauma cases.<sup>11,18</sup>

The difference in hospital policy related to the patient's end-of-life status, case-mix differences, insurance policies, step-down policy, and differences in clinical practice between USA and Indonesia affected the accuracy in predicting PLOS. This study has several limitations. Firstly, 9.8% of medical records cannot be taken and secondly only data for 1-year was taken, and more extensive data may give a different result.

## CONCLUSION

APACHE IV score has excellent accuracy for mortality prediction but poor accuracy for PLOS prediction in patients admitted in the ICU of SGH.

## ACKNOWLEDGMENT

This research is funded by RSUP Dr Sardjito grant no: HK.02.03/XI.2/8268/2019.

## CONFLICT OF INTEREST

None to declare.

## REFERENCES

1. Rapsang AG, Shyam DC. Scoring systems in the intensive care unit: A compendium. *Indian J Crit Care Med* 2014; 18(4): 220–8.
2. Myers PD, Ng K, Severson K, Kartoun U, Dai W, Huang W, et al. Identifying unreliable predictions in clinical risk models. *npj Digit Med*. 2020; 3(1): 1-8.
3. Shrestha GS. Developing a feasible and valid scoring system for critically ill patients in resource-limited settings. *Crit Care* 2018; 22(1): 1–2.
4. Sakr Y, Krauss C, Amaral ACKB, Réa-Neto A, Specht M, Reinhart K, et al. Comparison of the performance of SAPS II, SAPS 3, APACHE II, and their customized prognostic models in a surgical intensive care unit. *Br J Anaesth* 2008; 101(6): 798–803.
5. Zimmerman JE, Kramer AA, McNair DS, Malila FM. Acute Physiology and Chronic Health Evaluation (APACHE) IV: Hospital mortality assessment for today's critically ill patients. *Crit Care Med* 2006; 34(5): 1297–310.
6. Zimmerman JE, Kramer AA, McNair DS, Malila FM, Shaffer VL. Intensive care unit length of stay: Benchmarking based on Acute Physiology and Chronic Health Evaluation (APACHE) IV. *Crit Care Med* 2006; 34(10): 2517–29.
7. Shrope-Mok SR, Propst KA, Iyengar R. APACHE IV versus PPI for predicting community hospital ICU mortality. *Am J Hosp Palliat Care* 2010; 27(4): 243–7.
8. Choi JW, Park YS, Lee YS, Park YH, Chung C, Park DI, et al. The Ability of the Acute Physiology and Chronic Health Evaluation (APACHE) IV score to predict mortality in a single tertiary hospital. *Korean J Crit Care Med* 2017; 32(3): 275–83.
9. Ghorbani M, Ghaem H, Rezaianzadeh A, Shayan Z, Zand F, Nikandish R. A study on the efficacy of APACHE-IV for predicting mortality and length of stay in an intensive care unit in Iran. *F1000Res* 2017; 20(6): 2032.
10. Brinkman S, Bakhshi-Raiez F, Abu-Hanna A, de Jonge E, Bosman RJ, Peelen L, et al. External validation of Acute Physiology and Chronic Health Evaluation IV in Dutch intensive care units and comparison with Acute Physiology and Chronic Health Evaluation II and Simplified Acute Physiology Score II. *J Crit Care* 2011; 26(1): 105.e11–8.
11. Keegan MT, Gajic O, Afessa B. Comparison of APACHE III, APACHE IV, SAPS 3, and MPM0III and influence of resuscitation status on model performance. *Chest* 2012; 142(4): 851–8.
12. Lee H, Shon Y-J, Kim H, Paik H, Park H-P. Validation of the APACHE IV model and its comparison with the APACHE II, SAPS 3, and Korean SAPS 3 models for the prediction of hospital mortality in a Korean surgical intensive care unit. *Korean J Anesthesiol* 2014; 67(2): 115–22.
13. Costa e Silva VT, de Castro I, Liano F, Muriel A, Rodriguez-Palomares JR, Yu L. Performance of the third-generation models of severity scoring systems (APACHE IV, SAPS 3 and MPM-III) in acute kidney injury critically ill patients. *Nephrol Dial Transplant* 2011; 26(12): 3894–901.
14. Chan T. Evaluation of APACHE-IV predictive scoring in surgical abdominal sepsis: A retrospective cohort study. *J Clin Diagn Res* 2016; 10(3): PC16–8.
15. Wong RS, Ismail NA, Tan CC. An external independent validation of APACHE IV in a Malaysian intensive care unit. *Ann Acad Med* 2015; 44(4): 6.
16. Toker MK. SAPS 3 or APACHE IV: Which score to choose for acute trauma patients in intensive care unit? *Ulus Travma Acil Cerrahi Derg* 2018; 25(3): 247–52.
17. Vandenbrande J, Verbrugge L, Bruckers L, Geebelen L, Geerts E, Callebaut I, et al. Validation of the Acute Physiology and Chronic Health Evaluation (APACHE) II and IV Score in COVID-19 Patients. *Crit Care Res Pract* 2021; 2021(19): 1–9.
18. Chattopadhyay A and Chatterjee S. Predicting ICU length of stay using APACHE-IV in persons with severe sepsis – a pilot study. *J Epidemiol Res* 2016; 2(1): 1–8.

# Cholelithiasis in children: A characteristic study

**Emiliana Lia, Sp.BA (K), Kharuli Amri, MD**

Pediatric Surgery Division. Department of Surgery, Faculty of Medicine Padjadjaran University/ Dr. Hasan Sadikin Hospital, Bandung, West Java, Indonesia

## ABSTRACT

**Introduction:** Pediatric cholelithiasis (PC) is relatively rare when compared to adult cholelithiasis. This study is aimed to describe the clinical characteristics of pediatric cholelithiasis treated at Hasan Sadikin General Hospital (HSGH), Bandung, Indonesia.

**Materials and Methods:** This is a descriptive study of children aged 0–18 years who were diagnosed with and treated for cholelithiasis at the HSGH over 4–5 years. Variables collected during this study were sex, age, chief complaint, previous medical history, diagnostic test, definitive management, and clinical outcomes.

**Results:** There were 12 cases of pediatric cholelithiasis during the study period, including those of 5 boys (41.7%) and 7 girls (58.3%). The mean and median age of the patients was 10.75 years and 12 years, respectively. The most prevalent complaint of the patients was abdominal pain (75%), followed by jaundice (16.6%) and abdominal distension (8.4%). Thalassemia was the most frequently associated disorder among the patients (25%). Ultrasonography was diagnostic imaging used on 66.6% of patients. Fifty-eight percent of patients have performed the surgery. The most frequently used surgical technique to manage the patients included laparoscopic cholecystectomy (33.3%), followed by laparotomic cholecystectomy (16.7%).

**Conclusion:** PC is an uncommon disorder, but easier to diagnose reasonably with the development of imaging study. Minimally invasive procedures using laparoscopic cholecystectomy were the most frequently performed surgical treatment in this study.

## KEYWORDS:

*cholelithiasis, characteristics, pediatric surgery*

## INTRODUCTION

Cholelithiasis is a gallbladder disease commonly reported in adults. The incidence of cholelithiasis in children is relatively rare. An increasing trend of cholelithiasis in children has been noted.<sup>1-3</sup> Ultrasonography (USG) had been recommended for the diagnosis of cholelithiasis under clinical settings.<sup>4</sup> The worldwide prevalence of cholelithiasis in children was approximately 0.15%–0.22%. Ganesh et al. had reported a lower prevalence of PC in Kanchi Kamakoti Child Trust Hospital; from 13,675 children treated at the institute, 43 (0.3%) were diagnosed with pediatric

cholelithiasis. The gallbladder stones were of size <5 mm, and 56% of the cases involved solitary stones. Only 2 out of 43 children (5.7%) diagnosed with cholelithiasis presented with symptoms.<sup>5</sup> The publications for the epidemiology of PC remains unknown. This is partly because of the lack of symptoms in most cases. Thus, the present study was aimed to describe the characteristics of pediatric patients diagnosed with cholelithiasis.

## MATERIAL AND METHODS

This is a descriptive retrospective study of pediatric patients diagnosed and treated for cholelithiasis at the Pediatric Department of HSGH during January 1, 2016 to July 30, 2020. Secondary data was collected from medical records. Relevant data were collected for this study, which included sex, age, symptoms, medical history, diagnostic tests, and definitive management of patients.

## RESULTS

A total of 12 patients with cholelithiasis were treated during this period. The subjects included 5 boys (41.7%) and 7 girls (58.3%). The mean age of the patients was 10.75 years (0–18 years). Nine patients (75%) reported upper abdominal pain as the chief complaint. There were 2 patients (16.6%) who were admitted to the hospital for jaundice and 1 patient (8.4%) presented with abdominal distension.

According to their past medical history, 3 patients had thalassemia (25%), 2 had a past history of abdominal tuberculosis (16.5%), 1 had a past history of cholangitis (8.4%), 1 was obese (8.4%), and 1 had chronic bronchitis (8.4%). A total of 4 patients (33.3%) had no medical history.

Patients diagnosed with cholelithiasis underwent further supporting examination. Complete blood count and abdominal USG were performed in 8 patients (66.6%), and complete blood count without abdominal USG and computed tomography (CT) was performed in 3 patients (25%). One patient (8.4%) underwent an abdominal CT scan and complete blood count examination.

Varying definitive management was noted in the study. There was a total of 7 patients (58.4%) who had received surgical treatment, 5 patients (41.7%) had received laparoscopic cholecystectomy, and 2 patients (16.7%) had received open cholecystectomy. There was a total of 5 patients (41.6%) who refused to undertake any definitive treatment.

Corresponding Author: Kharuli Amri  
Email: ruliamridr@gmail.com



**Table I: Characteristic Demography Patients**

Parameter	n (%)	Mean	Median (Min-Max)
Gender			
Boy	5 (41.7%)		
Girl	7 (58.3%)		
Age		10.75	12 (0-18)

**Table II: Chief complaint and previous medical history**

Parameter	Proportion %
Chief complaint	
Abdominal pain	75%
Jaundice	16.6%
Abdominal distention	8.4%
Previous medical history	
No past medical history	33.3%
Thalassemia	25%
TBC abdominal	16.5%
Cholangitis	8.4%
Obesity	8.4%
Chronic bronchitis	8.4%

**Table III: Characteristic Diagnostic Examination**

Parameter	Proportion %
complete blood count, USG	66.6%
complete blood count, USG + CT Scan	25%
complete blood count + CT Scan	8.4%

**Table IV: Management**

Parameter	Proportion %
Surgical	58.4%
Laparoscopic cholecystectomy	33.3%
Open cholecystectomy	16.7%
Conservative treatment	41.6%

## DISCUSSION

In all there were a total of 12 patients who were diagnosed with cholelithiasis, predominantly girls. The data in the present study was different from those of previous study by Gunawan et al.<sup>6</sup> the latter study recorded a higher ratio of boys to girls (2.3:1) in cases of PC. The mean age of the patients was 10.75 years (0–18 years). The age demographics of this study were similar to those of a previous study by Bhasin et al.<sup>7</sup> who reported a mean age of pediatric patients with cholelithiasis as 10.1 years.

Upper right abdominal pain was the most commonly reported clinical symptom in our study. Bhasin et al.<sup>7</sup> recorded several symptoms associated with pediatric cholelithiasis: the recurrent upper right abdominal pain with or without nausea was recorded in 75% of the study population with the remaining subjects showing varying symptoms, such as jaundice and failure to thrive. Thalassemia and anemia were commonly recorded in patients with PC, accounting for 25% of all patients.<sup>7</sup> Tannuri et al.<sup>8</sup> noted that 62.3% of the pediatric patients with cholelithiasis were previously diagnosed with a hemolytic disorder such as sickle cell anemia or thalassemia.

The most commonly used diagnostic tool to confirm cholelithiasis in our study was USG, with 83.2% of the patients diagnosed with it. Real-time USG examination is highly accurate, reaching 96% in diagnostic accuracy, for the diagnosis of gallbladder and liver disorders. Cholelithiasis is readily diagnosed with a relatively high degree of accuracy by USG.<sup>4</sup>

Surgical treatment was the mainstay of management for cases of PC in this study. In our study, 58.4% of the patients received cholecystectomy, while 33.3% received laparoscopic cholecystectomy. Over the last decade, laparoscopic cholecystectomy has attained the status of the standard for definitive management of cholelithiasis.<sup>4</sup> Lugo-Vicente et al. reported that 71% of all infants and children with cholelithiasis received laparoscopic cholecystectomy, while the remaining received conventional or open cholecystectomy. There are several advantages in opting for laparoscopic intervention for the treatment of cholelithiasis, including the minimally invasive nature of this procedure that reduces the risk of postoperative pain, reduces the length of stay, and creates only small surgical wounds.<sup>9,10</sup>

## CONCLUSION

Cholelithiasis is often asymptomatic; occasionally, some cases may present with visible symptoms that require surgical treatment. Most cases can be diagnosed with USG. Minimally, invasive procedures using laparoscopic cholecystectomy demonstrate fewer morbidities when compared with the conventional approach.

## ACKNOWLEDGMENTS

We would like to thank the Pediatric Surgery Division, Department of Surgery, Dr. Hasan Sadikin Hospital/ Faculty of Medicine Padjadjaran University, Bandung, Indonesia for permission to publish this article.

## REFERENCES

1. Holcomb III GW, Murphy PJ, Ostlie DJ. Choledochal cyst and gallbladder disease. In: Peter SD, Editor. *Ashcraft's pediatric surgery, 6th Edition*. Elsevier Inc; 2014:599-603.
2. Puri P, Hollwarth ME. Cholecystectomy. In: *Pediatric Surgery, 2nd Edition*. Springer; 2019: 375-9.
3. Lesmana L. Batu empedu: Buku ajar penyakit dalam jilid I, 3rd ed. Balai Penerbit Fakultas Kedokteran; 2000: 380-394.
4. Grosfeld JL, O'Neill JA, Coran AG, Fonkalsrud EW. Gallbladder disease and hepatic infection. In: Caldamone AA, Editor. *Pediatric Surgery, 6th ed*. Elsevier Inc; 2006: 1635-46.
5. Maryan LF, Chiang W. Cholelithiasis 2013 [cited Dec 2020]. Available from: <http://www.emedicine.com/emerg/Gastrointestinal/topic97.htm>.
6. Gustawan IW, Aryasa KN, Karyana IPG, Putra S. Kolelitiasis pada anak. *Majalah Kedokteran Indonesia* 2007; 57(10): 353-62.
7. Bhasin SJ, Gupta A, Kumari S. Evaluation and management of cholelithiasis in children: A hospital-based study. *Int Surg J* 2017; 4(1): 246-51.
8. Tannuri AC, Leal AJG, Velhote MC, Tannuri U. Management of gallstone disease in children: A new protocol based on the experience of a single center. *J Pediatr Surg* 2012; 47(11): 2033-8.
9. Lobe TE. Cholelithiasis and cholecystitis in children. *Semin Pediatr Surg* 2000; 9: 170-6.
10. Vicente HL. Trends in management of gallbladder disorders in children. *Pediatr Surg Int* 1997; 12(5-6): 348-52.

# Circulating levels of Interferon-Gamma in patients with neovascular age-related macular degeneration in Yogyakarta

Supanji Supanji, PhD<sup>1</sup>, Ayudha Bahana Ilham Perdamaian, MSc<sup>1</sup>, Firman Setya Wardhana, MD<sup>1</sup>, Muhammad Bayu Sasongko, PhD<sup>1</sup>, Mohammad Eko Prayogo, MD<sup>1</sup>, Angela Nurini Agni, MD<sup>1</sup>, Chio Oka, PhD<sup>2</sup>

<sup>1</sup>Department of Ophthalmology, Faculty of Medicine, Public Health and Nursing, Universitas Gadjah Mada, Sekip Utara, Yogyakarta, Indonesia, <sup>2</sup>Laboratory of Gene Function in Animals, Nara Institute of Science and Technology, Takayama, Ikoma, Nara, Japan

## ABSTRACT

**Introduction:** Neovascular age-related macular degeneration (nAMD) is a major factor contributing to blindness and impaired visual acuity in elderly people. The pathophysiology of nAMD involves excessive inflammation events in the macula. Thus, it is crucial to study the dynamics of an important pro-inflammatory cytokine, interferon-gamma (IFN- $\gamma$ ).

**Materials and Methods:** This research is aimed to investigate plasma IFN- $\gamma$  profiles of patients with nAMD. In this cross-sectional study, blood plasma samples of 16 patients with AMD and 23 age-matched controls were collected. Samples were examined for two inflammatory cytokines (IFN- $\gamma$ ) using a commercially available enzyme-linked immunosorbent assay. Acquired data were log transformed to normalize any outliers before conducting student's t-test using the SPSS software.

**Results:** IFN- $\gamma$  levels were higher in the control group, without statistically significant difference between the two groups.

**Conclusion:** IFN- $\gamma$  levels were not significantly different between patients with AMD and controls.

## KEYWORDS:

Age-related macular degeneration, inflammation, inflammatory cytokines, IFN- $\gamma$ , ELISA

## INTRODUCTION

Neovascular age-related macular degeneration (nAMD) is a major risk factor for impaired central visual acuity and irreversible blindness.<sup>1,2</sup> Genetics plays a key role in the onset of nAMD. Epidemiological study conducted in Indonesia showed a strong association of rs11200638 High temperature requirement factor A1 (HTRA1),<sup>3</sup> rs10490924 HTRA1/Age-related maculopathy susceptibility 2 (ARMS2), del443ins54 ARMS2, and rs10490924 Complement factor H (CFH) polymorphisms with the onset of nAMD.<sup>4</sup> However, other studies have failed to show a correlation of interleukin-1beta (IL-1 $\beta$ )<sup>5</sup> and HTRA1<sup>6</sup> protein levels with nAMD pathogenesis.

The aetiology of nAMD is characterized by retinal swelling, which is caused by abnormal vascularization, leading to leaky blood vessel formation in the macula. Genetic and epidemiological evidence indicate the key role of inflammation in nAMD. An important pro-inflammatory cytokine, interferon-gamma (IFN- $\gamma$ ), is considered a vital factor in nAMD onset. Recent studies indicate an emerging relationship between IFN- $\gamma$  and mechanisms underlying AMD pathogenesis. Alone or along with other pro-inflammatory factors such as IL-1 $\beta$  and tumour necrosis factor-alpha, IFN- $\gamma$  appears to trigger inflammatory pathways<sup>7</sup> and its associated biomarkers, including the complement cascade, as well as recruit immune cells such as macrophages, microglia, natural killer, and T cells.<sup>8-11</sup> Reportedly, in the affected eyes, cytokines were observed in the outer retina and drusen.<sup>12-14</sup> Excessive cytokines could compromise photoreceptors,<sup>14,15</sup> leading to central vision impairment or blindness. The pathways activated by IFN- $\gamma$  are interconnected in a complicated manner and are not fully understood. Furthermore, clinical data related to IFN- $\gamma$  and AMD therapy are limited. The possibility of using IFN- $\gamma$  as target for AMD therapy remains debatable. Accordingly, the present research aimed to investigate IFN- $\gamma$  levels in patients with nAMD and age-matched controls.

## MATERIAL AND METHODS

This cross-sectional case control study was approved by the Medical and Health Research Ethics Committee, Faculty of Medicine, Public Health and Nursing (FK-KMK) UGM, Universitas Gadjah Mada (approval no.: KE-FK-0215-EC-2021). Following screening, 38 patients with AMD and 16 age-matched control were included. Recruitment was conducted from January until August 2019. All participants understood and signed informed consent form before undergoing ophthalmic testing and blood collection. Only patients without other retinal or systemic diseases were included to rule out the effect of other disease. All patients underwent standard eye examination, including visual acuity assessment, fundus imaging, and optical coherence tomography to diagnose nAMD or verify the control eye group. A structured questionnaire was used to collect baseline data regarding lifestyle, including smoking status (active or

Corresponding Author: Supanji S  
Email: supanji@ugm.ac.id

**Table I: Characteristics of patients with AMD and age-matched control**

Variables	nAMD (n:16; %)	Age-matched control (n:23/%)	p-value
Sex			
Male	58	52	0.301
Female	42	46	
Age (years)			
<59	23	8	0.235
60–69	35	52	
70–79	35	30	
>80	5	8	
Smoking status			
Yes	23	30.5%	0,23
No	76	69.5%	
Blood pressure (mmHg)			
Hypertension	35.2%	21.7%	0,4
Normal	64.8%	78.3%	
Cytokines (mean (±SD))			
IFN-γ (pg/mL)	14.88 (± 6.96)	18.70 (± 17.93)	0.087

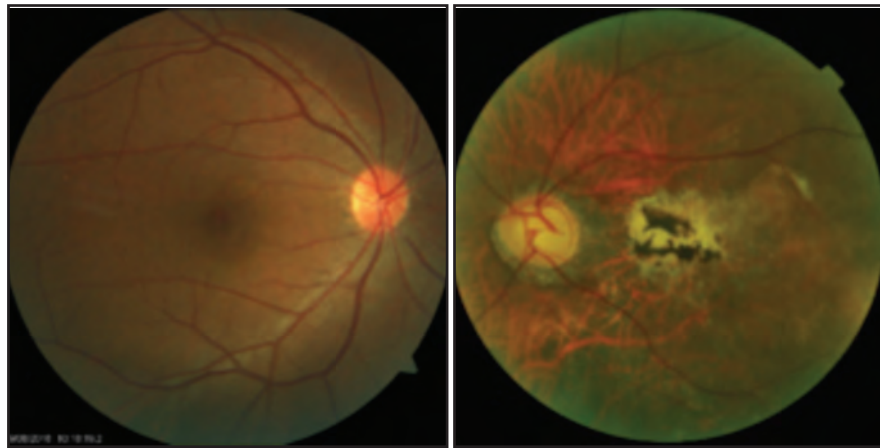


**Fig. 1:** Funduscopy image of the affected eye (left) and clear normal eye (right). Hemorrhage and neovascularization were observed in the affected eye.

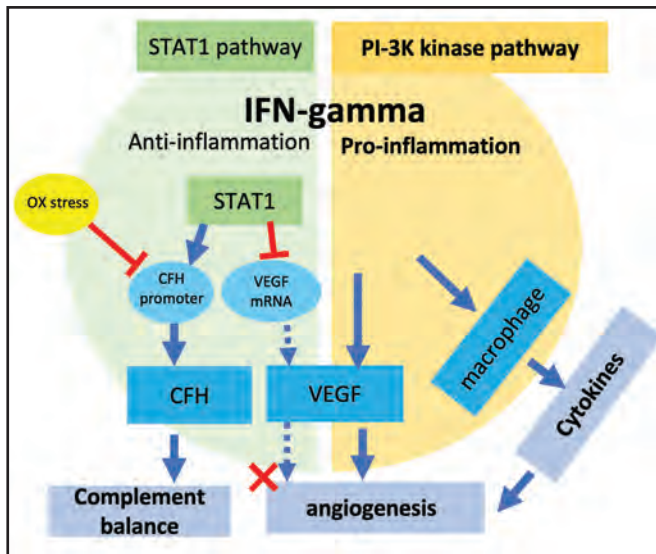


**Fig. 2:** Pro- and anti-inflammatory roles of IFN-γ in nAMD pathogenesis

passive) and indoor/outdoor working activity of AMD and control groups. The study was conducted at Dr. Sardjito Central General Hospital, Dr. S. Hardjolukito Air Force Main Hospital, and Dr. Yap Eye Hospital, Yogyakarta. ELISA was conducted at the Integrated Research Laboratory, FK-KMK, UGM.

Whole blood was centrifuged (1,000 ×g for 15 min), and the upper layer was collected to retrieve plasma. ELISA was performed in accordance with the manufacturer's protocol (Finetest®, Wuhan Fine Biotech, Wuhan, China). First, 100 μL of the plasma sample and the standard solution each was placed into 96-well plates, followed by incubation for 37°C for 90 min. After discarding the mixture and standard, the empty plate was washed twice, and 100 μL of Biotin was added to each well before incubating the plate at 37°C for 60 min. Next, the mixture was discarded, and the plate was washed three times. Subsequently, streptavidin conjugate buffer was added before incubating at 37°C for 30 min. Finally, the mixture was discarded, and the plate was washed five times. Then, 90 μL of TMB substrate buffer was added before incubating the plate at 37°C for 10–20 min (depending on the change in color) in the dark. Immediately after the color accurately changed according to the standard chart, 50 μL of



stop solution was added. Then, using a microplate reader, the optical density at 450 nm obtained, which was interpolated into nanogram per milliliter using the CurveExpert 1.4 software.

All acquired data were analyzed using the Mann-Whitney Test (SPSS) for unevenly distributed data. The obtained results were expressed as means and standard deviations with 95% confidence interval (CI) to determine any association between IFN- $\gamma$  level and the incidence of AMD.

## RESULTS

All patients with AMD or age-matched controls were diagnosed by an ophthalmologist (Fig. 1). For statistical analysis, the data from 16 patients with AMD and 23 age-matched controls were used.

In the nAMD and control groups, the mean value of circulating IFN- $\gamma$  was  $14.88 \pm 6.96$  pg/mL and  $18.70 \pm 17.93$  pg/mL, respectively. There was no positive association between cytokine level and AMD ( $p > 0.05$ , 95% CI: 12.650 – 21.606) (Table I).

Baseline parameters were similar in the case and control groups. The majority of subjects were non-smokers (76% in nAMD group and 69.5% in control group) and had normal blood pressure (64.8 mmHg in nAMD group and 78.3 mmHg in control group).

## DISCUSSION

To our knowledge, this is the first study reporting the association between circulating IFN- $\gamma$  level and neovascular AMD in an Indonesian population. The results suggest that IFN- $\gamma$  levels were not associated with AMD. Patients with AMD had lower IFN- $\gamma$  cytokine level than controls. However, there was no association between IFN- $\gamma$  cytokine level and nAMD onset ( $p > 0.05$ , 95% CI).

In exudative nAMD, it is not clear what the role of IFN- $\gamma$  is, since IFN- $\gamma$  can either maintain or inhibit inflammation in different ways (Figure 2). Several reports have demonstrated the role of IFN- $\gamma$  in initiating immunomodulatory and protective functions. However, IFN- $\gamma$  was reported as a pro-inflammatory factor in nAMD.<sup>8,16</sup> In addition, IFN- $\gamma$  inhibits the angiogenic activity of VEGF via the activation of the STAT1 pathway in human endothelial cells<sup>17</sup>, while also down-regulating Vascular endothelial growth factor (VEGF) mRNA in a dose-dependent manner<sup>18</sup>. This process might be of potential in AMD therapy. Therefore, IFN- $\gamma$ -associated STAT1 activation may be beneficial.

Interestingly, another study has suggested that IFN- $\gamma$  can mediate VEGF expression in Retinal pigment epithelium (RPE) cells through the PI-3K/Akt/mTOR/p70 S6 kinase pathway and is independent of STAT1.<sup>19</sup> Another piece of evidence comes from the study demonstrating IFN- $\gamma$  up-regulating CFH expression in RPE cells.<sup>20</sup> CFH can keep the complement cascade in check and prevent tissue injury from excessive complement activation.<sup>21</sup> CFH is transcriptionally upregulated by STAT1; however, oxidative stress, one of the

most important risk factors for AMD, can disrupt this process by acetylating FOXO3, which competes with STAT1 for binding to the CFH promoter.<sup>22,23</sup> Reportedly, STAT1-deficient mice were highly susceptible to autoimmune disorders<sup>24</sup>, and considering this response pattern, AMD may be considered an autoimmune disease.<sup>25,26</sup>

One limitation of this study was that only patients with nAMD who were only in the most severe stage of the disease were included. At this stage, IFN- $\gamma$  may no longer play an important role in inducing or maintaining AMD condition. Further studies should recruit patients in the early and intermediate stages of AMD to compare cytokines levels. Our findings may also be limited due to the lack of samples in the study groups. Future studies with larger number of samples are required to validate and better understand the association between IFN- $\gamma$  concentration and AMD incidence.

## CONCLUSION

Although insignificant, higher concentrations of IFN- $\gamma$  were observed in the control group than in the AMD group.

## ACKNOWLEDGMENT

The authors would like to acknowledge Universitas Gadjah Mada for providing the RTA grant (1185/UN1.P.III/SK/HUKOR/2021).

## REFERENCES

1. Resnikoff S, Pascolini D, Etya'ale D, Kocur I, Pararajasegaram R, Pokharel GP, et al. Global data on visual impairment in the year 2002. *Bull World Health Organ* 2004; 82(11): 844–51.
2. GBD 2019 Blindness and Vision Impairment Collaborators; Vision Loss Expert Group of the Global Burden of Disease Study. Causes of blindness and vision impairment in 2020 and trends over 30 years, and prevalence of avoidable blindness in relation to VISION 2020: The Right to Sight: An analysis for the Global Burden of Disease Study. *Lancet Glob Heal* 2021;9: e144–60.
3. Supanji S, Perdamaian ABI, Romdhoniyyah DF, Sasongko MB, Agni AN, Wardhana FS, et al. The association of HTRA1 rs11200638 polymorphism with neovascular age-related macular degeneration in Indonesia. *Ophthalmol Ther* 2021.
4. Supanji S, Romdhoniyyah DF, Sasongko MB, Agni AN, Wardhana FS, Widayanti TW, et al. Associations of ARMS2 and CFH gene polymorphisms with neovascular age-related macular degeneration. *Clin Ophthalmol* 2021; 15: 1101–8.
5. Supanji S, Perdamaian ABI, DianratriA, PrayogoME, Sasongko MB, Wardhana FS, et al. The circulating level of IL-1 $\beta$  in patients with age-related macular degeneration (AMD) in Yogyakarta: characteristics to disease activity. in *Proceedings of the 3rd KOBICongress, International and National Conferences (KOBICINC 2020)*. Atlantis Press 2021; 14: 434–6.
6. Supanji S, Perdamaian ABI, DianratriA, SyfarahmahA, WidayantiTW, WardhanaFS, et al. HtrA1 serine protease expression levels on age-related macular degeneration (AMD) patients in Yogyakarta. *BIO Web Conf* 2020; 28: 02004.
7. Jiang K, Cao S, Cui JZ, Matsubara JA. Immuno-modulatory effect of IFN-gamma in amd and its role as a possible target for therapy. *J Clin Exp Ophthalmol* 2013; Suppl 2, 0071.
8. Nagineni CN, Detrick B, Hooks JJ. Synergistic effects of gamma interferon on inflammatory mediators that induce interleukin-6 gene expression and secretion by human retinal pigment epithelial cells. *Clin Diagn Lab Immunol* 1994; 1: 569–77.

9. Chakrabarty P, Ceballos-Diaz C, Beccard A, Janus C, Dickson D, Golde TE, et al. IFN- $\gamma$  promotes complement expression and attenuates amyloid plaque deposition in amyloid  $\beta$  precursor protein transgenic mice. *J. Immunol* 2020; 184: 5333–43.
10. Huang Y, Krein PM, Muruve DA, Winston BW. Complement factor B gene regulation: synergistic effects of TNF- $\alpha$  and IFN- $\gamma$  in macrophages. *J Immunol* 2002; 169: 2627–35.
11. Juel HB, Faber C, Udsen MS, Folkersen L, Nissen MH. Chemokine expression in retinal pigment epithelial ARPE-19 cells in response to coculture with activated T cells. *Investig Ophthalmol Vis Sci* 2012; 53: 8472–80.
12. Dastgheib K, Green WR. Granulomatous reaction to bruch's membrane in age-related macular degeneration. *Arch. Ophthalmol* 1994; 112: 813–8.
13. Penfold PL, Wong JG, Gyory J, Billson FA. Effects of triamcinolone acetonide on microglial morphology and quantitative expression of MHC-II in exudative age-related macular degeneration. *in Clin Exp Ophthalmol* 2001; 29: 188–192.
14. Ding X, Patel M, Chan CC. Molecular pathology of age-related macular degeneration. *Prog Retin Eye Res* 2009; 28: 1–18.
15. Roque RS, Rosales AA, Jingjing L, Agarwal N, Al-Ubaidi MR. Retina-derived microglial cells induce photoreceptor cell death in vitro. *Brain Res* 1999; 836: 110–9.
16. Afarid M, Azimi A, Malekzadeh M. Evaluation of serum interferons in patients with age-related macular degeneration. *J Res Med Sci* 2019; 24.
17. Battle TE, Lynch RA, Frank DA. Signal transducer and activator of transcription 1 activation in endothelial cells is a negative regulator of angiogenesis. *Cancer Res* 2006; 66: 3649–57.
18. Kawano Y, Matsui N, Kamihigashi S, Narahara H, Miyakawa I. Effects of interferon- $\gamma$  on secretion of vascular endothelial growth factor by endometrial stromal cells. *Am J Reprod Immunol* 2000; 43: 47–52.
19. Liu B, Faia L, Hu M, Nussenblatt RB. Pro-angiogenic effect of IFN $\gamma$  is dependent on the PI3K/mTOR/ translational pathway in human retinal pigmented epithelial cells. *Mol Vis* 2010; 16: 184–193.
20. Fritsche, L. G. Igl W, Bailey JN, Grassmann F, Sengupta S, Bragg-Gresham JL, et al. A large genome-wide association study of age-related macular degeneration highlights contributions of rare and common variants. *Nat Genet* 2016; 48: 134–143.
21. Patel M, Chan CC. Immunopathological aspects of age-related macular degeneration. *Seminars in Immunopathology* 2008; 30: 97–110.
22. Wu Z, Lauer TW, Sick A, Hackett SF, Campochiaro PA. Oxidative stress modulates complement factor H expression in retinal pigmented epithelial cells by acetylation of FOXO3. *J Biol Chem* 2007; 282: 22414–25.
23. Beatty S, Koh H, Phil M, Henson D, Boulton M. The role of oxidative stress in the pathogenesis of age-related macular degeneration. *Surv Ophthalmol* 2000; 45: 115–34.
24. Nishibori T, Tanabe Y, Su L, David M. Impaired development of CD4+ CD25+ regulatory T cells in the absence of STAT1: increased susceptibility to autoimmune disease. *J Exp Med* 2004; 199: 25–34.
25. Iannaccone A, Neeli I, Krishnamurthy P, Lenchik NI, Wan H, Gerling IC, et al. Autoimmune biomarkers in age-related macular degeneration: A possible role player in disease development and progression. *Adv Exp Med Biol* 2012; 723: 11–6.
26. Morohoshi K, Goodwin AM, Ohbayashi M, Ono SJ. Autoimmunity in retinal degeneration: Autoimmune retinopathy and age-related macular degeneration. *J Autoimmun* 2009; 33: 247–54.

# Network pharmacology for deciphering molecular mechanism of mahogany in dyslipidemia treatment of menopausal conditions

Afivah Dewi Anggraeni, S. Farm<sup>1</sup>, Dhiya Ulhaq Salsabila<sup>1</sup>, Bayu Anggoro<sup>1</sup>, Adam Hermawan, Dr. rer. nat.<sup>1,2</sup>

<sup>1</sup>Cancer Chemoprevention Research Center, Faculty of Pharmacy, Universitas Gadjah Mada, Yogyakarta Indonesia, <sup>2</sup>Macromolecular Engineering Laboratory, Department of Pharmaceutical Chemistry, Faculty of Pharmacy, UGM, Yogyakarta, Indonesia

## ABSTRACT

**Introduction:** Estrogen deficiency during menopause is associated with pathological menopausal syndromes and metabolic disorders, including dysregulated lipid metabolism (dyslipidemia). Mahogany is a promising material for use in an alternative treatment for preventing dyslipidemia during menopause. This study investigated the potency of mahogany compounds and their molecular mechanism as an alternative treatment for preventing dyslipidemia during menopause.

**Method and Materials:** The determination of the potential of the compounds of interest was performed by machine learning using KNIME software to identify the potential compounds for HMG-CoA Reductase (HMGCR) inhibitor. Target genes for a potential mahogany compound were obtained from Swiss Target Prediction. Analysis of the KEGG-Pathways, Gene Ontology profiling, and protein-protein interaction networks of the target gene were analyzed.

**Results:** We identified five compounds:  $\beta$ -sitosterol, swietemacrophyllanin, 7-hydroxy-2-(4-hydroxy-3-methoxyphenyl)-chroman-4-on (7-HMC), scopoletin, and stigmasterol as candidates for HMGCR inhibitors. The target prediction results mined 294 genes. The top 20 hub genes with the highest degree included MAPK1/3, PI3K/AKT, ER1, and mTOR, which played a role in lipid metabolism.

**Conclusion:** The possible molecular mechanisms mainly involved direct inhibitory pathway of HMGCR and an indirect inhibitory pathway of HMGCR. The tidal inhibitory pathway was indirectly mediated via the PI3K/AKT, MAPK1/3, MTOR, ER1, and SREBP1/2 signaling pathways. Further investigation is warranted to validate the results of the present study.

## KEYWORDS:

Mahogany, Dyslipidemia, Menopause, HMG-CoA Reductase, and Bioinformatics

## INTRODUCTION

Menopause is a condition of the cessation of the menstrual cycle in women as a result of aging of the reproductive

organs.<sup>1</sup> A new hormonal pattern is established at menopause, which is characterized by low estrogen level.<sup>2</sup> Estrogen is a steroid hormone produced primarily in the ovaries that contributes to the regulation of some physiological mechanisms. Estrogen deficiency during menopause is associated with pathological menopausal syndromes, psychiatric disorders, cardiovascular diseases (CVDs), cancer, and metabolic disorders, including dysregulated lipid metabolism or dyslipidemia.<sup>3</sup> Hormone replacement therapy (HRT) using estrogen synthesis has been the primary treatment for preventing menopausal symptoms, CVD, and dyslipidemia.<sup>4</sup> However, clinical studies have demonstrated that HRT increases the risks of endometrial and breast cancers and hence cannot be used as an idealized therapy.<sup>5</sup> Seeking alternative dietary estrogenic compounds is believed to be crucial for the prevention of menopause-associated metabolic syndromes.<sup>6</sup>

Decreasing level of estrogen during menopause causes dyslipidemia through multiple mechanisms.<sup>7</sup> Decreased level of estrogen increases the hepatic HMG-CoA reductase (HMGCR) gene expression and activation, leading to the elevation of the serum cholesterol levels.<sup>8</sup> HMGCR is a rate-limiting enzyme that plays a pivotal role in cholesterol biosynthesis. Dysregulation of lipid metabolism during menopause can alter the level of various lipids circulating in the blood, such as lipoproteins, apolipoproteins, low-density lipoproteins (LDLs) high-density lipoproteins (HDL), and triacylglycerol (TG).<sup>9</sup>

Mahogany (*Swietenia macrophylla* and *Swietenia mahogany*) has the potential resource of phytoestrogen<sup>10</sup> Mahogany has been used in the preparation of traditional medicine in Asia to treat hypertension, diabetes, and pain.<sup>11</sup> Chemical compounds in mahogany include flavonoids, saponins, alkaloids, steroids, and tannins. Recent studies have demonstrated that mahogany seeds have an estrogenic activity that can increase the uterine weight and bone density, prolong the estrus phase, and increase the breast gland proliferation in ovariectomized rats.<sup>12</sup> Another study also showed that compound contained in the mahogany extract could decrease the cholesterol, triglyceride, low-density lipoprotein, increased high-density lipoprotein, and reduced atherogenic indexes.<sup>13-15</sup> According to the study performed by Kalpana and Pugalendi, the *in vivo* study of

Corresponding Author: Adam Hermawan  
Email: adam\_apt@ugm.ac.id

ethanolic extract of mahogany seeds on rats proved reduction in the level of total cholesterol, triglyceride, LDL, and VLDL and increase in the level of HDL.<sup>15</sup> This finding suggests that mahogany offers potential efficacy for preventing menopause syndrome and hyperlipidemia that often occur during menopause.

Mahogany is a promising plant for use in preventing dyslipidemia during menopause. However, the detailed therapeutic targets and signaling mechanisms behind the benefits of mahogany remain unknown.<sup>13</sup> Cholesterol in our body can arise from *de novo* synthesis in our cells or obtained through food consumption.<sup>16</sup> In the process of cholesterol biosynthesis, 3-hydroxy-3-methylglutaryl coenzyme A (HMG-CoA) reductase (HMGCR) catalyzes HMG-CoA conversion to mevalonate. It is known as a rate-limiting enzyme in cholesterol synthesis, signifying its important role. The multivalent system regulates HMGCR through various mechanisms.<sup>17</sup>

This study was conducted to investigate the potency of mahogany compound's molecular targets and signaling mechanisms as an alternative treatment for preventing dyslipidemia during menopause by focusing on the indirect effects. In this study, bioinformatics analysis was performed to investigate the potential compound of mahogany that can inhibit HMGCR, an enzyme that plays an essential role in lipid metabolism. The use of bioinformatics analysis can simplify and organize bioinformatics data such that it allows researchers to access existing information and submit new entries as they are produced and make new conclusions and understand new possibilities. In conclusion, we identified and developed potential compound candidates and predicted their molecular target and molecular signaling role in lipid metabolism.

## MATERIAL AND METHODS

### *Prediction inhibition activity prediction using KNIME*

The prediction model for the inhibition of mahogany compounds against HMGCR was developed using the dataset inhibitor compound activity against HMGCR obtained from ChEMBL (<https://www.ebi.ac.uk/chembl>), which were entered in ChEMBL ID and analyzed by the KNIME version 4.3.1 with the pipeline/workflow created. Mahogany metabolite profiles were analyzed to predict the inhibitory activity on HMGCR based on the prediction model prepared. The outputs produced were the "ROC curve" and "Prediction value," which provided method validation and prediction value of mahogany's metabolites. Furthermore, the potential compounds in mahogany's metabolites were selected by identifying the compounds that predicted the inhibitory activity based on the machine learning (ML) prediction outcomes.<sup>18</sup>

### *Target prediction and collection*

The potential compounds of mahogany metabolites were analyzed for their predictive target genes using online databases based on the SMILES code. The database used included Swiss Target Prediction (<http://www.swisstargetprediction.ch>) with the default settings. The total target genes were collected, combined, and then sliced using the InteractiVenn

(<http://www.interactivenn.net>) to ensure no duplicity in the target.<sup>19</sup>

### *Gene ontology (GO) and Kyoto Encyclopedia of Genes and Genomes (KEGG) pathway enrichment analysis*

KEGG pathways and GO enrichment analysis was conducted to explore the potential functions of the essential protein targets of mahogany metabolites with the Database for Annotation, Visualization, and Integrated Discovery (DAVID). GO analysis involved three categories: biological process (BP), cellular component (CC), and molecular function (MF).  $P < 0.05$  was set as the thresholds for significant enrichment analysis.<sup>20</sup>

### *Protein-protein interaction (PPI) network of predictive biomarkers and hub gene construction*

The PPI data were obtained from the Search Tool for the Retrieval of Interacting Genes (STRING) database (<https://string-db.org>), which can predict interactions among proteins. The prediction method of this database was derived from experiments, databases, and text mining of the neighborhood, gene fusion, co-occurrence, and co-expression. In the present study, PPIs with combined scores  $>0.4$  were selected for further research. The Cytoscape software (<http://www.cytoscape.org>) was used to establish a PPI network. In addition, the Cytohubba was applied to analyze the PPI network to obtain the top 20 nodes that were considered hub genes according to the degree value.<sup>21</sup>

## RESULTS

### *Predicted compounds of mahogany showed inhibitory activity against HMG-CoA reductase*

The study of mahogany metabolites on predicting HMGCR inhibition was performed using the KNIME software by predicting the inhibitory activity of one or more compounds at once against the targeted protein (mahogany-stated inhibition of HMGCR). The prediction model was constructed with the KNIME software by adapting the Teach-Open CADD pipeline.<sup>18</sup> The dataset for constructing the prediction model was a dataset of HMGCR inhibitory activity, which is provided in ChEMBL with ID dataset ChEMBL407. Based on the MACCS fingerprint of the inhibitor compounds from the dataset, ML had mapped all compound fingerprints to prepare a predictive model of the inhibitory activity from the targeted protein.<sup>22</sup> The HMGCR inhibitory compound data set was split into active and inactive compounds and used to train ML classifiers based on two ML algorithms: Random Forest (RF) and Artificial Neural Network (ANN). Validation of the prediction models from two different MLs suggested that all prediction models had an overall accuracy value  $>90\%$  (RF 92.07% and ANN 90.24%) and ROC curve p scores  $>0.75$  (RF 0.932 dan ANN 0.879). These results indicated that the prediction model was valid and could predict the inhibitory activity of compounds in mahogany.<sup>23</sup>

The results of the inhibitory activity prediction revealed that potential compounds of mahogany metabolites inhibited HMGCR. Based on the prediction model under ML algorithms, ANN showed 5 compounds, namely,  $\beta$ -sitosterol, swietemacrophyllanin, 7-hydroxy-2-(4-hydroxy-3-methoxyphenyl)-chroman-4-on (7HMC), scopoletin, and stigmaterol, which were predicted to possess inhibitory



activity against HMGCR based on the number of predictive values being 1.00 and 0.99. Analyzing the RF algorithm presented the same result as that with ANN, with the highest predictive value of 0.9 for scopoletin (Table I). These inhibitory activities were predicted based on the likeness of structure and inhibitory activity with those of known inhibitor compounds processed by the RF and ANN algorithms.

#### Targeted genes prediction of mahogany potential compounds

Predictive target genes of each potential mahogany metabolites using databases SwissTargetPrediction obtained from the default settings. We obtained 100 targets for each compound (Fig. 1). A Venn diagram was used to determine all compounds' total targeted genes to ensure no duplication of the targets. A total of 294 genes were known predicted as the target of the 5 potential compounds (Table II and Table III).

#### KEGG pathway and GO enrichment analysis

A total of 294 common targets were subjected to the DAVID v6.8 database for gene enrichments. GO and KEGG gene enrichment results were put in order according to the percentage of genes. The top 5 GO results in the KEGG pathway, biological process, cellular component, and molecular function were recorded.

KEGG pathway enrichment analysis revealed that the genes were regulated in the cancer signaling pathways, PI3K-Akt, neuroactive ligand-receptor interaction, proteoglycan in cancer, and viral carcinogenesis pathway (Table IV). The results for GO analysis were evaluated through the related term option of the DAVID database. According to biological process results, protein phosphorylation, signal transduction, response to drug, oxidation-reduction process, and positive regulation of transcription from RNA polymerase II promoter showed higher targeted numbers in the count. Molecular function results with higher targeted numbers included protein binding, ATP binding, protein kinase activity, protein serine/threonine kinase activity, and zinc ion binding, which were found to be related to at least one of the KEGG pathways such as the cancer signaling pathways, PI3K-Akt, neuroactive ligand-receptor interaction, proteoglycan in cancer, and viral carcinogenesis pathway. Moreover, based on the analysis, most of the genes were present in the cellular components of the plasma membrane, nucleus, cytoplasm, and integral component of membrane.

#### PPI network construction and hub gene selection

Construction of the PPIs network among the targeted genes of mahogany compounds and identification of the most significant modules using the online tool STRING with a cutoff score of  $\geq 0.4$ . A total of 294 genes were constructed to

the PPI network complex containing 294 nodes and 3150 edges, with an average node degree of 22.2, an average local clustering coefficient of 0.465, and a PPI enrichment p-value of  $<1.0e-16$  (Fig. 2a). Using the cytoHubba plugin Cytoscape, we detected the top 20 targeted genes with the uppermost degree score, including AKT1, MAPK3, EGFR, SRC, MAPK1, VEGFA, SKP90AA1, ESR1, PTGS2, MTOR, PIK3CA, APP, MMP9, MAPK14, AR, ERBB2, MDM2, KDR, BCL2L1, and STAT1 (Fig 2b, Table V).

## DISCUSSION

The present study investigated the potency of mahogany compounds and their molecular targets and signaling mechanism as an alternative treatment for preventing dyslipidemia during menopause through bioinformatics analyses. This study was conducted to determine which compounds were responsible for the anti-dyslipidemic effect of mahogany. Moreover, the predictive targeted genes of the compounds showed inhibit activity against HMGCR under hyperlipidemia conditions. It uses data on HMGCR inhibitor compounds that have been studied, which is then used to perform ML on the fingerprint pattern of the inhibitor compounds for the prediction of compounds in mahogany with inhibitory activity against HMGCR.<sup>18</sup> Past analysis suggests  $\beta$ -sitosterol, swietemachrophyllanin, 7-HMC, scopoletin, and stigmasterol as compounds that can be suspected to be responsible for the anti-dyslipidemia effect of mahogany through the inhibition of HMGCR (Table I). Targeted genes' exploration predicted 294 genes is the target of the 5 mahogany potential metabolites. Twenty potential hub genes including MAPK, AKT1, PI3K, MTOR, and ER1, and others were screened as effective targets of mahogany compounds (Fig. 2, Table V).

Past studies have shown that the ethanolic extract of the seeds, leaves, and bark of mahogany tree possesses hypolipidemic activity and can reduce the HMGCR activity.<sup>24</sup> HMGCR is a rate-limiting enzyme of cholesterol biosynthesis. HMGCR inhibitors (ex, statins) are currently the mainstay of treatment for dyslipidemia. Nevertheless, during the menopause condition, treatment with only a single statin cannot alleviate the other menopausal syndromes.<sup>25</sup> Under physiological conditions, HMGCR activity is regulated by multiple mechanisms. At the transcriptional level, the expression of the HMGCR gene is regulated by the sterol regulatory element-binding proteins (SREBP).<sup>26</sup> SREBPs can be mainly categorized as SREBP1 and SREBP2, where every subunit plays an essential role in lipid and cholesterol biosynthesis. SREBP1 activates mostly those genes that are related to fatty acid biosynthesis or carbohydrate metabolism, while SREBP2 primarily activates cholesterol synthesis-related genes.<sup>27</sup> SREBP2 was also predicted as a

Table I: The predicted value of HMG-CoA reductase inhibitory activity of mahogany metabolites

No	Compound	Prediction value (1.0)	
		ANN	RF
1	$\beta$ -sitosterol	0.99	0.84
2	Swietemacrophyllanin	1.00	0.79
3	(7HMC)	1.00	0.86
4	Scopoletin	1.00	0.9
5	Stigmasterol	1.00	0.83

Table II: Prediction 100 protein target of a potential mahogany compound through Swiss Target Prediction

No	B-sitosterol	Swietemacphyllanin	7HMC	Stigmasterol	Scopoletin
1	AR	PGF	CYP1B1	AR	CA7
2	HMGCR	VEGFA	CYP19A1	NPC1L1	CA12
3	CYP51A1	MMP2	TAS2R31	HMGCR	CA9
4	NPC1L1	MMP9	CA7	CYP51A1	CA13
5	NR1H3	SQLE	CA12	CYP19A1	CA1
6	CYP19A1	BACE1	CA4	NR1H3	CA14
7	CYP17A1	CA5B	ADORA1	CYP17A1	CA4
8	RORC	MMP13	ADORA3	RORC	EGFR
9	ESR1	MMP12	ESR1	ESR1	CA5A
10	ESR2	PTGS1	ESR2	ESR2	XDH
11	SREBF2	CA2	MAOB	SHBG	CA6
12	SHBG	CA1	HSD17B1	SREBF2	CA2
13	SLC6A2	DNM1	MMP13	ACHE	SRD5A1
14	CYP2C19	CA4	ABCG2	CYP2C19	CBR1
15	RORA	CA7	ABCC1	PTPN1	CDK2 CCNA1 CCNA2
16	PTPN1	CA12	SHBG	SLC6A2	MAOA
17	BCHE	CA9	CBR1	BCHE	ESR2
18	SERPINA6	CYP19A1	MMP12	RORA	ALOX5
19	SLC6A4	HIF1A	PTGS1	SERPINA6	CCND1 CDK4
20	CHRM2	BCL2	CA2	SLC6A4	FLT4
21	VDR	MMP14	CA1	CHRM2	INSR
22	ACHE	SYK	CA6	G6PD	PTK2
23	G6PD	MAPT	CA5A	VDR	PLK1
24	NR1H2	TERT	CA3	NR1H2	TEK
25	GLRA1	PGD	APP	HSD11B1	MAP3K8
26	CES2	ST3GAL3	KLK1	PTGER1	HSPA1A
27	PTGER1	FUT7	KLK2	PTGER2	NUAK1
28	PTGER2	FUT4	PLA2G1B	CDC25A	FGR
29	HSD11B1	PDK1	ACHE	GLRA1	CA5B
30	PTGES	ABCB1	CHRNA7	CES2	AKR1C1
31	CDC25A	PIK3CA PIK3R1	BACE1	PTGES	DAO
32	PPARA	PIK3CD PIK3R1	SRC	PPARA	GSK3B
33	PPARD	PIK3R1 PIK3CB	SGK1	PPARD	KCNA3
34	DHCR7	MTOR	ERN1	SQLE	PTGS2
35	SQLE	PIK3CG	RP56KB1	DHCR7	GSR
36	PTPN6	PIK3CA	AURKA	NR1I3	HSD17B3
37	NR1I3	MET	POLB	PTPN6	SRC
38	FDFT1	CA3	CA9	NR3C1	KDR
39	SIGMAR1	CA6	CA13	CDC25B	ACHE
40	NOS2	CA5A	CA5B	NOS2	CYP1A2
41	NR3C1	ALPL	GRM2	HSD11B2	NAT1
42	PPARG	PLAA	PLA2G5	TBXAS1	MAOB
43	CDC25B	FCER2	EDNRA	PPARG	PTPN1
44	UGT2B7	TYMP	MET	UGT2B7	ESR1
45	HSD11B2	PRKDC	MMP2	POLB	MB
46	POLB	MAPK3	NOX4	PREP	PARP1
47	PREP	MAPK1	PLG	SIGMAR1	KCNMA1
48	PTGER4	PCNA	MMP3	PTGER4	ERBB2
49	IDO1	POLB	MMP7	IDO1	SQLE
50	DRD2	FBP1	PPARG	MDM4	BACE1
51	TBXAS1	MMP7	MMP9	DRD2	MET
52	ATP12A	MMP8	SLC5A2	MDM2	COMT
53	MDM4	GABRA1 GABRB2 GABRG2	BCL2	ATP12A	GPR35
54	MDM2	PLA2G2A	CDK2 CCNA1 CCNA2	MGLL	CDK9 CCNT1
55	PTGIR	PLA2G5	DNM1	PTGIR	AKR1C3
56	DHCR7 EBP	PLA2G10	DYRK1A	DHCR7 EBP	ALPG
57	FABP4	GAK	RXRA	FABP4	PLAA
58	TERT	ERN1	BCHE	FABP3	AKR1B1
59	FABP3	HDAC2	HSD17B2	FABP5	AURKA
60	FABP5	P2RX3	CHEK1	FABP1	CHRM1
61	FABP1	CYP1B1	CDK2	BACE2	AOC3
62	ADORA3	PIM1	CDC7	ADORA3	AURKB
63	MAPK3	PIM2	KDR	MAPK3	CISD1
64	PTPN11	PIM3	BRAF	PTPN11	AKT1
65	AKR1B10	EDNRA	ODC1	AKR1B10	PLEC
66	PRKCG	KLK1	BCL2L1	CCR1	CSNK1A1
67	PRKCD	KLK2	CLK1	GABBR1	CSNK1D
68	PRKCB	ADAM17	DYRK1B	BACE1	HMGCR
69	PRKCE	NCOR2 HDAC3	DNMT1	PTPRF	ALPL

cont..... pg 70

cont from..... pg 69

**Table II: Prediction 100 protein target of a potential mahogany compound through Swiss Target Prediction**

No	B-sitosterol	Swietemacphyllanin	7HMC	Stigmasterol	Scopoletin
70	PRKCQ	HDAC5	PGD	PLA2G1B	BRAF
71	PTPRF	HDAC7	ST3GAL3	ACP1	ALDH5A1
72	PLA2G1B	PIK3CB	FUT7	SCD	ABAT
73	ACP1	HDAC4	FUT4	MAPK14	CSNK2A1
74	IGF1R	HDAC10	STAT1	GRM2	APEX1
75	SRC	HDAC3	SQLE	ACACB	CXCR1
76	KDR	PLG	MMP8	MTNR1A	PIK3CG
77	ALK	PLAU	CDK4	MTNR1B	CLK1
78	SCD	PLA2G7	CES1	TOP2A	DYRK1B
79	MGLL	CHRM1	SERPINE1	IGF1R	IGF1R
80	BACE1	TOP1	ABCB1	SRC	PTPRC
81	CCR1	CDK2	RPS6KA3	KDR	GRK6
82	TOP2A	CDK1	CHEK2	ALK	TNNC1 TNNT2 TNNI3
83	GABBR1	HSP90AA1	RPS6KA1	PRKCG	EPHB4
84	BACE2	KCNH2	WEE1	PRKCD	PDGFRB
85	MAPK14	JAK3	BMP1	PRKCB	PLK4
86	F11	JAK1	OPRK1	PRKCE	LYN
87	PTGFR	SCN9A	DUSP3	PRKCQ	PNP
88	PTGER3	CCNE2 CDK2 CCNE1	HDAC5	PTPN2	TAAR1
89	PTGDR	LCK	HDAC7	KCNA5	PIM3
90	TOP1	ITK	HDAC4	TACR1	HTR2B
91	HIF1A	JAK2	PNP	PTGFR	TERT
92	ACACB	TXK	YWHAG	PTGER3	CA3
93	PRKCH	F11	CES2	PTGDR	JAK1
94	PTPN2	PNMT	AKR1C3	AGTR1	JAK2
95	TACR1	KDR	TYMS	CNR1	TYK2
96	MTNR1A	FGFR1	ECE1	TOP1	F2
97	MTNR1B	HSD17B2	MMP14	HIF1A	CHEK1
98	NPY5R	HSD17B3	GABRA1 GABRB2 GABRG2	F11	WEE1
99	SLC22A6	ESR1	PTPN1	HTR2B	ADRA2A
100	MAP3K14	ESR2	TERT	AVPR1A	ADRA2C

**Table III: The total of 294 genes were known predicted as the target of the 5 potential compounds**

No	Genes	No	Genes	No	Genes
1	<i>FDFT1</i>	101	<i>NAT1</i>	201	<i>CDC25A</i>
2	<i>PRKCH</i>	102	<i>MB</i>	202	<i>PPARA</i>
3	<i>NPY5R</i>	103	<i>PARP1</i>	203	<i>PPARD</i>
4	<i>SLC22A6</i>	104	<i>KCNMA1</i>	204	<i>DHCR7</i>
5	<i>MAP3K14</i>	105	<i>ERBB2</i>	205	<i>PTPN6</i>
6	<i>PGF</i>	106	<i>COMT</i>	206	<i>NR1I3</i>
7	<i>VEGFA</i>	107	<i>GPR35</i>	207	<i>SIGMAR1</i>
8	<i>SYK</i>	108	<i>CDK9 CCNT1</i>	208	<i>NOS2</i>
9	<i>MAPT</i>	109	<i>ALPG</i>	209	<i>NR3C1</i>
10	<i>PDK1</i>	110	<i>AKR1B1</i>	210	<i>CDC25B</i>
11	<i>PIK3CA PIK3R1</i>	111	<i>AOC3</i>	211	<i>UGT2B7</i>
12	<i>PIK3CD PIK3R1</i>	112	<i>AURKB</i>	212	<i>HSD11B2</i>
13	<i>PIK3R1 PIK3CB</i>	113	<i>CISD1</i>	213	<i>PREP</i>
14	<i>MTOR</i>	114	<i>AKT1</i>	214	<i>PTGER4</i>
15	<i>PIK3CA</i>	115	<i>PLEC</i>	215	<i>IDO1</i>
16	<i>FCER2</i>	116	<i>CSNK1A1</i>	216	<i>DRD2</i>
17	<i>TYMP</i>	117	<i>CSNK1D</i>	217	<i>TBXAS1</i>
18	<i>PRKDC</i>	118	<i>ALDH5A1</i>	218	<i>ATP12A</i>
19	<i>MAPK1</i>	119	<i>ABAT</i>	219	<i>MDM4</i>
20	<i>PCNA</i>	120	<i>CSNK2A1</i>	220	<i>MDM2</i>
21	<i>FBP1</i>	121	<i>APEX1</i>	221	<i>PTGIR</i>
22	<i>PLA2G2A</i>	122	<i>CXCR1</i>	222	<i>DHCR7 EBP</i>
23	<i>PLA2G10</i>	123	<i>PTPRC</i>	223	<i>FABP4</i>
24	<i>GAK</i>	124	<i>GRK6</i>	224	<i>FABP3</i>
25	<i>HDAC2</i>	125	<i>TNNC1 TNNT2 TNNI3</i>	225	<i>FABP5</i>
26	<i>P2RX3</i>	126	<i>EPHB4</i>	226	<i>FABP1</i>
27	<i>PIM1</i>	127	<i>PDGFRB</i>	227	<i>PTPN11</i>
28	<i>PIM2</i>	128	<i>PLK4</i>	228	<i>AKR1B10</i>
29	<i>ADAM17</i>	129	<i>LYN</i>	229	<i>PRKCG</i>
30	<i>NCOR2 HDAC3</i>	130	<i>TAAR1</i>	230	<i>PRKCD</i>
31	<i>PIK3CB</i>	131	<i>TYK2</i>	231	<i>PRKCB</i>
32	<i>HDAC10</i>	132	<i>F2</i>	232	<i>PRKCE</i>

cont..... pg 71

cont from..... pg 70

**Table III: The total of 294 genes were known predicted as the target of the 5 potential compounds**

No	Genes	No	Genes	No	Genes
33	HDAC3	133	ADRA2A	233	PRKCO
34	PLAU	134	ADRA2C	234	PTPRF
35	PLA2G7	135	KCNA5	235	ACP1
36	CDK1	136	AGTR1	236	ALK
37	HSP90AA1	137	CNR1	237	SCD
38	KCNH2	138	AVPR1A	238	MGLL
39	JAK3	139	MMP2	239	CCR1
40	SCN9A	140	MMP9	240	TOP2A
41	CCNE2 CDK2 CCNE1	141	MMP13	241	GABBR1
42	LCK	142	MMP12	242	BACE2
43	ITK	143	PTGS1	243	MAPK14
44	TXK	144	DNM1	244	PTGFR
45	PNMT	145	BCL2	245	PTGER3
46	FGFR1	146	MMP14	246	PTGDR
47	TAS2R31	147	PGD	247	ACACB
48	ADORA1	148	ST3GAL3	248	PTPN2
49	HSD17B1	149	FUT7	249	TACR1
50	ABCG2	150	FUT4	250	MTNR1A
51	ABCC1	151	ABCB1	251	MTNR1B
52	APP	152	MMP7	252	PIK3CG
53	CHRNA7	153	MMP8	253	ALPL
54	SGK1	154	GABRA1 GABRB2	254	PLAA
			GABRG2		
55	RPS6KB1	155	PLA2G5	255	PIM3
56	NOX4	156	ERN1	256	CHRM1
57	MMP3	157	CYP1B1	257	JAK1
58	SLC5A2	158	EDNRA	258	JAK2
59	DYRK1A	159	KLK1	259	HSD17B3
60	RXRA	160	KLK2	260	GRM2
61	CDC7	161	HDAC5	261	SHBG
62	ODC1	162	HDAC7	262	BCHE
63	BCL2L1	163	HDAC4	263	CES2
64	DNMT1	164	PLG	264	PPARG
65	STAT1	165	CDK2	265	ADORA3
66	CDK4	166	HSD17B2	266	PLA2G1B
67	CES1	167	MAOB	267	HMGCR
68	SERPINE1	168	CBR1	268	IGF1R
69	RPS6KA3	169	AURKA	269	MAPK3
70	CHEK2	170	CA13	270	F11
71	RPS6KA1	171	CDK2 CCNA1 CCNA2	271	TOP1
72	BMP1	172	CHEK1	272	HIF1A
73	OPRK1	173	BRAF	273	CYP19A1
74	DUSP3	174	CLK1	274	POLB
75	YWHAG	175	DYRK1B	275	TERT
76	TYMS	176	WEE1	276	CA5B
77	ECE1	177	PNP	277	CA2
78	CA14	178	AKR1C3	278	CA1
79	EGFR	179	HTR2B	279	CA4
80	XDH	180	AR	280	CA7
81	SRD5A1	181	CYP51A1	281	CA12
82	MAOA	182	NPC1L1	282	CA9
83	ALOX5	183	NR1H3	283	MET
84	CCND1 CDK4	184	CYP17A1	284	CA3
85	FLT4	185	RORC	285	CA6
86	INSR	186	SREBF2	286	CA5A
87	PTK2	187	SLC6A2	287	PTPN1
88	PLK1	188	CYP2C19	288	ACHE
89	TEK	189	RORA	289	SRC
90	MAP3K8	190	SERPINA6	290	ESR1
91	HSPA1A	191	SLC6A4	291	ESR2
92	NUAK1	192	CHRM2	292	SQLE
93	FGR	193	VDR	293	KDR
94	AKR1C1	194	G6PD	294	BACE1
95	DAO	195	NR1H2		
96	GSK3B	196	GLRA1		
97	KCNA3	197	PTGER1		
98	PTGS2	198	PTGER2		
99	GSR	199	HSD11B1		
100	CYP1A2	200	PTGES		



**Table IV: Top five results of KEGG pathway dan Gene Ontology enrichment analysis of the potential targeted genes using DAVID v6.8.**

Term	Count	P-Value	Genes
hsa05200: Pathways in cancer	49	3.21162E-13	GSK3B, PIK3CD, PIK3CB, PIK3CG, IGF1R, EDNRA, CCND1, AKT1, JAK1, PDGFRB, PRKCG, HSP90AA1, PRKCB, MMP2, MMP9, PGF, AR, PIK3CA, CCNE2, CCNE1, AGTR1, PPARG, MET, PPAR, PTGER4, HDAC2, PTGER1, PTGER2, PTGER3, PIK3R1, PTGS2, HIF1A, EGFR, RXRA, ERBB2, MAPK1, MAPK3, NOS2, STAT1, BRAF, MTOR, PTK2, VEGFA, CDK4, CDK2, BCL2, MDM2, FGFR1, BCL2L1
hsa04151:PI3K-Akt signaling pathway	41	2.03355E-10	CHRM2, GSK3B, CHRM1, FLT4, PIK3CD, PIK3CB, PIK3R1, EGFR, PIK3CG, IGF1R, RXRA, CCND1, KDR, AKT1, MAPK1, JAK2, JAK3, YWHAG, JAK1, MAPK3, PDGFRB, HSP90AA1, SYK, INSR, MTOR, PGF, PTK2, VEGFA, PIK3CA, CCNE2, RPS6KB1, CCNE1, CDK4, CDK2, BCL2, MDM2, TEK, SGK1, MET, FGFR1, BCL2L1
hsa04080: Neuroactive ligand-receptor interaction	37	7.16148E-11	PTGER4, CHRM2, GABRB2, PTGFR, CHRM1, PTGER1, PTGER2, CHRNA7, PTGER3, HTR2B, PLG, NR3C1, GRM2, GLRA1, EDNRA, CNR1, ADORA3, ADORA1, DRD2, PTGDR, GABRA1, PTGIR, GABBR1, NPY5R, GPR35, OPRK1, TACR1, AVPR1A, ADRA2C, F2, TAAR1, GABRG2, ADRA2A, MTNR1A, P2RX3, MTNR1B, AGTR1
hsa05205: Proteoglycans in cancer	32	1.78808E-11	SRC, PIK3CD, PIK3CB, PIK3R1, HIF1A, EGFR, PIK3CG, IGF1R, CCND1, PLAU, ERBB2, KDR, AKT1, MAPK1, MAPK3, PRKCG, PRKCB, MMP2, PTPN11, BRAF, MAPK14, MMP9, ESR1, MTOR, PTK2, VEGFA, PIK3CA, RPS6KB1, MDM2, PTPN6, MET, FGFR1
hsa05203: Viral carcinogenesis	30	7.95804E-10	HDAC4, HDAC5, HDAC2, HDAC3, HDAC10, SRC, PIK3CD, PIK3CB, PIK3R1, PIK3CG, HDAC7, POLB, CCND1, CHEK1, MAPK1, JAK3, YWHAG, JAK1, MAPK3, LYN, SYK, CCNA2, CCNA1, PIK3CA, CCNE2, CCNE1, CDK4, CDK2, CDK1, MDM2

**Molecular function**

Term	Count	P-Value	Genes
GO:0005515~protein binding	199	2.66061E-07	APP, HDAC10, SERPINE1, PREP, RPS6KA3, EDNRA, CHEK2, RPS6KA1, CHEK1, KDR, AKT1, EPHB4, PDK1, PTGDR, CSNK2A1, PRKCB, PRKCE, PRKCD, CSNK1D, GABRG2, AR, AGTR1, PRKCQ, SLC22A6, ABCB1, PRKDC, TXK, PIK3R1, HIF1A, NUAK1, TERT, CCR1, LYN, PLK4, INSR, PLK1, CDC7, BRAF, PTK2, AKR1B10, NOX4, TOP2A, ACHE, ITK, SLC6A2, SLC6A4, JAK2, JAK3, JAK1, PARP1, SYK, TNNC1, AVPR1A, TYK2, TACR1, F2, SREBF2, GAK, BACE1, NCOR2, FCER2, MMP14, TNNT2, KCNMA1, PPARG, MAPT, SGK1, PPARA, PPAR, PTGER4, PCNA, ODC1, KCNA5, PTGS2, EGFR, GLRA1, RXRA, ALOX5, AOC3, GABBR1, STAT1, CSNK1A1, AKR1C1, NR1H2, F11, NR1H3, VEGFA, FABP1, FABP3, FABP5, APEX1, HSPA1A, CCNT1, RORC, RORA, COMT, NR3C1, IGF1R, CCND1, PLAU, ADORA1, PIM1, MAP3K8, PIM3, PIM2, PDGFRB, KCNH2, G6PD, DYRK1A, DYRK1B, PGF, CDC25A, CDC25B, ERN1, ADAM17, MTNR1A, CCNE2, CCNE1, MTNR1B, PLAA, ABCG2, DNMT1, ACACB, NPC1L1, GRK6, DRD2, VDR, ESR1, ESR2, CDK9, CLK1, DAO, BMP1, PTPRC, CDK4, CDK2, BCL2, MDM2, CDK1, ALPL, MDM4, MAP3K14, BCL2L1, FGFR1, ALK, GSK3B, FLT4, PIK3CD, ECE1, PIK3CB, PIK3CG, POLB, GRM2, CA1, CA2, CA4, ACP1, YWHAG, HSP90AA1, MMP2, MMP3, ADRA2C, MMP9, ADRA2A, DNMT1, FGR, CCNA2, CCNA1, PIK3CA, LCK, TOP1, MET, FBP1, PLEC, HDAC4, HDAC5, HDAC2, HDAC3, SRC, PLG, HMGR, AURKB, AURKA, HDAC7, ERBB2, MAPK1, TNNT3, MAPK3, PTPN1, NOS2, OPRK1, PTPN11, MAPK14, MTOR, WEE1, RPS6KB1, PTPN6, TEK, PTPN2
GO:0005524~ATP binding	83	2.15845E-21	ALK, TOP2A, GSK3B, ITK, FLT4, PIK3CD, PIK3CB, ATP12A, PIK3CG, IGF1R, RPS6KA3, CHEK2, RPS6KA1, CHEK1, PIM1, KDR, AKT1, PIM3, MAP3K8, PIM2, JAK2, JAK3, EPHB4, JAK1, PDK1, PDGFRB, PRKCG, ABCB1, HSP90AA1, PRKCH, CSNK2A1, SYK, PRKCB, PRKCE, PRKCD, DYRK1A, DYRK1B, CSNK1D, TYK2, GAK, ERN1, FGR, PIK3CA, LCK, PRKCQ, SGK1, MET, ABCG2, ABCB1, SRC, PRKDC, TXK, ACACB, EGFR, AURKB, AURKA, NUAK1, ERBB2, GRK6, MAPK1, MAPK3, LYN, PLK4, CSNK1A1, INSR, PLK1, BRAF, CDC7, MAPK14, MTOR, PTK2, CDK9, CLK1, WEE1, P2RX3, RPS6KB1, CDK4, CDK2, CDK1, TEK, MAP3K14, FGFR1, HSPA1A
GO:0004672~protein kinase activity	51	1.5312E-30	GSK3B, PIK3CG, RPS6KA3, CCND1, CHEK2, RPS6KA1, CHEK1, AKT1, PIM3, MAP3K8, PIM2, JAK2, PDK1, PRKCG, PRKCH, CSNK2A1, SYK, PRKCB, PRKCE, PRKCD, DYRK1A, DYRK1B, CSNK1D, TYK2, GAK, PRKCQ, MET, SRC, PRKDC, TXK, EGFR, AURKB, AURKA, NUAK1, ERBB2, CSNK1A1, PLK1, BRAF, CDC7, MAPK14, MTOR, PTK2, CDK9, CLK1, WEE1, RPS6KB1, CDK4, CDK2, CDK1, TEK, MAP3K14

cont from..... pg 72

**Table IV: Top five results of KEGG pathway dan Gene Ontology enrichment analysis of the potential targeted genes using DAVID v6.8.**

GO:0004674~protein serine/threonine kinase activity	45	9.24148E-24	GSK3B, CCNT1, PRKDC, PIK3CG, AURKB, AURKA, RPS6KA3, NUAK1, CHEK2, CHEK1, RPS6KA1, PIM1, AKT1, MAPK1, PIM3, MAP3K8, PIM2, MAPK3, PLK4, PRKCH, SYK, CSNK2A1, PRKCB, CSNK1A1, PRKCE, PRKCD, PLK1, DYRK1A, DYRK1B, BRAF, CSNK1D, CDC7, MAPK14, MTOR, CDK9, GAK, ERN1, CLK1, PIK3CA, CDK4, CDK2, CDK1, PRKCQ, SGK1, MAP3K14.
GO:0008270~zinc ion binding	43	8.45694E-06	HDAC4, DNMT1, NR1I3, RORC, RORA, NR3C1, GLRA1, CA1, RXRA, CA5B, CA3, CA2, CA5A, CA4, CA7, CA6, CA9, CA13, CA12, PRKCG, PTPN1, MMP7, PARP1, PRKCB, VDR, NR1H2, MMP2, MMP3, NR1H3, MMP8, MMP9, ESR1, ESR2, MMP12, AR, MMP14, BMP1, MMP13, MDM2, PPARG, MDM4, PPARA, PPARD.
<b>Biological process</b>			
<b>Term</b>	<b>Count</b>	<b>P-Value</b>	<b>Genes</b>
GO:0006468~protein phosphorylation	56	2.74809E-30	APP, GSK3B, CCNT1, PIK3CD, PIK3CG, RPS6KA3, CCND1, CHEK2, RPS6KA1, PIM1, AKT1, PIM3, MAP3K8, PIM2, JAK2, JAK3, JAK1, PDK1, PRKCG, PRKCH, CSNK2A1, SYK, PRKCB, PRKCE, PRKCD, DYRK1A, DYRK1B, CSNK1D, TYK2, CDC25B, GAK, ERN1, FGR, PIK3CA, CCNE1, LCK, SGK1, TXK, PIK3R1, AURKB, AURKA, NUAK1, ERBB2, GRK6, MAPK1, MAPK3, LYN, PLK4, CSNK1A1, PLK1, BRAF, MTOR, CDK9, RPS6KB1, CDK4, FGFR1.
GO:0007165~signal transduction	51	3.74565E-09	ALK, ITK, CHRM1, PIK3CD, PIK3CB, NR3C1, IGF1R, RPS6KA3, EDNRA, PLAU, RPS6KA1, ADORA1, AKT1, JAK2, PDGFRB, HSP90AA1, PRKCH, CSNK2A1, PRKCB, PRKCE, PRKCD, CSNK1D, ADRA2A, PGF, AR, PLAA, PPARG, MET, PTGES, SRC, PLA2G1B, NR1I3, CHRNA7, PIK3R1, HIF1A, EGFR, EBP, ERBB2, GRK6, MAPK1, LYN, CSNK1A1, VDR, MAPK14, ESR1, MTOR, ESR2, P2RX3, RPS6KB1, CDK4, TEK.
GO:0042493~response to drug	40	1.44432E-22	HDAC4, HDAC5, HDAC2, ABCB1, MAOB, SRC, HTR2B, ABAT, TYMS, COMT, PTGS2, SLC6A2, ACACB, SLC6A4, HSD11B2, PNP, CCND1, NPC1L1, CA9, DRD2, LYN, BCHE, ABCC1, HSP90AA1, STAT1, SRD5A1, PGF, CDK9, ADAM17, FABP3, RPS6KB1, LCK, CDK4, APEX1, BCL2, CDK1, MDM2, PPARG, TOP1, ABCG2.
GO:0055114~oxidation-reduction process	38	2.42738E-11	MAOB, MAOA, HSD17B3, AKR1B1, HMGCR, CYP2C19, PTGS2, CYP19A1, PTGS1, CYP17A1, HSD11B1, HSD11B2, HSD17B1, ALOX5, HSD17B2, CYP1B1, XDH, FDF1, AOC3, CBR1, G6PD, NOS2, SRD5A1, AKR1C1, GSR, CYP51A1, AKR1C3, PGD, SQLE, DAO, AKR1B10, SCD, APEX1, TBXAS1, CYP1A2, NOX4, DHCR7, IDO1.
GO:0045944~positive regulation of transcription from RNA polymerase II promoter	38	1.10342E-05	HDAC4, TOP2A, HDAC5, APP, GSK3B, HDAC2, HDAC3, CCNT1, PLA2G1B, PRKDC, NR1I3, TXK, SERPINE1, RORA, PIK3R1, NR3C1, HIF1A, EGFR, RPS6KA3, RXRA, RPS6KA1, AKT1, DRD2, MAPK3, PARP1, STAT1, VDR, NR1H2, NR1H3, MAPK14, ESR1, SREBF2, VEGFA, CDK9, AR, PPARG, PPARA, MET.
<b>Cell component</b>			
<b>Term</b>	<b>Count</b>	<b>P-Value</b>	<b>Genes</b>
GO:0005886~plasma membrane	123	8.03158E-13	CHRM2, APP, CHRM1, SERPINE1, COMT, ATP12A, IGF1R, EDNRA, PLAU, ADORA3, ADORA1, PIM1, KDR, AKT1, EPHB4, CA14, PTGDR, PDGFRB, KCNH2, PRKCG, PRKCH, CSNK2A1, PRKCB, PRKCE, PRKCD, CSNK1D, TAAR1, GABRG2, AR, MTNR1A, ADAM17, MTNR1B, AGTR1, PRKCQ, ABCG2, PTGFR, SLC22A6, ABCB1, CHRNA7, PIK3R1, PLA2G5, SLC5A2, TERT, NPC1L1, GRK6, DRD2, CCR1, LYN, TAS2R31, INSR, BRAF, ESR1, PTK2, PTPRC, MDM2, ALPL, FGFR1, GABRB2, ACHE, GSK3B, FLT4, HTR2B, PIK3CD, ECE1, PIK3CB, SLC6A2, PTPRF, PIK3CG, SLC6A4, GRM2, CA2, CA4, CA9, ABCC1, PTGIR, HSP90AA1, NPY5R, SYK, MMP2, AVPR1A, TACR1, F2, ADRA2C, ADRA2A, DNMT1, BACE1, FGR, FCER2, MMP14, PIK3CA, LCK, KCNMA1, MAPT, SGK1, MET, MGLL, PLEC, PTGER4, HDAC3, SRC, PTGER1, PTGER2, PTGER3, KCNA3, KCNA5, PLG, EGFR, GLRA1, CXCR1, CNR1, ERBB2, CA12, AOC3, PTPN1, GABRA1, GABBR1, CYP51A1, F11, PLA2G2A, OPRK1, P2RX3, TEK, PTPN2
GO:0005829~cytosol	118	4.75122E-18	PNMT, APP, COMT, RPS6KA3, PNP, CCND1, RPS6KA1, CHEK1, AKT1, MAP3K8, EPHB4, CA13, PRKCG, G6PD, PRKCH, CSNK2A1, PRKCB, PRKCE, PRKCD, CSNK1D, PGD, CDC25A, CDC25B, AR, CCNE2, CCNE1, PRKCQ, IDO1, CES1, PRKDC, PIK3R1, HIF1A, ACACB, LYN, PLK4, PLK1, BRAF, PTK2, DAO, AKR1B10, NAT1, CDK4, CDK2, BCL2, MDM2, CDK1, MAP3K14, BCL2L1, FGFR1, GABRB2, GSK3B, ITK, PIK3CD, AKR1B1, PIK3CB, PIK3CG, SLC6A4, CA1, CA3, CA2, CA7, CA6, JAK2, JAK3, YWHAG, JAK1, CBR1, PTGIR,

cont..... pg 74

cont from..... pg 73

**Table IV: Top five results of KEGG pathway dan Gene Ontology enrichment analysis of the potential targeted genes using DAVID v6.8.**

			<i>HSP90AA1, DUSP3, SYK, TNNC1, TYK2, SREBF2, GAK, FGR, CCNA1, PIK3CA, LCK, TNNT2, PPARG, MAPT, SGK1, FBP1, MGLL, PLEC, HDAC4, HDAC3, SRC, NR1I3, ODC1, TYMS, AURKB, TYMP, AURKA, HSD17B1, ALOX5, MAPK1, TNNI3, XDH, MAPK3, PTPN1, NOS2, STAT1, CSNK1A1, AKR1C1, GSR, AKR1C3, PTPN11, MAPK14, MTOR, FABP1, FABP3, FABP4, RPS6KB1, FABP5, PTPN6, HSPA1A</i>
GO:0005634~nucleus	110	0.006034134	<i>CCNT1, HDAC10, PREP, RORC, RORA, NR3C1, RPS6KA3, PNP, CCND1, RPS6KA1, CHEK1, PIM1, KDR, AKT1, PDGFRB, PRKCG, G6PD, CSNK2A1, PRKCB, PRKCE, PRKCD, DYRK1A, DYRK1B, CSNK1D, PGD, CDC25A, AR, CCNE2, CCNE1, PLAA, ABCG2, DNMT1, KLK1, TXK, PIK3R1, HIF1A, ACACB, NUA1, TERT, LYN, VDR, PLK1, CDC7, BRAF, ESR1, ESR2, PTK2, CLK1, CDK4, CDK2, BCL2, MDM2, CDK1, MDM4, FGFR1, TOP2A, ACHE, GSK3B, FLT4, PIK3CB, POLB, JAK2, JAK1, HSP90AA1, DUSP3, PARP1, SYK, MMP2, TYK2, SREBF2, CCNA2, NCOR2, CCNA1, PPARG, TOP1, SGK1, PPARA, PPARD, HDAC4, HDAC5, HDAC2, HDAC3, PCNA, SRC, NR1I3, PTGS2, TYMS, EGFR, AURKB, HDAC7, PTGS1, AURKA, RXRA, ERBB2, MAPK1, MAPK3, NOS2, STAT1, NR1H2, AKR1C3, NR1H3, PTPN11, MAPK14, MTOR, WEE1, FABP4, RPS6KB1, APEX1, PTPN6, PTPN2</i>
GO:0005737~cytoplasm	107	0.005336642	<i>APP, HDAC10, PREP, NR3C1, RPS6KA3, PNP, CCND1, RPS6KA1, PIM1, AKT1, MAP3K8, PIM3, PIM2, PDGFRB, G6PD, PRKCH, PRKCB, PRKCE, PRKCD, CDC25A, CDC25B, ERN1, AR, ADAM17, PLAA, PTGFR, TXK, PIK3R1, PLA2G7, HIF1A, NUA1, LYN, PLK1, CDC7, BRAF, ESR1, PTK2, CDK9, CLK1, CDK2, BCL2, MDM2, CDK1, MAP3K14, BCL2L1, TOP2A, GSK3B, FLT4, HTR2B, AKR1B1, PIK3CG, POLB, CA1, CA3, CA2, JAK2, ACP1, JAK1, HSP90AA1, DUSP3, NPY5R, SYK, TYK2, ADRA2C, SREBF2, ADRA2A, CCNA2, MMP14, MAPT, SGK1, FBP1, PLEC, HDAC4, HDAC5, HDAC2, HDAC3, PCNA, SRC, NR1I3, ODC1, PTGS2, TYMS, EGFR, HDAC7, PTGS1, HSD17B1, ERBB2, MAPK1, AOC3, GABBR1, NOS2, STAT1, NR1H2, AKR1C3, PTPN11, MAPK14, MTOR, VEGFA, FABP1, WEE1, FABP4, RPS6KB1, FABP5, APEX1, PTPN6, TEK, HSPA1A</i>
GO:0016021~integral component of membrane	101	0.026736903	<i>APP, CISD1, COMT, ATP12A, IGF1R, ADORA3, ADORA1, KDR, CYP1B1, CA14, PTGDR, PDGFRB, KCNH2, TAAR1, GABRG2, AR, MTNR1A, ADAM17, MTNR1B, AGTR1, PTGES, ABCG2, PTGFR, SLC22A6, ABCB1, MAOB, MAOA, CHRNA7, SLC5A2, CYP19A1, FUT4, HSD11B1, HSD11B2, EBP, FUT7, NPC1L1, ST3GAL3, FDFT1, CCR1, TAS2R31, SRD5A1, ESR1, SQLE, PTPRC, TBXAS1, CYP1A2, BCL2, NOX4, ALPL, DHCR7, BCL2L1, FGFR1, ALK, GABRB2, ACHE, HTR2B, ECE1, SLC6A2, PTPRF, SLC6A4, GRM2, CA4, CA9, ACP1, ABCC1, PTGIR, GPR35, SIGMAR1, AVPR1A, TACR1, ADRA2C, BACE1, FCER2, BACE2, MMP14, MMP13, KCNMA1, MET, UGT2B7, PTGER4, HDAC2, PTGER1, PTGER2, PTGER3, HMGR, EGFR, GLRA1, CXCR1, CNR1, ERBB2, HSD17B2, CA12, AOC3, BCHE, PTPN1, GABRA1, GABBR1, CYP51A1, OPRK1, SCD, PTPN2</i>

**Table V: Top 20 hub genes with the highest degree score**

No	Gene symbol	Full name	Score
1	<i>AKT1</i>	Serine/threonine-protein kinase AKT	123
2	<i>MAPK3</i>	MAP kinase ERK1	116
3	<i>EGFR</i>	Epidermal growth factor receptor erbB1	107
4	<i>SRC</i>	Tyrosine-protein kinase SRC	102
5	<i>MAPK1</i>	MAP kinase ERK3	101
6	<i>VEGFA</i>	Vascular endothelial growth factor A	98
7	<i>HSP90AA1</i>	Heat shock protein HSP 90-alpha	90
8	<i>ESR1</i>	Estrogen receptor alpha	84
9	<i>PTGS2</i>	Cyclooxygenase-2	82
10	<i>MTOR</i>	Serine/threonine-protein kinase mTOR	76
11	<i>PIK3CA</i>	PI3-kinase p110-alpha subunit	74
12	<i>APP</i>	Beta-amyloid A4 protein	65
13	<i>MMP9</i>	Matrix metalloproteinase 9	62
14	<i>MAPK14</i>	MAP kinase p38 alpha	59
15	<i>AR</i>	Androgen Receptor	58
16	<i>ERBB2</i>	Receptor protein-tyrosine kinase erbB-2	57
17	<i>MDM2</i>	p53-binding protein Mdm-2	57
18	<i>KDR</i>	Vascular endothelial growth factor receptor 2	56
19	<i>BCL2L1</i>	Apoptosis regulator Bcl-X	55
20	<i>STAT1</i>	Signal transducer and activator of transcription 1-alpha/beta	55

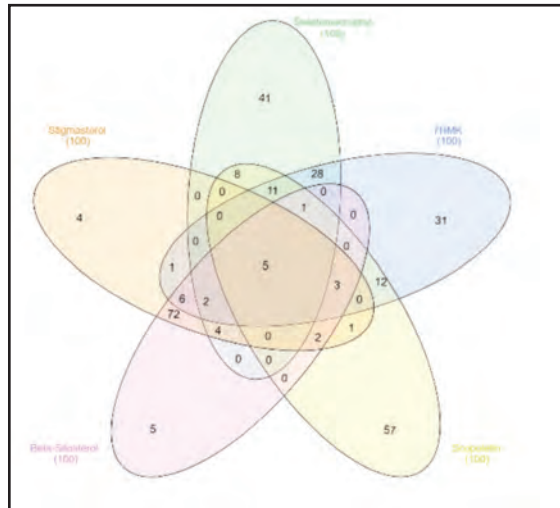


Fig. 1: Venn diagram of predicted genes target of 5 potential mahogany compounds, resulting in 294 potential targets.

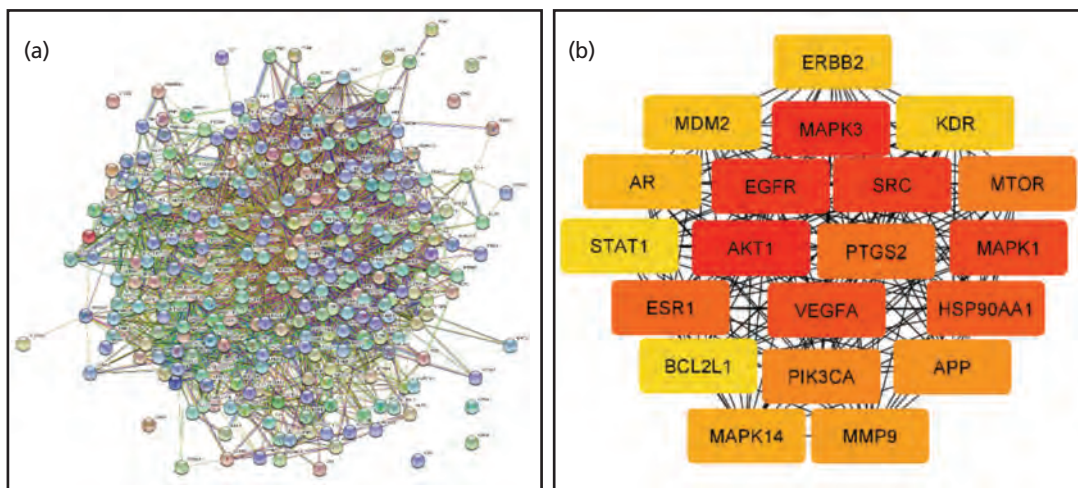


Fig. 2: (a) Protein-protein interaction networks of predictive mahogany metabolite target genes analyzed using STRING-DB and (b) the top 20 hub genes with the highest degree score analyzed using Cytoscape.

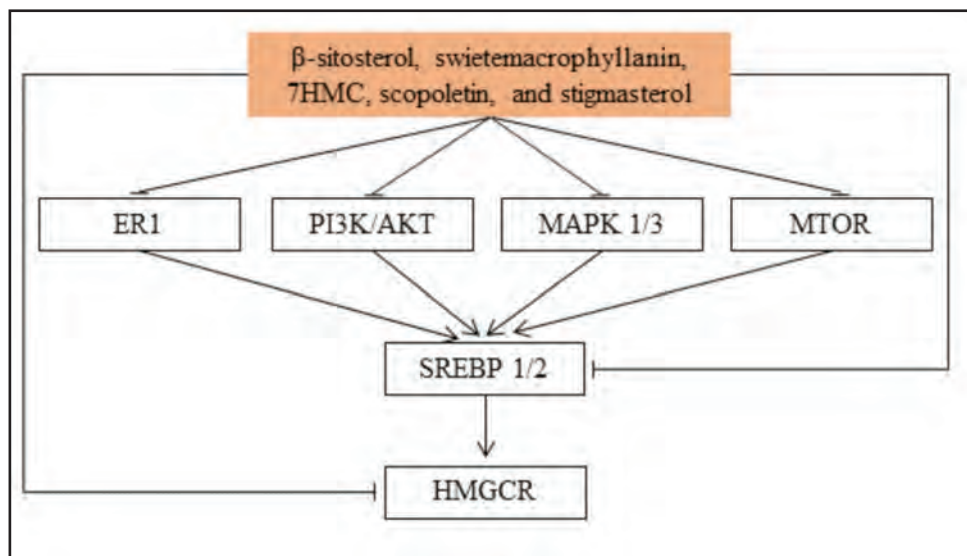


Fig. 3: Mechanism of antidiabetic activity of the 5 mahogany test compounds through the direct inhibition of HMGCR and indirect inhibition through SREBP, ER1, PI3K/AKT, MAPK 1/3, and MTOR.



target of mahogany compounds (Table II). SREBP was activated by MAPK, AKT1, PI3K, MTOR, and ER1.<sup>28-30</sup>

Intracellular mitogen-activated protein kinases (MAPKs) are an essential class of proline-dependent protein kinases involved in regulating various biological functions, such as inflammation, cell proliferation, and differentiation.<sup>31</sup> MAPK1 and MAPK3 (also known as ERK2 and ERK1, respectively) are the members of the MAPK family. The N-terminal domains of SREBP1a, SREBP1c, and SREBP2 are the substrates of MAPK1 and MAPK3.<sup>32</sup> The activation of the MAP kinase cascade increases the transcriptional activity of SREBP1a and SREBP2 to a similar degree (state). MAPK1/3 plays a role in regulating the lipid metabolism in the liver.<sup>33</sup> A past study also confirmed that the inhibition of MAPK3 had been known to reduce adipocytes and resistance to high-fat diet-induced obesity due to impaired adipocyte differentiation and higher postprandial metabolism.<sup>34</sup>

The phosphatidylinositol 3-kinase/protein kinase B (PI3K/AKT) pathway is considered as one of the upstream pathways of SREBP.<sup>29</sup> The Akt pathway positively modulates the activation of SREBP2, which selectively activates *de novo* cholesterol synthesis.<sup>35</sup> The inhibition of the AKT signaling pathway is known to inhibit the formation of SREBP2 and the downstream target genes of SREBP2, such as LDLR and HMGCR.<sup>35</sup>

The mechanistic target of rapamycin (mTOR) is the catalytic subunit of two structurally distinct complexes: mTORC1 and mTORC2, both of which localize to different subcellular compartments and also affect different activation and function.<sup>36</sup> During obesity and overnutrition conditions, mTORC1 is hyperactivated, resulting in the persistent activation of SREBP 1c in the liver, leading to the overproduction of lipids and hepatic steatosis hypertriglyceridemia.<sup>37</sup> The inhibition of mTORC1 is known to reduce the SREBP2 activity and cholesterol synthesis in the endoplasmic reticulum.<sup>28</sup> Moreover, the inhibition of mTORC1 is known to prevent lipid storage processes, increase low-density lipoprotein cholesterol levels, and activate lipolysis.<sup>38</sup> Thus, the inhibition of mTORC1 can be a potential therapeutic target for metabolic syndromes such as dyslipidemia.

Estrogen receptor alpha (ER $\alpha$ ) plays a significant role in adipocyte activity and sexual dimorphism in fat distribution.<sup>7</sup> For instance, ER  $\alpha$  modulates the process of transcription and the activation of proteins that play a role in fat metabolisms, such as PPAR gamma, SREBP, HMGCR, and LDLR.<sup>25,30,39</sup> Past research has shown that ER-alpha activation plays a role in activating the SREBP2 expression, which is correlated with the exhibition of the HMGCR expression for cholesterol synthesis and LDLR for the cellular uptake of LDL cholesterol.<sup>30,40</sup> However, past studies have shown that phytoestrogen genistein activation of SREBP2 did not significantly increase HMGCR expression, rather it increases LDLR expression.<sup>40</sup>

Our research suggests that mahogany contains  $\beta$ -sitosterol, swietemachropyllanin, swietenia, 7-HMC, and scopoletin, which are responsible for the estrogenic and anti-dyslipidemic activity with the mechanism through direct or indirect inhibition of HMGCR. Indirect inhibition of the

HMGCR activity through inhibition of the ERK1/2, AKT/PI3K, mTOR, and estrogen receptor alpha pathways mediated through SREBP1/2 (Fig. 3). This study demonstrates the potential of mahogany as an estrogenic agent and a dyslipidemia-preventing agent in postmenopausal women. This research was based on bioinformatics research that suspected the compound roles of its activity and mechanism pathways. Therefore, further research is warranted to confirm our results.

## CONCLUSION

In this study, a network pharmacology approach was proposed to explore the mechanism underlying the action of mahogany on dyslipidemia for menopausal conditions. The active ingredients of mahogany in the treatment of dyslipidemia consisted of five compounds  $\beta$ -sitosterol, swietemachropyllanin, 7-hydroxy-2-(4-hydroxy-3-methoxyphenyl)-chroman-4-one (7HMC), scopoletin, and stigmaterol. The possible molecular mechanisms mainly involved the direct inhibitory pathway of HMGCR and the indirect inhibitory pathway of HMGCR. The indirect inhibitory pathway was mediated through the PI3K/AKT, MAPK1/3, MTOR, ER1, and SREBP1/2 signaling pathways. Our findings suggested the use of mahogany as an alternative herbal therapy to prevent dyslipidemia in menopause conditions and exert estrogenic activity. This research provides new insights for further research on the anti-dyslipidemic effect of mahogany.

## ACKNOWLEDGMENTS

Thanks to *Program Kreativitas Mahasiswa 2020 (PKM 2020)* from the Directorate of Learning and Student Affairs, Ministry of Education and Culture of the Republic of Indonesia, for funding this research. We are also grateful to Prof. Dr. apt. Edy Meiyanto, M.Si, for excellent discussion and suggestion while finishing this study.

## REFERENCES

1. Santoro N, Worsley R, Miller KK, Parish SJ, Davis SR. Role of estrogens and estrogen-like compounds in female sexual function and dysfunction. *J Sex Med* 2016; 13(3): 305–16.
2. Yeasmin N, Akhter QS, Mahmuda S, Nahar S, Rabbani R, Hasan M, et al. Effect of estrogen on serum total cholesterol and triglyceride levels in postmenopausal women. *Journal of Dhaka Medical College* 2017; 26(1): 25–31.
3. Dalal PK, Agarwal M. Postmenopausal syndrome. *Indian J Psychiatry* 2015; 57(2): S222–32.
4. Fait I. Menopause hormone therapy: latest developments and clinical practice [cited Sep 2020]. Available from: <https://www.ncbi.nlm.nih.gov/pmc/articles/PMC6317580/>.
5. Davidson MH, Maki KC, Karp SK, Ingram KA. Management of hypercholesterolaemia in postmenopausal women. *Drugs Aging*. 2002; 19(3): 169–78.
6. Kuiper GG, Lemmen JG, Carlsson B, Corton JC, Safe SH, van der Saag PT, et al. Interaction of estrogenic chemicals and phytoestrogens with estrogen receptor beta. *Endocrinology* 1998; 139(10): 4252–63.
7. Lizcano F, Guzmán G. Estrogen deficiency and the origin of obesity during menopause. *Biomed Res Int* 2014; 757461.
8. Ness GC, Chambers CM. Feedback and hormonal regulation of hepatic 3-hydroxy-3-methylglutaryl coenzyme A reductase: the concept of cholesterol buffering capacity. *Proc Soc Exp Biol Med* 2000; 224(1): 8–19.

9. Ko S-H, Kim H-S. Menopause-associated lipid metabolic disorders and foods beneficial for postmenopausal women. *Nutrients* 2020; 12(1): 202.
10. Moghadamtousi SZ, Goh BH, Chan CK, Shabab T, Kadir HA. Biological activities and phytochemicals of *Swietenia macrophylla* King. *Molecules* 2013; 18(9): 10465–83.
11. Goh BH, Kadir HA. In vitro cytotoxic potential of *Swietenia macrophylla* King seeds against human carcinoma cell lines. *JMPR* 201; 5(8): 1395–404.
12. Hasibuan PAZ, Sitanggang RG, Angkat RS. Estrogenic Activity of mahoni seed ethanolic extract [*Swietenia mahogany* (L.) Jacq] on uterus weight, bone density and mammae gland proliferation on ovariectomized rats. *Indonesian Journal of Cancer Chemoprevention* 2020; 11(2): 75–83.
13. Lau WK, Goh BH, Kadir HA, Shu-Chien AC, Tengku Muhammad TS. Potent PPAR $\gamma$  ligands from *swietenia macrophylla* are capable of stimulating glucose uptake in muscle cells. *Molecules* 2015; 20(12): 22301–14.
14. Ayunda RD, Prasetyastuti P, Hastuti P. Effect of 7-hydroxy-2-(4-hydroxy -3-methoxyphenyl)-chroman-4-one on level of mangan-superoxide dismutase (mn-sod) and superoxide dismutase 2 (sod2) gene expression in hyperlipidemia rats. *Indonesian Journal of Pharmacy* 2019; 30(3):180.
15. Kalpana K, Pugalendi KV. Antioxidative and hypolipidemic efficacy of alcoholic seed extract of *Swietenia macrophylla* in streptozotocin diabetic rats [cited Aug 2020]. Available from: <https://www.degruyter.com/view/j/jbcpp.2011.22.issue-1-2/jbcpp.2011.001/jbcpp.2011.001.xml>
16. Cerqueira NMFSA, Oliveira EF, Gesto DS, Santos-Martins D, Moreira C, Moorthy HN, et al. Cholesterol biosynthesis: A mechanistic overview. *Biochemistry* 2016; 55(39): 5483–506.
17. DeBose-Boyd RA. Feedback regulation of cholesterol synthesis: Sterol-accelerated ubiquitination and degradation of HMG CoA reductase. *Cell Res* 2008; 18(6): 609–21.
18. Sydow D, Morger A, Driller M, Volkamer A. TeachOpenCADD: A teaching platform for computer-aided drug design using open source packages and data [cited Mar 2021]. Available from: <https://www.ncbi.nlm.nih.gov/pmc/articles/PMC6454689/>
19. Wulandari F, Ikawati M, Meiyanto E, Kirihata M, Hermawan A. Bioinformatic analysis of CCA-1.1, a novel curcumin analog, uncovers furthest noticeable target genes in colon cancer. *Gene Reports* 2020; 21: 100917.
20. Hermawan A, Putri H, Utomo RY. Functional network analysis reveals potential repurposing of  $\beta$ -blocker atenolol for pancreatic cancer therapy. *DARU J Pharm Sci* 2020; 28(2): 685–99.
21. Chin C-H, Chen S-H, Wu H-H, Ho C-W, Ko M-T, Lin C-Y. cytoHubba: identifying hub objects and sub-networks from complex interactome. *BMC Syst Biol* 201; 8: S11.
22. Nicola G, Berthold MR, Hedrick MP, Gilson MK. Connecting proteins with drug-like compounds: Open source drug discovery workflows with BindingDB and KNIME [cited May 2021]. Available from: <https://doi.org/10.1093/database/bav087>
23. Ben-David A. About the relationship between ROC curves and Cohen's kappa. *Engineering Applications of Artificial Intelligence* 2008; 21(6): 874–82.
24. Yelaware Puttaswamy N, Urooj A. In vivo antihypercholesterolemic potential of *swietenia mahagoni* leaf extract. *Cholesterol* 2016; 2016: e2048341.
25. Trapani L, Pallottini V. Age-related hypercholesterolemia and HMG-CoA reductase dysregulation: Sex Does Matter (A Gender Perspective) [cited Sep 2020]. Available from: <https://www.ncbi.nlm.nih.gov/pmc/articles/PMC2863156/>
26. Wu N, Sarna LK, Hwang S-Y, Zhu Q, Wang P, Siow YL, et al. Activation of 3-hydroxy-3-methylglutaryl coenzyme A (HMG-CoA) reductase during high fat diet feeding. *Biochimica et Biophysica Acta (BBA) - Molecular Basis of Disease* 2013; 1832(10): 1560–8.
27. DeBose-Boyd RA, Ye J. SREBPs in lipid metabolism, insulin signaling, and beyond. *Trends Biochem Sci* 2018; 43(5): 358–68.
28. Eid W, Dauner K, Courtney KC, Gagnon A, Parks RJ, Sorisky A, et al. mTORC1 activates SREBP-2 by suppressing cholesterol trafficking to lysosomes in mammalian cells. *PNAS* 2017; 114(30): 7999–8004.
29. Krycer JR, Sharpe LJ, Luu W, Brown AJ. The Akt-SREBP nexus: cell signaling meets lipid metabolism. *Trends in Endocrinology & Metabolism* 2010; 21(5): 268–76.
30. Meng Y, Zong L. Estrogen stimulates SREBP2 expression in hepatic cell lines via an estrogen response element in the SREBP2 promoter. *Cellular & Molecular Biology Letters* 2019 Dec; 24(1): 65.
31. Upadhya D, Ogata M, Reneker LW. MAPK1 is required for establishing the pattern of cell proliferation and for cell survival during lens development. *Development* 2013 Apr; 140(7): 1573–82.
32. Roth G, Kotzka J, Kremer L, Lehr S, Lohaus C, Meyer HE, et al. MAP kinases Erk1/2 phosphorylate sterol regulatory element-binding protein (SREBP)-1a at serine 117 in vitro. *Journal of Biological Chemistry* 2000; 275(43): 33302–7.
33. Xiao Y, Liu H, Yu J, Zhao Z, Xiao F, Xia T, et al. Activation of ERK1/2 ameliorates liver steatosis in leptin receptor-deficient (db/db) mice via stimulating ATG7-dependent autophagy. *Diabetes* 2016; 65(2): 393–405.
34. Bost F, Aouadi M, Caron L, Even P, Belmonte N, Prot M, et al. The Extracellular signal-regulated kinase isoform ERK1 Is specifically required for in vitro and in vivo adipogenesis. *Diabetes* 2005; 54(2): 402–11.
35. Luu W, Sharpe LJ, Stevenson J, Brown AJ. Akt acutely activates the cholesterolgenic transcription factor SREBP-2. *Biochimica et Biophysica Acta (BBA) - Molecular Cell Research* 2012; 1823(2): 458–64.
36. Wullschlegel S, Loewith R, Hall MN. TOR Signaling in Growth and Metabolism. *Cell* 2006; 124(3): 471–84.
37. Ai D, Baez JM, Jiang H, Conlon DM, Hernandez-Ono A, Frank-Kamenetsky M, et al. Activation of ER stress and mTORC1 suppresses hepatic sortilin-1 levels in obese mice. *J Clin Invest* 2012; 122(5): 1677–87.
38. Xie X, Zhang L, Li X, Liu W, Wang P, Lin Y, et al. Liangxue Jiedu Formula Improves Psoriasis and Dyslipidemia Comorbidity via PI3K/Akt/mTOR Pathway. *Front Pharmacol* 2021; 12: 591608.
39. Jeong S, Yoon M. 17 $\beta$ -Estradiol inhibition of PPAR $\gamma$ -induced adipogenesis and adipocyte-specific gene expression. *Acta Pharmacologica Sinica* 2011; 32(2): 230–8.
40. Kartawijaya M, Han HW, Kim Y, Lee S-M. Genistein upregulates LDLR levels via JNK-mediated activation of SREBP-2. *Food Nutr Res* 2016; 60: 10.3402/fnr.v60.31120.
21. Patel M, Chan CC. Immunopathological aspects of age-related macular degeneration. *Seminars in Immunopathology* 2008; 30: 97–110.
22. WuZ, Lauer TW, Sick A, Hackett SF, Campochiaro PA. Oxidative stress modulates complement factor H expression in retinal pigmented epithelial cells by acetylation of FOXO3. *J Biol Chem* 2007; 282: 22414–25.
23. Beatty S, Koh H, Phil M, Henson D, Boulton M. The role of oxidative stress in the pathogenesis of age-related macular degeneration. *Surv Ophthalmol* 2000; 45: 115–34.
24. Nishibori T, Tanabe Y, Su L, David M. Impaired development of CD4<sup>+</sup> CD25<sup>+</sup> regulatory T cells in the absence of STAT1: increased susceptibility to autoimmune disease. *J Exp Med* 2004; 199: 25–34.
25. Iannaccone A, Neeli I, Krishnamurthy P, Lenchik NI, Wan H, Gerling IC, et al. Autoimmune biomarkers in age-related macular degeneration: A possible role player in disease development and progression. *Adv Exp Med Biol* 2012; 723: 11–6.
26. Morohoshi K, Goodwin AM, Ohbayashi M, Ono SJ. Autoimmunity in retinal degeneration: Autoimmune retinopathy and age-related macular degeneration. *J Autoimmun* 2009; 33: 247–54.

# Assessment of association between PD-L1 expression and clinicopathological characteristics of Indonesian patients with high grade bladder urothelial carcinoma

Hanggoro Tri Rinonce, PhD, Theresia Hening Dwi Ambarwati, MD, Muh Syaebani, MD, Maria Fransiska Pudjohartono, MD, Stella Adevita, MD, Paranita Ferronika, PhD, Irianiwati Widodo, PhD

Department of Anatomical Pathology, Faculty of Medicine, Public Health and Nursing, Universitas Gadjah Mada/ Dr. Sardjito Hospital, Sleman, Yogyakarta, Indonesia

## ABSTRACT

**Introduction:** Urothelial carcinoma (UC) is the most common type of bladder cancer. One of the treatments that are currently being explored for UC involves the use of immune checkpoint inhibitors, especially those targeting PD-1/PD-L1 interaction. This interaction has been previously suggested to aid in the prediction of outcomes. This study was aimed to investigate PD-L1 expression in high grade UC cases in Indonesia, both at mRNA and protein levels, and assess its associated clinicopathological characteristics.

**Materials and Methods:** The study involved analysis of 51 formalin-fixed paraffin-embedded (FFPE) tissue samples, obtained from patients diagnosed with high grade UC. PD-L1 expression was measured using immunohistochemistry (IHC) and quantitative real-time polymerase chain reaction.

**Results:** PD-L1 IHC staining was found to be positive in five (9.80%) cases. Upregulated expression of PD-L1 mRNA was reported in the patients belonging to older age group ( $p = 0.049$ ) and mainly involved less invasive cases ( $p = 0.019$ ), when compared with normoregulated group. Age was positively correlated with PD-L1 expression, as observed in IHC ( $r = 0.281$ ,  $p = 0.046$ ). In comparison to this, mitotic index was found to be inversely correlated with PD-L1 mRNA levels ( $r = -0.369$ ,  $p = 0.008$ ).

**Conclusion:** IHC staining results showed that PD-L1 expression was lower as compared to previous studies, which might suggest poor response to anti PD-1/PD-L1 agents. The results of the study showed that higher mRNA levels were associated with lower proliferation and less invasive behavior. Thus, the study suggested the potential of PD-L1 mRNA levels to be used as a predictive factor for patient outcomes.

## KEYWORDS:

Bladder Cancer, Immune Checkpoint Inhibitors, Immunohistochemistry, Immunotherapy, Real-Time PCR

## INTRODUCTION

Urothelial carcinoma (UC) is known to be the most common type of bladder malignancy. It accounts for over 500,000 new cases and over 200,000 deaths per year.<sup>1</sup> Patient outcomes for

UC patients at later stages remain dismal, necessitating the development of new treatment strategies. One of the treatment modalities that are currently being explored for treatment of UC involves the use of immune checkpoint inhibitors (ICI), especially the ones that target PD-1/PD-L1 interaction. Currently, there are five ICI agents targeting PD-1 or PD-L1 that have been approved for UC patients.<sup>2</sup>

Despite the advancements in this field, responses of patients toward ICI therapy have been reported to be significantly variable. It has been previously suggested that testing for PD-L1 expression using immunohistochemistry (IHC) staining might help in predicting therapy response and patient outcomes, in general.<sup>3</sup> However, very limited studies have previously explored patient characteristics and outcomes in relation to PD-L1 expression in UC cases. The results in most of these studies were mainly inconclusive. Interestingly, one of the studies reported that PD-L1 mRNA levels could predict prognosis better than PD-L1 expression assessed using IHC.<sup>4</sup>

In Indonesia, studies focused on the associations between PD-L1 status and clinicopathological features are still limited. In fact, the results for these studies are quite conflicting. A study involving colorectal cancer (CRC) patients reported lower levels of mRNA expression for PD-L1 in peripheral blood as compared to healthy controls. Importantly, these mRNA levels correlated with gender but showed no correlation with age, stage, histological type, patient status, and body mass index.<sup>5</sup> Inversely, Al Azhar et al. (2021) reported higher PD-L1 mRNA expression in peripheral blood of nasopharyngeal carcinoma patients as compared to healthy controls. These levels were not associated with any of the clinicopathological features that were analyzed.<sup>6</sup> A study involving analysis of formalin-fixed paraffin-embedded (FFPE) tissue of bladder UC showed an association of PD-L1 expression with depth of invasion.<sup>7</sup>

Although ICI treatment has not been routinely used in case of most of Indonesian patients, data for the expression of immune checkpoint molecules would assist clinicians in considering the potential effectiveness of these treatment strategies in Indonesia. This study was aimed to investigate PD-L1 expression, at mRNA and protein levels, in high grade UC cases in Indonesia, and assessed its association with clinicopathological characteristics.

Corresponding Author: Hanggoro Tri Rinonce  
Email: hanggoro\_rinonce@ugm.ac.id



## MATERIAL AND METHODS

This cross-sectional study included 51 FFPE tissue samples, obtained from patients diagnosed with high grade UC at Dr. Sardjito Hospital, Yogyakarta, Indonesia (longitude of  $-7.768393056636577$  and latitude of  $110.37345273846378$ ), during January 2014 to December 2019. Grading for tissue samples was determined on the basis of 2016 WHO Classification of Tumors of the Urinary System and Male Genital Organs.<sup>8</sup> Cases with incomplete clinicopathological data or degraded specimens were excluded from the study.

PD-L1 expression was measured using IHC and quantitative real-time polymerase chain reaction (RT-PCR). IHC staining was performed on 3  $\mu\text{m}$ -thick tissue sections, using PD-L1 antibody clone 22C3 (Dako Agilent Technologies, Santa Clara, CA, USA). UltraTek<sup>®</sup> HRP Anti-Polyvalent Lab Pack (Scytek Laboratories, Logan, UT, USA) was used for visualization. Normal tonsil tissue was used as positive control. The expression of PD-L1 was determined using combined positive score (CPS), which was calculated using the following formula:

$$\text{CPS} = \frac{\text{number of PD-L1 staining cells (tumor cells, lymphocytes, and macrophages)}}{\text{total number of viable tumor cells}} \times 100$$

Samples with  $\text{CPS} \geq 10$  was classified as PD-L1 positive, while samples with  $\text{CPS} < 10$  were classified as PD-L1 negative.

Tumor RNA was extracted from FFPE tissue using GeneAll<sup>®</sup> Ribospin<sup>™</sup> II (GeneAll Biotechnology, Seoul, South Korea). Quantification of PD-L1 mRNA was done using RT-PCR with AccuPower<sup>®</sup> GreenStar<sup>™</sup> RT-qPCR PreMix on Exicycler<sup>™</sup> 96 (Bioneer Corp., Daejeon, South Korea). RT-PCR was performed according to the protocol previously described by Vassilakopoulou et al.<sup>9</sup> In particular, this study provided sequences for the primer pairs and thermocycler conditions used in the present study. PD-L1 mRNA levels were calculated and normalized from the quantification cycle ( $C_q$ ). GAPDH was used as an internal control. Samples were classified as normoregulated if the expression was lower or equal to the average of PD-L1 mRNA levels of the entire subject group, while the samples with levels above the average were classified as upregulated.

Detailed clinical data (age, sex, and lymph node metastasis) were obtained from the medical records. The collected pathological data included information regarding invasion of muscularis propria, mitotic index, and tumor-infiltrating lymphocytes (TILs). Muscle invasion and TILs were assessed from hematoxylin-eosin slides, while mitotic index was measured using Ki-67 IHC stained slides. Presence of muscle invasion was assessed in terms of whether tumor cells had invaded muscularis propria layer or not. If muscle invasion could not be assessed from the sample, the sample was excluded from analysis for muscle invasion. TILs were grouped as intense and non-intense using a 10% cut-off, according to previous studies.<sup>10,11</sup> The samples with 10% or more stromal TILs were classified as intense, while the samples with less than 10% stromal TILs were classified as non-intense. For mitotic index assessed using Ki-67 IHC stained slides, observed under the microscope, 20% cut-off value was used. The number of tumor cells with brown-stained nuclei was calculated for at least 1000 tumor cells.

Chi-square analysis was used to compare clinicopathological characteristics for PD-L1 positive and negative groups for the categorical variables. T-test and Mann-Whitney test were used to compare continuous variables for normally distributed variables and non-normal distribution, respectively. Correlation between continuous variables was analyzed using Pearson correlation. The experiments performed in this study were approved by the Medical and Health Research Ethics Committee of Faculty of Medicine, Public Health and Nursing, Universitas Gadjah Mada, Yogyakarta, Indonesia (KE/FK/0733/EC/2019).

## RESULTS

The characteristic features for the whole group and group comparisons made on the basis of PD-L1 expression are presented in Table I. The study mainly included male patients (76.47%), with an average age of 65.78 years (range: 45–83 years). PD-L1 IHC staining was reported to be positive in five (9.80%) cases. Representative results for PD-L1 immunohistochemistry are shown in Fig. 1.

Fig. 2 shows the distribution of PD-L1 mRNA expression levels of the PD-L1 expression groups based on immunohistochemistry assessment. Patients with upregulated PD-L1 mRNA belonged to older age group ( $p = 0.049$ ). In fact, these cases were less invasive cases ( $p = 0.019$ ) as compared to normoregulated group (Table I). No other differences were found to be statistically significant in case of clinicopathological characteristics.

Pearson correlations between continuous parameters are shown in Table II. Age was found to be positively correlated with PD-L1 expression, as assessed using IHC examination ( $r = 0.281$ ,  $p = 0.046$ ). In contrast to this, mitotic index was inversely correlated to PD-L1 mRNA levels ( $r = -0.369$ ,  $p = 0.008$ ).

## DISCUSSION

This study investigated the associations between PD-L1 expression (both at mRNA and protein levels) and clinicopathological characteristics of high-grade UC cases in Indonesia. The results for IHC staining showed that PD-L1 expression was positive in 9.80% of the cases. Upregulated mRNA levels were found to be associated with less invasive behavior and lower mitotic index. Importantly, higher PD-L1 expression was associated with older age.

For IHC staining, five out of 51 samples tested positive for PD-L1, resulting in a prevalence of 9.80%. This rate is comparatively lower as compared to previous studies, wherein it ranged from 15.1%–46.39%.<sup>12–15</sup> It has been previously reported that differences in populations and histological variants might affect PD-L1 expression.<sup>13</sup> Another factor that might contribute is the variation in the antibody clone used, which is known to cause differences in sensitivity and specificity.<sup>16</sup> Low PD-L1 expression might suggest that ICI treatment in Indonesian patients would exhibit poorer response. However, the predictive role of PD-L1 still remains inconclusive, thus requiring further research.



Table I: Associations between PD-L1 expression and clinicopathological characteristics

	All subjects (n = 51)	PD-L1 expression on IHC		p **	PD-L1 mRNA expression		p **
		Positive	Negative		Upregulated	Normoregulated	
Age, mean $\pm$ SD*	65.78 $\pm$ 8.76	71.00 $\pm$ 9.54	65.20 $\pm$ 8.59	0.163	68.24 $\pm$ 8.53	63.4 $\pm$ 8.47	0.049
Age category, n (%)							
<65 years	22 (43.13)	2 (3.92)	20 (39.22)	0.632	9 (17.65)	13 (25.49)	0.400
$\geq$ 65 years	29 (56.87)	3 (5.88)	26 (50.98)		16 (31.37)	13 (25.49)	
Sex, n (%)							
Male	39 (76.47)	4 (7.84)	35 (68.63)	0.665	20 (39.22)	19 (37.25)	0.743
Female	12 (23.53)	1 (1.96)	11 (21.57)		15 (29.41)	7 (13.73)	
Lymph node metastasis, n (%)							
Present	7 (13.73)	1 (1.96)	6 (11.76)	0.538	1 (1.96)	6 (11.76)	0.055
Absent	44 (86.27)	4 (7.84)	40 (78.43)		24 (47.06)	20 (39.22)	
Muscle invasion, n (%)							
Yes	37 (72.55)	4 (8.89)	33 (73.33)	0.443	15 (33.33)	22 (48.89)	0.019
No	8 (15.69)	0 (0.00)	8 (17.78)		7 (15.56)	1 (2.22)	
Indeterminate	6 (11.76)						
Mitotic index, mean $\pm$ SD*	36.64 $\pm$ 15.80	47.40 $\pm$ 20.11	35.47 $\pm$ 15.07	0.110	33.04 $\pm$ 13.56	40.11 $\pm$ 17.24	0.111
Mitotic index category, n (%)							
$\geq$ 20%	42 (82.35)	4 (7.84)	38 (74.51)	0.638	19 (37.25)	23 (45.10)	0.213
<20%	9 (17.65)	1 (1.96)	8 (15.69)		6 (11.76)	3 (5.88)	
TILs, mean $\pm$ SD*	17.21 $\pm$ 10.88	11.00 $\pm$ 8.21	17.89 $\pm$ 10.98	0.237	15.32 $\pm$ 11.62	19.03 $\pm$ 10.00	0.128
TILs category, n (%)							
Intense ( $\geq$ 10%)	35 (68.63)	2 (3.92)	33 (64.71)	0.171	14 (27.45)	21 (41.18)	0.075
Non-intense (<10%)	16 (31.37)	3 (5.88)	13 (25.49)	0.099	11 (21.57)	5 (9.80)	
PD-L1 mRNA, mean $\pm$ SD*	9.78 $\pm$ 4.13	6.89 $\pm$ 2.54	10.10 $\pm$ 4.16				
PD-L1 mRNA category							
Upregulated	25 (49.02)	1 (1.96)	24 (47.06)	0.187			
Normoregulated	26 (50.98)	4 (7.84)	22 (43.13)				

\*SD = standard deviation.

\*\*p value &lt; 0.05 was considered significant.

**Table II: Correlation between PD-L1 expression and clinicopathological parameters**

	Mitotic Index	TILs	PD-L1 (IHC)	PD-L1 (mRNA)
Age	0.007 (0.959)	-0.060 (0.676)	<b>0.281</b> <b>(0.046)</b>	0.133 (0.351)
Mitotic Index		-0.049 (0.732)	0.233 (0.101)	<b>-0.369</b> <b>(0.008)</b>
TILs			-0.238 (0.093)	-0.027 (0.851)
PD-L1 (IHC)				-0.196 (0.167)
PD-L1 (mRNA)				

Statistically significant values are indicated in bold

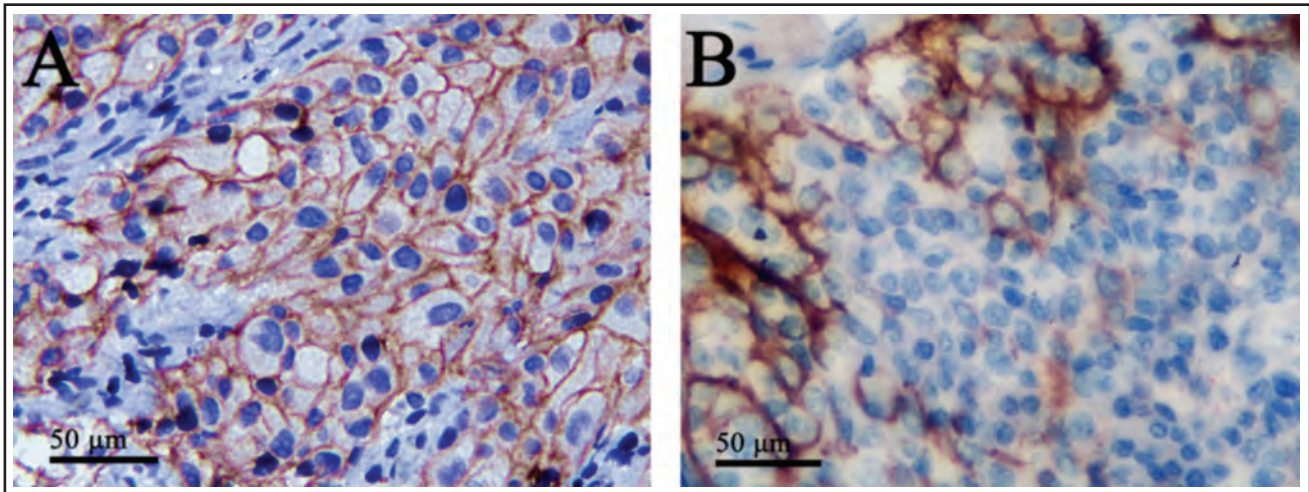


**Fig. 1:** (A) Immunohistochemistry staining image for representative urothelial carcinoma case stained positive for PD-L1, with combined positive score 100 (400x magnification). (B) Normal tonsil tissue as positive control showed positive membranous expression on reticulated epithelium of crypts.

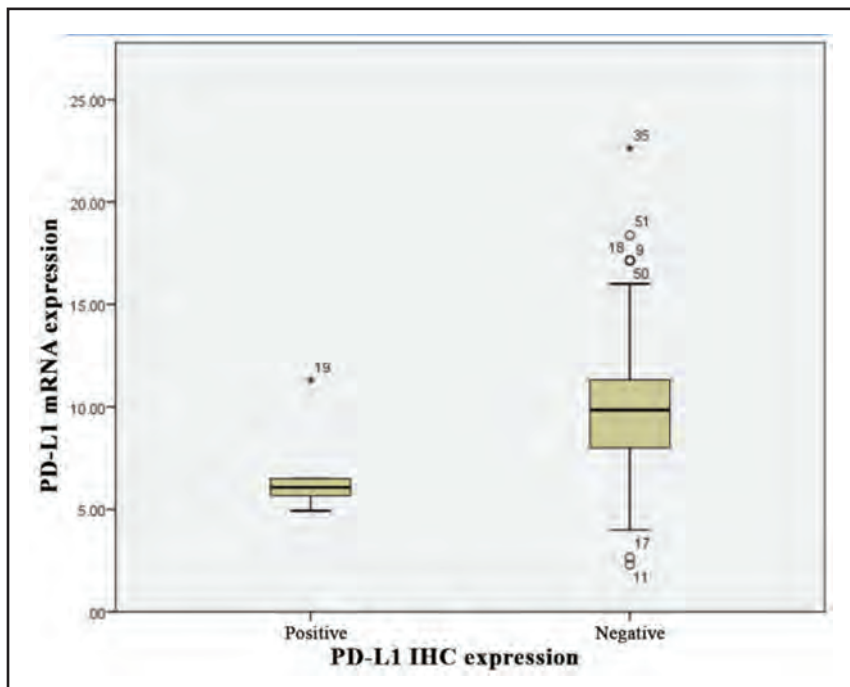


**Fig. 2:** Blox plot showing distribution of PD-L1 mRNA expression levels in positive and negative PD-L1 expression groups based on immunohistochemistry.

Importantly, it was observed that PD-L1 protein expression was not directly proportional to mRNA levels. PD-L1 expression levels observed for IHC and quantitative PCR even appeared to be negatively correlated. However, it was not statistically significant. Studies in UC have been previously shown to be variable in terms of the correlation between expression of PD-L1 mRNA and protein. Le Goux et al. reported a positive correlation between both these molecules.<sup>17</sup> However, Eckstein et al. reported that over 80% of urothelial bladder tumors that showed high expression of PD-L1 mRNA were negative for PD-L1 when IHC staining was performed.<sup>4</sup>

The type of PD-L1 expression (whether constitutive or inducible) might affect the correlation between the expression of PD-L1 mRNA and protein. In steady state conditions, mRNA levels tend to be proportional to protein levels.<sup>18</sup> However, in dynamic cell settings, such as proliferation, correlations between mRNA and protein expression become more variable. In fact, it can even reach negative correlation in certain cases. Variations in the findings of several studies might reflect the involvement of different expression modes in different populations. In this study, lack of positive correlation between PD-L1 mRNA and protein suggested that PD-L1 expression in Indonesian UC patients was inducible or reactive. The mode of expression might affect the prognostic role of PD-L1 in cancers, with reactive PD-L1 expression marking better prognosis and improved response to therapies targeting PD-L1.<sup>19</sup>

Post-transcriptional factors, including miRNA, involved in PD-L1 expression pathway might also affect the correlation between mRNA and protein levels. Several oncogenic miRNAs, such as miR-873 and miR-34a, are known to target the genes that encode PD-L1.<sup>20</sup> Consequently, inhibited translation could result in low protein expression, regardless of mRNA levels. Polymorphism of untranslated regions of PD-L1 mRNA can also affect the mRNA stability, which in turn can affect the measured mRNA levels.

Several post-translational processes, such as N-glycosylation, phosphorylation, and ubiquitination, can also affect PD-L1 protein levels. Glycosylation has been previously shown to protect PD-L1 from degradation, while phosphorylation and ubiquitination marked PD-L1 for degradation.<sup>21</sup> Increased degradation of PD-L1 protein might also account for a poor correlation between PD-L1 mRNA and protein levels.

This discrepancy between PD-L1 mRNA and protein expression might also explain the other associations that were found. Expression of PD-L1 in urothelial cancer cells is known to be associated with more aggressive tumors and higher recurrence.<sup>22,23</sup> Conversely, the results of this study showed that upregulated PD-L1 mRNA is associated with lower muscle invasiveness. Two previous studies also reported that bladder cancer cases with higher PD-L1 mRNA exhibit longer patient survival.<sup>4,24</sup> Differences in the prognostic role of protein and mRNA might arise from their different roles. A failure to express the PD-L1 protein, despite high levels of mRNA, might lead to stronger immune responses toward the tumor, thereby resulting in improved patient outcomes.

Interestingly, both upregulated PD-L1 mRNA and increased PD-L1 protein expression were found to be associated with older age. There is a possibility that PD-L1 transcription increases with age, which resulted in an overall increase in PD-L1 mRNA and protein expression levels. Very few studies have previously reported an association with age. Interestingly, one study conducted in United States of America reported that PD-L1 expression on IHC was linked to younger age.<sup>10</sup>

Although the samples analyzed in this study were limited and retrospective data collection might lead to information bias, the results of this study suggested that PD-L1 mRNA levels have the potential to be used as a prognostic factor for UC cases. Further research with larger sample size is required to investigate the correlation between PD-L1 expression (using both IHC and RT-PCR) and outcomes among subjects who do not receive immunotherapy.

## CONCLUSIONS

The results of this study suggested that PD-L1 expression at mRNA and protein levels exhibited different clinicopathological associations and possibly prognostic implications. The study particularly highlighted the potential of PD-L1 mRNA levels to be used as a predictive factor for patient outcomes. Studies with larger subject group are required to further ascertain the prognostic role of PD-L1 expression in Asian patients.

## ACKNOWLEDGMENT

The authors would like to thank Nur Eka Wiraditya (Department of Anatomical Pathology, Faculty of Medicine, Public Health and Nursing, Universitas Gadjah Mada, Yogyakarta, Indonesia) and Agustina Supriyanti (Department of Integrated Laboratory, Dr. Sardjito Hospital, Yogyakarta, Indonesia) for providing assistance in the laboratory processes during this study.

## CONFLICT OF INTEREST

All authors declare no conflict of interest.

## REFERENCES

1. Sung H, Ferlay J, Siegel R, Laversanne M, Soerjomataram I, Jemal A, et al. Global cancer statistics 2020: GLOBOCAN estimates of incidence and mortality worldwide for 36 cancers in 185 countries. *Ca-Cancer J Clin* 2021;71(3):209-49.
2. Kim H, Seo H. Immune checkpoint inhibitors for urothelial carcinoma. *Investig Clin Urol* 2018; 59(5):285-96.
3. Tang H, Liang Y, Anders R, Taube J, Qiu X, Mulgaonkar A, et al. PD-L1 on host cells is essential for PD-L1 blockade-mediated tumor regression. *J Clin Invest* 2018; 128(2):580-88.
4. Eckstein M, Wirtz R, Pfannstiel C, Wach S, Stoehr R, Breyer J, et al. A multicenter round robin test of PD-L1 expression assessment in urothelial bladder cancer by immunohistochemistry and RT-qPCR with emphasis on prognosis prediction after radical cystectomy. *Oncotarget* 2018; 9(19):15001-14.
5. Ajoedi A, Azhar M, Nadliroh S, Hartini S, Andalusia R, Witarto A. The mRNA expression profile of PD-1 and PD-L1 in peripheral blood of colorectal cancer patients. *Indonesian Journal of Cancer* 2019;13(3):80-5.

6. Al Azhar M, Nadliroh S, Prameswari K, Handoko H, Tobing D, Herawati C. Profile of PD-1 and PD-L1 mRNA expression in peripheral blood of nasopharyngeal carcinoma. *Molecular Cellular Biomedical Sci* 2020; 4(3):121-7.
7. Widayanti LA, Dewi I, Saputra H, Susraini AAAN, Sriwidayanti NP, Muliarta IM. Hubungan antara tumor infiltrating lymphocytes (TIL), ekspresi programmed death-ligan 1 (PD-L1) pada sel tumor dan TIL dengan kedalaman invasi pada karsinoma urothelial kandung kemih tipe tidak spesifik di RSUP Sanglah, Bali, Indonesia. di RSUP Sanglah, Bali, Indonesia. *Intisari Sains Medis* 2020; 11(3):1119-25.
8. Moch H, Cubilla A, Humphrey P, Reuter V, Ulbright T. The 2016 WHO classification of tumours of the urinary system and male genital organs—Part A: Renal, Penile, and Testicular Tumours. *Eur Urol* 2016; 70(1):93-105.
9. Vassilakopoulou M, Avgeris M, Velcheti V, Kotoula V, Rampias T, Chatzopoulos K, et al. Evaluation of PD-L1 expression and associated tumor-infiltrating lymphocytes in laryngeal squamous cell carcinoma. *Clin Cancer Res* 2015; 22(3):704-13.
10. Rouanne M, Betari R, Radulescu C, Signolle N, Allory Y, Marabelle A, et al. Association of stromal lymphocyte infiltration with tumor invasion depth and high-grade T1 bladder cancer. *J Clin Oncol* 2018; 36(6\_suppl):488.
11. Huang H, Su H, Li P, Chiang P, Huang C, Chen C, et al. Prognostic impact of tumor infiltrating lymphocytes on patients with metastatic urothelial carcinoma receiving platinum-based chemotherapy. *Sci Rep* 2018; 8(7485):1-7.
12. Faraj S, Munari E, Guner G, Taube J, Anders R, Hicks J, et al. Assessment of tumoral PD-L1 expression and intratumoral CD8+ T Cells in urothelial carcinoma. *Urology* 2015; 85(3): 703.e1-e6.
13. Kim B, Lee C, Kim Y, Moon K. PD-L1 expression in muscle-invasive urinary bladder urothelial carcinoma according to basal/squamous-like phenotype. *Front Oncol* 2020; 10(527385):1-7.
14. Nechifor-Boilă I, Loghin A, Nechifor-Boilă A, Decaussin-Petrucci M, Voidăzan S, Chibelea B, et al. PD-L1 expression in muscle invasive urothelial carcinomas as assessed via immunohistochemistry: correlations with specific clinical and pathological features, with emphasis on prognosis after radical cystectomy. *Life* 2021;11(5):404.
15. Kim D, Kim JM, Kim JS, Kim S, Kim KH. Differential expression and clinicopathological significance of HER2, indoleamine 2,3-dioxygenase and PD-L1 in urothelial carcinoma of the bladder. *J Clin Med* 2020; 9(5): 1-15.
16. Reis H, Serrette R, Posada J, Lu V, Chen Y, Gopalan A, et al. PD-L1 expression in urothelial carcinoma with predominant or pure variant histology. *Am J Surg Pathol* 2019; 43(7):920-7.
17. Le Goux C, Damotte D, Vacher S, Sibony M, Delongchamps NB, Schnitzler A, et al. Correlation between messenger RNA expression and protein expression of immune checkpoint-associated molecules in bladder urothelial carcinoma: a retrospective study. *Urol Oncol: Semin Orig* 2017; 35(5): 257-63.
18. Liu Y, Beyer A, and Aebersold R. On the dependency of cellular protein levels on mRNA abundance. *Cell* 2016; 165(3): 535-50.
19. Hao D, Wang G, Yang W, Gong J, Li X, Xiao M, et al. Reactive versus constitutive: reconcile the controversial results about the prognostic value of PD-L1 expression in cancer. *Int J Biol Sci* 2019; 15(9): 1933-41.
20. Yi M, Niu M, Xu L, Luo S, Wu K. Regulation of PD-L1 expression in the tumor microenvironment. *J Hematol Oncol* 2021; 14(1): 10.
21. Hsu JM, Li CW, Lai YJ, Hung MC. Posttranslational modifications of PD-L1 and their applications in cancer therapy. *Cancer Res* 2018; 78(22): 6349-53.
22. Bellmunt J, Mullane SA, Werner L, Fay AP, Callea M, Leow JJ, et al. Association of PD-L1 expression on tumor-infiltrating mononuclear cells and overall survival in patients with urothelial carcinoma. *Ann Oncol* 2015; 26(4): 812-7.
23. Pierconti F, Raspollini MR, Martini M, Larocca LM, Bassi PF, Bientinesi R, et al. PD-L1 expression in bladder primary in situ urothelial carcinoma: evaluation in BCG-unresponsive patients and BCG responders. *Virchows Archiv* 2020; 477(2): 269-77.
24. Kubon J, Sikić D, Eckstein M, Weyerer V, Stöhr R, Neumann A, et al. Analysis of CXCL9, PD1 and PD-L1 mRNA in stage T1 non-muscle invasive bladder cancer and their association with prognosis. *Cancers* 2020; 12(10): 1-13.



# Neutrophil-to-lymphocyte ratio, platelet-to-lymphocyte ratio, and absolute lymphocyte count as mortality predictor of patients with Coronavirus Disease 2019

Farida Anwari, MPH<sup>1</sup>, Martina Kurnia Rohmah, MBiomed<sup>2</sup>, Iif Hanifa Nurrosyidah, MFarm<sup>2</sup>, Acivrida Mega Charisma, MSi<sup>1</sup>, Adinugraha Amarullah, MFarm<sup>2</sup>, Geo Firnanda A, Md<sup>1</sup>

<sup>1</sup>Departement of Medical Laboratory Technology, STIKES RumahSakit Anwar Medika, Sidoarjo, Indonesia, <sup>2</sup>Departement of Pharmacy, STIKES RumahSakit Anwar Medika, Balongbendo, Sidoarjo, Indonesia

## ABSTRACT

**Introduction:** Coronavirus Disease 2019 (COVID-19) has a various spectrum of symptoms from asymptomatic to severe. In previous research, hematological examination could predict the severity of the infection. This study is aimed to evaluate Neutrophil-to-Lymphocyte Ratio (NLR), Platelet-to-Lymphocyte Ratio (PLR), and Absolute Lymphocyte Count (ALC) as a predictor of COVID-19 mortality.

**Materials and Methods:** The study was a cross sectional research with retrospective design by collecting data from medical records of the COVID-19 patients at a General Hospital Anwar Medika of East Java, for the period June 2020 to January 2021. A comparative test was performed using the Mann-Whitney test. The predictive ability was assessed using the ROC curve.

**Results:** A total of 70 subjects were involved in this study with 16 (22.9%) mortality. And the average NLR and PLR were 4.11 and 174.39. The Mann-Whitney test showed significant results ( $p < 0.05$ ) on leukocytes, NLR, PLR, and ALC of the patients. The ROC curve showed that under the curve of leukocytes, NLR, PLR, and ALC were 0.749, 0.731, 0.719, and 0.306, respectively.

**Conclusion:** With higher sensitivity and specificity by leukocytes 75% and 70.4%. Leukocytes, NLR, and PLR showed good ability to predict patient mortality from COVID-19.

## KEYWORDS:

Coronavirus, mortality, predictive tools

## INTRODUCTION

Coronavirus is a family of viruses found in humans and animals, the emergence of a new virus outbreak belonging to the coronavirus group was first discovered in the city of Wuhan, China. Within a few weeks, this virus spread to various parts of the continent. On February 20, 2020, the World Health Organization (WHO) announced that the outbreak caused by this new type of Coronavirus, namely Coronavirus Disease 2019 (COVID-19), was global. It is recorded that at this time, around 184 million people have

been affected, and almost 4 million deaths due to Coronavirus, which has infected 222 countries around the world.<sup>1</sup>

In Indonesia alone, there were 2.3 million confirmed cases with nearly 60,000 deaths.<sup>2</sup> In SARS-CoV-2 infection, there are changes in several laboratory indicators which are also found in several other viral infections, because the hematopoietic system is a system that feels the impact of a viral infection.<sup>3,4</sup> Several previous studies have shown that there is lymphocytopenia, neutrophilia, eosinopenia, thrombocytopenia, or thrombocytosis, as well as the presence of reactive lymphocytes which indicate an acute infection.<sup>4</sup> Apart from the changes in the results of the hematological examination, the results can also be used to predict the severity of COVID-19. A meta-analysis stated that leukocytosis, lymphopenia, and thrombocytopenia are predictors of the severity of COVID-19 and increase the incidence of mortality with these results.<sup>5</sup>

Several other studies have also shown that NLR, PLR, and ALC can predict mortality from COVID-19 infection.<sup>6,7</sup> In this study, we evaluated the COVID-19 mortality hematologic predictors at Anwar Medika General Hospital as one of the COVID-19 referral hospitals in Indonesia

## MATERIAL AND METHODS

The study used an observational analytic cross-sectional research with retrospective design. The profile description is carried out retrospectively by collecting data from medical records of the COVID-19 patients' data consisting of age, gender, leukocytes and the differential count, platelets, length of stay, and mortality status. The hematological result was then calculated to produce NLR (neutrophil-to-lymphocyte ratio), PLR (platelet-to-lymphocyte ratio), and ALC (absolute lymphocyte count).

These were the following equation:

$$NLR = \frac{NLR = (\text{Absolute neutrophil count (Cells}/\mu\text{L)})}{(\text{Absolute lymphocyte count (Cells}/\mu\text{L)})}$$

$$PLR = \frac{\text{Thrombocyte count (Cells}/\mu\text{L)}}{\text{Absolute lymphocyte count (Cells}/\mu\text{L)}}$$

Corresponding Author: Farida Anwari  
Email: faridamph@gmail.com

The sample used in this study were patients infected with COVID-19 at the Anwar Medika General Hospital during the period of June 2020 to January 2021. With the inclusion criteria of patients who have been confirmed positive for COVID-19 through PCR examination results, while patients with a history of blood transfusions were excluded from this study.

Furthermore, comparative tests were conducted between the hematological profile to the length of stay (LoS) and patient mortality. Comparative tests were conducted using a two-sample independent t2 test on data with a normal distribution and using the Mann-Whitney test on data with an abnormal distribution. Variables that have significant values were then tested for predictive ability using the ROC curve then interpreted as sensitivity and specificity. The highest sensitivity and specificity are obtained by the curve reading that produced by IBM® SPSS®

## RESULTS

A total of 70 subjects were involved in this study. From the subjects, 10 subjects (14.3%) were males, and the rest were females (85.7%). The average age of the research subjects was 51.03 years with the youngest being 30 years old and the oldest 82 years old.

From the results of the hematological examination, the average leukocytes, platelets, neutrophils, and lymphocytes were 9,730/ $\mu$ L, 265,671/ $\mu$ L, 5,960/ $\mu$ L, and 1,830/ $\mu$ L. And from the calculation, the average NLR and PLR were 4.11 and 174.39. With an average length of stay (LoS) of 10.91 days.

From the mortality data, 16 patients (22.9%) died. The average age of the subjects who died was 53.19 years, higher than the group who survived 50.58 years. From the calculation of leukocytes, platelets, neutrophils, NLR, and PLR, it was found that the average death group was higher than the survival group. Meanwhile, ALC and LoS were lower in the mortal group than in the surviving group. The comparative test showed significant results ( $p < 0.05$ ) on leukocytes, NLR, PLR, ALC, and length of stay (LoS) of the patients.

The results of the receiver operating characteristic (ROC) curve the largest area under the curve (AUC) was produced by leukocytes, 0.749, followed by NLR and PLR. Meanwhile, ALC has the lowest AUC of 0.306. From the results of the highest sensitivity obtained PLR of 81.3% and the highest specificity is 70.4% leukocytes.

## DISCUSSION

The number of deaths due to COVID-19 is increasing every day in Indonesia, with the number of deaths reaching a thousand on 07/08/2021.<sup>2</sup> In addition, there are also more than 300,000 active cases of confirmed patients infected with COVID-19, which further reduces the ability of hospitals to handle patients.<sup>2</sup> However, clinical manifestations of the confirmed patients vary from asymptomatic to severe symptoms.<sup>8,9</sup> Because of this, it is necessary to stratify individuals with confirmed COVID-19 to optimize the capacity of the available hospitals.

From our research, it was found that from 70 subjects consisted of 16 subjects (22.9%) who died during the observation and the rest recovered. The mortality rate of 22.9% was higher if were looked at the death rate throughout Indonesia, which was 2.6%.<sup>2</sup> This finding could be related to community stigma regarding COVID-19 which causes patients to be late in seeking help to health centers which is associated with increased patient mortality.<sup>10,11</sup>

From the findings in our study, it was found that the average age of the covid patients we treated was 51.03 years, which is the age group at risk of severe infection in COVID-19.<sup>12-14</sup> This result is also supported by the finding of an older age in mortality cases compared to the survivors. However, in our study, there were no significant results between age and mortality status which was not in line with previous studies which stated that age was associated with patient mortality.<sup>14</sup>

The comparison test result from mortality status and hematological results were found that there was a relationship between mortality status with leukocytes, NLR, PLR, and ALC. There was also a significant relationship between mortality status and length of stay (LoS) of the patients. In the previous study, evaluation of the hematological component compared to the severity of COVID-19 infection showed that there was a relationship between either NLR, PLR, or ALC and infection severity with various degrees of association.<sup>15-17</sup> Our findings showed that leukocytes, NLR, and PLR were higher in subjects with mortality compared to surviving subjects. While the ALC showed the opposite results which decreased in subjects who experienced mortality. This finding is in line with research.<sup>18</sup> So that leukocytes, NLR, PLR, and ALC could be used as predictors of severity and mortality from COVID-19 patients. From the ROC curve, it was found that leukocytes, NLR, and PLR had AUC more than 0.50, but not with ALC. From the results of the best sensitivity and specificity, leukocytes were obtained with a sensitivity of 75% and a specificity of 70.4%, followed by PLR with a sensitivity of 81.3% and a specificity of 63%. Although ALC has a relationship with the patient's mortality status, the predictive ability of ALC on mortality status is quite low, seeing the AUC of only 0.306. In the previous predictive value testing in the research conducted by Yang et al. the sensitivity from NLR and PLR were 88% and 77%, respectively.<sup>6</sup> These results indicate that this modality can be used as a basis for predicting mortality in COVID-19 patients.

The association of leukocytes and NLR in infection cases in previous studies has been associated with the occurrence of cytokine storms that often occur in severe COVID-19 patients.<sup>19</sup> Although in this study no further investigation was carried out regarding the cause of death suffered by the patients, the increase in the number of leukocytes, which were dominated by polymorphonuclear cells, indicated that this finding was a predictor of increased immune activity in the patients' body which could be a sign of a cytokine storm. In line with the investigation Xiong et al. stated that the increase in neutrophil was a result of the release of CXCL-2 and CXCL-8 which increased neutrophil recruitment and indicated high cytokine activity in the patient's body.<sup>20</sup>

From our findings, it was found that there was a higher PLR

**Table I: Characteristic of the subject**

Variable	Mortality status	
	Survive, n (%)	Mortal, n (%)
Gender		
Male	7 (70%)	3 (30%)
Female	47 (78.3%)	13 (21.7%)

**Table II: Comparison variable between mortality status**

Variable	Mean±SD			p
	Total subject	Survived subject	Dead subject	
Age (years old)	51.03±11.77	50.58±12.814	53.19±7.332	NS
Leukocyte (μL)	9,730±4,720	8,672±3,687	13,200±6,219	0.003
Thrombocyte (μL)	265,671±101,263	259,113±106,998	286,812.5±82,743.1	NS
Neutrophil (μL)	5,960±3,310	5,183.8±2,287.4	8,505.3±4,820.2	NS
NLR	4.11±3.40	3.23±2.10	11±5.02	0.005
PLR	174.40±97.80	160.76±94.797	223.55±96.64	0.008
ALC (μL)	1,830±981.5	1,895.4±967.3	1,572.4±1,035.8	0.019
Length of stay (days)	10.91±4.52	11.91±4.42	75±3.45	0.001

NS, Not significant

**Table III: The highest sensitivity and specificity of the variable**

Predictive variable	AUC	Sensitivity	Specificity
Leukocyte	0.749	75%	70.4%
NLR	0.731	75%	57.4%
PLR	0.719	81.3%	63%
ALC	0.306	56.3%	20.4%

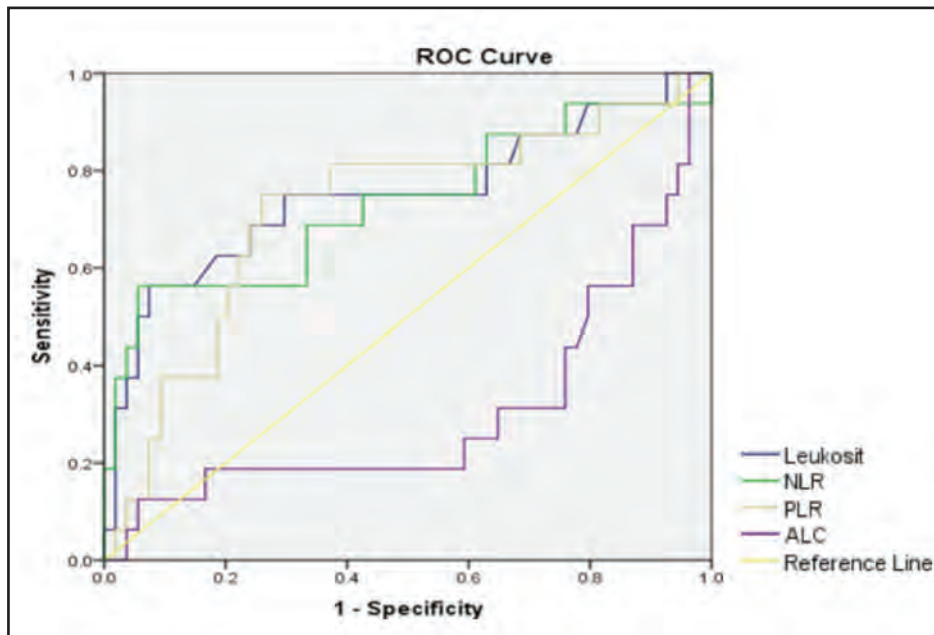


**Fig. 1: ROC Curve of the predicting variable**

in the mortal group compared to the surviving group. This finding is in line with previous research.<sup>21</sup> However, the increase in PLR was not in line with increase in platelets, there was no significant difference between the survivors and the mortality group from the platelet count. The increase in PLR is due to a decrease in the denominator component which is ALC. Several hypotheses that the decrease in ALC in COVID-19 patients is due to the P53 signaling process and FAS signaling which causes lymphocytes to undergo apoptosis.<sup>20,22</sup>

The findings in this study can be used to detect the possible severity and mortality of COVID-19 patients. So that it can be used as consideration for determining the room and therapy to be given to patients. However, this study has limitations mainly because the focus of this study was to evaluate the predictive ability of NLR, PLR, and ALC on COVID-19 mortality in one of the COVID-19 referral sites in Indonesia. Therefore, the subjects involved in this study are limited and cannot represent subjects in Indonesia in general. However, this study can be the basis that NLR, PLR, and leukocytes can be used as predictors of COVID-19 mortality that are easy and inexpensive.

## CONCLUSION

Hematological components (Leukocytes, NLR, PLR, and ALC) have a relationship with mortality status in COVID-19 patients. However, only leukocytes, NLR, and PLR showed good ability to predict patient mortality so it could be used as a triage consideration for COVID-19 patients in the conclusions with the goals of the study but avoid unqualified statements and conclusions not completely supported by the data.

## REFERENCES

- American Library Association. Covid-19 Coronavirus Pandemic [cited 2020] Accessed from: <https://www.worldometers.info/coronavirus/>
- Gugus Tugas COVID-19. Data Sebaran Kasus Positif [cited 2020] Accessed from: <https://covid19.go.id/>
- Debut B, Smadja DM. Is COVID-19 a new hematologic disease? *Stem Cell Rev Reports* 2021;17(1):4–8.
- de Oliveira Toledo SL, Nogueira LS, das Graças Carvalho M, Rios DRA, de Barros Pinheiro M. COVID-19: Review and hematologic impact. *Clin Chim Acta* 2020;510:170–6.
- Henry BM, De Oliveira MHS, Benoit S, Plebani M, Lippi G. Hematologic, biochemical and immune biomarker abnormalities associated with severe illness and mortality in coronavirus disease 2019 (COVID-19): A meta-analysis. *Clin Chem Lab* 2020; 58: 1021–8.
- Yang AP, Ping LJ, Qiang TW, Ming LH. The diagnostic and predictive role of NLR, d- NLR and PLR in COVID-19 patients. *Int Immunopharmacol* 2020;84.
- Wagner J, DuPont A, Larson S, Cash B, Farooq A. Absolute lymphocyte count is a prognostic marker in Covid-19: A retrospective cohort review. *Int J Lab Hematol* 2020;42(6):761–5.
- Hafez MAF. The mean severity score and its correlation with common computed tomography chest manifestations in Egyptian patients with COVID-2019 pneumonia. *Egypt J Radiol Nucl Med* 2020;51(1).
- Storch-de-Gracia P, Leoz-Gordillo I, Andina D, Flores P, Villalobos E, Escalada-Pellitero S, et al. Clinical spectrum and risk factors for complicated disease course in children admitted with SARS-CoV-2 infection. *An Pediatr* 2020;93(5):323–33.
- Abdelhafiz AS, Alorabi M. Social stigma: The hidden threat of COVID-19. *Front in Public Health* 2020; 8.
- Alaa A, Qian Z, Rashbass J, Bengler J, van der Schaar M. Retrospective cohort study of admission timing and mortality following COVID-19 infection in England. *BMJ Open* 2020;10(11):e042712.
- Wolff D, Nee S, Hickey NS, Marscholke M. Risk factors for Covid-19 severity and fatality: a structured literature review. *Infection* 2021; 49: 15–28.
- Li X, Xu S, Yu M, Wang K, Tao Y, Zhou Y, et al. Risk factors for severity and mortality in adult COVID-19 inpatients in Wuhan. *J Allergy Clin Immunol* 2020;146(1):110–8.
- Zheng Z, Peng F, Xu B, Zhao J, Liu H, Peng J, et al. Risk factors of critical & mortal COVID-19 cases: A systematic literature review and meta-analysis. *J Infect* 2020; 81: e16–25.
- Imran MM, Ahmad U, Usman U, Ali M, Shaukat A, Gul N. Neutrophil/lymphocyte ratio—A marker of COVID-19 pneumonia severity. *Int J Clin Pract* 2021;75(4).
- Qu R, Ling Y, Zhang Y, Wei L, Chen X, Li X, et al. Platelet-to-lymphocyte ratio is associated with prognosis in patients with coronavirus disease-19. *J Med Virol* 2020;92(9):1533–41.
- Zeng F, Li L, Zeng J, Deng Y, Huang H, Chen B, et al. Can we predict the severity of coronavirus disease 2019 with a routine blood test? *Polish Arch Intern Med* 2020;130(5):400–6.
- Illg Z, Muller G, Mueller M, Nippert J, Allen B. Analysis of absolute lymphocyte count in patients with COVID-19. *Am J Emerg Med*. 2021;46:16–9.
- Wang J, Jiang M, Chen X, Montaner LJ. Cytokine storm and leukocyte changes in mild versus severe SARS-CoV-2 infection: Review of 3939 COVID-19 patients in China and emerging pathogenesis and therapy concepts. *J Leukoc Biol* 2020;108: 17–41.
- Xiong Y, Liu Y, Cao L, Wang D, Guo M, Jiang A, et al. Transcriptomic characteristics of bronchoalveolar lavage fluid and peripheral blood mononuclear cells in COVID-19 patients. *Emerg Microbes Infect* 2020;9(1):761–70.
- Lin S, Mao W, Zou Q, Lu S, Zheng S. Associations between hematological parameters and disease severity in patients with SARS-CoV-2 infection. *J Clin Lab Anal* 2021;35(1).
- Feng Z, Diao B, Wang R, Wang G, Wang C, Tan Y, et al. The novel severe acute respiratory syndrome coronavirus 2 (SARS-CoV-2) directly decimates human spleens and lymph nodes. *medRxiv* 2020.